Tailor-made carrier particles
for dry powder inhalers

Dissertation

to obtain the academic degree of "Doktorin der Naturwissenschaften" at

Graz University of Technology

Dipl.-Ing. Mag.pharm. Eva Maria Littringer

Eva Maria Littringer

Tailor-made carrier particles
for dry powder inhalers

Dissertation

First assessor

Prof. Mag. Dr.rer.nat. Nora Anne Urbanetz

Research Center Pharmaceutical Engineering GmbH

and

Institute for Process and Particle Engineering

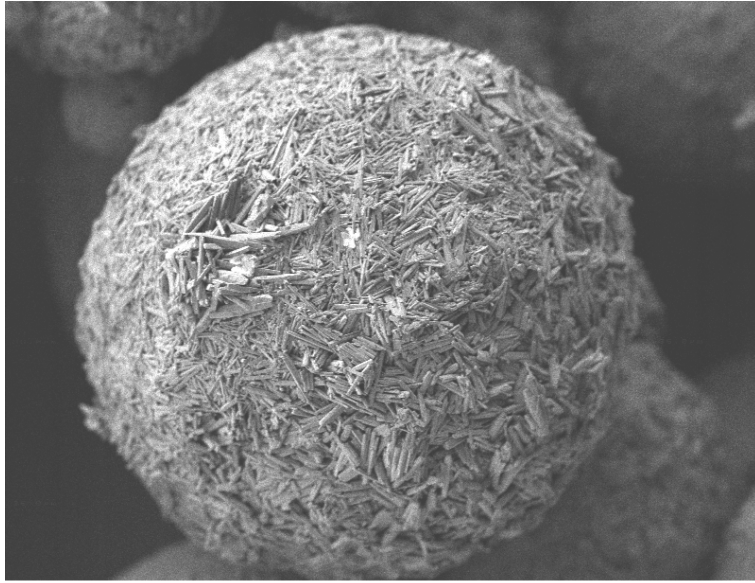Graz University of Technology

Second assessor

Prof. Mag. Dr.phil.nat. Andreas Zimmer
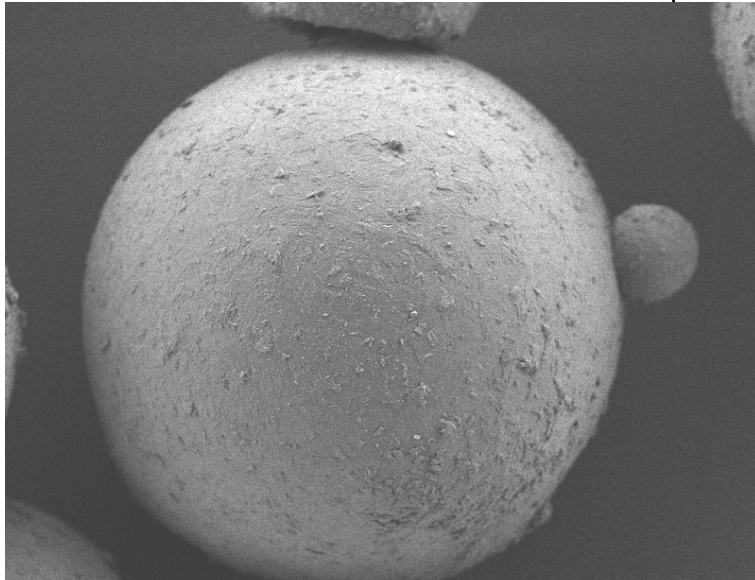
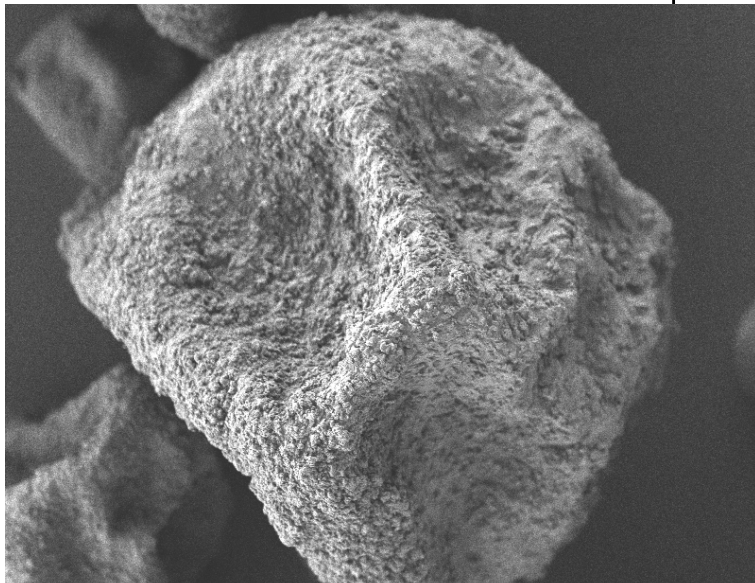Department of Pharmaceutical Technology

University of Graz
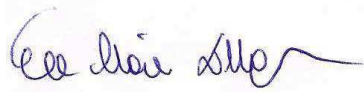
30 µm

30 µm

30 µm

STATUTORY DECLARATION

I declare that I have authored this thesis independently, that I have not used other than the declared sources / resources, and that I have explicitly marked all material which has been quoted either literally or by content from the used sources.

(Ich erkläre an Eides statt, dass ich die vorliegende Arbeit selbstständig verfasst, andere als die angegebenen Quellen/Hilfsmittel nicht benutzt, und die den benutzten Quellen wörtlich und inhaltlich entnommene Stellen als solche kenntlich gemacht habe.)

August, 2012

Eva Maria Littringer

Table of contents

1. Abstract

Active pharmaceutical ingredients (APIs) intended for pulmonary drug delivery must have aerodynamic particle sizes in the range of 1 μm to 5 μm. For this reason they are cohesive, show poor flowability and are difficult to dose. In order to overcome this problem the fine API particles are attached in a mixing process to coarser carrier particles of sufficient flowability. During inhalation the API particles must detach again from the carrier surface to reach the lung. Consequently interparticle forces must be high enough to ensure mixing homogeneity and stability of the mixture during powder handling and transport but low enough to allow detachment during inhalation. Therefore the control of interparticle forces is of vital importance for the quality of the dry powder inhalate. The aim of this work is the preparation of tailored carrier particles with respect to interparticle forces by surface modification via spray drying.

Wirkstoffe, die die Lunge über Inhalation erreichen sollen, müssen aerodynamische Partikelgrößen zwischen 1 μm und 5 μm aufweisen. Auf Grund dessen sind sie kohäsiv, fließen schlecht und sind schlecht dosierbar. Daher werden die feinen Wirkstoffpartikel in einem Mischprozess auf einen gröberen Träger, der ausreichende Fließfähigkeit aufweist, aufgebracht. Bei Inhalation muss sich der Wirkstoff wieder vom Träger lösen, damit er die Lunge erreicht. Dementsprechend müssen die interpartikulären Kräfte groß genug sein, um die Homogenität und Stabilität der Mischung während der Pulververarbeitung und des Transports zu gewährleisten, jedoch klein genug, dass er sich bei Inhalation wieder löst. Aus diesem Grund kommt der Steuerung der Wechselwirkung entscheidende Bedeutung für die Qualität eines Pulverinhalates zu. Ziel des Forschungsvorhabens ist die Gewinnung hinsichtlich der interpartikulären Kräfte maßgeschneiderter Trägerpartikel durch Oberflächenmodifikation mittels Sprühtrocknung.

1. Introduction

1.1. Pulmonary drug delivery

The delivery of active pharmaceutical ingredients (APIs) via the lung is a well established route of administration. Preferably pulmonary administration is used to treat respiratory diseases such as asthma, cystic fibrosis, chronic pulmonary infections and COPD. Here the active is locally administered. This allows higher doses at the site of drug action and concomitantly reduces systemic side effects. Because of the large surface area of the lung accessible to drug absorption and the low metabolic activity an increasing number of formulations is developed for systemic delivery also.

The European Pharmacopoeia lists four types of inhalation devices: nebulizers, pressurized metered-dose inhalers (pMDIs), non-pressurized metered-dose inhalers (MDIs) and powder inhalers (dry powder inhalers – DPIs). For nebulizers, pMDIs and MDIs the corresponding preparations are liquid (solutions, suspensions or emulsions) whereas solid state formulations are used in DPIs.

Depending on the device used the principle of aerosol generation differs. Nebulizers, which deliver the active over an extended period of time involving consecutive inhalations, and MDIs make use of high-pressure gases, ultrasonic vibration or other methods to generate the aerosol. In pMDIs a liquefied propellant is employed. The driving force of aerosol generation in DPIs is the inspired air. Because of the underlying aerosolization principles and the preparations used each class of inhalation devices has its strengths and weaknesses which will be shortly summarized below.

Nebulizers are historically considered the oldest [17] and are indispensable in intensive care treatment. Nevertheless disadvantages encountered are a low efficiency, poor reproducibility, great variability, large size and long time that is needed for inhalation as well as cleaning [5]. Most of those disadvantages were overcome by the development of the first pMDIs in the late 1950s [17]. Until now pMDIs are the gold standard in asthma therapy [15]. The reason for their popularity is the small size. Further they are simple, cheap and easy-to-use. However the high velocity of the aerosol plume and the required co-ordination of actuation and inhalation, which has been overcome by the development of breath-actuated pMDI devices as well as the knowledge about the impact of propellants, especially chlorofluorocarbons (CFCs), on the environment and the final ban of CFCs led to the development of alternative devices. One of those alternatives are non pressurized metered dose inhalers which are also termed soft mist inhalers. The major improvements of those devices are the low velocity of the generated aerosol plume and therefore enhanced lung deposition as well as the absence of propellants. Another alternative are dry powder inhalers administering a dry powder to the lung. DPIs combine the advantages mentioned above of being small, cheap, more or less easy-to-use and having a short administration time, a reduced aerosol plume velocity, no required co-

ordination of actuation and inhalation, the potential of delivering a high range of doses, the absence of propellants as well as the plus of increased stability and reduced risk of microbial contamination compared to liquid formulations. One drawback of some of those dosage forms is the varying amount of active reaching the lung depending on the inspiratory flow rate of the patient.

A precondition for successful pulmonary drug delivery is that aerosol particles with aerodynamic diameters of 1 µm to 5 µm [14, 7, 17] are delivered. Particles that are too large cannot follow the air stream. They will impact in the throat and will have no access to the bronchiolar region. However if the particle size is too small the particles will travel deeper into the lung during inhalation and will be deposited mainly in the alveolar region. The latter might be desirable for APIs intended for systemic delivery, however not for the treatment of asthma and COPD.

In DPIs this desired aerodynamic diameter is commonly achieved by milling of the API. However particles of this size are rather cohesive and precise as well as reproducible dosing is difficult due to poor powder flowability. Especially in multi-dose dry powder inhalers (DPIs) where usually the powder is metered by flowing of the powder from a reservoir into well defined orifices, sufficient flowability is crucial in order to guarantee adequate dosing [5]. To ensure flowability the fine API particles may be mixed with coarser carrier particles. Those carrier particles carrying the API particles on their surface generally have particle sizes in the range of 50 µm to 200 µm and are large enough to allow the adhesive mixture to flow well. Further they may act as diluents for highly active APIs.

1.2. Objectives

In carrier based dry powder inhaler formulations interparticle forces between carrier and API particles play an important role. On the one hand adhesion force must be high enough to ensure mixing homogeneity and stability of the mixture during powder handling, dosing and transport, but low enough to allow the detachment of the API particles from the carrier upon inhalation in order to allow the API particles to travel along the tiny airways into the deep lung and not to impact together with the coarse carrier particles in the upper airways. For this reason the control of interparticle forces is of vital importance for the quality of the dry powder inhalate. Furthermore the tailoring of interparticle forces may open-up the possibility to optimize the performance of the inhalate.
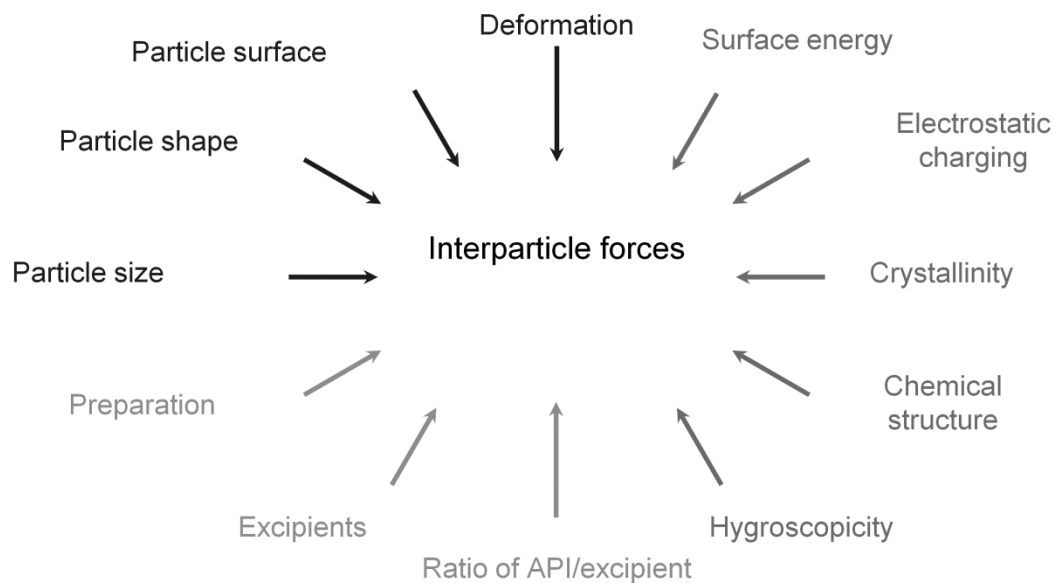
Figure 1. Factors influencing interparticle forces.

Interparticle forces are influenced by a multitude of factors such as factors that are related to physico-chemical properties (surface energy, electrostatic charging, crystallinity / amorphicity, chemical structure, hygroscopicity), geometric characteristics (size, shape, surface, deformation) and mixture properties (preparation methods, excipients, ratio of API/excipient) (Figure 1).

Due to the fact that interparticle forces are highly dependent on the contact area of carrier and API, surface roughness of the carrier might be an important parameter to optimize such formulation. This is also verified by multiple studies (see below). Figure 2 shows that depending on the scale of the surface roughness the contact area of carrier and API differs. If the distance between the surface roughness spacings is larger than the size of the API (Figure 2, left, macroscopic roughness) the contact area is high. The advantages of a high contact area are a good content uniformity and stability of the mixture. However increased adhesion and consequently decreased drug detachment have to be mentioned as drawbacks. In contrast nanoscopic roughness (Figure 2, right) reduces the contact area. This facilitates the detachment of the API particles from the carrier surface but results in poorer content uniformities and the risk of blend segregation.

The ideal carrier might have a surface roughness just in between macro- and nanoscopic ensuring sufficient mixing stability but concomitantly as much API detachment during inhalation as possible (Figure 2, middle).

Figure 2. Schematic of potential drug-carrier interactions for carriers of different surface roughness.

Almost all DPI formulations on the market are based on α-lactose monohydrate as a carrier [15]. For this reason many scientific papers are about the surface modification and optimization of lactose carrier particles for example by controlled dissolution of the surface [6, 5], carrier surface covering by magnesium stearate, sucrose stearate or lactose, surface modification by milling [24, 13] or the addition or removal of carrier fines [1, 6, 12, 2]. Despite the fact that α-lactose monohydrate has a well-investigated toxicology profile and its supply is assured at low price [20] there are also some disadvantages which might affect the inhaler performance. For example α-lactose monohydrate is not the excipient of choice for APIs with primary amino groups (e.g. budesonide, formoterol, peptides and proteins) due to incompatibility reactions (Maillard-reaction) which might occur. Another disadvantage is that the physico-chemical (e.g. amorphous content) and morphological properties might vary due to the production processes (milling [23], crystallization, sieving) and storage [20]. However the most important aspect with respect to this study is that α-lactose monohydrate becomes partially or fully amorphous upon spray drying [11, 9]. Mannitol in contrast which has been investigated as an alternative carrier for dry powder inhalers by Steckel and Bolzen [20], Saint-Lorant et al. [16], Kaialy et al. [10] and Tee et al. [21] is found crystalline after spray drying [14].

Spray drying is an ideal technique for the preparation of carrier particles because it allows the generation of spherical particles, provided that appropriate process parameters are adjusted. However also non-spherical particles might be obtained when modifying these conditions as will be shown in this study also. To the knowledge of the authors all marketed spray dried mannitol products in the size range of 50 μm to 200 μm are of non-spherical shape (e.g. Pearlitol SD (Roquette), Mannogem EZ (SPI Pharma); Figure 3).
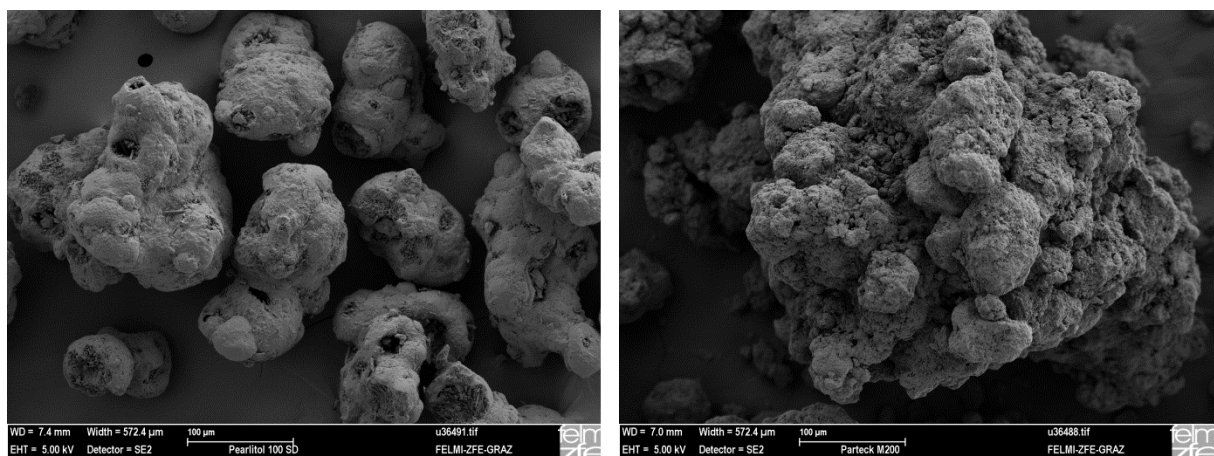
Figure 3. SEM of the commercially available Pearlitol 100 SD (Roquette, left) Mannogem EZ mannitol powder (SPI Pharma, right).

Spherical particles have the advantage of offering similar adhesion conditions to every API particle attached to the surface. This is in contrast to single crystals with different crystal faces that might vary in their affinity to the active due to different surface properties.

Further spray dried particles are usually considered as well-flowing. The reason for this is that on the one hand they often are narrowly particle size distributed (cyclone classifier effect) and on the other hand they are of spherical shape usually. Moreover it was shown by Maas [20] that spherical mannitol carrier particles of different surface roughness can be prepared by adjusting the spray drying outlet temperature.

For this reason the aim of this work is the preparation of tailored mannitol carrier particles with respect to interparticle forces to the API by surface modification via spray drying.

References

[1]   Handoko Adi, Ian Larson, Herbert Chiou, Paul Young, Daniela Traini, and Peter Stewart. Agglomerate strength and dispersion of salmeterol xinafoate from powder mixtures for inhalation. *Pharmaceutical research*, 23:2556–2565, 2006. ternary mixture.

[2]   B.H.J. Dickhoff, A.H. de Boer, D. Lambregts, and H.W. Frijlink. The effect of carrier surface treatment on drug particle detachment from crystalline carriers in adhesive mixtures for inhalation. *International Journal of Pharmaceutics*, 327(1-2):17 – 25, 2006. surface.

[3]   Dina El-Sabawi, Stephen Edge, and Robert Price. Continued investigation into the influence of loaded dose on the performance of dry powder inhalers: surface smoothing effects. *Drug development and industrial pharmacy*, 32:1135–1138, 2006.

[4]   Dina El-Sabawi, Robert Price, and Stephen Edge. Novel temperature controlled surface dissolution of excipient particles for carrier based dry powder inhaler formulation. *Drug development and industrial pharmacy*, 32:243–251, 2006. surface.

[5]   Henderik Willem Frijlink and Anne Haaije de Boer. *Pulmonary drug delivery - Basics, Application and Opportunities for Small Molecules and Biopharmaceutics- Chapter III Application Devices*. Editio Cantor Verlag für Medizin und Naturwissenschaften GmbH, 2007.

[6]   R. Guchardi, M. Frei, E. John, and J.S. Kaerger. Influence of fine lactose and magnesium stearate on low dose dry powder inhaler formulations. *International Journal of Pharmaceutics*, 348(1-2):10 – 17, 2008. surface.

[7] Anthony J. Hickey. Lung deposition and clearance of pharmaceutical aerosols: What can be learned from inhalation toxicology and industrial hygiene? *Aerosol Science and Technology*, 18(3):290–304, 1993.

[8] Kotaro Iida, Yukari Inagaki, Hiroaki Todo, Hirokazu Okamoto, Kazumi Danjo, and Hans Luenberger. Effects of surface processing of lactose carrier particles on dry powder inhalation properties of salbutamol sulfate. *Chem. pharm. bull.*, 52:938–942, 2004. surface.

[9] M. I. U. Islam, R. Sherrell, and T. A. G. Langrish. An investigation of the relationship between glass transition temperatures and the crystallinity of spray-dried powders. *Drying technology*, 28:361–368, 2010. lactose and amorphous.

[10] Waseem Kaialy, Mohammed N. Momin, Martyn D. Ticehurst, John Murphy, and Ali Nokhodchi. Engineered mannitol as an alternative carrier to enhance deep lung penetration of salbutamol sulphate from dry powder inhaler. *Colloids and Surfaces B: Biointerfaces*, In Press, Corrected Proof:–, 2010. Mannitol, DPI.

[11] Yoshiaki Kawashima, Takanori Serigano, Tomoaki Hino, Hiromitsu Yamamoto, and Hirofumi Takeuchi. Effect of surface morphology of carrier lactose on dry powder inhalation property of pranlukast hydrate. *International Journal of Pharmaceutics*, 172(1-2):179 – 188, 1998.

[12] Margaret D. Louey, Sultana Razia, and Peter J. Stewart. Influence of physico-chemical carrier properties on the in vitro aerosol deposition from interactive mixtures. *International Journal of Pharmaceutics*, 252(1-2):87 – 98, 2003. surface.

[13] Stephan Gerhard Maas. *Optimierung trägerbasierter Pulverinhalate durch Modifikation der Trägeroberfläche mittels Sprühtrocknung*. PhD thesis, Heinrich-Heine-Universität Düsseldorf, 2009.

[14] Venkatesh Naini, Peter R. Byron, and Elaine M. Phillips. Physicochemical stability of crystalline sugars and their spray-dried forms: Dependence upon relative humidity and suitability for use in powder inhalers. *Drug Development and Industrial Pharmacy*, 24(10):895–909, 1998.

[15] Gabrielle Pilcer and Karim Amighi. Formulation strategy and use of excipients in pulmonary drug delivery. *International Journal of Pharmaceutics*, 392(1-2):1 – 19, 2010. review.

[16] G. Saint-Lorant, P. Leterme, A. Gayot, and M.P. Flament. Influence of carrier on the performance of dry powder inhalers. *International Journal of Pharmaceutics*, 334(1-2):85 – 91, 2007. Mannitol.

[17] Mark Sanders. Inhalation therapy: an historical review. *Primary Care Respiratory Journal*, 16:71–81, 2007.

[18] Gerhard Scheuch, William C. Zimerlich, and Ruediger Siekmeier. *Pulmonary drug delivery - Basics, Application and Opportunities for Small Molecules and Biopharmaceutics- Chapter I Biophysical Parameters Determing Pulmonary Drug Delivery*. Editio Cantor Verlag für Medizin und Naturwissenschaften GmbH, 2007.

[19] H. Steckel, P. Markefka, H. teWierik, and R. Kammelar. Effect of milling and sieving on functionality of dry powder inhalation products. *International Journal of Pharmaceutics*, 309(1-2):51 – 59, 2006.

[20] Hartwig Steckel and Nina Bolzen. Alternative sugars as potential carriers for dry powder inhalations. *international journal of pharmaceutics*, 270:297–306, 2004.

[21] S. K. Tee, C. Marriott, X. M. Zeng, and G. P. Martin. The use of different sugars as fine and coarse carriers for aerosolised salbutamol sulphate. *international journal of pharmaceutics*, 208:111–123, 2000.

[22] Claudius Weiler, Marc Egen, Michael Trunk, and Peter Langguth. Force control and powder dispersibility of spray dried particles for inhalation. *Journal of pharamceutical sciences*, 2009.

[23] Paul M. Young, Herbert Chiou, Terrance Tee, Daniela Traini, Hak-Kim Chan, Frank Thielmann, and Dan Burnett. The use of organic vapor sorption to determine low levels of amorphous content in processed pharmaceutical powders. *Drug Development and Industrial Pharmacy*, 33(1):91–97, 2007.

2. Results and discussion

The results of this thesis are presented in form of publications (see chapter Research papers, page 14) and are briefly summarized and discussed in this chapter.

2.1. Spray drying at lab scale

In order to prepare spherical mannitol particles intended to be used as carrier in dry powder inhaler formuations spray drying experiments were carried out on a lab scale spray dryer (Figure 4) equipped with a rotary atomizer (*The impact of spray drying outlet temperature on the particle morphology of mannitol, page 14*). Products were spray dried at three different outlet temperatures. Depending on the outlet temperature adjusted particles of different surface topography were obtained. At low temperatures spherical particles with a smooth surface were formed whereas higher temperatures led to round particles with a rough surface. All products were crystalline after spray drying. This work shows that spray drying mannitol at different outlet temperatures offers the opportunity to adjust surface roughness. This surface modification opens up the possibility to tailor interparticle interactions between the carrier and the API in DPI formulations. However the spray dried products prepared on the lab scale spray dryer had a mean particle size of approximately 13 µm. Particles of this size are too small to be used as carrier in dry powder inhaler formulations. As larger droplets, which will after solidification form larger particles, require longer drying times and consequently a larger spray dryer than smaller ones scale-up experiments were carried out using a pilot scale spray dryer.
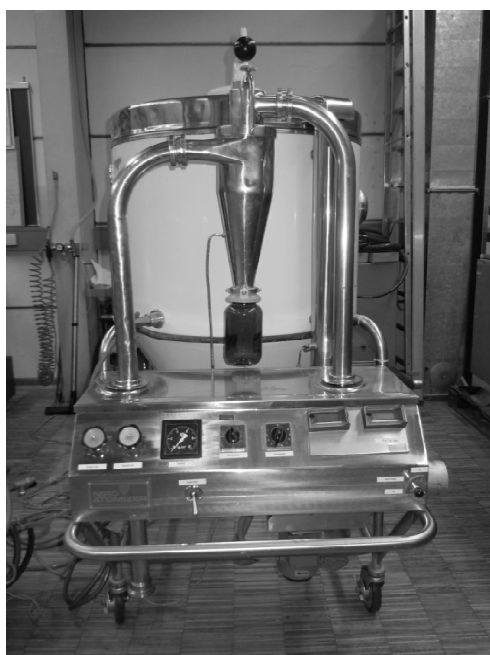

Figure 4. Image of the lab scale spray dryer (Niro MOBILE MINOR™).

2.2. Spray drying at pilot scale

The generation of mannitol carrier particles, sufficiently large to be used as carrier in DPI formulations was carried out on a pilot scale spray dryer (Figure 5) equipped with a rotary atomizer.

Figure 5. Images of the pilot scale spray dryer (proprietary construction, group Prof. Walzel, Dortmund University of Technology

A full-factorial statistical design was employed to study the influence of the factors considered to be important namely feed concentration, gas heater temperature, feed rate and atomizer rotation speed on particle size and morphology. Additionally the impact of process parameters on breaking strength and crystallinity was investigated. By using the larger spray dryer particles of the appropriate size could be prepared (*Spray drying of mannitol as a drug carrier – The impact of process parameters on product properties,* page 24). The spray dried products had mean particles sizes of 71.4 μm to 90.0 μm. Surface roughness was significantly impacted by gas heater temperature, feed rate and feed concentration. By correlating the outlet temperature and the obtained particle surface roughness it could be shown that also at pilot scale outlet temperature is a major factor governing the particle surface topography. Particles prepared at high feed rates and/or low gas heater temperatures, both leading to low outlet temperatures, had a rough surface whereas lower feed rates and/or higher gas heater temperatures, causing higher outlet temperatures, resulted in the formation of particles with a comparably smoother surface.

Spray drying at several outlet temperature supported these findings but also showed that powders spray dried at lower temperatures are prone to break upon mechanical stress of powder handling and processing procedures (*Tailoring particle morphology of spray dried manntiol carrier particles by variation of the outlet temperature, page 37*).

As the performance of carrier based dry powder inhaler formulations is highly sensitive to morphological changes and in order to get a better understanding of the dependence of carrier stability on outlet temperature particle morphology as well as several single particle and powder bulk properties of mannitol carriers which had been prepared at different outlet temperatures were thoroughly investigated (*The morphology and various densities of spray dried mannitol, page 43*). In contrast to the products prepared at lab scale at pilot scale besides surface roughness also particle shape changed. With increasing temperature the shape changes from spherical to raisin-like. The indentations of the particle, which give the particles the raisin-like appearance, reduce the hollow space volume. This reduced hollow space volume increases the mechanical stability and leads to higher effective particle densities. The particles prepared at different outlet temperatures consist of a shell and a porous inside.

Studies on the performance of adhesive mixtures containing the API salbutamol sulphate and mannitol carriers of tailored surface roughness in DPI formulations showed that surface roughness as well as particle shape influenced the detachment of the API from the carrier (*Spray dried mannitol carrier particles with tailored surface properties - The influence of carrier surface roughness and shape, page 59*). The highest fine particle fraction was achieved with carriers of spherical shape and rough surface. Smoother surfaces and surface cavities reduced the fine particle fraction released from the carrier. SEM images of the carrier particles after mixing and after delivery via the inhaler show that all of the products, also those prepared at low outlet temperatures, have sufficient stability to be used as a carrier in DPIs.

In contrast to the lab scale experiments, where a conventional rotary atomizer was used, the pilot spray dryer was equipped with a laminary operated rotary atomizer (LAMROT). The characteristic of this type of atomizer is the generation of narrowly distributed droplets and consequently particle sizes (*Homogene Produkteigenscahften in der Sprühtrocknung durch laminare Rotationszerstäubung, page 73*). By the use of this type of atomizer the span values, which characterize the width of the distribution, were much lower (< 1) than at lab scale (1.43 – 1.78).

2.3. Differences at lab and pilot scale

As mentioned above at pilot scale rough surfaces were observed at low and smoother surfaces at higher outlet temperatures. These results are in contrast to those at lab scale where smooth surfaces were observed at low outlet temperatures and rough surfaces at higher ones. Additionally at pilot scale besides surface roughness also particle shape changed. Higher temperatures led to particles with multiple surface indentations. Depending on the scale of the used spray dryer particle morphology differed (Figure 6).
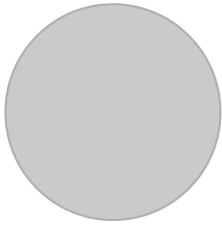
Droplet		Particle					
Size / μm		Size / μm	T1	<	T2	<	T3
27		13					
137		80					

Figure 6. Scheme of the morphologies obtained at lab and pilot scale.

It was found out that depending on the scale of the used spray dryer, more precisely depending on the droplet size two different crystallization regimes of aqueous mannitol solutions were observed (*The morphology of spray dried mannitol particles - The vital importance of droplet size, page 80*). Either there was crystallization from a solution or delayed crystallization from a highly supersaturated and viscous melt. For small droplets which are generated at lab scale at low temperatures crystallization from a solution results in particles with a smooth surface that is composed of numerous small crystals at the surface. At higher temperatures crystallization takes place from a highly viscous liquid where crystals grow larger giving the surface a rougher appearance. For small droplets and high temperatures the increase in concentration is so fast that there is no time for nucleation from a diluted solution allowing the formation of a highly viscous liquid. When drying larger droplets at pilot scale no viscous liquid is formed because of a slower drying and a lower particle temperature. For that reason for all temperatures studied at pilot scale crystallization from a solution takes place. Here low temperatures, hence slow crystallization, results in the formation of larger crystals that form the particle surface, whereas higher temperatures lead to higher nucleation rates and consequently smaller crystals at the surface giving the particles a smoother appearance.

2.4.   Outlook- API morphology and size optimization

As beside optimizing carrier surface roughness (spacing distance) the use of API particles of appropriate size might be a useful approach to optimize the performance of carrier-based inhalates and in order to further study the complex interplay of carrier surface roughness and API size in dry powder inhaler formulations (Figure 7), an attempt was made to prepare salbutamol sulfate particles in different sizes in the range of 1 μm to 5 μm as a first preliminary step (Spray drying of aqueous salbutamol sulfate solutions using the Nano Spray Dryer B-90 - The impact of process parameters on particle size, page 106).
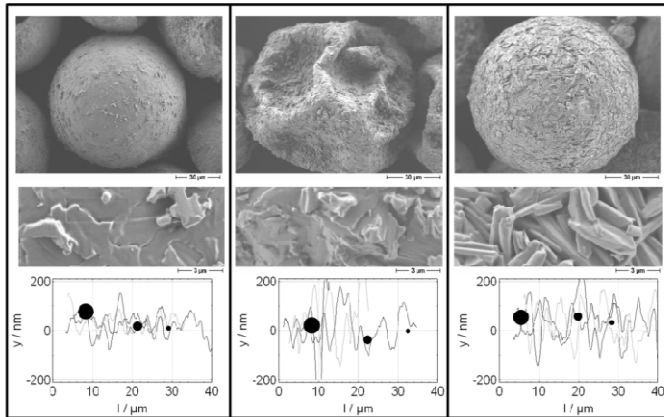
Figure 7. SEM micrographs of mannitol samples spray dried at different outlet temperatures (upper and middle line) and schema of the influence of API size in relation to the spacing distance of the surface roughness peaks of mannitol samples spray dried at different outlet temperatures (lower line).

Usually the preparation of particles in the low micrometer range involves micronization. The disadvantage of this procedure is the need of high energy input and the high variability of the morphology of the obtained single particles (Figure 8) leading to unpredictable dry powder inhaler (DPI) performance. For that reason narrowly size distributed, isometric, preferably spherical particles would be desirable.
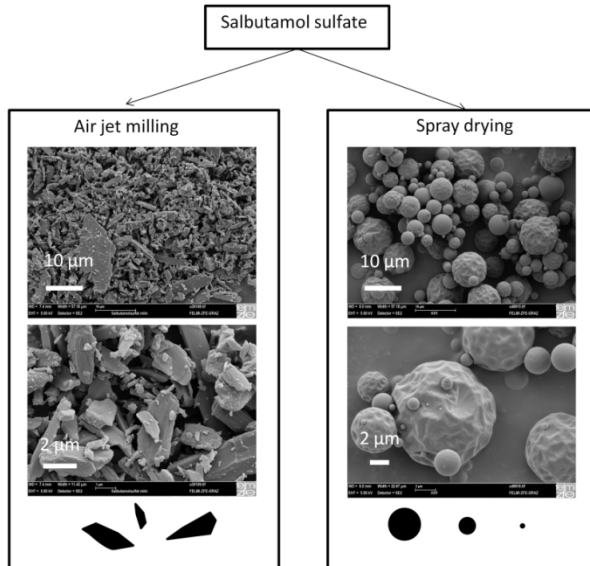
Figure 8. Morphology of API particles prpared by air jet milling (left) and spray drying (right).

By using the recently launched Nano Spray Dryer B-90 it was shown that spray drying of aqueous salbutamol sulfate solutions, as a model API, results in the formation of spherical particles. A 33 full factorial design was used to investigate the influence of process parameters (mesh size, feed concentration and drying air temperature) on particle size. The median particle size was significantly

influenced by all three factors of the statistical design. Within the design space studied particle sizes of 1.01 µm to 6.39 µm were obtained.

2.5. Conclusion

This study demonstrates that spray drying mannitol is an appropriate technique for the preparation of alternative carriers. It was shown that surface roughness can be tailored by adjusting appropriate process parameters, particularly the appropriate outlet temperature. In order to get particles of adequate size to be used as carrier in DPI formulations experiments were not only carried out on a lab ($X_{50.3} \approx$ 13 µm) but also on a pilot scale spray dryer ($X_{50.3} \approx$ 80 µm). Interestingly the increase in particle size when using the pilot scale spray dryer led to a change of the dependence of surface roughness on outlet temperature. At lab scale rough particles were obtained at high temperatures whereas at pilot scale rough particles were observed at low temperatures. The reasons leading to a different surface roughness depending on the outlet temperature adjusted and the scale of the spray dryer could be explained by extensively studying the underlying crystallization and particle formation mechanisms.

Not only roughness and shape but also the inner structure, which determines the mechanical stability of the particles and their aerodynamic characteristics, could be analyzed by using appropriate and highly sophisticated techniques.

Most importantly this work shows that surface roughness as well as particle shape influences the detachment of the active particles from the carrier. The highest fine particle fraction was achieved with carrier particles of spherical shape and a rough surface. Smoother surfaces and surface cavities reduced the amount of fine particles released from the carrier. These results highlight the importance of tailoring carrier morphology with respect to the performance of the dry powder inhalate and emphasize the potential of spray dried mannitol.

All these results will contribute to a platform knowledge by which, dependant on the API used, interparticle forces between API and spray dried mannitol can be adjusted by using carriers with tailored surface roughness and shape. This will finally lead, irrespective of the chemical identity and size of the API, to a product with optimized performance. The establishment of a platform like this, especially by using a single process step, has not been shown before for lactose and certainly not for mannitol.

3. Research papers

3.1. Spray drying at lab scale

3.1.1. The impact of spray drying outlet temperature on the particle morphology of mannitol

Stephan Gerhard Maas, Gerhard Schaldach, Eva Maria Littringer, Axel Mescher, Ulrich Griesser, Doris Braun, Peter Walzel , Nora Anne Urbanetz

The impact of spray drying outlet temperature on the particle morphology of mannitol

Stephan G. Maas [a], Gerhard Schaldach [b], Eva M. Littringer [c], Axel Mescher [b], Ulrich J. Griesser [d], Doris E. Braun [d], Peter E. Walzel [b], Nora A. Urbanetz [c,*]

[a] Institute of Pharmaceutics and Biopharmaceutics, Heinrich-Heine-University, Universitaetsstrasse 1, 40225 Duesseldorf, Germany
[b] Department of Biochemical and Chemical Engineering, Technische Universitaet Dortmund, Emil-Figge-Strasse 68, 44227 Dortmund, Germany
[c] Research Center Pharmaceutical Engineering GmbH, Inffeldgasse 21A, 8010 Graz, Austria
[d] University of Innsbruck, Institute of Pharmacy, Pharmaceutical Technology, Josef-Moeller-Haus, Innrain 52c, A-6020 Innsbruck, Austria

ARTICLE INFO

ABSTRACT

The motivation for this study was to find an adequate substitute for lactose as carrier in dry powder inhalers and to overcome some drawbacks inherent to lactose. Mannitol appears to be the ideal replacement of lactose because it lacks the risk of transmitting the transmissible spongiform encephalopathy, mannitol does not carry reducing groups, that may cause chemical interactions with drugs such as proteins, and is highly crystalline even upon spray drying. Spray drying in turn is a dedicated technology to prepare carrier particles for dry powder inhalers. Typically spherical particles are generated constituting comparable interparticle forces to every drug particle attached to their surface. This study shows, that mannitol particles of different surface roughness can be prepared by spray drying at different outlet temperatures, providing the opportunity of tailoring the contact area respectively the interparticle interactions between the drug and the carrier. The emergence of different surface roughness was attributed to different crystallization mechanisms. Surface roughness was quantified by confocal laser-scanning microscopy. Quantitative Raman spectroscopy revealed, that the spray dried products consist mainly of the thermodynamically stable modification I° besides small amounts (5 to 15%) of the metastable modification II, irrespective of the drying temperature and the crystallization mechanisms taking place. This renders mannitol a most suitable substitute of lactose for the use in dry powder inhalers.

© 2011 Elsevier B.V. All rights reserved.

1. Introduction

This study was carried out in order to provide a substitute for α-lactose monohydrate used as carrier in dry powder inhalates. As the active of dry powder inhalates need to exhibit aerodynamic diameters between 1 μm and 5 μm, the powder is very cohesive, poorly flowable and dosable. In order to improve flowability and dosing, the drug particles are attached to coarse carrier particles, which are large enough to ensure reproducible dosing. Upon inhalation, in turn, the active has to detach from the carrier again in order to travel along the narrow airways into the deep part of the lungs. By substituting α-lactose monohydrate several drawbacks inherent to α-lactose monohydrate like its bovine origin making it likely to transmit the Transmissible Spongiform Encephalopathy (TSE) can be avoided. In addition, α-lactose monohydrate carries a reducing group rendering it incompatible with drug substances containing amino groups like peptides and proteins. Finally, α-lactose monohydrate tends to

become partially or fully amorphous upon mechanical treatment like milling or spray drying (Briggner et al. [1]; Gombas et al. [2]; Lehto et al. [3]), which makes the substance unsuitable for this particle generation process due to the risk of instability during storage (Buckton et al. [4]; Price and Young [5]).

Spray drying in turn is a dedicated technology to prepare carrier particles for dry powder inhalers (DPIs) as typically spherical particles are generated (Vehring [6]), that, due to homogeneous surface properties, offer similar adhesion conditions to every particle of the attached active. This is in contrast to crystals with different crystal faces varying broadly in their affinity to the active, possibly causing inadequate detachment from crystal sites of high affinity upon inhalation.

Moreover, spray drying offers the opportunity of altering the particle morphology depending on the spray drying conditions. The influence of surface topography on interparticle interactions between the active and the carrier is discussed in literature extensively -even though adhesive forces also depend on other factors like particle size (Danjo et al. [7]; Mullins et al. [8]) and shape, chemical identity (Podczeck et al. [9]) as well as hygroscopic and crystalline properties (Iqbal and Fitzpatrick [10]; Pilpel [11]; Teunou and Fitzpatrick [12];

Tomas and Schubert [13]) of the interacting partners. Consequently spray drying may also offer the opportunity of tailoring the adhesion force between active and carrier by carrier surface modification. Adhesion forces have to be strong enough in order to ensure proper adhesion of the active substance to the carrier during manufacturing and dosing, but weak enough in order to allow drug detachment from the carrier upon inhalation.

Due to the fact, that the majority of commercially available powder inhalers use α-lactose monohydrate as carrier and that α-lactose monohydrate is approved for pulmonary applications, the existing literature mainly deals with modifications of the surface of α-lactose monohydrate. The surface modification of the carrier by dispersion and subsequent removal of the dispersion agent is described by Dickhoff et al. [14], El-Sabawi et al. [15,16], Islam et al. [17–19], Iida et al. [20,21] and Zeng et al. [22] for example. Furthermore Iida et al. [23] and Chan et al. [24] report about changing the surface topography by coating it with solutions or suspensions of different substances. A modification of the surface topography by adding fine particle (micronized) carrier material or a third fine particle component is documented by Guchardi et al. [25], Adi et al. [26,27], Iida et al. [28–30], Louey et al. [31,32], Tee et al. [33] and Podczeck [34]. The modification of the surface topography by applying mechanical stress in mills or mixers with and without adding dispersion agents was analyzed by Steckel et al. [35], Ferrari et al. [36], Iida et al. [28] and Young et al. [37]. Finally Larhrib et al. [38] and Zeng et al. [39–42] were successful in modifying the surface topography by crystallization under different conditions.

However, mannitol seems to be ideally suited to substitute α-lactose monohydrate as carrier in DPIs, because it does not contain and is not made of animal material, does not carry reducing groups, is highly crystalline even upon spray drying (Naini et al., 1998 [43]) and is approved for pulmonary delivery. Even though mannitol is considered as alternative for α-lactose monohydrate in literature (Adi et al. [26], Harjunen et al. [44], Kaialy et al. [45,46], Saint-Lorant et al. [47], Steckel et al. [48], Tee et al. [33]), there is no systematic study analyzing the surface topography of spray dried mannitol in dependence on the spray drying parameters, although the surface topography is of high importance for the strength of the particle interaction between active substance and carrier. Furthermore the possibility of specifically modifying the surface topography of mannitol is not discussed in literature. Solely the generation of different particle sizes in dependence on the spray drying parameters is described by Chew et al. [49] and Elversson et al. [50].

The present study is dedicated to the investigation of the influence of spray drying conditions on particle morphology using a rotary atomizer, especially on the surface roughness of spray dried mannitol, to its crystal structure as it exists in different polymorphic forms and to the elucidation of the particle forming mechanism.

2. Materials and methods

2.1. Materials

Mannitol (Pearlitol SD 200) was kindly provided by Roquette, F-Lestrem.

2.2. Spray drying of mannitol

Aqueous mannitol solutions were fed into a spray dryer (Niro Atomizer, Niro, DK-Copenhagen) with a feeding rate of 14 ml/min by a flexible-tube pump and atomized to small droplets by a rotary atomizer with a rotational speed of 27 500 rpm (4.9 bar air pressure at turbine). The diameter of the atomizing wheel was 50 mm. It contained 24 channels, which were 6 mm in height and 3 mm in width. Outlet air temperature and mannitol concentration were varied. The obtained products were stored in desiccators containing

silica gel until further required. Batches of samples spray dried at the outlet temperatures of 60 °C, 90 °C and 120 °C using a 15% aqueous mannitol solution were prepared in triplicate, all other formulations were prepared just once. The abbreviations M60, M90 and M120 are used in this manuscript for spray dried products obtained at these three outlet temperatures.

2.3. Particle characterization

2.3.1. Scanning electron microscopy (SEM)

The spray dried mannitol powder samples were examined using a Hitachi H-S4500 FEG scanning electron microscope (Hitachi High-Technologies Europe, DE-Krefeld) operating under vacuum (ca. 10^{-7} mbar) at 1 kV and 10 μA. For the study of particle cross sections samples were embedded in epoxy resin and cut using a microtome (Jung Rm2055, Leica, DE-Wetzlar).

2.3.2. Confocal laser-scanning microscopy

Surface roughness was quantified using confocal laser-scanning microscopy (LEXT OLS3100, Olympus, DE-Hamburg). Samples were positioned using a movable sample holder (OLS30-CS150AS, Olympus, DE-Hamburg). The laser was run at 408 nm and ca. 900 μW. The lateral resolution was 120 nm, the minimum roughness detectable was 10 nm. Samples were scanned at 1024×768 points. Intensities of less than 147 counts were eliminated and set to zero. Fourier transformation was used to distinguish between smaller scale roughnesses and larger scale roughnesses also affecting particle shape. The SRa value was calculated using the software LEXT OLS, Olympus, JP-Tokio). The SRa value represents the mean of the absolute value of the deviations of each single height value from the average height value of the area scanned.

2.3.3. Hot stage microscopy

The investigation of the drying process was carried out using an Olympus BH2 polarization microscope (Olympus Optical, AT-Vienna) equipped with a Kofler hot stage (Reichert Thermovar, AT-Vienna). A small droplet of a 15% aqueous mannitol solution was prepared on a glass slide (no cover slip), which was placed on the preheated (60 °C or 120 °C) hot stage. The drying and crystallization process was watched instantly and while slowly cooling down the stage. Photomicrographs were acquired using the Olympus BH2 polarization microscope (Olympus Optical, AT-Vienna) and a stereomicroscope (Olympus SZX-12, Olympus Optical, AT-Vienna) equipped with a ColorViewIII CCD camera using the software Cell-D (Olympus Optical, AT-Vienna).

2.3.4. Laser diffraction

Laser light diffraction (Helos/KF-Magic, Sympatec, DE-Clausthal-Zellerfeld) including a dry dispersing system (Rodos, Sympatec, DE-Clausthal-Zellerfeld) was used to determine particle size distributions. The powder was fed to the diperser via a vibrating chute (Vibri, Sympatec, DE-Clausthal-Zellerfeld.). The measurements were carried out at the dispersing pressure of 2.1 bar and the negative pressure of 71 mbar. Evaluation of the data was performed using the software Window 4 (Sympatec, DE-Clausthal-Zellerfeld).

2.3.5. Differential Scanning Calorimetry (DSC)

Thermal Analysis was performed with a Differential Scanning Calorimeter DSC 821e (Mettler-Toledo, DE-Gießen). Sample amounts of about 3 mg were recorded at a heating rate of 10 K/min under nitrogen atmosphere. The nitrogen flow was adjusted at 50 mL/min. An aluminium pan with a pierced lid was used. Experiments were performed in duplicate.

2.3.6. FT-Raman spectroscopy

FT-Raman spectra were recorded with a Bruker RFS 100 FTRaman spectrometer, equipped with a diode pumped Nd:YAG laser (1064 nm),

and a liquid nitrogen cooled, high sensitivity Ge detector (Bruker Optik GmbH, DE-Ettlingen). A few milligrams of the samples were packed into aluminum sample cups. For each spectrum 128 scans were recorded at a resolution of 4 cm^{-1} in the range between 30 cm^{-1} and 4000 cm^{-1}. A Blackman-Harris B4 term was used as apodization function. Evaluation of the data was performed according to Braun et al. [51].

3. Results and discussion

3.1. Investigations on particle morphology by Scanning Electron Microscopy (SEM)

Scanning electron micrographs of spray dried mannitol display spherical particles with a smooth surface (Fig. 1a and d) when spray drying is performed at an outlet temperature of 60 °C (M60). A smooth surface (Fig. 1b and e) is also obtained when an outlet temperature of 90 °C is used (M90). In contrast, at the outlet temperature of 120 °C, spherical particles (M120) showing a rough surface is obtained, due to the formation of larger mannitol crystals (Fig. 1c and f).

This result is somewhat surprising because high temperatures are expected to cause rapid drying of the droplets, which usually favors the formation of small crystals, whereas the opposite is expected to be true for low drying temperatures. In order to obtain an insight into the mechanisms causing the differences of surface roughness depending on the outlet temperature, hot stage microscopy studies were performed, which will be discussed in Section 3.3.

Another difference of the particles obtained by spray drying at different temperatures is the presence or absence of a hole in the particle shell. The outlet temperature of 90 °C generally results in hollow particles with a well visible orifice in their shell. This is also true for most of the M120 particles. However, the M60 particles do not show a hole but mostly a single indentation at their surface (Fig. 1a). The presence of the hole in the particle shell of M90 and M120 particles is caused by the evaporating liquid that escapes from the inner of the droplet through the solid crust already built in the course of the drying process on the surface of the droplet. The indentation of
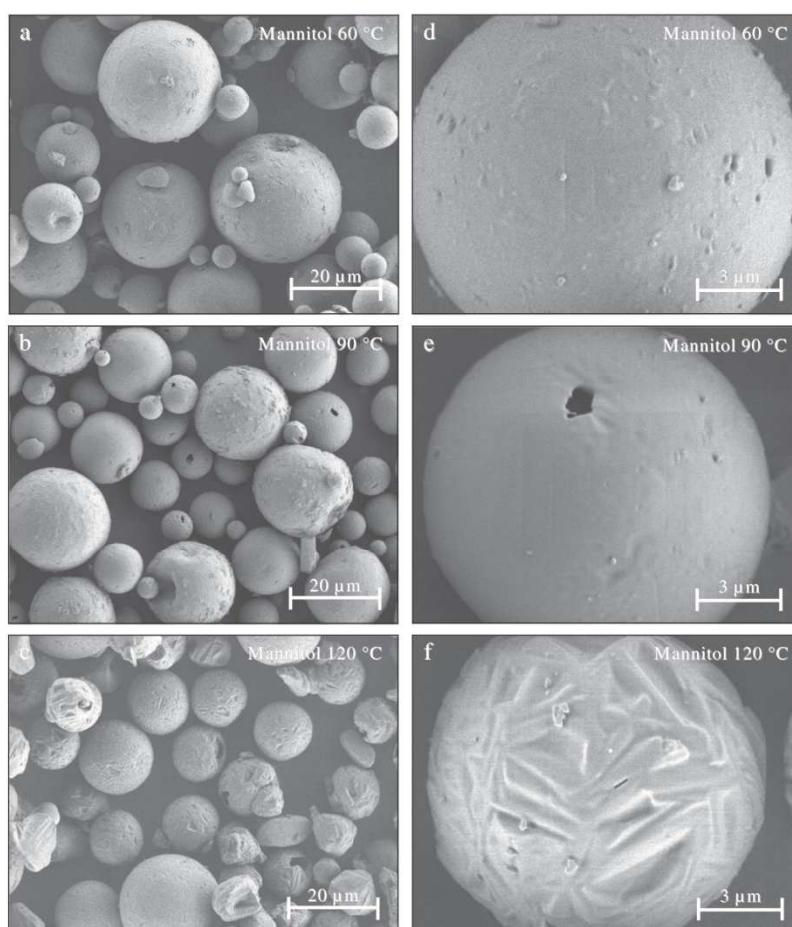

Fig. 1. Scanning electron micrographs of mannitol samples spray dried at 60 °C (Mannitol 60 °C, a and d), 90 °C (Mannitol 90 °C, b and e) and 120 °C (Mannitol 120 °C, c and f) outlet temperature.

the M60 particles in contrast, indicates that even though also here a crust is formed, the majority of the solvent now may escape through the crust by diffusion. This is possible, because the pressure exerted by the evaporating liquid is lower at 60 °C than at 90 °C and 120 °C, giving the vapour enough time to escape without rupturing the crust. At the end of the drying process capillary forces and underpressure within the void space lead to deformations in the shell and form the observed indentations of the M60 particles. In separate trials we observed crystal growth and transformation processes in hot stage microscopy experiments (Section 3.3) at the final stage of the drying process of droplets of mannitol solutions at 60 °C.

In order to confirm that lower spray drying temperatures result in hollow spheres, samples were embedded in an epoxy resin and cut. The obtained cross sections were examined using a scanning electron microscope. Results are discussed in Section 3.4.

Interestingly, the morphology of large particles spray dried at higher temperature is similar to that of small particles spray dried at lower temperature. For example, large particles spray dried at 90 °C outlet temperature do not show a hole in their shell as most of the particles spray dried at 90 °C outlet temperature do, but an indentation like those particles spray dried at the outlet temperature of 60 °C (Fig. 1). This means that larger droplets spray dried at higher temperatures show similar drying behaviour and consequently result in similar morphology as smaller droplets spray dried at lower temperature and vice versa.

3.2. Investigation and quantification of surface roughness by confocal laser-scanning microscopy

The surface roughness of the M60 and M120 particles was investigated with a confocal laser-scanning microscope. This method is commonly applied for evaluating the roughness of flat material surfaces and we were curious whether the method can be applied for the challenging and thus rarely applied analysis of small spherical particles. The micrographs in Fig. 2 show a circle of high peaks (artefacts) indicating the limits where the angle of the curved particle surface exceeds the recordable surface angle of the scanning method. The area within this circle (slightly smaller than the diameter of the particles) shows the roughness of the particle surface. M60 particles exhibit only some minor peaks in this area (Fig. 2a) confirming the smoothness of the surface, whereas M120 particles show a much rougher surface (Fig. 2b).

The surface roughness was quantified by the SRa value and was determined for three batches of M60 and M120 respectively. Three particles of each batch were scanned and the mean of these values was calculated. In Fig. 3 the mean SRa value and the standard deviation of these three means per batch are depicted. The mean SRa

value of the M120 particles is significantly higher than that of the M60 particles which is expected from the SEM images. Additionally, the experiment indicates that the technical developments in laser-scanning microscopy provide a simple quantitative technique to evaluate the surface roughness of small, spherical particles, which is a critical parameter in particle technology.

3.3. Visualization of the drying process on a hot stage

To gain insight into the formation mechanisms of the spray dried particles at different outlet temperatures simple hot stage microscopy experiments were performed. Droplets of an aqueous mannitol solution on a glass slide were placed on a hot stage that was preheated to 60 °C or 120 °C and the changes upon drying were observed using a polarized light microscope.

At 60 °C recrystallization starts after a few seconds and results in mostly small acicular crystals that grow in radial manner from several emerging nucleation centers (Fig. 4a, b). The nucleation occurs clearly at the surface of the droplets, which is quickly covered by the growing crystals, whereas the core of the droplets shows the presence of liquid. From the optical appearance we can derive that two polymorphic forms are formed in these experiments. Fine acicular crystals with low birefringence characterize mod. II (or α-form), whereas larger, prismatic crystals with higher birefringence indicate the presence of the stable mod. I (β-form). This was confirmed by the observation of a subsequent transformation process and PXRD experiments. During the drying process of the droplets, the growth of mod. I in the remaining liquid can be observed, and it can also be noticed that in the presence of residual water mod. II is transformed to some extent into the more stable mod. I°.

Droplets placed on the hot stage at 120 °C shrink quickly due to the fast evaporation of water but most of them remain liquid and do not recrystallize, indicating that the nucleation rate is low at this temperature (Fig. 4b). The highly supersaturated solution recrystallizes instantly in the presence of seed crystals or when the temperature is lowered by 10 °C to 20 °C. Though the crystal growth is fast, significantly larger crystals occur than at 60 °C. Domains of high and low birefringence indicate that both orthorhombic forms (mods. I and II) crystallize, but an ambiguous distinction by optical methods is difficult because of the similar morphologies of these two polymorphs.

These hot stage microscopy experiments show clearly that the differences in surface topography of the spray dried particles are based on diverse crystallization processes. At low temperatures (around 60 °C) fine needles crystallize from the supersaturated solution resulting in hollow spheres with smooth surfaces. In contrast, at high temperatures (around 120 °C) the mannitol solution dries
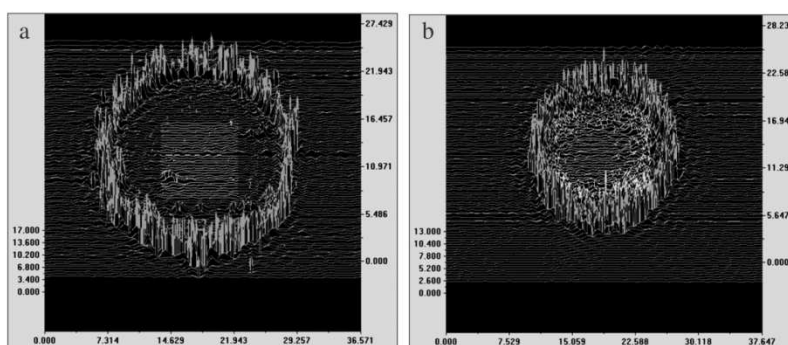

Fig. 2. Confocal laser micrographs of mannitol samples spray dried at 60 °C (a) and 120 °C (b) outlet temperature, x- and y-axis in μm.
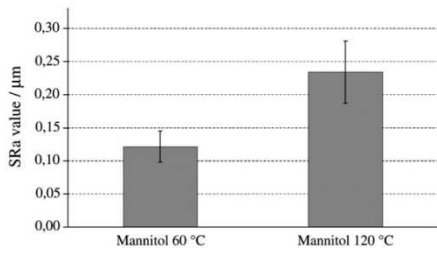
Fig. 3. SRa values obtained by confocal laser microscopy of mannitol samples spray dried at 60 °C and 120 °C outlet temperature, (n = 3 per batch, three batches, mean ± s.d.).

quickly to a highly supersaturated, viscous liquid since the solvent evaporation rate is high and the nucleation rate of crystalline mannitol is low at this temperature. This metastable supersaturated liquid crystallizes to coarse crystals resulting in particles or spheres with rough surfaces. The crystallization is triggered most likely by a secondary nucleation process (contact with other, already crystalline particles in the spray dryer which act as seeds).

3.4. Investigation of particle cross sections by Scanning Electron Microscopy (SEM)

Scanning electron micrographs of the M90 and M120 particles show a hole in the shell of most of these particles, whereas micrographs of the M60 particles mostly do not. In order to visualize the interior of the M60 and M120 particles, samples of M60 and M120 were embedded in epoxy resin and cut. The obtained cross sections were investigated by scanning electron microscopy. As shown by the SEM micrographs (Fig. 5), both particle species are hollow inside. The void of the M120 particles is filled with epoxy resin, which entered the particle via the orifice in the particle shell, whereas the M60 particles

do not contain epoxy resin because the particle shell is completely closed.

3.5. Estimation of droplet size

Due to the low volumetric flow rate a pulsifying spray generation was observed and no reliable information on droplet sizes could be gained by laser diffraction analysis. Instead, in order to estimate the droplet size of the atomizing spray and afterwards to relate it to the particle size of the final product a balance of forces for water at room temperature was calculated first. High circumferential speed (27500 rpm) and low volumetric flow rate (14 ml/min) leads to droplet formation by dripping (equation 1). In this droplet formation regime the droplet size is only influenced by the forces caused by the centrifugal acceleration ($R\omega^2$) and the capillary force caused by surface tension (σ). Low deformation velocities allow for neglecting viscous effects on the droplet formation (Walzel [52]). Estimates of the drop sizes are difficult as the distribution of the liquid onto the vanes is not well defined. However, the drop size can be expected close to the capillary length $Lc = (\sigma/\rho a)^{1/2}$ (Walzel [52]). ρ is the density of the liquid and $a = R\omega^2$ is the centrifugal acceleration, R the radius of the atomizer and ω the angular speed of the wheel. The nondimensional droplet size is defined as $d^* = d/Lc$ and the expected non-dimensional drop size typically lies in the range

$$1.5 < d^* < 2.8 \tag{1}$$

the smaller values corresponding to low flow rates as in the given case. The drop size then is obtained from:

$$d^* = d_{50.3} \cdot \left(\frac{\rho \cdot a}{\sigma}\right)^{0.5} \tag{2}$$

When atomizing the mannitol solution (surface tension: 70.0 mN/m, density: 1050 kg/m^3) at 27500 rpm with a flow rate of 14 ml/min according to equation 1 and 2 droplets formed have an average diameter
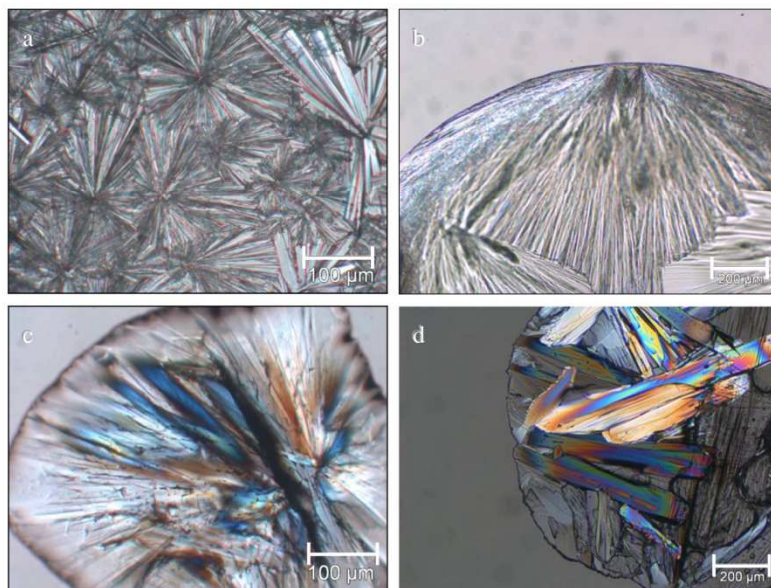

Fig. 4. Microscopic images of droplets of aqueous mannitol solutions heated and dried at 60 °C (a, b) and 120 °C (c, d).
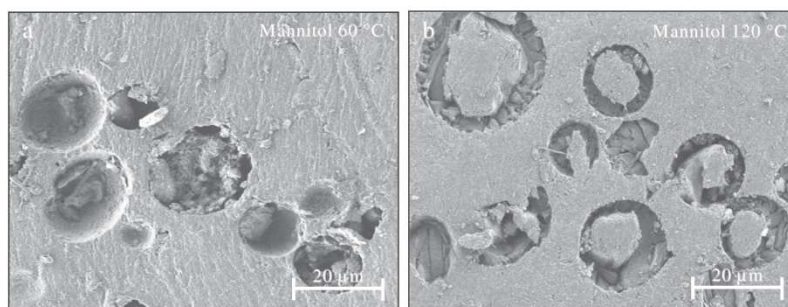
Fig. 5. Scanning electron micrographs of cross sections of mannitol particles spray dried at 60 °C (Mannitol 60 °C, a) and 120 °C (Mannitol 120 °C, b) outlet temperature embedded in epoxy resin, each micrograph represents a sample taken from the second of three batches.

of about 27 μm. Considering the material density of mannitol with $\rho_s = 1520$ kg/m^3 as well as an average porosity of the dried particles at $\varepsilon = 40\%$, the mean particle size after removal of the solvent is expected at around d = 15 μm.

3.6. Investigation of particle size distribution by laser diffraction

In order to evaluate the particle size characteristics of the spray dried products prepared at different temperatures laser diffraction was applied. Despite the observed differences in particle formation, the particle size distributions of the M60, M90 and M120 samples are very close (Fig. 6). Nevertheless, the particle sizes obtained here are very low compared to particles used in commercially available products, which typically range between 50 μm and 200 μm. The mean particle size and standard deviation of M60 is 13,5 μm ± 0,3 μm. M90 samples exhibit a mean particle size of 13,6 μm ± 0,2 μm, and that of M120 was found to be 13,2 μm ± 0,4 μm. Comparing these results with the estimate of the droplet size shows, that during drying droplets lose about 90% of their initial volume. As will be shown the void space within the dried particles may also lead to hollow structures.

The reason why there is no difference between M60 and M120 is related to the crystallization process that occurs in an early drying stage at the surface of the droplets, once the solution becomes supersaturated at the droplet surface. At lower spray drying temperatures the droplets are quickly covered with a crystalline layer, which is more or less rigid and determines the size of the final particles. The evaporation process of water is hindered by this shell and in order to vent the water vapor inside the particle, an orifice is formed through which the release of the water vapour is possible. The shell becomes thicker in this way and the particles become hollow.
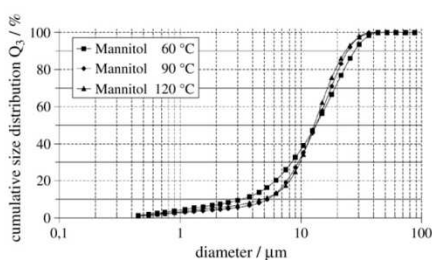

Fig. 6. Cumulative size distribution of mannitol samples spray dried at 60 °C, 90 °C and 120 °C outlet temperature obtained by laser diffraction.

At higher temperatures the water of spray dried droplets evaporates much faster and as observed by hot stage microscopy, the droplets do not recrystallize readily because of the low nucleation rate at this temperature. Thus, it is expected that a substantial amount of water evaporates prior to crystallization. However, since there is no difference of particle size, it may be assumed that the nucleation and growth of crystalline mannitol in the droplets spray dried at 120 °C also occurs in a rather early drying stage due to the high dynamics in the spray dryer and the presence of crystalline seeds that triggers this crystallization. Since the crystals grow larger in the higher temperature range and because of the fast solvent evaporation, the forming shell becomes quickly very rigid and the openings of the hollow particles become (and stay) rather large.

3.7. Investigations on polymorphism

Mannitol exists in three different modifications, which tend to crystallize concomitantly (Burger et al., 2000; Yu, 2007) and may also emerge under spray drying conditions. Mod. I° (modification I°) is the thermodynamically stable form at 20 °C (this fact is distinguished by the superscript zero), whereas the mods. II and III represent metastable forms with a high kinetic stability. The polymorphic forms can be well identified with spectroscopic methods (IR, Raman) and powder X-ray diffractometry, whereas thermal analysis allows the detection of form III as well as impurities such as sorbitol (Burger et al., 2000) but is not able to discriminate unambiguously between mod. I° and II.

3.7.1. Differential scanning calorimetry (DSC)

The DSC curves of the M60, M90 and M120 samples (Fig. 7) show only a single sharp melting peak at 166 °C (onset temperature) and thus match well with the DSC curve of the starting product. The melting point at 166 °C indicates the presence of either mod. I or mod II (Burger et al [53]). Moreover the enthalpies of fusion of the spray dried samples are more or less indistinguishable and the thermograms do not reveal any other thermal events such as a glass transition or eutectic peaks due to the presence of common impurities (e.g. sorbitol). The presence of larger amounts of mod. III can be excluded by the fact that no melting event emerges in the DSC curve at about 155 °C. The absence of mod. III was also confirmed with PXRD and Raman measurements.

3.7.2. Raman spectroscopy

Investigations by Raman spectroscopy and evaluation of the data according to Braun et al. [51] revealed, that mainly mod. I° is formed by the spray dying process besides smaller amounts of mod. II. The fraction of mod. I° in M60 and M90 samples is approximately 95% (Fig. 8), whereas in M120 samples the content of mod. II exceeds 10%.
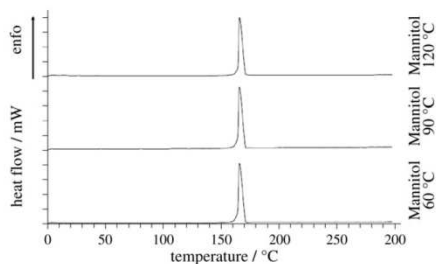
Fig. 7. DSC traces of mannitol samples spray dried at 60 °C (Mannitol 60 °C), 90 °C (Mannitol 90 °C) and 120 °C (Mannitol 120 °C) outlet temperature, heating rate: 10 K/min, one tick mark of the y-axis represents 10 mW.

Fig. 9. FT Raman spectra of mannitol samples spray dried at 60 °C (Mannitol 60 °C), 90 °C (Mannitol 90 °C) and 120 °C (Mannitol 120 °C).

4. Conclusion

The amount of mod. III is below the limit of quantification (3%). Representative Raman spectra of M60, M90 and M120 samples are supplied in Fig. 9.

In order to check for the existence of a correlation between the spray drying temperature and the occurrence of the two polymorphic forms, a larger set of spray dried products was prepared at outlet temperatures between 60 °C and 140 °C in 10 °C steps. As shown in Fig. 10, the amount of mod. I° is more or less constant (95%) in samples spray dried between 60 °C and 110 °C. Further increasing the spray drying outlet temperature results in a clear rise of the mod. II amount that achieves about 16% in the 140 °C sample.

These results may suggest that the rough surface of mannitol spray dried at 120 °C outlet temperature is related to the amount of mod. II. However, preliminary studies on the influence of the mannitol concentration of spray dried aqueous solutions on the surface topography and the occurrence of different polymorphic forms reveal that increasing the concentration from 10% to 24% at a constant outlet temperature of 90 °C results in a significant increase of the amount of mod. II. The ratio rises from 2% to 12% (Fig. 11), whereas no significant influence on surface topography is observable. Consequently, there is no direct relation between the amount of mod. II and surface roughness. Also in these samples no mod. III was detected.

Spray drying of mannitol at different outlet temperatures offers the opportunity of modifying particle surface topography, which, for example, may be useful for tailoring interparticle interactions between the drug and the carrier in interactive mixtures of dry powder inhalates. The emergence of different surface topographies is caused by the occurrence of different crystallization mechanisms. Drying at 60 °C leads to the formation of small acicular crystals forming a smooth particle surface as the concentration of the aqueous mannitol solution becomes supersaturated. In contrast, a fast evaporation of water occurs at high temperatures until a highly concentrated, viscous liquid is obtained, from which larger crystals emerge finally leading to rough particle surfaces. Confocal laser-scanning microscopy was successfully used for the quantification of surface roughness. However, particle size is largely unaffected by the spray drying outlet temperature. Raman spectroscopic studies revealed that the products consist mainly of mannitol mod. I° besides small amounts of mod. II. The amount of mod. II is about 5% at spray drying temperatures at/below 90 °C but increases gradually to 15% when the outlet temperature is raised to 140 °C. Nevertheless, it is shown that surface topography is not directly related to the ratio of these two polymorphic forms in the spray dried products. The crystallization process of mannitol under the stated spray drying conditions is obviously rather complex and its understanding requires additional experimental efforts. Furthermore, emphasis will be put on

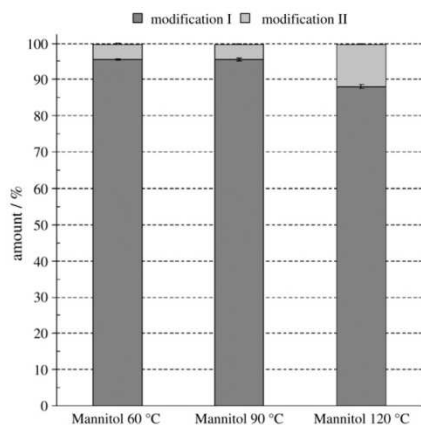**Fig. 8.** Relative amount of mannitol polymorphs in samples spray dried at 60 °C, 90 °C and 120 °C outlet temperature determined by FT Raman spectroscopy, (n = 1 per batch, three batches, mean ± s.d.).
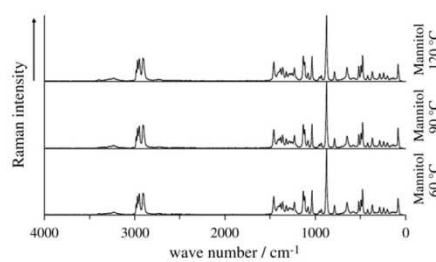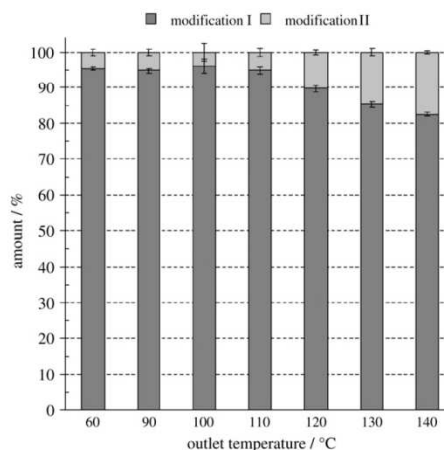

Fig. 10. Crystal modifications of mannitol samples spray dried at outlet temperatures between 60 °C and 140 °C determined by FT Raman spectroscopy, (n = 5 per batch, one batch, mean ± s.d.).
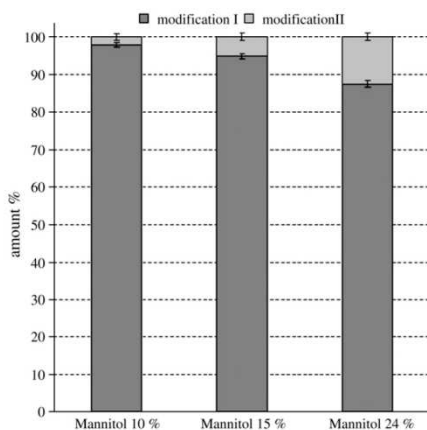
Fig. 11. Relative amount of mannitol polymorphs in samples spray dried at an outlet temperature of 90 °C using aqueous mannitol solutions containing 10%, 15% and 24% (w/w) of mannitol determined by FT Raman spectroscopy, (n = 5 per batch, one batch, mean ± s.d.).

the scale up from the lab scale to the pilot scale in order to obtain larger carrier particles that are typically used as carrier material in dry powder inhalers. Finally, the impact of surface topography on interparticle forces between the drug and the carrier as well as the detachment of the drug from the carrier surface upon inhalation will be investigated. If there is a correlation between surface roughness and respirable fraction, spray drying will offer the opportunity to modify interparticle interactions between the drug and the carrier of dry powder inhalers and to tailor the performance of dry powder inhalates.

Acknowledgements

References

[1] L.E. Briggner, G. Buckton, K. Bystrom, P. Darcy, The Use of Isothermal Microcalorimetry in the Study of Changes in Crystallinity Induced During the Processing of Powders, International Journal of Pharmaceutics 105 (1994) 125–135.
[2] A. Gombas, I. Antal, P. Szabo-Revesz, S. Marton, I. Eros., Quantitative determination of crystallinity of alpha-lactose monohydrate by Near Infrared Spectroscopy (NIRS), International Journal of Pharmaceutics 256 (2003) 25–32.
[3] V.P. Lehto, M. Tenho, K. Vaha-Heikkila, P. Harjunen, M. Paallysaho, J. Valissaari, P. Niemela, K. Jarvinen, The comparison of seven different methods to quantify the amorphous content of spray dried lactose, Powder Technology 167 (2006) 85–93.
[4] G. Buckton, E. Yonemochi, J. Hammond, A. Moffat, The use of near infra-red spectroscopy to detect changes in the form of amorphous and crystalline lactose, International Journal of Pharmaceutics 168 (1998) 231–241.
[5] R. Price, P.M. Young, Visualization of the crystallization of lactose from the amorphous state, Journal of Pharmaceutical Sciences 93 (2004) 155–164.
[6] R. Vehring, Pharmaceutical particle engineering via spray drying, Pharmaceutical Research 25 (2008) 999–1022.
[7] K. Danjo, K. Kinoshita, K. Kitagawa, K. Iida, H. Sunada, A. Otsuka, Effect of Particle-Shape on the Compaction and Flow Properties of Powders, Chemical & Pharmaceutical Bulletin 37 (1989) 3070–3073.
[8] M.E. Mullins, L.P. Michaels, V. Menon, B. Locke, M.B. Ranade, Effect of Geometry on Particle Adhesion, Aerosol Science and Technology 17 (1992) 105–118.
[9] F. Podczeck, J.M. Newton, M.B. James, The influence of chemical structure on the friction properties between particles and compacted powder surfaces, Journal of Materials Science 31 (1996) 2213–2219.
[10] T. Iqbal, J.J. Fitzpatrick, Effect of storage conditions on the wall friction characteristics of three food powders, Journal of Food Engineering 72 (2006) 273–280.
[11] N. Pilpel, Some Effects of Moisture on Flow and Cohesiveness of Powders, Manufacturing Chemist 41 (1970) 19–22.
[12] E. Teunou, J.J. Fitzpatrick, Effect of relative humidity and temperature on food powder flowability, Journal of Food Engineering 42 (1999) 109–116.
[13] J. Tomas, H. Schubert, About Modeling of the Strength and the Flow Properties of Moist and Soluble Mineral Bulk Materials.1. Bulk Materials with Liquid Bridges Bonding, Chemische Technik 34 (1982) 130–134.
[14] B.H.J. Dickhoff, A.H. de Boer, D. Lambregts, H.W. Frijlink, The effect of carrier surface treatment on drug particle detachment from crystalline carriers in adhesive mixtures for inhalation, International Journal of Pharmaceutics 327 (2006) 17–25.
[15] D. El-Sabawi, S. Edge, R. Price, P.M. Young, Continued investigation into the influence of loaded dose on the performance of dry powder inhalers, Surface smoothing effects, Drug Development and Industrial Pharmacy 32 (2006) 1135–1138.
[16] D. El-Sabawi, R. Price, S. Edge, P.M. Young, Novel temperature controlled surface dissolution of excipient particles for carrier based dry powder inhaler formulations, Drug Development and Industrial Pharmacy 32 (2006) 243–251.
[17] N. Islam, P. Stewart, I. Larson, P. Hartley, Surface roughness contribution to the adhesion force distribution of salmeterol xinafoate on lactose carriers by atomic force microscope, Journal of Pharmaceutical Sciences 94 (2005) 1500–1511.
[18] N. Islam, P. Stewart, I. Larson, P. Hartley, Effect of carrier size on the dispersion of salmeterol xinafoate from interactive mixtures, Journal of Pharmaceutical Sciences 93 (2004) 1030–1038.
[19] N. Islam, P. Stewart, I. Larson, P. Hartley, Lactose surface modification by decantation: Are drug-fine lactose ratios the key to better dispersion of salmeterol xinafoate from lactose-interactive mixtures? Pharmaceutical Research 21 (2004) 492–499.
[20] K. Iida, Y. Hayakawa, H. Okamoto, K. Danjo, H. Leuenberger, Preparation of dry powder inhalation by surface treatment of lactose carrier particles, Chemical & Pharmaceutical Bulletin 51 (2003) 1–5.
[21] K. Iida, Y. Hayakawa, H. Okamoto, K. Danjo, H. Leuenberger, Evaluation of flow properties of dry powder inhalation of salbutamol sulfate with lactose carrier, Chemical & Pharmaceutical Bulletin 49 (2001) 1326–1330.
[22] X.M. Zeng, G.P. Martin, C. Marriott, J. Pritchard, Lactose as a carrier in dry powder formulations: The influence of surface characteristics on drug delivery, Journal of Pharmaceutical Sciences 90 (2001) 1424–1434.
[23] K. Iida, H. Todo, H. Okamoto, K. Danjo, H. Leuenberger, Preparation of dry powder inhalation with lactose carrier particles surface-coated using a Wurster fluidized bed, Chemical & Pharmaceutical Bulletin 53 (2005) 431–434.
[24] L.W. Chan, L.T. Lim, P.W.S. Heng, Immobilization of fine particles on lactose carrier by precision coating and its effect on the performance of dry powder formulations, Journal of Pharmaceutical Sciences 92 (2003) 975–984.
[25] R. Guchardi, M. Frei, E. John, J.S. Kaerger, Influence of fine lactose and magnesium stearate on low dose dry powder inhaler formulations, International Journal of Pharmaceutics 348 (2008) 10–17.
[26] H. Adi, I. Larson, P.J. Stewart, Adhesion and redistribution of salmeterol xinafoate particles in sugar-based mixtures for inhalation, International Journal of Pharmaceutics 337 (2007) 229–238.
[27] H. Adi, I. Larson, H. Chiou, P. Young, D. Traini, P. Stewart, Agglomerate strength and dispersion of salmeterol xinafoate from powder mixtures for inhalation, Pharmaceutical Research 23 (2006) 2556–2565.
[28] K. Iida, Y. Inagaki, H. Todo, H. Okamoto, K. Danjo, H. Luenberger, Effects of surface processing of lactose carrier particles on dry powder inhalation properties of salbutamol sulfate, Chemical & Pharmaceutical Bulletin 52 (2004) 938–942.
[29] K. Iida, Y. Hayakawa, H. Okamoto, K. Danjo, H. Luenberger, Influence of storage humidity on the in vitro inhalation properties of salbutamol sulfate dry powder with surface covered lactose carrier, Chemical & Pharmaceutical Bulletin 52 (2004) 444–446.
[30] K. Iida, Y. Hayakawa, H. Okamoto, K. Danjo, H. Luenberger, Effect of surface covering of lactose carrier particles on dry powder inhalation properties of salbutamol sulfate, Chemical & Pharmaceutical Bulletin 51 (2003) 455–1457.
[31] M.D. Louey, S. Razia, P.J. Stewart, Influence of physico-chemical carrier properties on the in vitro aerosol deposition from interactive mixtures, International Journal of Pharmaceutics 252 (2003) 87–98.
[32] M.D. Louey, P.J. Stewart, Particle interactions involved in aerosol dispersion of ternary interactive mixtures, Pharmaceutical Research 19 (2002) 1524–1531.
[33] S.K. Tee, C. Marriott, X.M. Zeng, G.P. Martin, The use of different sugars as fine and coarse carriers for aerosolised salbutamol sulphate, International Journal of Pharmaceutics 208 (2000) 111–123.
[34] F. Podczeck, The influence of particle size distribution and surface roughness of carrier particles on the in vitro properties of dry powder inhalations, Aerosol Science and Technology 31 (1999) 301–321.
[35] H. Steckel, P. Markefka, H. teWierik, R. Kammelar, Effect of milling and sieving on functionality of dry powder inhalation products, International Journal of Pharmaceutics 309 (2006) 51–59.
[36] F. Ferrari, D. Cocconi, R. Bettini, F. Giordano, P. Santi, M. Tobyn, R. Price, P. Young, C. Caramella, P. Colombo, The surface roughness of lactose particles can be modulated by wet-smoothing using a high-shear mixer, AAPS Pharmscitech 5 (2004).
[37] P.M. Young, D. Cocconi, P. Colombo, R. Bettini, R. Price, D.F. Steele, M.J. Tobyn, Characterization of a surface modified dry powder inhalation carrier prepared by "particle smoothing", Journal of Pharmacy and Pharmacology 54 (2002) 1339–1344.
[38] H. Larhrib, G.P. Martin, C. Marriott, D. Prime, The influence of carrier and drug morphology on drug delivery from dry powder formulations, International Journal of Pharmaceutics 257 (2003) 283–296.

[39] X.M. Zeng, G.P. Martin, C. Marriott, J. Pritchard, The use of lactose recrystallised from carbopol gels as a carrier for aerosolised salbutamol sulphate, European Journal of Pharmaceutics and Biopharmaceutics 51 (2001) 55–62.

[40] X.M. Zeng, G.P. Martin, C. Marriott, J. Pritchard, The effects of carrier size and morphology on the dispersion of salbutamol sulphate after aerosolization at different flow rates, Journal of Pharmacy and Pharmacology 52 (2000) 1211–1221.

[41] X.M. Zeng, G.P. Martin, C. Marriott, J. Pritchard, The influence of crystallization conditions on the morphology of lactose intended for use as a carrier for dry powder aerosols, Journal of Pharmacy and Pharmacology 52 (2000) 633–643.

[42] X.M. Zeng, G.P. Martin, C. Marriott, J. Pritchard, The influence of carrier morphology on drug delivery by dry powder inhalers, International Journal of Pharmaceutics 200 (2000) 93–106.

[43] V. Naini, P.R. Byron, E.M. Phillips, Physicochemical stability of crystalline sugars and their spray-dried forms: Dependence upon relative humidity and suitability for use in powder inhalers, Drug Development and Industrial Pharmacy 24 (1998) 895–909.

[44] P. Harjunen, T. Lankinen, H. Salonen, V.P. Lehto, K. Jarvinen, Effects of carriers and storage of formulation on the lung deposition of a hydrophobic and hydrophilic drug from a DPI, International Journal of Pharmaceutics 263 (2003) 151–163.

[45] W. Kaialy, G.P. Martin, M.D. Ticehurst, M.N. Momin, Ali Nokhodchi, The enhanced aerosol performance of salbutamol from dry powders containing engineered mannitol as excipient, International Journal of Pharmaceutics 392 (2010) 178–188.

[46] W. Kaialy, M.N. Momin, M.D. Ticehurst, J. Murphy, Ali Nokhodchi, Engineered Mannitol as an alternative carrier to enhance performance of dry powder inhaler, Colloids and Surface B: Biointerfaces 79 (2010) 345–356.

[47] G. Saint-Lorant, P. Leterme, A. Gayot, M.P. Flament, Influence of carrier on the performance of dry powder inhalers, International Journal of Pharmaceutics 334 (2007) 85–91.

[48] H. Steckel, N. Bolzen, Alternative sugars as potential carriers for dry powder inhalations, International Journal of Pharmaceutics 270 (2004) 297–306.

[49] N.Y.K. Chew, H.K. Chan, Influence of particle size, air flow, and inhaler device on the dispersion of mannitol powders as aerosols, Pharmaceutical Research 16 (1999) 1098–1103.

[50] J. Elversson, A. Millqvist-Fureby, Particle size and density in spray drying - Effects of carbohydrate properties, Journal of Pharmaceutical Sciences 94 (2005) 2049–2060.

[51] D.E. Braun, S.G. Maas, N. Zencirci, C. Langes, N.A. Urbanetz, U.J. Griesser, Simultaneous quantitative analysis of ternary mixtures of d-mannitol polymorphs by FT-Raman spectroscopy and multivariate calibration models, International Journal of Pharmaceutics 385 (2010) 29–36.

[52] P. Walzel, Spraying and Atomizing of Liquids in Ullmann's Encyclopedia of Industrial Chemistry, Electronic Release, 7th ed. Wiley-VCH, Weinheim, 2010.

[53] A. Burger, J.O. Henck, S. Hetz, J.M. Rollinger, A.A. Weissnicht, H. Stottner, Energy/temperature diagram and compression behavior of the polymorphs of D-mannitol, Journal of Pharmaceutical Sciences 89 (2000) 457–468.

3.2. Spray drying at pilot scale

3.2.1. Spray Drying of Mannitol as a Drug Carrier - The Impact of Process Parameters on Product Properties

Eva Maria Littringer, Axel Mescher, Susanna Eckhard, Hartmuth Schröttner, Christoph Langes, Manfred Fries, Ulrich Griesser , Peter Walzel, Nora Anne Urbanetz

Taylor & Francis
Taylor & Francis Group

Spray Drying of Mannitol as a Drug Carrier—The Impact of Process Parameters on Product Properties

Eva Maria Littringer,[1] Axel Mescher,[2] Susanna Eckhard,[3] Hartmuth Schröttner,[4] Christoph Langes,[5] Manfred Fries,[3] Ulrich Griesser,[5] Peter Walzel,[2] and Nora Anne Urbanetz[1]

[1]*Research Center Pharmaceutical Engineering GmbH, Graz, Austria*
[2]*Department of Biochemical and Chemical Engineering, Technische Universitaet Dortmund, Dortmund, Germany*
[3]*Fraunhofer Institute for Ceramic Technologies and Systems, Dresden, Germany*
[4]*Austrian Centre for Electron Microscopy and Nanoanalysis, Graz University of Technology, Graz, Austria*
[5]*Institute of Pharmacy, Pharmaceutical Technology, University of Innsbruck, Innsbruck, Austria*

Powders intended for the use in dry powder inhalers have to fulfill specific product properties, which must be closely controlled in order to ensure reproducible and efficient dosing. Spray drying is an ideal technique for the preparation of such powders for several reasons. The aim of this work was to investigate the influence of spray-drying process parameters on relevant product properties, namely, surface topography, size, breaking strength, and polymorphism of mannitol carrier particles intended for the use in dry powder inhalers. In order to address this question, a full-factorial design with four factors at two levels was used. The four factors were feed concentration (10 and 20% [w/w]), gas heater temperature (170 and 190°C), feed rate (10 and 20 L/h), and atomizer rotation speed (6,300 and 8,100 rpm). The liquid spray was carefully analyzed to better understand the dependence of the particle size of the final product on the former droplet size. High gas heater temperatures and low feed rates, corresponding to high outlet temperatures of the dryer (96–98°C), led to smoother particles with surfaces consisting of smaller crystals compared to those achieved at low outlet temperatures (74–75°C), due to lower gas heater temperatures and higher feed rates. A high solution concentration of the feed also resulted in the formation of comparably rougher surfaces than a low feed concentration. Spray-dried particles showed a volume-weighted mean particle size of 71.4–90.0 μm and narrow particle size distributions. The mean particle size was influenced by the atomizer rotation speed and feed concentration. Higher rotation speeds and lower feed concentrations resulted in smaller particles. Breaking strength of the dried particles was significantly influenced by gas heater temperature and feed rate. High gas heater temperatures increased the breaking strength, whereas high feed rates decreased it. No influence of the process parameters on the polymorphism was observed. All products were crystalline, consisting of at least 96.9% of mannitol crystal modification I.

INTRODUCTION

The application of active pharmaceutical ingredients via the lung is a very promising route of administration because local as well as systemic treatment can be achieved. High drug efficiency, however, can only be expected when the active pharmaceutical ingredient is able to penetrate into the lower parts of the lung. In order to enable deep lung deposition, the aerodynamic diameter of the aspirated aerosol particles should be between 1 and 5 μm. Larger particles will be separated from the air by deflection and impact in the inhaler or within the pharynx. Particles that are too small can only reach the lung's surface by diffusion but do not have enough time to reach the lung tissue during a breathing cycle. In dry powder inhalers the required particle size is usually achieved by micronizing the active substance. Powders of this size are extremely cohesive and show poor flowing and dosing properties. Therefore, in order to ensure sufficient flowability of the particles stored inside a dry powder inhaler, the fine active particles are mixed with coarser carrier particles. Those carrier particles are usually in the size range of 50–100 μm.

The amount of the active ingredient that reaches the lung and reproducible dosing are two important characteristics of such dry powder inhalers. Both can be affected by the variation of interparticle forces between carrier and active fines. On the one hand, adhesion forces must be high enough to guarantee homogeneity of the mixtures and, on

the other hand, low enough to allow the detachment of the active ingredient from the carrier upon inhalation. By variation of the contact area between the active ingredient and the carrier, adhesion forces can be modified. The contact area, in turn, is largely affected by the surface roughness of the carrier. Hence, by variation of the surface roughness it would be possible to tailor interparticle forces and thereby the performance of dry powder inhalers.

Most commercially available dry powder inhaler formulations consist of α-lactose monohydrate carrier particles. Therefore, much work can be found on the influence of surface modification of α-lactose monohydrate carrier particles on the performance of dry powder inhalers.[1–5] The advantages of this excipient are its well-investigated toxicity profile and broad availability at a low price.[6]

However, α-lactose monohydrate may have several disadvantages, for example, the incompatibility reactions of the sugars' reducing aldehyde group with active pharmaceutical ingredients like budesonide, formoterol, peptides, and proteins. Another drawback is that product quality may vary due to production processes (milling, crystallization, sieving) and storage.[7]

Steckel and Bolzen[6] and Tee et al.[8] investigated the use of alternative carriers for dry powder inhalers. They showed the suitability of mannitol as carrier in dry powder inhalers but they also mentioned that there might be problems similar to those experienced with α-lactose monohydrate.

However, by using mannitol, several constraints inherent to α-lactose monohydrate can be avoided. For example, using mannitol instead of α-lactose monohydrate opens up the possibility to apply spray-drying procedures for particle generation. Unlike α-lactose monohydrate, mannitol does not become partially or fully amorphous upon mechanical treatment such as milling or spray drying.[9] Spray drying is a dedicated technology to prepare carrier particles for dry powder inhalers because typically spherical particles are generated. Due to their homogeneous surface properties, those carrier particles offer similar adhesion conditions to active particles attached to the surface. This is in contrast to single lactose carrier crystals with different crystal faces that vary broadly in their affinity to the active ingredient. Furthermore, spray-dried particles of the desired size of 50–100 μm usually exhibit excellent flowing properties because of their typically spherical shape. Moreover, Maas[10] found that it is possible to prepare mannitol carrier particles of different surface roughnesses by varying the spray-drying outlet temperature. Additionally, Maas et al.[11] showed that the amount of the active ingredient that reaches the lung significantly depends on the surface roughness of the spray-dried mannitol carrier particles. However, these carrier particles, which were prepared in a lab-scale spray dryer, were too small (approximately 13 μm) and did not show sufficient flowability.[10]

Therefore, the aim of this study is the preparation of larger (50–100 μm) surface-modified mannitol carrier particles by spray drying. In order to produce particles with the desired size, it was necessary to use a pilot-scale spray dryer, ensuring the drying of larger droplets. Maas[10] mentioned that, depending on the width of the particle size distribution, the surface roughness varied within one product. Therefore, a laminar operated rotary atomizer, characterized by the formation of narrow droplet size distributions, was used for spraying of the mannitol solution.[12] A full-factorial design was applied to study the influence of process parameters on particle size and surface roughness. Furthermore, the breaking strength of the particles produced was analyzed. It is important that carrier particles show a minimum breaking strength, ensuring the stability of the particles during preparation, dosing, and administration of a dry powder inhalate. Mannitol may crystallize in three different polymorphs during spray drying, with slightly different crystal habits and possibly leading to different surface topographies. The phase composition of the spray-dried products was therefore examined. The detailed influence of process parameters when spraying mannitol solutions on the air outlet temperature of the dryer was determined and the outlet temperature was identified as an appropriate parameter to predict the surface morphology of the dried particles.

MATERIALS AND METHODS
Setup of Spray Dryer

A pilot-scale cocurrent spray dryer (Fig. 1) with a diameter of 2.7 m and an overall height of 3.7 m was used. The spray was produced by a laminar operated rotary atomizer;[12] see Fig. 2. The liquid feed was dosed with a screw pump. The pressure was controlled by reducing the air flow to the outlet blower via a flap in order to obtain ambient pressure. Products were collected at the bottom of the spray dryer. Fines were separated by a cyclone and a filter.
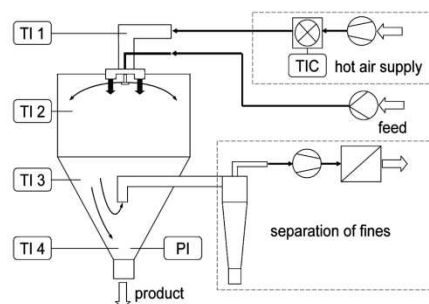

FIG. 1. Schematic diagram of the pilot-scale spray dryer. TIC, temperature inlet control; TI, temperature indicators; PI, pressure indicators.
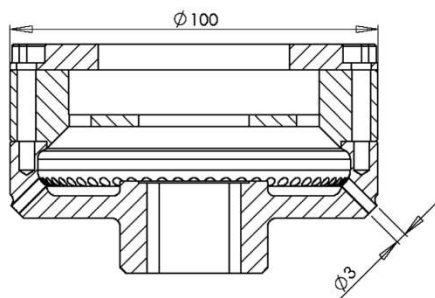
FIG. 2.   Sketch of the rotary atomizer.

The spray-dried products were further dried in an oven for 1 h at 100°C to remove residual moisture. The final product was sealed and stored at room temperature.

Statistical Design

A 2^4 full-factorial design was performed to study the influence of the spray-drying process parameters on particle surface, size, breaking strength, and polymorphism. Additionally, outlet temperature (see TI 4 in Fig. 1) was monitored. Experiments were carried out in a pilot-scale spray dryer (Fig. 1). A statistical experimental design was chosen instead of a mechanistic model due to the unknown crystallization behavior of mannitol and its very complex interaction with the drying course.

Process parameters studied were feed concentration (A), gas heater temperature (B), feed rate (C), and atomizer rotation speed (D). Each factor was studied at two levels, as listed in Tables 1 and 2. Three center points were added to check model linearity (curvature) and to calculate random scattering. No three-way interactions were considered.

TABLE 1
Process parameters used in the 2^4 full-factorial design

Process parameter	Low (−)	Center (o)	High (+)	Unit
A (feed concentration)	15.0	17.5	20.0	% (w/w)
B (gas heater temperature)	170	180	190	°C
C (mannitol solution feed rate)	10	15	20	L/h
D (atomization rotation speed)	6,300	7,200	8,100	rpm

To determine the significance and impact of process parameters as well as their interactions on the product characteristics, statistical analysis of variance (ANOVA) was used. Statistical significance was defined at $p < 0.05$.

The relationships linking the main factors and interactions with the response were determined and presented as quadratic equations of the general form in the following equation:

$$Y = \text{intercept} + \Sigma\,\text{main effects}/2 + \Sigma\,\text{interactions}/2$$

with coefficients for each term of that equation that are shown in Table 3. To graphically quantify the influence of the single factors on the targeted values, standardized effect estimate plots were created. They display the t-values of the test statistic of the standardized effects of the factors on the target values (e.g., particle size). The larger the effect, and hence the influence on the target values, the higher the corresponding value and the more likely the statistical significance. If the value exceeds the t-value that corresponds to a confidence level of $p < 0.05$ (dashed line in the graphs), there is a statistically significant effect. A positive value indicates, like the coefficients of the equation above (Table 3), that the output parameter increases with increasing variable level, and a negative coefficient indicates that the output parameter increases with decreasing variable level.

The high setting for the feed concentration was limited to 20.0% due to the solubility of mannitol at room temperature. Gas heater temperatures above 190°C had been studied prior to these experiments at 10 and 20 L/h solution feed rates. Particles of category 5 were produced under these conditions (Fig. 3), meaning that further increasing the gas heater temperature did not lead to further changes in particle morphology. Therefore, the highest gas heater temperature was set at 190°C. Drying of particles below 170°C is difficult due to the large amount of residual moisture and the stickiness of particles, which tend to form large agglomerates at the bottom of the spray dryer. Feed rates and wheel rotation speed were chosen based on the knowledge of droplet size analysis, in order to obtain carrier particles of the desired particle size. Statistical analysis was carried out using Statistica 8 software (StatSoft, Hamburg, Germany).

Experimental Analysis

Mannitol (Pearlitol 200SD, Roquette Freres, Lestrem, France) was used for the spray-drying experiments. For the analysis and as reference material, polymorphic crystal modifications II and III of mannitol were produced from modification I according to the procedure of Burger et al.[13]

The droplet size analysis was performed by laser diffraction (Malvern 2600, Malvern Instruments, Malvern, UK) at room temperature. The LAMROT atomizer[12] (wheel

TABLE 2
Design matrix of the 2^4 full-factorial design and the data collected from the analyses

Sample ID	Process parameters[a] A	B	C	D	Mean particle size (μm)	Particle span $[(d_{90.3a}-d_{10.3a})/d_{50.3a}]$	Surface category, 1–5	Outlet temperature (°C)	Breaking strength (MPa)	Amount of modificiation I (%)
1	+	−	+	−	88.5	0.82	2	75	4.2 ± 1.1	100.0
2	+	−	+	+	82.7	0.86	2	75	2.7 ± 0.8	100.0
3	−	−	+	+	74.4	0.91	3	74	4.2 ± 1.1	100.0
4	−	−	+	−	81.7	0.87	3	75	4.6 ± 1.1	96.9
5	o	o	o	o	76.9	0.90	4	85	6.4 ± 2.1	99.0
6	o	o	o	o	80.0	0.80	4	86	6.2 ± 1.7	98.8
7	−	+	+	−	79.6	0.87	4	87	6.1 ± 2.2	100.0
8	+	+	+	+	78.7	0.87	4	85	5.0 ± 1.8	100.0
9	+	+	+	−	85.6	0.83	4	85	5.4 ± 2.5	100.0
10	−	+	+	+	74.5	0.91	4	84	5.1 ± 1.9	99.5
11	−	+	−	+	72.7	0.85	5	96	8.5 ± 3.8	98.7
12	−	+	−	−	80.7	0.76	5	97	7.7 ± 2.9	100.0
13	+	+	−	+	79.3	0.83	5	98	9.5 ± 4.0	100.0
14	+	+	−	−	90.0	0.68	5	98	7.9 ± 3.2	100.0
15	−	−	−	−	76.3	0.83	4	85	6.3 ± 2.6	100.0
16	−	−	−	+	71.4	0.82	4	86	7.3 ± 2.6	100.0
17	+	−	−	+	77.2	0.87	4	87	5.6 ± 1.9	100.0
18	+	−	−	−	85.3	0.76	4	88	6.4 ± 2.6	100.0
19	o	o	o	o	78.6	0.85	4	87	6.0 ± 2.5	100.0

[a]A, feed concentration; B, gas heater temperature; C, mannitol solution feed rate; D, atomization rotation speed. −, Low; o, center; +, high.

TABLE 3
Coefficients of the equation linking the spray-drying process parameters to responses

Parameter	Mean particle size (μm)	Surface category, 1–5	Outlet temperature (°C)	Breaking strength (kPa)
Mean/intercept	**79.91**	**3.9**	**85.9**	**6.03**
Curvature	−2.89	0.3	0.1	0.34
A (feed concentration)	**7.00**	**−0.3**	0.9	−0.39
B (gas heater temperature)	0.47	**1.3**	**10.6**	**1.74**
C (feed rate)	1.61	**−1.3**	**−11.9**	**−2.74**
D (atomization rotation speed)	**−7.13**	0.0	−0.6	−0.09
A × B	−0.47	**0.3**	−0.4	0.49
A × C	−0.68	**−0.3**	−0.9	−0.29
A × D	−0.76	0.0	0.4	−0.19
B × C	**−2.67**	**0.3**	−0.1	−0.26
B × D	−0.53	0.0	−0.4	0.34
C × D	0.84	0.0	−0.4	**−0.74**
R^2	0.9709	0.9819	0.9949	0.9659

R^2 values are given to indicate the quality of fit of the statistical models to the experimental values (also see Statistical Design section). Parameters of significance are in bold. No model for polymorphism is given because there was no significant influence of process parameters on polymorphism.
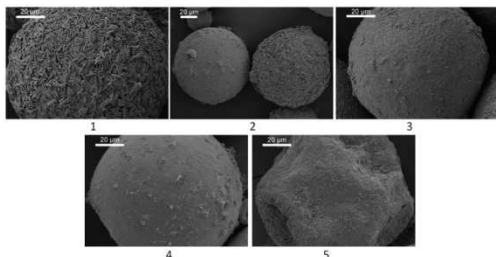
FIG. 3. Roughness categories from 1 (rough) to 5 (smooth) used for the categorization of the spray-dried products in the statistical design. Categorization was based on micrographs obtained from samples of different spray-drying outlet temperatures.

diameter: 100 mm) contained 60 bores of 3 mm, inclined in the radial direction (Fig. 2). Two aqueous mannitol solutions (7.5 and 15.0% [w/w]) were studied at two feed rates (10 and 20 L/h) and at four rotation speeds (5,400, 6,300, 7,200, and 8,100 rpm). Parameters used for spray characterization were volumetric mean droplet size ($d_{50.3}$) and droplet span $= (d_{90.3} - d_{10.3})/d_{50.3}$. The droplet span characterizes the width of the droplet size distribution by relating the characteristic droplet sizes at the 10 and 90% quantiles of the volumetric distribution to the volume mean droplet size.

In order to determine the surface roughness of the powder samples, they were examined using an Ultra 55 scanning electron microscope (SEM; Zeiss, Oberkochen, Germany) operating at 5 kV. Particles were sputtered with gold–palladium prior to analysis. SEM micrographs were classified with respect to surface topography (five categories) from coarse crystalline (category 1, Fig. 3) to smooth (category 5, Fig. 3). Categorization was based on micrographs obtained from samples at different spray-drying outlet temperatures.

Particle size analysis was carried out with a HELOS/L laser diffraction system (Sympatec, Clausthal-Zellerfeld, Germany) with a dry dispersing unit (RHODOS/L with VIBRI/L, Sympatec, Clausthal-Zellerfeld, Germany). The adjusted volumetric mean particle size $d_{50.3,a}$ and particle span span $= (d_{90.3a} - d_{10.3a})/d_{50.3a}$ were obtained from the data. Particles larger than 125 μm were considered as agglomerates originating from the merging of several wet particles during the spray-drying process. They were excluded when calculating the adjusted particle diameters. The assumption of agglomerates was checked by analysis of sieve fractions. They showed that the majority of particles above 125 μm represented agglomerates (picture not shown).

Dried particle strength was examined with a granule strength measuring system (granule strength test system

lab version, Etewe GmbH, Karlsruhe, Germany). The mean and standard deviation of 30 measurements were determined. During the compression test, the required force to break a particle between two plates was measured.

The X-ray powder diffraction (XRPD) patterns of the spray-dried products and the three pure mannitol polymorphs were obtained with an X'Pert PRO diffractometer (PANalytical, Almelo, The Netherlands) equipped with a theta/theta coupled goniometer in transmission geometry and Cu-Kα 1,2 radiation source. The patterns were recorded with a step size of 0.013° 2 Θ in the angular range of 2° to 40° 2 Θ. Refinement of the sample's phase composition was done by Fullprof.2k (Laboratoire Léon Brillovin, CEA-CNRS, France). Crystal structures DMANTL07, DMANTL08, DMANTL10 were received from the Cambridge structural database.[14–16]

RESULTS AND DISCUSSION
Droplet Size Analysis

Preliminary measurements of the mean droplet size and the size distribution were performed in order to approximate the particle size distribution (PSD) of the final spray-dried product. For particles used as carriers in dry powder inhalers, the PSD should exhibit a volume mean diameter between 50 and 100 μm. The atomizer wheel is operated in the jetting regime and laminar liquid threads are formed prior to droplet formation.[12] Among other parameters, the mean droplet size mostly depends on the wheel revolution rate and is reduced with increasing rotation speed (Fig. 4).[12] Because of the higher centrifugal acceleration under such conditions, the liquid threads are
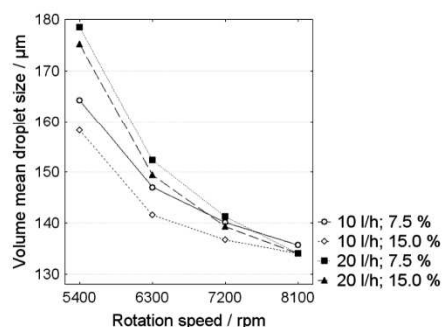
FIG. 4. Dependence of volume mean droplet size on rotation speed, feed rate (10 and 20 L/h), and feed concentration (7.5 and 15.0%) at room temperature (23°C). An increase in atomizer rotation speed decreased the mean droplet size. Assuming a porosity of the dried particles $\varepsilon = 0.5$, droplet sizes in the range of 130 to 155 μm are needed, leading to particles in the desired size range. For that purpose, atomizer rotation speeds of 6,300 and 8,100 rpm were used for the factorial design of experiments.

distinctly attenuated and smaller droplets are produced from decreased thread diameters.

Especially at low rotation speed (5,400 rpm), the feed rate also affects the droplet size. Because only open channel flows can be found inside atomizers of this type, higher volumetric flow rates lead to larger liquid thread diameters[12] and finally to larger droplets.

The influence of the feed concentration on droplet size is comparably low. Even though the breakup length of the liquid jets slightly increases with higher mannitol concentration, due to a slightly increased viscosity, the mean droplet size is hardly affected by the feed concentration. The low sensitivity of the mean droplet size on the liquid viscosity was also shown by Schneider.[17] At a higher rotation speed, the influence of feed concentration and feed rate diminish, because of the strong influence of the atomizer revolution rate. The reduction of the particle size at different solid concentrations due to release of the water volume along the drying process is, then, only insignificantly different.[18] Assuming a porosity of the dried particles $\varepsilon = 0.5$, droplet sizes in the range of 130–155 μm are needed, leading to particles in the desired size range. The desired droplet size can be achieved at wheel speeds of 6,300 rpm and above (Fig. 4). The span was also still low, with $\text{span} = (d_{90.3} - d_{10.3})/d_{50.3} < 0.6$. Therefore, rotation speeds of 6,300 and 8,100 rpm were chosen for the spray-drying experiments.

Particle Size

The desired mean particle size for carrier particles in dry powder inhalers within the range of 50–100 μm was successfully achieved for all samples within the set of tested parameters. Values from 71.4 to 90.0 μm were confirmed with narrow particle size distributions (span <0.91; see Table 2).

Figure 5 shows that feed concentration, wheel rotation speed, and the two-way interaction of gas heater temperature and feed rate significantly affected the particle size. A two-way interaction means that the influence of one factor on the target value differs depending on the level of the other factor. The interaction of gas heater temperatures and feed rates will not be discussed, because none of the factors involved were significant on their own. A major effect on the particle size was found for the atomizer revolution rate. A negative t-value of -10.23 (Fig. 5) for the atomizer rotation speed describes an inverse proportional relation. The higher the atomizer rotation speed, the smaller the particles. This is in agreement with the data from the spray analysis, where smaller droplets—and, consequently, smaller particles after drying—were found at higher rotation speeds. The feed concentration (t-value = 10.06) showed a directly proportional behavior. The higher the feed concentration, the larger the observed mean particle size, even though the preceding droplet size was found to

FIG. 5. Standardized effect estimate of the influence of spray-drying process parameters on mean particle size. Atomizer rotation speed, feed concentration, and the two-way interaction of gas heater temperature and feed rate (2 × 3) significantly influenced the mean particle size. Low rotation speeds and high feed concentrations led to larger particles.

be almost independent on the feed concentration in the range of high atomizer revolution rates used in the drying experiments (Fig. 4). Therefore, another explanation for the increase in particle size with increasing feed concentration must be found. Even though higher concentrations simply mean larger amounts of dryable solids per droplet, larger particles may also result from shell formation at increased concentrations, as described by Elversson and Millqvist-Fureby for spray-dried lactose.[19] At high feed concentrations, the saturation of mannitol at the surface of the drying droplet may be reached earlier and particle shell formation takes place. A stable shell may then fix the apparent particle diameter at its outskirts.[19]

Surface Roughness

In order to obtain carrier particles exhibiting different interparticle forces between carrier and active pharmaceutical ingredient in dry powder inhaler formulations, the influence of the spray-drying process parameters on the surface roughness was studied. The variation of interparticle forces between the active ingredient and the carrier is intended to be achieved by changing the surface roughness of the carrier particles.

Figure 6 shows that particle surface topography was affected by feed concentration, feed rate, and gas heater temperature. All three factors were involved in two-way interactions. Because the effect estimate plot (Fig. 6) provides no direct information regarding the influence of the single factors of the two-way interaction on the value of the surface category, contour plots of the two-way interactions are shown (Figs. 7–9). These plots show regions,

distinctly attenuated and smaller droplets are produced from decreased thread diameters.

Especially at low rotation speed (5,400 rpm), the feed rate also affects the droplet size. Because only open channel flows can be found inside atomizers of this type, higher volumetric flow rates lead to larger liquid thread diameters[12] and finally to larger droplets.

The influence of the feed concentration on droplet size is comparably low. Even though the breakup length of the liquid jets slightly increases with higher mannitol concentration, due to a slightly increased viscosity, the mean droplet size is hardly affected by the feed concentration. The low sensitivity of the mean droplet size on the liquid viscosity was also shown by Schneider.[17] At a higher rotation speed, the influence of feed concentration and feed rate diminish, because of the strong influence of the atomizer revolution rate. The reduction of the particle size at different solid concentrations due to release of the water volume along the drying process is, then, only insignificantly different.[18] Assuming a porosity of the dried particles $\varepsilon = 0.5$, droplet sizes in the range of 130–155 μm are needed, leading to particles in the desired size range. The desired droplet size can be achieved at wheel speeds of 6,300 rpm and above (Fig. 4). The span was also low, with span $= (d_{90.3} - d_{10.3})/d_{50.3} < 0.6$. Therefore, rotation speeds of 6,300 and 8,100 rpm were chosen for the spray-drying experiments.

Particle Size

The desired mean particle size for carrier particles in dry powder inhalers within the range of 50–100 μm was successfully achieved for all samples within the set of tested parameters. Values from 71.4 to 90.0 μm were confirmed with narrow particle size distributions (span <0.91; see Table 2).

Figure 5 shows that feed concentration, wheel rotation speed, and the two-way interaction of gas heater temperature and feed rate significantly affected the particle size. A two-way interaction means that the influence of one factor on the target value differs depending on the level of the other factor. The interaction of gas heater temperatures and feed rates will not be discussed, because none of the factors involved were significant on their own. A major effect on the particle size was found for the atomizer revolution rate. A negative t-value of −10.23 (Fig. 5) for the atomizer rotation speed describes an inverse proportional relation. The higher the atomizer rotation speed, the smaller the particles. This is in agreement with the data from the spray analysis, where smaller droplets—and, consequently, smaller particles after drying—were found at higher rotation speeds. The feed concentration (t-value = 10.06) showed a directly proportional behavior. The higher the feed concentration, the larger the observed mean particle size, even though the preceding droplet size was found to
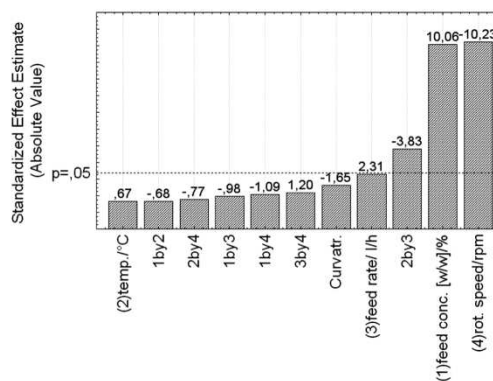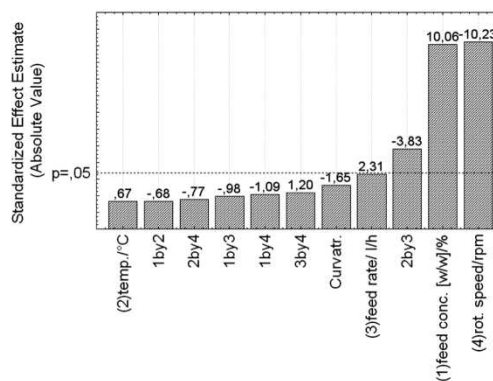

FIG. 5. Standardized effect estimate of the influence of spray-drying process parameters on mean particle size. Atomizer rotation speed, feed concentration, and the two-way interaction of gas heater temperature and feed rate (2 × 3) significantly influenced the mean particle size. Low rotation speeds and high feed concentrations led to larger particles.

be almost independent on the feed concentration in the range of high atomizer revolution rates used in the drying experiments (Fig. 4). Therefore, another explanation for the increase in particle size with increasing feed concentration must be found. Even though higher concentrations simply mean larger amounts of dryable solids per droplet, larger particles may also result from shell formation at increased concentrations, as described by Elversson and Millqvist-Fureby for spray-dried lactose.[19] At high feed concentrations, the saturation of mannitol at the surface of the drying droplet may be reached earlier and particle shell formation takes place. A stable shell may then fix the apparent particle diameter at its outskirts.[19]

Surface Roughness

In order to obtain carrier particles exhibiting different interparticle forces between carrier and active pharmaceutical ingredient in dry powder inhaler formulations, the influence of the spray-drying process parameters on the surface roughness was studied. The variation of interparticle forces between the active ingredient and the carrier is intended to be achieved by changing the surface roughness of the carrier particles.

Figure 6 shows that particle surface topography was affected by feed concentration, feed rate, and gas heater temperature. All three factors were involved in two-way interactions. Because the effect estimate plot (Fig. 6) provides no direct information regarding the influence of the single factors of the two-way interaction on the value of the surface category, contour plots of the two-way interactions are shown (Figs. 7–9). These plots show regions,
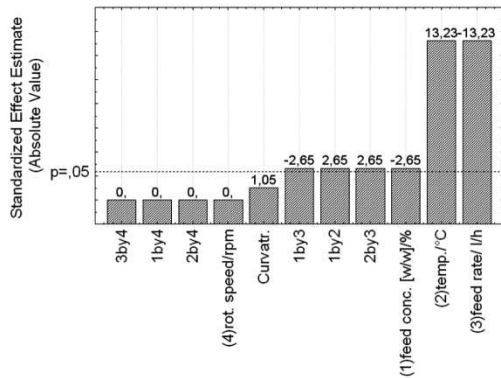
FIG. 6. Standardized effect estimate of the influence of process parameters on surface category. Higher feed rates, lower gas heater temperatures, and higher feed concentrations led to rough particles, of low surface category.

which are indicated by different grey scales, where the surface roughness categories have a constant value. The variables of the two-way interactions can be found on the x- and y-axes. One can see that these lines do not change linearly with the two factors. This clearly shows the interaction of the two factors, which means that the influence of one factor on the target value differs depending on the level of the other factor. For example, the effect of feed concentration on surface topography was only detectable at high feed rates (Fig. 8) or low gas heater temperatures (Fig. 9) but not at low feed rates or high gas heater temperatures.

Figure 3 shows particles with different surface roughnesses classified into different categories from 1 to 5.

FIG. 8. Contour plot of the influence of feed rate and feed concentration on the surface category of the spray-dried products.

Category 1 (Fig. 3) contains particles with a very rough surface consisting of large, rod-shaped single crystals of approximately 3 μm. At higher roughness categories, the single crystals at the surface of the spray-dried particles become smaller and the surface appears smoother. As a consequence, the differences in surface roughness of spray-dried mannitol particles are caused by the size of the single crystals that form the particle shell.

With a t-value of −13.23 (Fig. 6), higher feed rates lead to particles of a smaller surface category with large single crystals at the surface. The higher the gas heater temperature (t-value = 13.23), the smoother the particles, due to smaller crystals at the surface. Our results coincide with the theory that drying at low mass transfer rates favors crystal growth at the expense of nucleation.

The influence of feed concentration on the surface topography is only detectable at high feed rates (Fig. 8) or
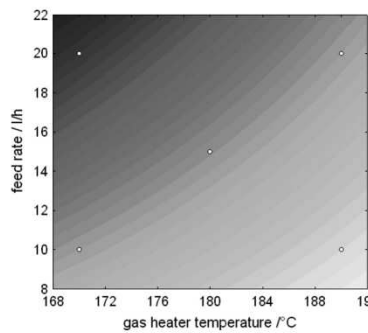

FIG. 7. Contour plot of the influence of feed rate and gas heater temperature on the surface category of the spray-dried products.

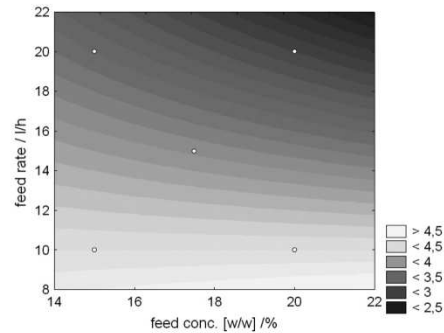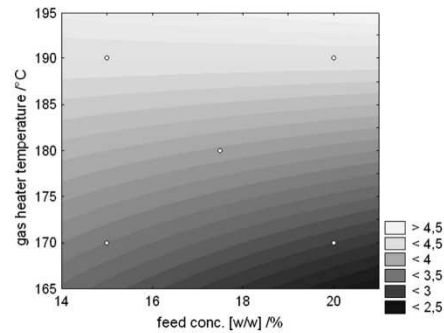FIG. 9. Contour plot of the influence of gas heater temperature and feed concentration on the surface category of the spray-dried products.

low gas heater temperatures (Fig. 9). Both conditions characterize a comparable low mass transfer rate at the droplet surface. Drying of a 20.0% solution then leads to particles with coarser crystals at the surface (lower categories) compared to those dried from solutions of 15.0% (Figs. 8 and 9). Mannitol concentration may influence the crystallization behavior by altering drying kinetics due to different viscosities. However, the formation mechanism of the mannitol particles is definitely more complex and not yet fully understood.

Although a narrowly distributed spray was generated (see droplet size analysis), a certain variability of surface roughness within one spray-dried product could be found, as also reported by Maas.[10] Especially at conditions leading to low surface categories, hence rough particles, a higher variability within one run was detected.

Even though the width of the PSD was low, particles of different sizes existed that had different trajectories inside the spray dryer, leading to different residence times and different drying kinetics. Mazza et al.[20] and Kieviet and Kerkhof[21] experimentally showed the residence time distributions of radio-traced droplets in a pilot-scale spray dryer equipped with a rotary atomizer or pressure nozzles. A comparatively broad residence time distribution of the particles was found in their experiments.

Outlet Temperature

As can also be estimated from a simple heat and mass balance, the outlet temperature at the given air flow rate depends significantly on the feed rate and the gas heater temperature (Fig. 10). An increase in feed rate leads to a decrease in outlet temperature (t-value $= -27.26$). An

FIG. 11. Comparison of surface roughness (y-axis, right) and outlet temperature (y-axis, left). Three regions can be observed: high outlet temperatures (96–98°C) with corresponding high surface categories (5; see Fig. 14); particles with a smooth surface, middle outlet temperatures (84–87°C), and products of surface categories 3–4 (see Fig. 13); and low outlet temperatures (74–75°C) with rough particles of low surface category (2; see Fig. 12).

increase in heater outlet/air inlet temperature causes higher outlet temperatures (t-value $= 24.39$).

For all experiments, three distinct groups of outlet temperatures were observed due to the experimental adjustments: low (74–75°C), intermediate (84–88°C) and high (96–98°C) temperature groups (Fig. 11). These groups each correlate with a distinct surface category (Figs. 12–14). A high surface category (5) corresponds to the high outlet temperature group (Fig. 14) and a low surface category (2) is found within the low outlet temperature group (Fig. 12). However, the latter is only true for high feed concentrations. When low feed concentrations are supplied, comparably higher categories are observed; see section on surface roughness.

The match of surface structure and outlet temperature (Fig. 11) suggests that this parameter is a major indicator

FIG. 10. Standardized effect estimate of the influence of process parameters on outlet temperature. The outlet temperature, which is significantly influenced by feed rate and gas heater temperature, is inversely proportional to feed rate and proportional to gas heater temperature.

FIG. 12. SEM micrograph of sample 1 of the statistical design (see Table 2) shows rough particles of category 2. The product was spray dried at 75°C outlet temperature, which corresponds to the low outlet temperature range.
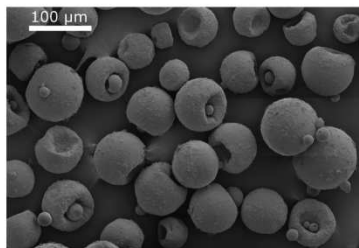
FIG. 13. SEM micrograph of sample 10 of the statistical design (see Table 2) shows particles of surface category 4. The product was spray dried at 84°C outlet temperature, which corresponds to the intermediate temperature range.

for the prediction of the particle surface structure. The outlet temperature is directly related to the particle temperature and therefore to the drying crystallization rate of the droplets.[22] However, as demonstrated in the section on surface roughness, at low outlet temperatures, the feed concentration has to be taken into account in addition to the outlet temperature.

Surprisingly, the influence of the air outlet temperature on surface roughness at the lab scale differed from the findings of Maas,[10] who found rough particles with large crystals at the surface at high outlet temperatures and smooth particles at low outlet temperatures. We conclude that this behavior might be due to two different crystallization mechanisms at the lab and pilot scales: Larger droplets as in these trials dry at a much slower rate, allowing for more time for the crystallization step compared to small droplets, as in Maas.[10] In the case of very small droplets, however, it is expected that heating of the particles and evaporation of the solvent is much faster. Crystallization then may occur faster at higher temperatures from supersaturated mannitol solutions. Further studies will cover this interesting aspect.
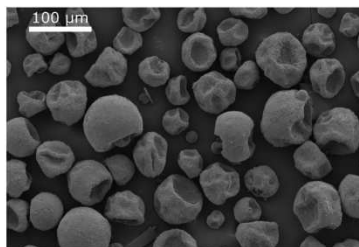
FIG. 14. SEM micrograph of sample 11 of the statistical design (see Table 2) shows smooth particles of surface category 5. The product was spray dried at 96°C outlet temperature, which corresponds to the high temperature range.

Breaking Strength

Because it is important to prevent the carrier particles from breaking during preparation, dosing, and administration of a dry powder inhalate, a minimum breaking strength is required. All products showed a breaking strength of at least 2.7 MPa (Table 2), indicating appropriate stability. Figure 15 shows that feed rate and gas heater temperature significantly affected the breaking strength. A higher feed rate decreased the breaking strength (t-value $= -11.23$), whereas a higher heater temperature increased the breaking strength (t-value $= 7.13$), which also corresponded to small crystals and rather smooth particles. Feed rate and gas heater temperature may influence the breaking strength by changing the mechanism of the particle formation, thus affecting the internal structure of the particles.

Crystallinity

In order to determine whether differences in surface topography or particle structure may arise due to the presence of different polymorphs, XRPD patterns of the samples of the statistical design (Fig. 16), as well as of the three pure mannitol polymorphs were recorded (Fig. 17). The proportion of each polymorph in the samples from the drying experiments was calculated. All products were crystalline after spray drying, showing no modification III. Table 2 shows that modification I, which is the thermodynamically stable polymorph at room temperature,[13] is dominant ($\geq 96.9\%$). Samples 4, 5, 6, 10, and 11 contain a small amount of modification II. The statistical evaluation revealed that there was no significant influence of process parameters on polymorphism. The independence of polymorphism on process parameters within the range examined
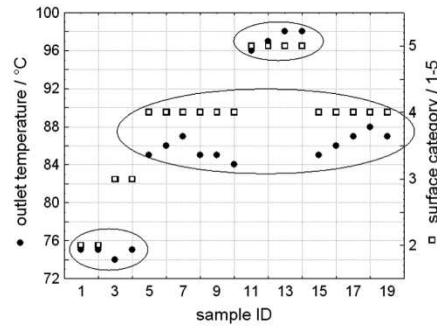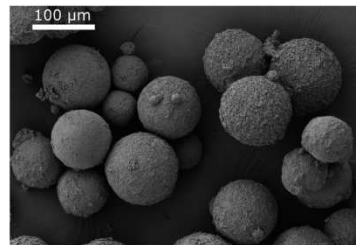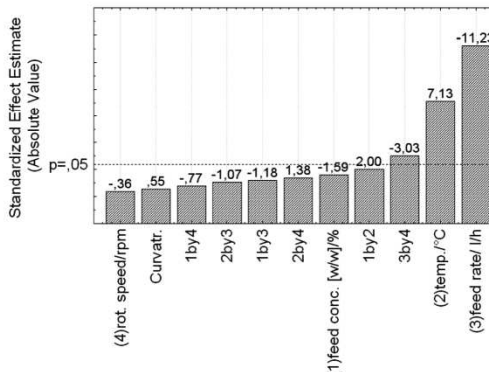

FIG. 15. Standardized effect estimate of the influence of process parameters on breaking strength. The breaking strength of the spray-dried products increased with higher gas heater temperatures and decreased with higher feed rates.

FIG. 16. XRPD patterns of the three mannitol polymorphs. Experimental patterns were recorded at room temperature.

FIG. 17. XRPD patterns of the samples of the statistical design. Modification I was the dominant polymorph. Samples 4, 5, 6, 10, and 11 contained a small amount of modification II.

and the presence of very small amounts of modification II indicate that differences in surface topography or particle structure are not caused by different polymorphs.
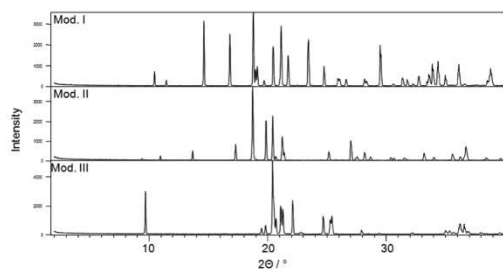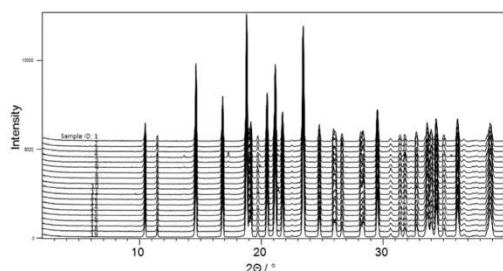
CONCLUSION

The aim of this study was the preparation of carrier particles for dry powder inhalers of sufficient size and variable surface roughness. It could be shown that spray drying mannitol at the pilot scale allows the preparation of carrier particles of different surface roughnesses and proper sizes (71.4–90.0 μm). Furthermore, it was shown that drying air outlet temperature is a key parameter for variations in surface properties of spray-dried mannitol. Low temperatures result in rough surfaces, consisting of larger, rod-shaped single crystals, whereas high temperatures cause smoother surfaces, due to smaller crystals at the particle surface. At low outlet temperatures, surface topography can be further modified by the variation in feed concentration. The changes in surface roughness are most likely caused by different crystallization rates, leading to single crystals of different sizes. The measured breaking strength

of at least 2.7 kPa indicates appropriate stability of the spray-dried carrier particles for their application in a dry powder inhalation. All products were crystalline after spray drying, consisting of at least 96.9% of modification I. Interestingly, the dependence of surface roughness on the outlet temperature was found to differ at the lab and pilot scales. At the lab scale, rough particles with coarse crystals at the surface were obtained at high temperatures, whereas at the pilot scale, rough particles were obtained at low outlet temperatures. Further work will focus on the differences at the lab and pilot scales and on the influence of the carrier surface roughness on the performance attributes of dry powder inhalers.

REFERENCES

1. Dickhoff, B.; de Boer, A.; Lambregts, D.; Frijlink, H. The effect of carrier surface treatment on drug particle detachment from crystalline carriers in adhesive mixtures for inhalation. *International Journal of Pharmaceutics* **2006**, *327*, 17–25.
2. El-Sabawi, D.; Edge, S.; Price, R. Continued investigation into the influence of loaded dose on the performance of dry powder inhalers: Surface smoothing effects. *Drug Development and Industrial Pharmacy* **2006**, *32*, 1135–1138.
3. Chan, L.W.; Lim, L.T.; Heng, P.W.S. Immobilization of fine particles on lactose carrier by precision coating and its effect on the performance of dry powder formulations. *Journal of Pharmaceutical Sciences* **2003**, *92*, 975–984.
4. Zeng, X.M.; Martin, G.P.; Marriott, C.; Pritchard, J. The use of lactose recrystallised from carbopol gels as a carrier for aerosolised salbutamol sulphate. *European Journal of Pharmaceutics and Biopharmaceutics* **2001**, *51*, 55–62.
5. Islam, N.; Stewart, P.; Larson, I.; Hartley, P. Lactose surface modification by decantation: Are drug–fine lactose ratios the key to better dispersion of salmeterol xinafoate from lactose-interactive mixtures? *Pharmaceutical Research* **2004**, *21*, 492–499.
6. Steckel, H.; Bolzen, N. Alternative sugars as potential carriers for dry powder inhalations. *International Journal of Pharmaceutics* **2004**, *270*, 297–306.
7. Steckel, H.; Brandes, H.G. A novel spray-drying technique to produce low density particles for pulmonary delivery. *International Journal of Pharmaceutics* **2004**, *278*, 187–195.
8. Tee, S.K.; Marriott, C.; Zeng, X.M.; Martin, G.P. The use of different sugars as fine and coarse carriers for aerosolised salbutamol sulphate. *International Journal of Pharmaceutics* **2000**, *208*, 111–123.
9. Islam, M.I.U.; Sherrell, R.; Langrish, T.A.G. An investigation of the relationship between glass transition temperatures and the crystallinity of spray-dried powders. *Drying Technology* **2010**, *28*, 361–368.
10. Maas, S.G.; Schaldach, G.; Littringer, E. M.; Mescher, A.; Griesser, U. J.; Braun, D. E.; Walzel, P. E.; Urbanetz, N. A. The impact of

spray drying outlet temperature on the particle morphology of manni-tol. *Powder Technology* **2011**, *213*, 27–35.

11. Maas, S.G.; Schaldach, G.; Walzel, P.E.; Urbanetz, N.A. Tailoring dry powder inhaler performance by modifying carrier surface top-ography by spray drying. *Atomization and Sprays* **2010**, *20*, 763–774.

12. Schröder, T.; Walzel, P. Design of laminary operated rotary atomizer under consideration of the out flow geometry. *Chemie Ingenieur Tech-nik* **1998**, *70*, 400–405 (in German).

13. Burger, A.; Henck, J.-O.; Hetz, S.; Rollinger, J.M.; Weissnicht, A.A.; Stöttner, H. Energy/temperature diagram and compression behaviour of the polymorphs of D-mannitol. *Journal of Pharmaceutical Sciences* **2000**, *89*, 457–468.

14. Berman, H.M.; Jeffrey, G.R.R. The crystal structures of the alpha and beta forms of D-mannitol. *Acta Crystallographica – Section B: Structural Crystallography & Crystal Chemistry* **1968**, *24*, 442–449.

15. Fronczek, F.R.; Kamel, H.N.; Slattery, M. Three polymorphs (alpha, beta and delta) of D-mannitol at 100 K. *Acta Crystallographica C* **2003**, *59*, o567–o570.

16. Kaminsky, W.; Glazer, A. Crystal optics of mannitol, $C_6H_{14}O_6$: Crystal growth, structure, basic physical properties, birefring-ence, optical activity, Faraday effect, electro-optic related effect and model calculations. *Zeitschrift für Kristallographie* **1997**, *212*, 238–296.

17. Schneider, S. Generation and break-up of stretched laminar flows in the gravity field. Ph.D. Thesis, TU Dortmund, Dortmund, Germany, 2002 (in German).

18. Walzel, P. Influence of spray method on product quality and mor-phology in spray drying. *Chemical Engineering & Technology* **2011**, *34*, 1039–1048.

19. Elversson, J.; Millqvist-Fureby, A. Particle size and density in spray drying—Effects of carbohydrate properties. *Journal of Pharmaceutical Sciences* **2005**, *94*, 2049–2060.

20. Mazza, M.G.G.; Brandão, L.E.B.; Wildhagen, G.S. Characterization of the residence time distribution in spray dryers. *Drying Technology* **2003**, *21*, 525–538.

21. Kieviet, F.; Kerkhof, P.J. Measurements of particle residence time dis-tributions in a co-current spray dryer. *Drying Technology* **1995**, *13*, 1241–1248.

22. Tsotsas, E.; Mujumdar, A.S., Eds. *Computational Tools at Different Scales*, Vol. 1; Wiley-VCH: Weinheim, 2007.

3.2.2. Tailoring particle morphology of spray dried mannitol carrier particles by variation of the outlet temperature

Eva Maria Littringer, Axel Mescher, Hartmuth Schröttner, Peter Walzel, Nora Anne Urbanetz

Tailoring particle morphology of spray dried mannitol carrier particles by variation of the outlet temperature

E. M. Littringer[‡]*, A. Mescher[†], H. Schröttner[•], P. Walzel[†], N.A. Urbanetz[‡]

[‡] Research Center Pharmaceutical Engineering GmbH
Inffeldgasse 21a/II, 8010 Graz, Austria
[†] Department of Biochemical and Chemical Engineering
Technische Universität Dortmund
Emil-Figge-Str. 68, 44227 Dortmund, Germany
[•] Austrian Centre for Electron Microscopy and Nanoanalysis,
Technische Universität Graz
Steyrergasse 17/III, 8010 Graz, Austria

Abstract

The aim of this work is to study the influence of spray drying outlet temperature on particle morphology and size of spray dried mannitol samples. Particles are prepared on a pilot scale spray dryer with rotary atomization operating within the laminar open channel flow range. Obtained products which should have a mean particle size of 50 μm to 100 μm are intended to be used as carrier particles in dry powder inhalers (DPIs). Seven samples at outlet temperatures between 67 °C and 102 °C are prepared. At 84 °C three replicates are spray dried to check reproducibility. Our experiments show that particle surface topography can be successfully impacted by the variation of the outlet temperature. The mean particle size of spray dried mannitol samples lies within 77 μm to 84 μm.

Introduction

The delivery of active pharmaceutical ingredients (APIs) to the lung is an emerging route in pharmaceutical drug delivery. It allows local as well as systemic treatment. The European Pharmacopoeia lists three classes of inhaler devices: nebulizers, metered dose inhalers (MDIs) and dry powder inhalers (DPIs) [1]. The related aerosolization principles are nebulization of aqueous suspensions or solutions, atomization of suspensions or solutions by the use of liquefied propellants or dispersion of dry powders in the inspired air, respectively. A precondition for all these devices is that they generate aerosol particles with aerodynamic diameters in the range of 1 μm to 5 μm [2, 3]. Because of the lung geometry particles larger than 5 μm tend to fly straight ahead due to their inertness during inhalation and impact mainly on their way to the alveolar region on the upper airways. In contrast, particles smaller than 1 μm, which depend on deposition by diffusion, often don't have enough time to diffuse to the alveolic tissue and are exhaled instead.

In DPIs this desired aerodynamic diameter is usually achieved by milling of the API. Due to their size these milled powders are rather cohesive and show poor flowing properties. However constant dosing, which is done volumetrically, relies on good flowability. Therefore ordered mixtures of API particles with coarse carrier particles providing sufficient flowability are used. Upon inhalation the API has to be detached from the carrier in order to be able to reach the lower airways. Among the commercially available carriers α-lactose monohydrate is the most prominent one although showing several disadvantages. An unwanted attribute for example is incompatibility of the sugars´ reducing aldehyde group with APIs such as formoterol, budesonide or peptides and proteins [4]. In addition commercially available carriers may show great variability in surface composition depending on the production process (crystallisation, milling, sieving) resulting in varying adhesion forces between the drug and the carrier and consequently varying drug detachment [5].

The aim of this study is to prepare an alternative carrier with excellent flowing properties and adjustable surface roughness thereby tailoring the adhesion forces between the drug and the carrier and consequently drug detachment from the carrier upon inhalation. A powder which fulfills these demands is spray dried mannitol. Maas [6] found out that spray dried mannitol particles showed different surface roughness depending on the spray drying air outlet temperature. However problems encountered by Maas were on the one hand a broad particle size distribution (span from 1,43 to 1,78) leading to varying surface roughness within the same batch and on the other hand a low mean particle size (d50,3=14 μm). For this reason the aim of this study is to carefully

---

* Corresponding author: eva.littringer@tugraz.at

study the influence of drying temperature on particle size, particle size distribution and surface roughness using a pilot scale spray dryer with rotary atomization operating within the laminar open channel flow range.

Materials and Methods

Material

Mannitol (Pearlitol® 200SD) was kindly provided by Roquette Frères (Lestrem, France).

Droplet size analysis

Rotary atomizing spray of a 15 % [w/w] aqueous mannitol solution at room temperature with a feed rate of 10 l/h and rotation speed of 7200 rpm of a 100 mm rotary atomizer containing 60 bores of 3 mm was measured by laser diffraction (Malvern 2600, Malvern Instruments, Malvern, UK). The laser beam was positioned 30 cm vertically from the atomizer edge. Parameters used for spray characterization were volume mean droplet size and droplet span $[(d_{90,3}\text{-}d_{10,3})/d_{50,3}]$.

Spray drying

A pilot-scale cocurrent spray dryer with a diameter of 2.7 m and an overall height of 3.7 m was used. The spray was produced by rotary atomization (100 mm, 60 bores of 3 mm). Feeding was done with a peristaltic pump. Fines were separated by a cyclone and a filter. Temperature was measured and controlled along the dryer. The pressure was controlled by reducing the inlet to the blower via a flap in order to obtain ambient pressure. Products were collected at the bottom of the spray dryer. Particles were prepared from a solution of mannitol dissolved in water (15 % [w/w]) at room temperature with a feed rate of 10 l/h. Seven different samples with outlet air temperatures varying between 67 °C and 102 °C were produced. Outlet temperature was in the range of the indicated temperature ± 2 °C. At 84 °C outlet temperature (named M84) three replicates were spray dried to check reproducibility. Spray dried products were further dried in an oven for one hour at 100 °C to remove residual moisture. Afterwards the powder was hand sieved through a 160 μm sieve to remove agglomerates. The final product was stored closed sealed at room temperature.

Particle surface investigations

The powder samples were examined using a scanning electron microscope (SEM) (Hitachi H-S4500 FEG, Hitachi High-Technologies Europe, Krefeld, Germany) operating at 1 kV.

Particle size distribution

Particle size distribution of spray dried product was determined by analytical sieving for 15 min (amplitude 20 %) on a sieving machine (Analysette Type 3010, Fritsch GmbH, Idar-Oberstein, Germany).

Paricle structure investigations

Spray dried particles were embedded in epoxy-resin (Epofix Struers, Willich, Germany) and after polymerisation cross sections were prepared by manual breaking of the resin. Cross sections were investigated by SEM (Hitachi H-S4500 FEG, Hitachi High-Technologies Europe, Krefeld, Germany) at 1 kV.

Results and discussion

Analysis of the rotary atomizing spray shows a volume mean droplet diameter of 137 μm and a span of 0.28. This low span was intended and can only be achieved when atomizing within the laminar open channel flow range.

Sieve analysis of spray dried products reveals that the mean particle size is in the range of 77 μm to 84 μm (Table 1). The highest mean particle diameter (84 μm) was observed at 67 °C whereas the lowest (77 μm) was seen at 102 °C. Our experiments show that the mean particle size may decrease with rising outlet temperature and vice versa. However these conclusions have to be handled with care due to the fact that all mean particle diameters lie within the standard deviation of samples dried at 84 °C. An explanation for this behavior may be that particle shape thus size changes with outlet temperature (Figure 3). Drying at low temperatures (67 °C) favors spherical particles. Products dried at intermediate temperatures (84 °C) show a collapsed surface giving the particles a mulberry like shape. High temperatures lead to shriveled particles of irregular shape (102 °C). Spray dried samples had span values from 0,64 to 0,82. Compared to Maas [6] who found spans from 1,43 to 1,78 our results seem to be quite promising.

SEM micrographs of sieve fractions of mannitol samples spray dried at different temperatures are presented in Figure 2. The ground sieve fraction of the sample M67 (0 μm-45 μm) clearly contains broken particles. Some broken particles can be still found at sieve fractions 45 μm-53 μm, 53 μm-63 μm and 63 μm-90 μm. Also at the

2

ground sieve fraction of sample M75 several broken particles can be seen. From sample M80 to M102 no broken particles are observed. This finding suggests that particles spray dried at outlet temperatures form 67 °C to 75 °C have lower mechanical strength than products prepared at higher temperatures. For all samples agglomerates are observed at sieve fraction 125 µm-160 µm.

Table 1. Particle size distribution of mannitol samples spray dried at exhaust air temperatures between 67 °C (M67) and 102 °C (M102)

SampleID	d_{10}/ µm	d_{50}/ µm	d_{90}/ µm	span
M67	55	84	124	0,82
M75	63	84	118	0,65
M80	65	84	119	0,64
M84 (n=3)	56 ± 1 (SD)	80 ± 3 (SD)	113 ± 3 (SD)	$0,73 \pm 0$ (SD)
M89	56	78	112	0,72
M92	56	77	111	0,71
M102	53	77	113	0,78

Analysis of atomization spray shows a mean diameter of 137 µm. Spray dried particles have mean diameters in the range of 80 µm. This means that during drying droplets lose about 81 % of their initial volume. Based on the concentration of mannitol in the aqueous solution non-porous mannitol particles should be even smaller, thus suggesting hollow or porous spray dried particles. Particle structure investigations prove these assumptions. SEM micrographs of epoxy-resin embedded particles show hollow particles (Figure 1). Many of the hollow particles contain large prismatic rods.
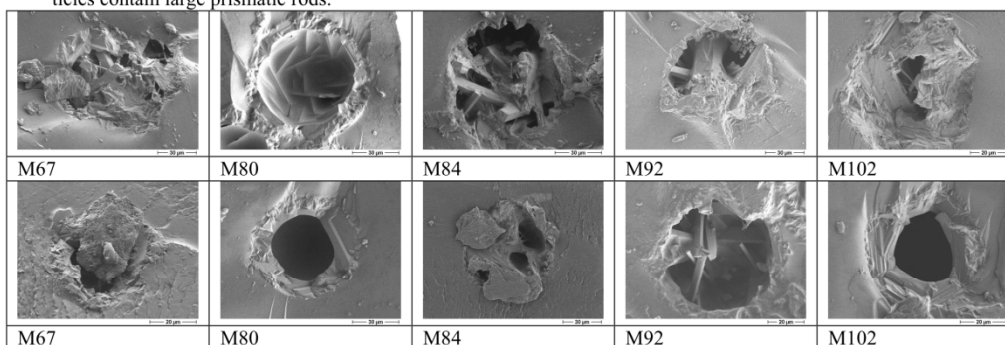
Figure 1. Particle structure of mannitol samples spray dried at different outlet temperatures (from 67 °C to 102 °C)

The results of SEM analysis on the surface of spray dried mannitol particles are shown in Figure 2. Pilot scale spray drying at low outlet temperature (67 °C, Figure 2, lower line) leads to particles of coarse crystalline surface. Single crystals, which can be clearly distinguished, have the shape of prismatic rods. At 84 °C outlet temperature (Figure 2, second line from below) crystal edges fuse to form a relatively smooth surface. At 92 °C (Figure 2, second line form above) outlet temperature single crystals reappear and the surface gets coarser again. However those crystals are smaller and not of that perfect prismatic rod like shape as experienced at 67 °C. At 102 °C (Figure 2, upper line) single crystals form irregular structures thus enhancing surface roughness.

From Figure 2 and Figure 3 it is obvious that despite the narrow span particles dried within one run show certain variability in surface structure and shape. This results from initial different droplet sizes and diverse drying tracks each with distinct temperature gradients leading to somewhat unequal drying conditions for single

3

droplets and therefore to a variability in product quality. Even for single particles variability in surface structure is observed.

Interestingly according to Maas [6] samples spray dried at high outlet air temperature consist of larger crystals, than products spray dried at lower temperatures, which is in contrast to our studies. However, the median diameter of particles determined by Maas is about 15 µm. Such particles may be found in our samples as so called "satellite particles" attached to the main particles. These satellite particles exhibit similar sizes reported by Maas and show similar morphology. Therefore we conclude that different drying kinetics for small and large droplets lead to different crystallization conditions and thus to different surface roughness.

Figure 2. SEM micrographs of mannitol samples, spray dried at outlet temperatures between 67 °C (M67) and 102 °C (M102)

4

| M92 | |
| M102 | |

Figure 3. SEM micrographs of sieve fractions of mannitol samples dried at different outlet temperatures (from 67 °C - M67 - to 102 °C - M102).

Conclusion

This study demonstrates that spray drying mannitol at pilot scale allows the preparation of particles sufficiently large to be used as carrier in DPI formulations. Further it is shown that surface properties of mannitol can be adjusted by changing the spray drying air outlet temperature. Low temperatures lead to surfaces of coarse crystalline structure whereas high temperatures cause surfaces which consist of smaller crystals. Hence the performance of inhalates can be tailored and optimized. Further experiments will focus on the dependence of mechanical strength of spray dried products on spray drying outlet temperature.

Nomenclature

API	active pharmaceutical ingredient	*DPI*	dry powder inhaler
SEM	scanning electron microscopy	*Sp*	span $(d_{90,3} - d_{10,3}) / d_{50,3}$

Acknowledgement

References

[1] European pharmacopoiea 6th edition, Directorate for the Quality of Medicines & Health Care of the Council of Europe, Strasbourg Cedex, France, Preparations for inhalation (2009)
[2] Daniher, D.I., and Zhu, J., *Particuology* 6:225-238 (2008).
[3] Labiris, N.R., and Dolovich, M.B., *British Journal of Clinical Pharmacology* 56:588-599 (2003).
[4] Patton J. S., and Platz, R. M., *Advanced drug delivery reviews* 8:179 – 228 (1992).
[5] Steckel H., Markefka, P., Tewierik, H., and Kammelar, R., *European journal of pharmaceutics and biopharmaceutics* 57:495 – 505(2004).
[6] Maas, S. G., *Optimierung trägerbasierter Pulverinhalate durch Modifikation der Trägeroberfläche mittels Sprühtrocknung, phD-thesis, Heinrich-Heine-Universität Düsseldorf* (2009).

5

3.2.3. The morphology and various densities of spray dried mannitol

Eva Maria Littringer, Michael F. Noisternig, Axel Mescher, Hartmuth Schröttner, Peter Walzel, Nora Anne Urbanetz

The morphology and various densities of spray dried mannitol

Eva M. Littringer[1*], Michael F. Noisternig[2], Axel Mescher[3], Hartmuth Schroettner[4], Peter Walzel[3], Ulrich J. Griesser[2], Nora A. Urbanetz[1]

[1] *Research Center Pharmaceutical Engineering GmbH, Inffeldgasse 21/A, 8010 Graz, Austria*

* corresponding author: Tel: +43 316 873 9743; Fax: +43 316 873 109743; Email: eva.littringer@tugraz.at

[2] *Institute of Pharmacy, Department of Pharmaceutical Technology, Innrain 52c, 6020 Innsbruck, Austria*

[3] *Department of Biochemical and Chemical Engineering, TU Dortmund, Emil-Figge-Str. 68, Dortmund, Germany*

4 Austrian Centre for Electron Microscopy and Nanoanalysis, TU Graz, Steyrergasse 17/III, Graz, Austria

Abstract

As the performance of carrier based dry powder inhaler formulations is highly sensitive to morphological changes carrier morphology must be precisely known and characterized. This work describes characteristic parameters (size, shape, morphology, bulk and effective particle density) of mannitol carriers which had been prepared at outlet temperatures of 67 °C (M67), 84 °C (M84) and 102 °C (M102). The study highlights that a thorough evaluation of the morphological properties requires a multiple method approach.

Scanning electron microscopy (SEM) images showed clear differences in surface roughness and shape of the spray dried products. At low outlet temperatures spherical, rough particles were obtained whereas higher spraying temperatures resulted in particles with multiple surface indentations and a smoother surface. The measurement of surface roughness was challenging due to the shape and small size of the spray dried particles. However, it was possible to analyse this parameter with confocal-scanning microscopy and SEM tilted-image analysis. Even more challenging was the determination of the effective particle density. Mercury intrusion porosimetry (MIP) turned out to be a higly valuable experimental tool for this task.

All spray drying conditions resulted in particles with a shell and a more or less hollow or porous inside. The inner hollow space volume decreases with increasing temperature. For this reason particles prepared at higher temperatures exhibit a higher mechanical stability (M67: 2.46 ± 0.77 MPa; M84: 5.03 ± 1.51 MPa; M102: 11,75 ± 4,01 MPa). The products prepared at 67 °C showed the lowest bulk and effective particle densities. The effective particle densities were determined to be 0.832 ± 0.002 g/cm^3 (M67), 1.004 ± 0.008 g/cm^3 (M84) and 1.111 ± 0.011 g/cm^3 (M102) respectively.

Introduction

In dry powder inhaler formulations, usually the micronized active pharmaceutical ingredient (API) is mixed with coarser carrier particles. Due to the low size of the API particles (1 µm to 5 µm aerodynamic diameter) the API particles stick to the carrier particle surface via Van der Waals forces. These interparticle forces are crucial and affect for example the homogeneity and stability of the mixtures, the flowability and most importantly the amount of active that is detached from the carrier surface during inhalation. Rumpf [9, 10] described that slight changes of particle morphology hugely impact interparticle forces. Furthermore Schubert et al. [11] reported that particle deformability, which is related to the morphological composition of the particle, influences interparticle forces via a change of the contact area. Additionally any change of particle morphology might lead to changes of the aerodynamic behaviour of the powder particles resulting in unpredictable powder performance.

There are many studies which demonstrate the importance of carrier morphology in dry powder inhaler formulations. However, the results of these studies are often controversial as different methods were used for the morphological characterization or insufficient characterization has been performed. Depending on the morphological properties of the powder several complementary characterization methods must be used in order to compensate for the weaknesses of any of the individual techniques.

Spray drying is a preferred method for the preparation of carrier particles for pulmonary drug delivery as it allows the preparation of spherical particles, provided that appropriate process parameters are adjusted. It was shown that the surface roughness of mannitol spheres can be tailored by spray drying aqueous mannitol solutions at different outlet temperatures [18, 19, 10]. However, depending on the selected process parameters and the size of the generated particles [4] not only a change of surface roughness , but also the particle shape was observed.

The present manuscript reports the characterization of spray dried mannitol carrier particles and the dependence of particle morphology and density on the spray drying outlet temperature. In order to get a better understanding of the influence of carrier morphology on the performance of DPI formulations we aimed a thorough characterization of the morphological particle characteristics..

Materials and Methods

Materials

Mannitol (Pearlitol® 200SD) was kindly provided by Roquette Frères (Lestrem, France).

Spray drying

Particles were prepared as described by Littringer et al. [11]. Shortly a laminar operated rotary atomizer (LAMROT-atomizer [5]) with a diameter of 100 mm and containing 60 bores of 3 mm was used in order to produce particles of the desired mean size with a narrow particle size distribution. The atomizer was running at a speed of 7200 min^{-1}. The dimensions of the pilot scale spray dryer were: diameter 2.7 m, conical height 2.2 m, total height 3.7 m. The spray was produced from a solution of mannitol dissolved in water (15 % [w/w]) at room temperature with a feed rate of 10 L/h. Three products at 67 °C, 84 °C and 102 °C outlet temperature, termed M67, M84 and M102, were prepared. The spray dried products were additionally dried in an oven for one hour at 100 °C to remove residual moisture. The powder was hand sieved through a 63 μm and a 160 μm sieve to remove broken particles and/or agglomerates from the tower wall.

Particle size distribution

Laser light diffraction (Helos/KF-Magic, Sympatec, Clausthal-Zellerfeld, Germany) including a dry dispersing system (Rodos, Sympatec, Clausthal-Zellerfeld, Germany) was used to determine particle size distributions of the spray dried powders. The powder was fed to the disperser via a vibrating chute (Vibri, Sympatec, Clausthal-Zellerfeld, Germany). The measurements were carried out at a dispersing pressure of 0.2 bar. Evaluation of the data was performed using the software Windox 4 (Sympatec, Clausthal-Zellerfeld, Germany).

Particle surface investigations

The powder samples were examined using a scanning electron microscope (SEM) (Hitachi H-S4500 FEG, Hitachi High-Technologies Europe, Krefeld, Germany; Particles were not sputtered) operating at 1kV.

Surface roughness

Confocal laser-scanning microscopy

Surface roughness was determined using a confocal laser-scanning microscope (LEXT, OLS4000, Olympus, Hamburg, Germany) and software (LEXT OLS, Olympus, Tokio, Japan). Positioning of the samples was done using a movable sample holder (Olympus, Hamburg, Germany). The laser was operated at a wavelength of 405 nm and a maximal power of approx. 900 μW. The lateral resolution was 120 nm. Per sample a grid of 1024 x 1024 points was scanned. In order to get the height information the sample was moved in z-direction in 60 nm steps. A roughness filter of 8 μm was applied. The Sa value represents the arithmetic mean of the absolute value of the deviations of each single height value from the average height value of the area scanned. Five particles per sample were analysed.

SEM tilted image analysis

SEM micrographs (FEI Nova 200 Nanolab, FEI, Netherlands) were recorded with 5 kV at two angles (0 ° and 10 °). Particles were sputtered with gold-palladium prior to analysis. Subsequently a 3-D reconstruction software (MeX 5.0.1, Alicona, Austria) was used and the mean R_a values were determined based on the following formula, where Z is the deviation of all points from a plane fit to the test surface over sampling length l:

$$R_a = \frac{1}{l}\int_0^l |Z(x) \times dx| \qquad (1)$$

The mean R_a values are calculated by averaging the R values of many line profiles over the analyzed surface. A roughness filter of 8 µm was applied. Three particles per sample were analyzed.

Breaking strength

The breaking strength of the products was examined with a granule strength measuring system (GFP lab-version, Etewe GmbH, Karlsruhe, Germany). The mean and the standard deviation of thirty measurements were determined. During this compression test the breakage force is measured while the individual particle is compressed by a punch to an upper fixed plate. In order to exclude the influence of particle size on the mechanical stability the breaking strength of particles of similar size (sieve fraction 45 µm to 63 µm) was analyzed.

Particle structure investigations

Spray dried particles were embedded into epoxy resin (Spezifix 40, Struers, Willich, Germany) and after polymerization cross sections were prepared by using a microtom (Ultracut UCT, Leica Microsystems, Wetzlar, Germany). Cross sections were investigated by SEM (Zeiss Ultra 55, Zeiss, Oberkochen, Germany; Particles were sputtered with pure carbon prior to analysis) at 5 kV.

Helium pycnometry

Powder density was analyzed by helium pycnometry (AccuPycII1340, Micromeritics, Aachen, Germany). Powder samples were dried in an oven for 1.5 hours at 95 °C and were than let cooled down to room temperature in a desiccator filled with silica gel prior to measurements. Analyzed sample size was between 1.6 g and 2.8 g. Samples were analyzed in triplicate.

Bulk and tapped density

Bulk and tapped densities were measured according to the European Pharmacopoeia (2.9.34: Bulk density and tapped density of powders, Ph. Eur. 7.0) using method 1. Due to a reduced sample size the method was slightly modified. Instead of a 250 mL graduated cyslinder a 10 ml graduated

cylinder (readable to 0.2 ml) filled with each 3.0 g of sample was used for testing. 1250 taps were applied. Each experiment was carried out three times.

Mercury Intrusion Porosimetry (MIP)

MIP measurements were carried out with a low-pressure (Pascal 140, Thermo Fisher Scientific, Milano, Italy) and a high-pressure unit (Porosimeter 2000, Carlo Erba, Milano, Italy). Low-pressure MIP measurements were performed using the Pascal 140 with an evaluable pressure range of ~0.13 bar to 4 bar, detecting pore radii between ~58 µm and 1.84 µm. After the low-pressure analysis the dilatometer is placed into the high-pressure storage tank of the high-pressure unit (Porosimeter 2000), operating from atmospheric pressure up to 2000 bar, detecting pore radii from 7355 nm to 3.7 nm. The mathematical relationship of pressure to pore radius distribution is calculated with the Washburn equation (Washburn, 1921), assuming that all pores are cylindrical, a surface tension of 480 mN/m and a contact angle of 141.3°.

$$r_P = \frac{2 \cdot \sigma}{p} \cdot \cos \vartheta$$

r_p Poreradius / m

σ Hg-Surface tension / Nm^{-1}

p Pressure / at (1 at = 0.980655 bar)

ϑ Contact angle (Mercury – Sample)

Results and Discussion

Table 1 shows that products spray dried at 67 °C, 84 °C and 102 °C have a similar median particle size of approximately 80 µm. The span, which characterizes the width of the particle size distribution, is below 1 which indicates narrowly distributed particles.

In order to get qualitative information about the shape and surface roughness of the spray dried products SEM micrographs were taken. Figure 1 shows the morphologies at 67 °C, 84 °C and 102 °C outlet temperature. As already described by Littringer et al. [11] it is obvious that the lowest outlet temperature (M67, Figure 1, left) yields particles with the roughest surface. The surface is covered by lots of small crystals of rod-like shape besides larger single crystals, which are approximately 3 µm in length. The crystals seem to be randomly oriented. At 84°C outlet temperature the surface gets smoother and the borders of the individual mannitol single crystals become more obscured (M84, Figure 1, middle). At the surface of particles obtained at 102 °C one can identify smaller mannitol

single crystals with blurred boundaries and a more isometric shape compared to those obtained at 67°C outlet temperature (M102, Figure 1, right).

Concerning the particle shape, Figure 1 (left) shows that spray drying aqueous mannitol solutions at low outlet temperatures (67 °C) results in the formation of perfectly round particles. With increasing temperatures the particles progressively lose their spherical shape due to the occurrence of indentations. The particles dried at 102 °C are shriveled and have a raisin like appearance (Figure 1, right).

The mechanisms leading to different shape and surface roughness when spray drying aqueous mannitol solutions at different outlet temperatures have been described earlier [4].

The quantification of surface roughness of carriers intended for pulmonary drug delivery is commonly performed with scanning probe microscopy [3, 14]. However, due to the curvature of the particles and the relatively small size the cantilever would have only access to a very small area resulting in data with limited representativity. Furthermore, analyzing an adequate number of particles allowing statistical analysis is a tedious work. There are several studies suggesting the calculation of the surface roughness parameters from the specific surface area determined by nitrogen adsorption [2, 4]. However, in the case of the particles of the present study (see below, hollow particles with permeable shell) both, the outer as well as the inner surface area will be measured. Therefore nitrogen adsorption cannot be used to calculate reliable roughness parameters off such particles.

The individual surface roughness of the products was thus analyzed with confocal laser-scanning microscopy as well as SEM tilted image-analysis. The obtained roughness profiles and the average surface roughness values (Sa, mean Ra) are displayed in Figure 2 and Figure 3.

The authors are aware of the fact that there is a multitude of different roughness parameters which can be derived from the measured roughness profiles and which are precisely described in ISO DIN norms (e.g. "Geometrical product specifications (GPS) - ISO 4287:1997, ISO 25178-602:2010). As the arithmetic mean of the absolute distances of the single points of the roughness profile from the middle line is a well established and widely used parameter it was used in this study.

Like the SEM micrographs (Figure 1) the roughness profiles determined by confocal laser scanning (Figure 2) and SEM tilted-image analysis (Figure 3) reveal that the three products exhibit clear differences in surface roughness. Both profiles show that the surface of M67 is made-up of rod-shaped single crystals of approximately 3 μm in length. At intermediate temperature (M84) the surface appears smoother and with higher temperatures smaller, isometrically grown grown crystals are observed at the particle surface.

Although the roughness profiles determined by the two different methods are similar the corresponding roughness values, their trends differ.

The Sa value (confocal laser-scanning microscopy) continually increases from M67 to M102. (0.27±0.07 nm to 1.33.56±0.54 nm) (Figure 2). However the mean Ra (SEM tilted image analysis) value first decreases (1.40±0.28 nm to 0.90±0.08 nm) and then increases again (1.25±0.20 nm).

It is not unusual that the single roughness values of the different products vary depending on the method used for characterization. However the overall trend should be the same irrespective of the method used. One reason for the different outcome might be that the analyzed area used for the calculation of the roughness values differed. The whole area displayed in Figure 2 was used for the calculation of the roughness values determined by confocal laser-scanning microscopy. However the values obtained from SEM tilted-image analysis were calculated from a smaller area (Figure 3, dark grey). Additionally this area was chosen not to contain any roughness valleys. Although for both methods a roughness filter of 8 μm was used (distinguishes between roughness and waviness and should eliminate the influence of surface indentations on the roughness value), this choice might not have been sufficient to eliminate all errors caused by surface indentations.

Several studies showed [15, 25] that depending on the chemical properties (e.g. solubility) of the spray dried material and the applied process parameters, spray drying might either result in the formation of solid or porous particles. In order to find out whether the products of this study are hollow or porous the amount of dissolved mannitol in a droplet and the final particle volume was evaluated. The measurement of the droplet size was performed in a previous work (Littringer et al. [10]) and revealed a mean droplet size of approximately 140 μm when atomizing aqueous mannitol solutions (15 % m/m) at 7200 rpm with the LAMROT rotary atomizer. As described above (Table 1) the spray dried particles have mean diameters in the range of 80 μm. This means that the droplets lose about 82 % of their initial volume during drying. Based on the concentration of mannitol present in the aqueous solution non-porous mannitol particles should be even smaller suggesting the presence of hollow or porous particles.

Particle structure investigations verify these assumptions. The SEM micrographs of cross sections, which are shown in Figure 4, reveal that all spray dried products, consist of an outer shell and a porous inside, independent on the outlet temperature. The core of M67 (Figure 4, left) particles contains large single crystals. With higher temperatures the crystals located at the inside of the particles become smaller (Figure 4, right) and also the hollow space volume decreases because of the already above mentioned surface indentations.

As the porosity of the particles affects their mechanical stability the breaking strength of the products was determined via a granule strength testing system. Littringer et al. showed [10] that

both, a higher gas inlet temperature as well as lower feed rates (leading to higher outlet temperatures), increase the mechanical stability. This was also observed here. With increasing outlet temperature the mechanical stability of the particles increased. Figure 5 shows that M67 has a mean breaking strength and standard deviation of 2,46 ± 0,77 MPa, M84 of 5,03 ± 1,51 MPa and M102 of 11,75 ± 4,01 MPa. It is assumed that with higher spraying temperatures the hollow space volume decreases and consequently there is more solid material per volume leading to a higher effective particle density and an increased mechanical stability. However, it has been demonstrated that all spray dried mannitol carrier particles have sufficient stability to withstand powder mixing and DPI delivery including those prepared at low outlet temperature [10].

Because of the fact that the density of the spray dried products is needed to calculate for example the aerodynamic diameter of the carrier or the carrier surface coverage with the API and to get more information about the correlation between mechanical stability and particle density several methods were employed that are suitable to determine the density characteristics of the products. As will be shown below depending on the method used different densities are obtained all of them needing particular interpretation.

A common way to determine the powder bulk density is the measurement of the bulk and tapped densities. Those densities are related to the "bulk" properties of the powders. A known mass of the powder is poured into a graduated cylinder, which is then tapped a defined number of times (see materials and methods). The volume read from the graduated cylinder before (bulk volume) and after tapping (tapped volume) is used to calculate the bulk densities. For M67 the bulk as well as the tapped density was lower than those of M84 and M102 (Table 2, bulk measurements). The reason for this might be a different particle packing arrangement, caused by the different morphologies and/or differences of the effective density of the single powder particles. The effective particle density is the mass of the particle divided by the volume of the particle (including closed and open pores).

A method to assess the "apparent" density is helium pycnometry. Here a measuring chamber of defined volume is filled with a known mass of sample. The chamber is then, after evacuation, filled with helium. The difference in volume of the chamber and the volume of helium that was needed to fill the chamber is used to calculate the density of the sample. In the case of solid particles without any inner voids the helium density represents the "true" density. The true density is the mass of the sample divided by the volume provided that there are not any open or closed pores as well as crystal defects. The true density might also be calculated from single crystal structure data. Helium pycnometry measurements of M67 show a density of 1.492 ± 0.001 g/cm^3 (Table 2) which is equal to the true density of mannitol (Mod. I [11]), indicating that the shell of the particles is permeable for helium. For M84 a lower density of 1.421 ± 0.001 g/cm^3 was found slightly increasing to

1.471 ± 0.003 g/cm^3 for product M102. Also the densities of M84 and M102 are quite close to the true density which means that most particles contain pores in their shells allowing the permeation of helium.

As proposed by Vehring et al. [15] the effective particle density can be calculated by dividing the mass of mannitol dissolved in the atomized droplet by the volume of the solidified particle. The dissolved mass of mannitol is calculated by multiplying the volume of the droplet by the mannitol concentration of the solution. The corresponding volume is obtained from the droplet size measurements. However this approach is only valid for perfect spheres and can therefore only be used for the calculation of the effective particle density of M67. In the case of droplets of 140 μm [10] and spray dried particles of 80 μm an effective particle density of 0.84 g/cm^3 is obtained.

A different well established, however less often used method to determine the particle density is mercury intrusion porosimetry (MIP). Here mercury, as a non-wetting liquid, is forced with increasing pressure into a volume calibrated chamber that contains a defined mass of sample.

With increasing pressure mercury will fill up the interparticular volume between the single powder particles first. At higher pressures mercury will then intrude into the inner porous core of the spray dried particles via the shell pores allowing the determination of the intraparticular volume. Knowing these volumes enables the calculation of different types of particle densities. However this determination is only possible when the mercury intrusion into the interparticular volume occurs in a different pressure range than the intrusion into the intraparticular volume.

Figure 6 shows one of the three mercury intrusion profiles which were recorded for each sample. It can be seen that the inter- and the intraparticular volumes are clearly separated. This enables the determination of the different particle densities by considering the penetrated volume that is recorded at 0.1 bar, 3.5 bar and 2000 bar. The corresponding densities are shown in Table 2.

The densities determined at 0.1 bar, when both the inter - and the intraparticular volume is unfilled, are similar to the bulk and tapped density determined above. Similar to those, the density of M67 is lower (0.432±0.002 g/cm^3) than that of M84 (0.537±0.006 g/cm^3) and M102 (0.515±0.004 g/cm^3) (Table 2).

Because of the fact that at 3.5 bar all the interparticular volume is filled with mercury whereas the intraparticular volume is still unfilled, this value can be used for the calculation of the effective particle density. For the rather perfect spheres (M67) an effective particle density of 0.832 ± 0.002 g/cm^3 was found by MIP. This value is close to the theoretical particle density values calculated above (0.84 g/cm^3; Method proposed by Vehring). Due to the occurrence of surface indentations in samples sprayed at higher temperatures the particle density is expected to increase. This is also clearly verified by the MIP measurements. The M84 products have a density of

1.004 ± 0.008 g/cm^3. The particles with the largest amount of surface indentations (M102) show the highest particle density (1.111 ± 0.011 g/cm^3). Recalling the results of the bulk measurements reported above, the the lower bulk densities determined for M67 can be assigned at least partially to the lower effective density of the single powder particles of M67. This highlights once more the potential of MIP with respect to the determination of the effective particle density of non-spherical particles.

If all the inner voids are accessible via pores the density obtained at 2000 bar should be equal to the true density. Table 2 shows that the MIP apparent densities are slightly lower than the ones obtained by helium pycnometry. This indicates that there are pores that are permeated by helium but are not accessible by mercury (isolated or very small pores - a minimal pore size radius of 3.7 nm is accessible with MIP).

Figure 7 shows that the samples M67, M84 and M102 have different mean pore radii (mode) within the shell ranging from 92 ± 4 nm (M102) to 453 ± 56 nm (M67). This suggests that lower spray drying temperatures result in particles with larger crystals and consequently larger pores than those produced at higher temperatures. The different pore sizes might be the reason for the change of shape with higher temperatures. The pores of M67 are sufficiently large to allow the evaporation of water that is still trapped inside the solidifying particle during drying after the formation of the shell. However at higher temperatures not only the evaporation rate is higher but also the pores are smaller. Therefore a pressure might form inside the particle which will, once large enough, lead to a rupture and subsequent collapse of the particle shell leading to particles of irregular shape.

Conclusion and outlook

The particles prepared at different outlet temperatures consist of a shell and a porous inside. With increasing temperature the shape changes from spherical to raisin-like. The indentations at the particle surface, which give the particles the raisin-like appearance, reduce the hollow space volume. This reduced hollow space volume increases the mechanical stability and leads to higher effective particle densities.

At this point it has to be mentioned that because of the fact that the particles not always exhibit spherical shape, the hollow structure and the permeable shell the determination and interpretation of the density data obtained from bulk and tapped density as well as helium pycnometry measurements is difficult.

Here MIP turned out to be a valuable tool not only to determine the bulk density but especially to evaluate the effective particle density.

This study shows that the thorough characterization of carrier morphology is utterly necessary. Depending on the method used and the prior knowledge about the particle morphology different interpretation of the results are required. Furthermore, a detailed knowledge of the particle morphology might lead to a better understanding of the particle formation process and the mechanisms that are responsible for occurrence of different morphologies.

References

[1]   B.H.J. Dickhoff, A.H. de Boer, D. Lambregts, and H.W. Frijlink. The interaction between carrier rugosity and carrier payload, and its effect on drug particle redispersion from adhesive mixtures during inhalation. *European Journal of Pharmaceutics and Biopharmaceutics*, 59:197 – 205, 2005.

[2]   B.H.J. Dickhoff, A.H. de Boer, D. Lambregts, and H.W. Frijlink. The effect of carrier surface treatment on drug particle detachment from crystalline carriers in adhesive mixtures for inhalation. *International Journal of Pharmaceutics*, 327(1-2):17 – 25, 2006.

[3]   Nazrul Islam, Peter Stewart, Ian Larson, and Patrick Hartley. Surface roughness contribution to the adhesion force distribution of salmeterol xinafoate on lactose carriers by atomic force microscopy. *Journal of pharmaceutical sciences*, 94:1500–1511, 2005.

[4]   E. M. Littringer, R Paus, A. Mescher, H. Schroettner, P. Walzel, and N. A. Urbanetz. The morphology of spray dried mannitol particles – the vital importance of droplet size. *European Journal of Pharmaceutics and Biopharmaceutics*, page submitted for publication, 2012.

[5]   Eva Maria Littringer, Axel Mescher, Susanna Eckhard, Hartmuth Schröttner, Christoph Langes, Manfred Fries, Ulrich Griesser, Peter Walzel, and Nora Anne Urbanetz. Spray drying of mannitol as a drug carrier – the impact of process parameters on the product properties. *Drying Technology*, 30:114–124, 2012.

[6]   Eva Maria Littringer, Axel Mescher, Hartmuth Schroettner, Peter Walzel, and Nora Anne Urbanetz. Spray-dried mannitol carrier particles with optimized surface properties – the influence of carrier surface roughness and shape. *European Journal of Pharmaceutical Sciences*, page in press, 2011.

[7]   S. G. Maas, G. Schaldach, E. M. Littringer, A. Mescher, U. J. Griesser, D. E. Braun, P. Walzel, and N. A. Urbanetz. The impact of spray drying outlet temperature on the particle morphology of mannitol. *Powder Technology*, 213:27–35, 2011.

[8]   Stephan G. Maas, Gerhard Schaldach, Peter E. Walzel, and Nora A. Urbanetz. Tailoring dry powder inhaler performance by modifying carrier surface topography by spray drying. *Atomization and Sprays*, 20:763–774, 2010.

[9]   H. Rumpf. Grundlagen und methoden des granulierens. *Chemie Ingenieur Technik*, 30(3):144–158, 1958.

[10]   Hans Rumpf. Die wissenschaft des agglomerierens. *Chemie Ingenieur Technik*, 46(1):1–11, 1974. interparticle forces and surface roughness.

[11]   Helmar Schubert, Karl Sommer, and Hans Rumpf. Plastische verformung des kontaktbereiches bei der partikelhaftung. *Chemie Ingenieur Technik*, 48(8):716–716, 1976.

[12]   Reinhard Vehring. Pharmaceutical particle engineering via spray drying. *Pharmaceutical research*, 25:1000–1022, 2008.

[13]   Reinhard Vehring, Willard R. Foss, and David Lechuga-Ballesteros. Particle formation in spray drying. *Aerosol Science*, 38:728–746, 2007.

[14]   P. M. Young, D. Cocconi, P. Colombo, R. Bettini, R. Price, D. F. Steele, and M. J. Tobyn. Characterization of a surface modified dry powder inhalation carrier prepared by "particle smoothing". *Journal of Pharmacy and Pharmacology*, 54:1339–1344, 2002.

Table 1. Particle size distribution and span of mannitol particles spray dried at different outlet temperatures, laser diffraction (mean ± SD, n=3).

Mean (n=3)±SD	$X_{10.3}$ / µm	$X_{50.3}$ / µm	$X_{90.3}$ / µm	Span
M67	45.68 ± 1.11	81.37 ± 0.79	122.37 ± 0.81	0.94
M84	54.71 ± 0.60	83.45 ± 0.56	119.52 ± 0.61	0.78
M102	59.03 ± 0.35	86.37 ± 0.34	122.04 ± 0.35	0.73

Table 2. Bulk measurements as well as densities from helium pycnometry and mercury intrusion porosimetry of mannitol samples spray dried at different outlet temperatures (mean (n=3) ±SD).

Mean (n=3) ±SD	Bulk measurements		Helium pycnometry	Mercury intrusion porosimetry (MIP)		
	Bulk density / g/cm3	Tapped density / g/cm3	Apparent density / g/cm3	Bulk density at 0.1 bar / g/cm^3	Effective particle density at 3.5 bar / g/cm^3	Apparent density at 2000 bar / g/cm^3
M102	0.49±0.01	0.60±0.01	1.471±0.003	0.515±0.004	1.111±0.011	1.353±0.017
M84	0.50±0.01	0.60±0.01	1.421±0.001	0.537±0.006	1.004±0.008	1.409±0.022
M67	0.41±0.00	0.48±0.00	1.492±0.001	0.432±0.002	0.832±0.002	1.453±0.018
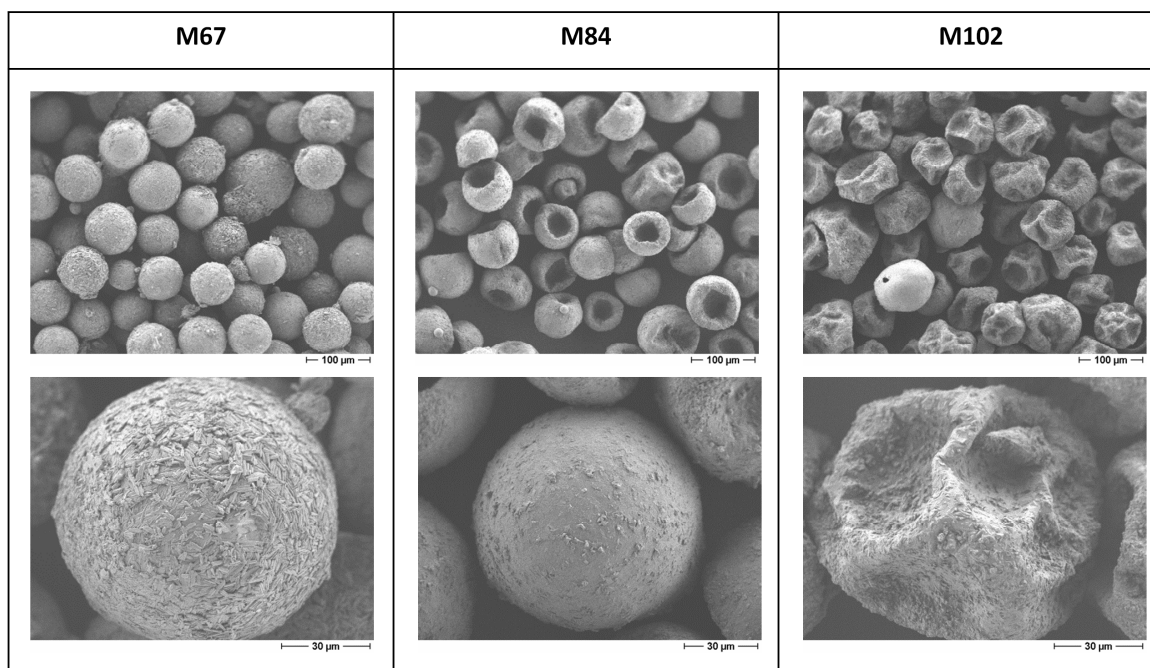
Figure 1. SEM micrographs of mannitol samples spray dried at different outlet temperatures.

M67	M84	M102
Sa= 0.27 ± 0.07 µm	Sa= 0.56 ± 0.50 µm	Sa= 1.33 ± 0.54 µm
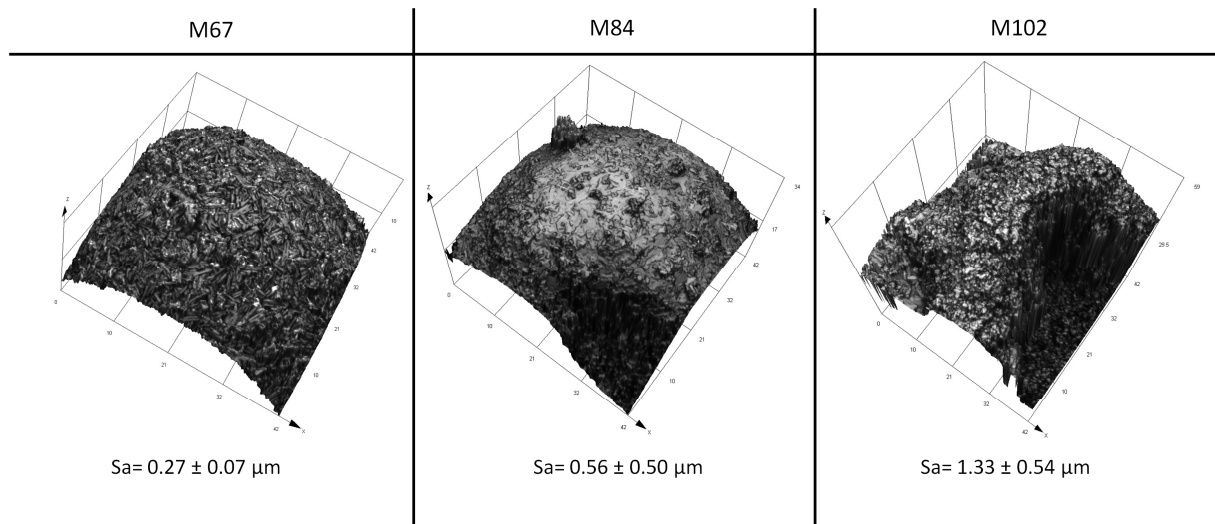
Figure 2. Surface roughness profiles and calculated roughness values (Sa) (mean (n=5) ±SD) of mannitol samples spray dried at different outlet temperatures, confocal laser-sanning microscopy.

M67	M84	M102
meanRa= 1.40 ± 0.28 µm	meanRa= 0.90± 0.08 µm	meanRa= 1.25± 0.20 µm
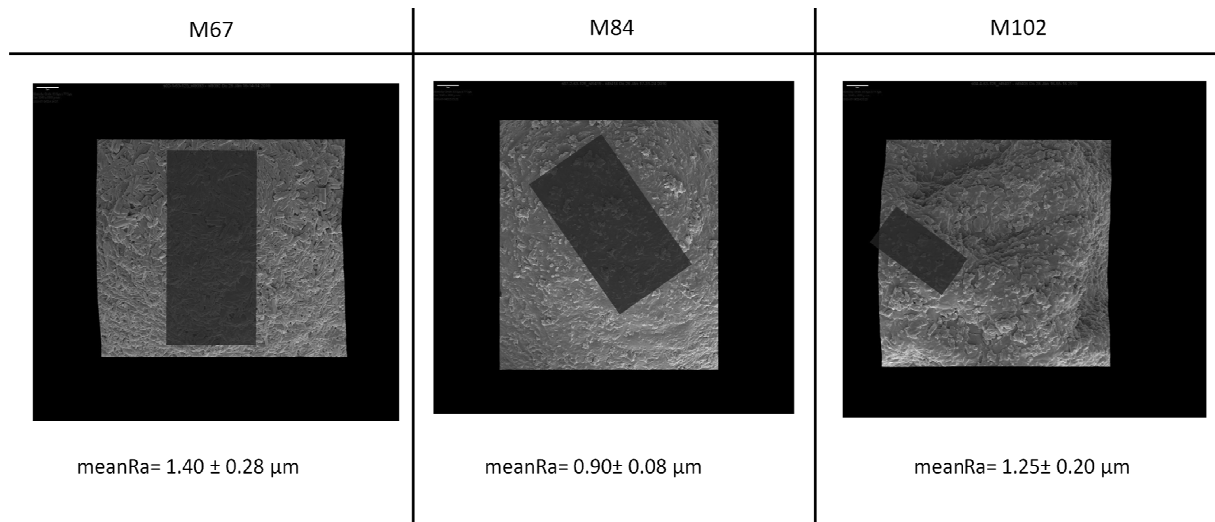
Figure 3. Surface roughness profiles and calculated roughness value (mean Ra) (mean (n=3) ±SD) of mannitol samples spray dried at different outlet temperatures, SEM tilted image analysis.
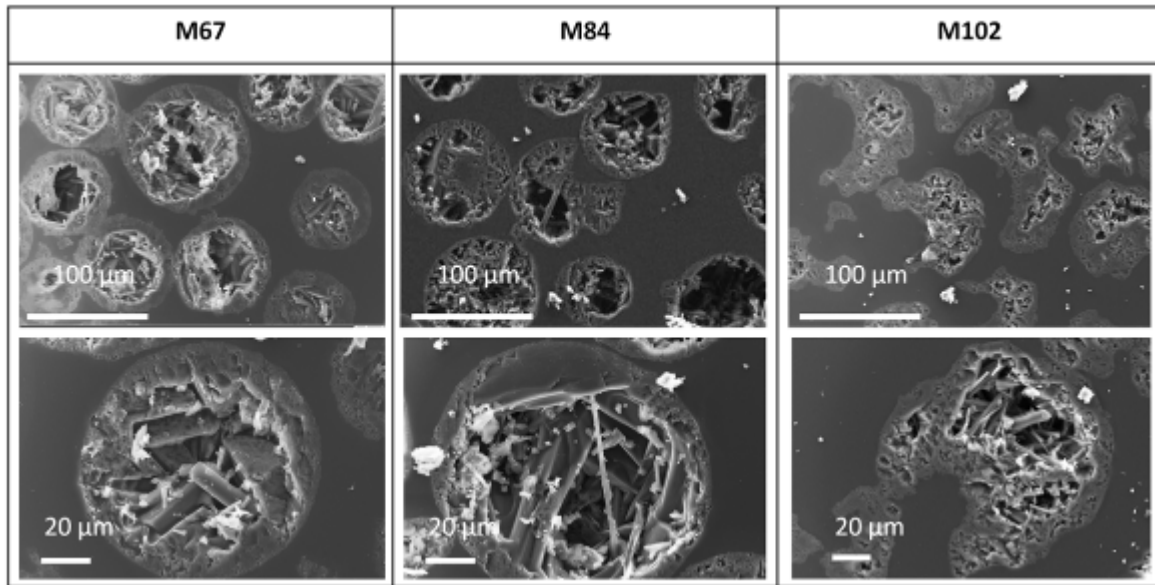
Figure 4. SEM micrographs of cross sections of mannitol samples spray dried at different outlet temperatures.
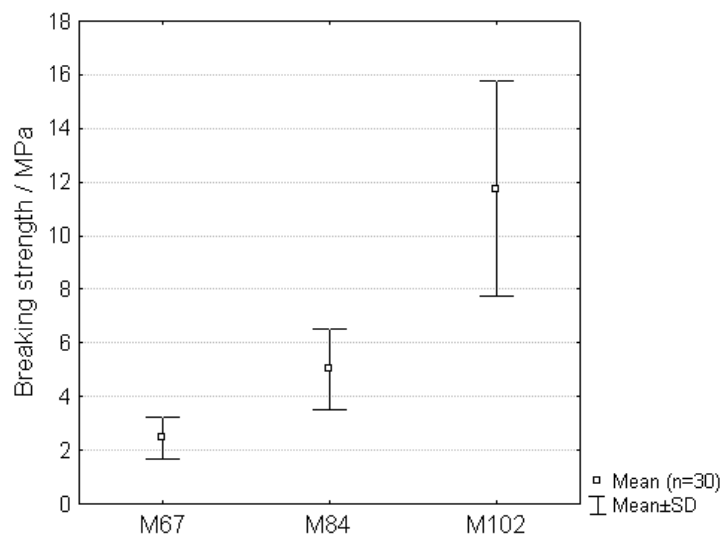
Figure 5. Breaking strength (mean (n=30) ±SD) of mannitol samples spray dried at different outlet temperatures, granule strength testing system.
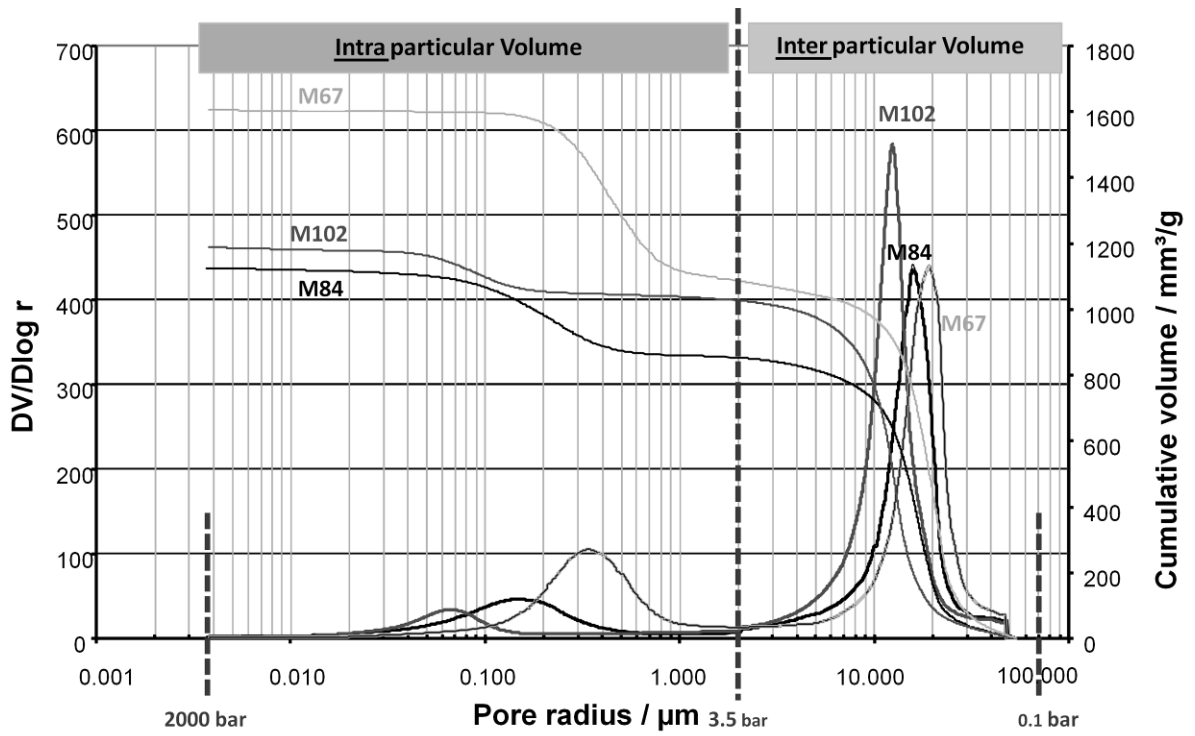
Figure 6. Porosimetry data (cumulative volume and pore size density distribution) of mannitol samples spray dried at different outlet temperatures.
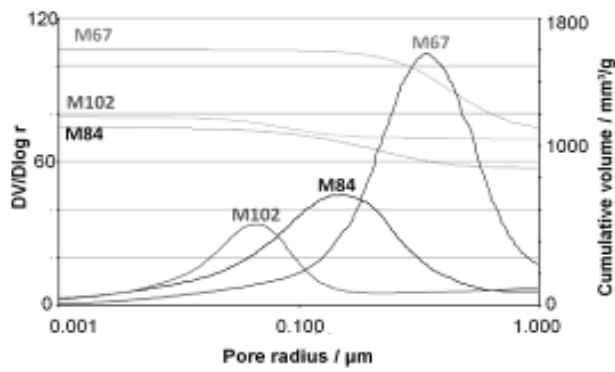
Figure 7. Intraparticular cumulative volume and pore size density distribution of mannitol samples spray dried at different outlet temperatures.

3.2.4. Spray dried mannitol carrier particles with tailored surface properties - The influence of carrier surface roughness and shape

Eva Maria Littringer, Axel Mescher, Hartmuth Schroettner, Lydia Achelis, Peter Walzel, Nora Anne Urbanetz

Research paper

Spray dried mannitol carrier particles with tailored surface properties – The influence of carrier surface roughness and shape

E.M. Littringer [a,*], A. Mescher [b], H. Schroettner [c], L. Achelis [d], P. Walzel [b], N.A. Urbanetz [a]

[a] Research Center Pharmaceutical Engineering GmbH, Graz, Austria
[b] Institute of Mechanical Engineering, Dortmund, Germany
[c] Austrian Centre for Electron Microscopy and Nanoanalysis, Graz, Austria
[d] Department of Mechanical Engineering, University Bremen, Bremen, Germany

ABSTRACT

The aim of this work was to study the performance of mannitol carrier particles of tailored surface roughness in dry powder inhaler formulations. Carrier particles of different surface roughness were prepared by spray drying of aqueous mannitol solutions at different outlet temperatures at a pilot-scale spray dryer. However, the carrier particles did not only change in surface roughness but also in shape. This is why the impact of carrier shape on the performance of carrier based dry powder inhalates was evaluated also. The highest fine particle fraction (FPF), that is the amount of active pharmaceutical substance, delivered to the deep lung, is achieved when using rough, spherical carrier particles (FPF = 29.23 ± 4.73%, mean arithmetic average surface roughness (mean R_a) = 140.33 ± 27.75 nm, aspect ratio = 0.925). A decrease of surface roughness (mean R_a = 88.73 ± 22.25 nm) leads to lower FPFs (FPF = 14.62 ± 1.18%, aspect ratio = 0.918). The FPF further decreases when irregular shaped particles are used. For those particles, the micronized active accumulates within the cavities of the carrier surface during the preparation of the powder mixtures. Upon inhalation, the cavities may protect the active from being detached from the carrier.

© 2012 Elsevier B.V. All rights reserved.

1. Introduction

In order to reach therapeutically relevant areas of the lung, active pharmaceutical ingredient (API) particles should have aerodynamic diameters of 1–5 μm [1–3]. However, particles of this size are rather cohesive and precise dosing is difficult due to poor powder flowability. Especially in multi-dose dry powder inhalers (DPIs) where usually the powder is metered by flowing of the powder from a reservoir into well defined orifices, sufficient flowability is crucial in order to guarantee reproducible dosing [4]. To ensure sufficient flowability, the fine API particles may be mixed with coarser carrier particles. Those carrier particles carrying the API particles on their surface usually have a particle size in the range of 50–200 μm. Further they may act as diluents for highly active APIs. Interparticle forces between carrier and API particles play an important role in such mixtures, which are called adhesive mixtures [5]. On the one hand, adhesion force must be high enough to ensure mixing homogeneity and stability of the mixture during powder handling, dosing, and transport, but low enough to allow the detachment of the API particles from the carrier upon inhalation.

Due to the fact that interparticle forces are highly dependent on the contact area of carrier and API, surface roughness of the carrier might be an important parameter to optimize such formulations. Nearly all DPI formulations on the market are based on α-lactose monohydrate as a carrier [6]. For this reason, many scientific papers are about the surface modification and optimization of lactose carrier particles for example by controlled dissolution of the surface [7,8], carrier surface covering [9–11], surface modification by milling [12,13], or the addition or removal of fines [14–17]. Despite the fact that α-lactose monohydrate has a well-investigated toxicology profile and an assured supply at low price [18], there are also some disadvantages which might affect the inhaler performance. For example, α-lactose monohydrate is not the excipient of choice for APIs with primary amino groups (e.g., budesonide, formoterol, peptides, and proteins) due to incompatibility reactions (Maillard-reaction) which might occur. Another disadvantage is that the physico-chemical (e.g., amorphous content) and morphological properties might vary due to the production processes (milling [19], crystallization, sieving) and storage [18]. However, the most important aspect with respect to this study is that α-lactose monohydrate becomes partially or fully amorphous upon spray drying [20,21]. Mannitol in contrast that has been

* Corresponding author. Research Center Pharmaceutical Engineering GmbH, Inffeldgasse 21a/II, Graz, Austria. Tel.: +43 316 873 9743; fax: +43 316 873 109743.
   E-mail address: eva.littringer@tugraz.at (E.M. Littringer).

investigated as an alternative carrier for dry powder inhalers by Steckel and Bolzen [18], Saint-Lorant et al. [22], Kaialy et al. [23], and Tee et al. [24] is found crystalline after spray drying [25].

Spray drying is an ideal technique for the preparation of carrier particles because it allows the generation of spherical particles, provided that appropriate process parameters are adjusted. However, also non-spherical particles might be obtained when modifying these conditions as will be shown in this study. To the knowledge of the authors, all marketed spray dried mannitol products in the size range of 50–200 μm are of non-spherical shape (e.g., Pearlitol® SD, Mannogem™ EZ).

Spherical particles have the advantage of offering similar adhesion conditions to every active particle attached to the surface. This is in contrast to single lactose carrier crystals with different crystal faces that might vary in their affinity to the active due to different surface energies.

Further spray dried particles are usually considered as well-flowing. The reason for this is that on the one hand, they often have a narrow particle size distribution (cyclone classifier effect), and on the other hand, they are of spherical shape usually.

Moreover, it was shown by Maas [26] that spherical mannitol carrier particles of different surface roughness can be prepared by variation of the spray drying outlet temperature. Maas et al. found out that the fine particle fraction is significantly dependent on the mannitol carrier surface roughness [27]. However, one problem encountered was that those carrier particles prepared on a lab-scale spay dryer did not exhibit sufficient flowability because of their small particle size ($X_{50.3} \sim 14\,\mu m$) [26].

By using a pilot-scale spray dryer, the preparation of surface modified mannitol carrier particles of approximately 80 μm was possible [25]. Littringer et al. [25] extensively studied the influence of spray drying process parameters on product properties such as particle size, surface roughness, breaking strength, and crystallinity. However, unlike the particles prepared at lab-scale, the larger particles prepared at pilot-scale did not only change their surface roughness but also their shape, both depending on the dryer outlet temperature. The aim of this work is to carefully study the influence of carrier shape and surface roughness of pilot-scale spray dried mannitol carrier particles on the performance of dry powder inhalates.

2. Materials and methods

2.1. Materials

Mannitol (Pearlitol® 200SD) was kindly provided by Roquette Frères (Lestrem, France), Polyoxyethylene-20-cetylether by Croda (Nettetal, Germany), and salbutamol sulfate (USP25 quality) by Selectchemie (Zurich, Switzerland).

For the analysis of mannitol polymorphism, Mannitol mod. II and III were produced from mod. I according to the procedure described by Burger et al. [28].

2-Propanol (p.a.), acetic acid (p.a.), glycerin (p.a.), and acetonitrile (UV-IR gradient grade) were purchased from Carl Roth (Karlsruhe, Germany).

2.2. Spray drying of the carrier

Spray dried particles were produced in a pilot-scale dryer built at the Institute of Mechanical Engineering (TU Dortmund, Germany) with a 100 mm rotary atomizer containing 60 bores of 3 mm that was running at a speed of 7200 rpm. The tower dimensions were: diameter 2700 mm, total height 3700 mm. Particles were prepared by spraying a solution of mannitol dissolved in water (15% [m/m]) at room temperature with a feed rate of

10 l/h. Five samples of different surface roughness were prepared by varying the outlet temperature between 67 °C and 102 °C and were named M67, M80, M84, M92, and M102. During the production of the particles, outlet temperatures were in the range of the indicated temperature ±2 °C. The spray dried products were additionally dried in an oven for 1 h at 100 °C to remove residual moisture. The powder was hand sieved through a 63 μm and a 160 μm sieve to remove broken particles and/or agglomerates from the tower wall. The final product was stored desiccated at room temperature.

2.3. Particle size distribution of the carriers and micronized salbutamol sulfate

Particle size distribution of the carrier products and the micronized API salbutamol sulfate was determined by laser diffraction (HELOS/KR, Sympatec GmbH, Clausthal-Zellerfeld, Germany) using a dry dispersing unit (Rodos/L, Sympatec, Clausthal-Zellerfeld, Germany). A dispersion pressure of 4.0 bar was used for the measurement of the micronized active. In order to prevent possible break-up of the carrier particles during measurement, a lower dispersion pressure of 0.2 bar was applied. Measurements were performed in triplicate. The software Windox 5 (Sympatec, Clausthal-Zellerfeld, Germany) was used for data evaluation.

2.4. Surface roughness of the carriers

SEM micrographs (FEI Nova 200 Nanolab, FEI, Netherlands) were recorded with 5 kV at two angles (0° and 10°). Particles were sputtered with gold–palladium prior to analysis. Subsequently, a 3-D reconstruction software (MeX 5.0.1, Alicona, Austria) was used and the mean R_a values were determined based on the following formula, where Z is the deviation of all points from a plane fit to the test surface over sampling length l:

$$R_a = \frac{1}{l} \int_0^l |Z(x) \times dx| \tag{1}$$

The mean R_a values are calculated by averaging the R_a values of several line profiles over the analyzed surface. A roughness filter of 8 μm was applied. Three particles per sample were analyzed.

2.5. Particle shape of the carriers

The aspect ratio, which is the ratio of the width of the particle to its length, of at least 3200 particles was determined by using the Morphology G3 (Malvern Instruments GmbH, Herrenberg, Germany) image analyzing system. Particles of 65–100 μm were analyzed in order not to measure any agglomerates or broken-up particles, which were caused by the sample preparation. Subsequently, the $d_{50.0}$ values of the cumulative aspect ratio distribution were calculated.

2.6. Powder density

Powder density was analyzed by helium pycnometry (Accu-PycII1340, Micromeritics, Aachen, Germany). Powder samples were dried in an oven for 1.5 h at 95 °C and were than let cool down to room temperature in a desiccator filled with silica gel prior to measurements. Analyzed sample size was between 1.6 g and 2.8 g. Samples were analyzed in triplicate.

2.7. Bulk and tapped density

Bulk and tapped densities were measured according to the European Pharmacopoeia (bulk density and tapped density of

powder, Ph. Eur. 7.0) using method 1. Due to a reduced sample size, a 10 ml graduated cylinder (readable to 0.2 ml) filled with each 3.0 g of sample was used for testing. Each experiment was carried out three times. The Hausner ratio was calculated using the following equation:

$$HR = \frac{V_0}{V_f} \qquad (2)$$

where V_0 stands for the unsettled apparent volume and V_f for the final volume after 1250 taps. High values of HR indicate poor dry powder flowability.

2.8. Powder crystallinity

In order to determine the X-ray powder diffraction (XRPD) patterns of the spray dried products and the three pure mannitol polymorphs, an X'Pert PRO diffractometer (PANalytical, Almelo, Netherlands) equipped with a theta/theta coupled goniometer in transmission geometry and a CuKα1,2 radiation source (wavelength 0.15419 nm) with a focusing mirror was used. The patterns were recorded at a tube voltage of 40 kV, tube current of 40 mA, applying a stepsize of 0.013° 2Θ with 80 s per step in the angular range of 2–40° 2Θ. About 5 mg of each mannitol sample was placed without further preparation in a well of a 40 position-plate holder covered with mylar foil of 3 μm. Fullprof.2 k software, Version 3.40 was used for the refinement of the sample's phase composition. The crystal structures of three polymorphs (DMANTL07, DMANTL08, and DMANTL10) were received from the Cambridge structural database [29–31]. Samples were analyzed in triplicate.

2.9. Micronization of salbutamol sulfate

Salbutamol sulfate, used as model active, was micronized using an air jet mill 50 AS (Hosokawa Alpine, Augsburg, Germany). The injection pressure was 6.0 bar and the milling pressure 2.0 bar. A feed rate of 1 g/min was used. The micronized material showed a mean particle diameter of 1.69 μm ($x_{10.3} = 0.46$ μm ± 0.00 μm, $x_{50.3} = 1.69 ± 0.01$ μm, $x_{90.3} = 5.65 ± 0.05$ μm). Particle size distributions were determined by laser diffraction.

2.10. Surface topography investigation of the spray dried carriers, micronized salbutamol sulfate, and interactive mixtures

The powder samples were examined using a scanning electron microscope (SEM) (Zeiss Ultra 55, Zeiss, Oberkochen, Germany; particles sputtered with gold–palladium prior to analysis) operating at 5 kV and a SEM (Hitachi H-S4500 FEG, Hitachi High-Technologies Europe, Krefeld, Germany; Particles unsputtered) operating at 1 kV.

2.11. Preparation of powder blends

A 0.1 g of salbutamol sulfate and 4.0 g of the carrier (drug content of 2.4% (m/m)) were weighed into stainless steel mixing vessels (diameter: 3.2 cm, height: 3,4 cm; filling volume approximately 70%) using the sandwich method. The vessel was then fixed in a Turbula blender TC2 (Willy A. Bachofen Maschinenfabrik, Muttenz, Switzerland) and mixed for 90 min at 62 rpm. All blends were prepared in triplicate.

2.12. Blend homogeneity

Ten samples of 10 mg to 20 mg were sampled from the powder blends via a spatula—three from the top, four from the center, and three from the bottom of the vessel. The powder samples were dis-

solved in 10 ml of water of pH = 3 (adjusted by acetic acid) and subsequently analyzed by reversed phase high performance liquid chromatography (HPLC). In order to determine the homogeneity of the samples, the coefficient of variation (CV) of the content of the active of the 10 samples was calculated (Table 3).

2.13. Carrier stability during inhaler testing

Several doses of the pure carriers were delivered through the Novolizer® (Meda Pharma, Bad Homburg, Germany), collected in the unit sampling apparatus (see delivered dose), and subsequently examined using a light microscope (Leica DM 4000 M, Leica Microsystems, Wetzlar, Germany). Hardly any broken-up particles were observed (data not shown).

2.14. Metering reproducibility of the carrier particles and the adhesive mixtures/metered mass

In order to determine the metering reproducibility of the carrier, 50 doses were delivered via the Novolizer® (Meda Pharma, Bad Homburg, Germany) multi-dose inhaler, which was filled with 1 g of the carrier. The procedure was performed in triplicate. The metering reproducibility of the adhesive mixtures was determined accordingly, by delivering 50 doses of each of the three batches of the powder blends. After each delivery, the inhaler was weighed and the metered mass was calculated as the difference between the weight before and after the delivery. The coefficient of variation (CV) of the 50 metered masses was calculated and used to characterize the metering reproducibility.

2.15. Delivered dose and uniformity of delivered dose

The delivered dose was determined by discharging one dose from the Novolizer® (Meda Pharma, Bad Homburg, Germany) multi-dose inhaler using the experimental setup as described by the European Pharmacopoeia (powders for inhalation, Ph. Eur., 7.0). Glass fiber filters (Type A/E, 47 mm, PALL GmbH, Dreieich, Germany) were inserted into the unit sampling apparatus. The unit sampling apparatus including the mouthpiece adaptor was rinsed with 20 ml of diluted acetic acid (pH = 3). For each batch of the three powder blends, the procedure was repeated ten times (dose 1–5 and 46–50 from a series of 50 discharges). The amount of the active was determined by HPLC. The Novolizer® was filled with 1 g of the interactive mixture.

In order to know how much of the active was lost during testing, the percentage of recovery of the delivered dose (PRDD) was calculated according to the following equation:

$$PRDD = \frac{DD * 100}{m_{DD} * c} \qquad (3)$$

whereby m_{DD} is the weighed mass of the puff and c is the concentration of the active in the adhesive mixture. The concentration of the active is calculated by dividing the weight of active by the total weight of the adhesive mixture multiplied by 100.The uniformity of the delivered dose was determined according to the European Pharmacopoeia (preparations for inhalation: inhalanda, Ph. Eur., 7.0).

2.16. Assessment of fine particles—fine particle fraction, emitted dose, fine particle dose

The aerodynamic assessment of fine particles (2.9.18. preparations for inhalation: aerodynamic assessment of fine particles, Ph. Eur., 7.0) was performed using the apparatus E (NGI, Copley Scientific, Nottingham, United Kingdom). In order to prevent bouncing of the active, the small cups of the impactor were coated with 2 ml, the large cups with 4 ml of coating agent (solution of 5% of

a mixture of glycerol and polyoxyethylene-20-cetylether (95:5) in isopropanol). The preseparator was filled with 10 ml of diluted acetic acid. A flow rate, which was measured with an electronic digital flowmeter (DFM3, Copley Scientific, Nottingham, United Kingdom), of 78.2 l/min was adjusted, which corresponds to an inhaler pressure drop of 4.0 kPa. The solenoid valve of the critical flow controller (TPK, Copley Scientific, Nottingham, United Kingdom) was kept open for three seconds so that 4 l of air were sucked (SV1025, Busch, Chevenez, Switzerland) through the apparatus. A leak test was performed prior to each experiment. Within 60 s, the pressure of the closed NGI must not increase by more than 2.0 kPa. The adhesive mixture (1 g) was filled in the powder container of a Novolizer® (Meda Pharma, Bad Homburg, Germany), which was fixed to the artificial throat of the impactor by a suitable mouth piece adaptor. For each batch of the three powder blends, 10 doses were discharged into the impactor (dose 21–30 form a series of 50 discharges). The active on the cups was then dissolved in 10 ml of diluted acetic acid (pH = 3). The preseparator was rinsed with 50 ml and the introduction port together with the mouthpiece with 10 ml of diluted acetic acid. The amount of drug was determined by HPLC. The cut-off diameter of the preseparator was calculated according to Marple et al. [32] with the following equation $D_{50} = 12.8 - 0.07(Q - 60)$, with the air flow rate Q (here 78.2 l/min). The cut-off diameters for the NGI stages were calculated according to the European Pharmacopoeia (preparations for inhalation, Ph. Eur., 7.0). The fine particle dose (FPD) is calculated as the dose of the active ingredient exhibiting an aerodynamic diameter of <5 μm. The emitted dose is the amount of the active found in the whole impactor (mouthpiece adaptor, introduction port, preseparator, impaction stages). The fine particle fraction (FPF) is defined as the fine particle dose divided by the emitted dose.

In order to know how much of the active was lost during testing, the percentage of recovery of the emitted dose (PRED) was calculated according to the following equation:

$$PRED = \frac{ED * 100}{m_{ED} * c} \qquad (4)$$

whereby m_{ED} is the weighed mass of the puff and c is the concentration of the active in the adhesive mixture. The concentration of the active is calculated by dividing the weight of active by the total weight of the adhesive mixture multiplied by 100.

2.17. HPLC

Salbutamol sulfate samples were analyzed by a HPLC method using a HP1090 liquid chromatograph (Agilent technologies, Boeblingen, Germany). A CC 8/4 Nucleodur 100-5 C18 ec precolumn (Macherey-Nagel, Dueren, Germany) and a EC250/4 Nucleodur 100-5 C18ec column (Macherey-Nagel, Dueren, Germany) was used as reversed phase stationary phase. The temperature of the column oven was adjusted to 40 °C. Detection of the active was performed at 276 nm and integration of the peaks was carried out using the software Chemstation (Agilent technologies, Boeblingen, Germany). The mobile phase was a mixture of acetonitrile and diluted acetic acid (pH = 3) at the ratio of 312/688. The flow rate

was set to 0.9 ml/min and 10 μl of the sample was injected per run. Each sample was analyzed three times. Linearity of the method was checked in the range of 6.36 μg/ml and 61.50 μg/ml. Every twenty samples a calibration curve, consisting of six solutions of known concentration, was recorded.

2.18. Statistical analysis

Statistical differences were studied by independent t-test using Statistica8 software (Statsoft, Hamburg, Germany). P-values of less than 0.05 were considered as statistically significant.

3. Results and discussion

3.1. Carrier characterization

Spray dried particles were prepared in a pilot-scale dryer at five different outlet temperatures between (67°C, 80°C, 84°C, 92°C and 102°C). In order to remove agglomerates and/or broken-up particles, which beneath the determination of surface roughness and particle shape may impact the performance of the inhalate, sieve fractions between 63 μm and 160 μm were used in the whole study. Table 1 shows that all carrier particles have a median particle size of approximately 80 μm. The products show a narrow particle size distribution which is characterized by span-values $[(x_{90.3} - x_{10.3})/x_{50.3}]$ for all products below 1.

Fig. 1 shows that spray drying of mannitol at different outlet temperatures leads to the formation of particles of different surface roughness. At 67 °C outlet temperature (M67), the carrier surface consists of rod shaped crystals of approximately 3 μm in length that give the particles a rough appearance. For those particles, the highest mean R_a-value of 140.33 ± 27.75 nm was measured (Fig. 3). At intermediate temperatures (M84) the particle surface gets smoother (88.73 ± 22.25 nm), due to smudging of the single crystals at the particle surface. At even higher temperatures (M102), the surface roughness increases again (125.00 ± 19.92 nm) due to the presence of smaller, single crystals at the surface.

Because of the coarse crystalline nature of M67 it is not much of a surprise that the XRPD analysis reveals that the product is crystalline (Fig. 2), consisting of 100.00 ± 0.00% of the thermodynamically stable polymorph I [28]. Also for M80 and M92, 100.00 ± 0.00% of mod. I was found. For M84 and M102, a small amount of mod. II apart from mod. I was determined (0.17 ± 0.14% and 0.5 ± 0.47%, respectively). However, the limit of detection is 1% and the results of the Rietveld calculations can be accepted within a confidence of ±1%. This means that the small amounts of mod. II determined might even be errors of the applied calculation method. As already shown by Littringer et al. [25], no correlation between process parameters and polymorph composition could be found within the range examined. The spray dried products under investigation are crystalline.

Unlike at lab-scale [33], particles do not only change in surface roughness but also in shape. At 67 °C, spherical particles are obtained (M67). With higher temperatures, the particles get a mulberry like shape and the surface is partially collapsed (M84).

Table 1
Particle size distribution of the carrier particles spray dried at different outlet temperatures and determined by laser diffraction (mean ± SD, n = 3).

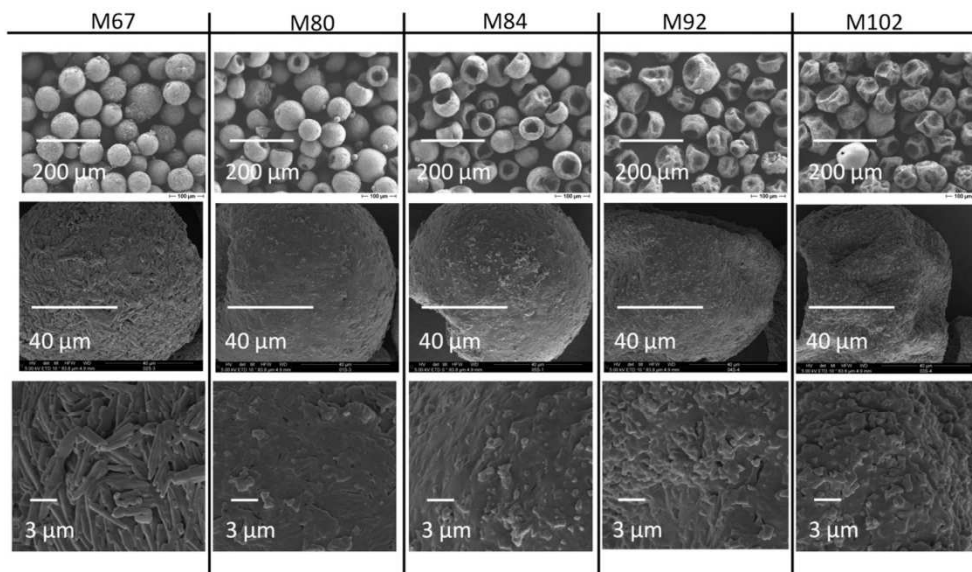|	M67	M80	M84	M92	M102
$X_{10.3}$ (μm)	45.7 ± 1.1	44.9 ± 2.3	54.7 ± 0.6	57.6 ± 0.5	59.0 ± 0.4
$X_{50.3}$ (μm)	81.4 ± 0.8	78.4 ± 0.5	83.4 ± 0.6	85.0 ± 0.6	86.4 ± 0.3
$X_{90.3}$ (μm)	122.4 ± 0.8	115.2 ± 0.6	119.5 ± 0.6	121.1 ± 0.9	122.0 ± 0.3
Span/$(X_{90.3} - X_{10.3})/X_{50.3}$	0.9 ± 0.0	0.9 ± 0.0	0.8 ± 0.0	0.7 ± 0.0	0.7 ± 0.0

Fig. 1. SEM micrographs (Hitachi – upper line, Zeiss – middle and lower line) of the spray dried carrier particles.
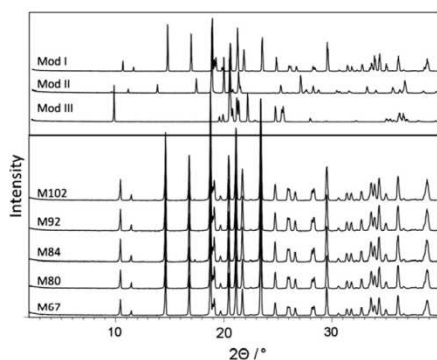

Fig. 2. XRPD patterns of the pure mannitol polymorphs (mod. I, II, and III) and the spray dried samples (M67, M80, M84, M92, and M102).

Fig. 3. Mean R_a of the spray dried carrier particles determined by tilted images of SEM and 3D reconstruction (mean ± SD, n = 3).

With further increasing temperatures, the surface is collapsed at multiple spots so that the whole particle looks shriveled like a raisin (M102). In order to quantify the particle shape, the aspect ratio, which is the ratio of the particle length to its width, was calculated. Fig. 4 clearly shows that the aspect ratio decreases with increasing outlet temperatures; however, the decrease is little for M67 (0.925) and M80 (0.918) because only few particles have the mulberry like shape at 80 °C. At 84 °C outlet temperature, nearly all particles have a collapsed surface (0.905). For M102, the lowest aspect ratio of 0.870 was measured. The influence of pilot-scale spray drying process parameters on carrier properties such as surface roughness and particle size had been studied in detail prior to these experiments and can be found at Littringer et al. [25]. Interestingly, the impact of the outlet temperature on the surface roughness of the smaller particles spray dried by Maas et al. [27] at a lab-scale spray dryer was different. Smooth particles were obtained at lower spray drying outlet temperatures, whereas higher temperatures caused rougher surfaces. The reason for the differences of surface roughness and shape depending on the scale of the spray dryer is not fully understood by now and will be the focus of further research.

Littringer et al. [34] showed that the spray dried products are porous. Because of the permeable or partly permeable shell (see helium pycnometry) and the porous nature of the particles, BET surface values were not used to calculate surface roughness parameters as proposed by Kou et al. [35] or done by Dickhoff et al. [36].

In order to characterize the powder bulk properties of the spray dried mannitol carrier particles, the bulk and tapped densities were determined. Table 2 shows that for M67 the bulk as well as the tapped density is lower than for all the other powders. For M67 and M80, the bulk density differs about 24%. The reason for
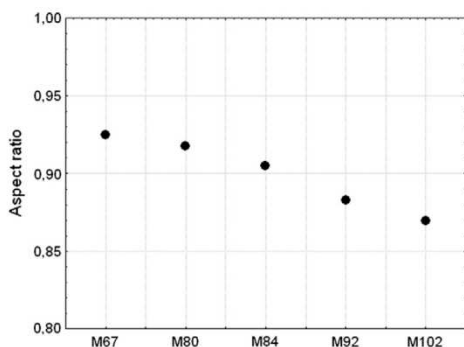
Fig. 4. Aspect ratio of the spray dried carrier particles determined by morphology G3 image analysis system ($d_{50.0}$, $n \geqslant 3200$).

this might be either a lower density of the single powder particles or a lower packing density of the powder. It was not possible to determine the particle density of the single particles by helium pycnometry due to the porous nature of the spray dried products [34] and the permeable or partly permeable shell. Table 2 shows that for M67 a density of 1.492 ± 0.001 g/cm^3 was measured, which is according to Burger et al. [28] the true density of mannitol (mod. I), indicating a helium permeable shell. As the initial droplet size of the different particles is the same, thus the amount of mannitol within the drying droplet, and the spray dried particles have a similar particle size, it is not likely that the different particles differ in the density of the single particles. It is more likely that the differences are caused by different packing arrangements of the solidified material. The consequences of this lower packing density of M67 with respect to the metered and delivered mass of the adhesive mixtures will be discussed below.

As powder flow is important for reproducible dosing, the Hausner ratio was determined from bulk and tapped density measurements. Table 2 shows that all powders have a mean Hausner ratio of 1.18–1.22 indicating good to fair flowability. Compared to the mannitol carrier particles that had been spray dried at lab-scale by Maas [26], a significant improvement in powder flowability could be achieved due to the increase of the median particle size from approximately 14 μm to 80 μm. The particles spray dried at lab-scale showed a Hausner ratio of 1.56–1.62 corresponding to very poor to very very poor flowing behavior.

3.2. Metering reproducibility of the carrier particles

In order to determine the metering reproducibility of the different carrier particles with respect to their use as carrier particles in dry powder inhalers, a method related to the DPI device was employed. Therefore, 50 puffs were released via the Novolizer® and the loss of mass of the inhaler after each puff was recorded (Fig. 5). The mean mass and the coefficient of variation of the 50 puffs was calculated (Table 4).

Fig. 5. Masses of the pure carrier particles released from a Novolizer® multi-dose inhaler.

Table 3
Mixing homogeneity expressed as the coefficient of variation of the drug content of $n = 10$ samples drawn from the adhesive mixtures of micronized salbutamol sulfate and mannitol carrier particles spray dried at different outlet temperatures.

	M67	M80	M84	M92	M102
Batch 1 (%)	0.85	2.80	2.48	2.96	2.26
Batch 2 (%)	1.73	2.74	2.74	2.13	1.20
Batch 3 (%)	4.35	5.89	1.67	1.28	3.75

Fig. 5 shows that all released masses of the three batches of the different carrier particles are approximately the same indicating reproducible metering. This is also verified by the coefficients of variation (Table 4) which are between 4.30% and 7.04%. Compared to the lab-scale carrier particles of Maas et al. [27] who found coefficients of variation of 21.2–36.2%, all pilot-scale spray dried particles performed better regarding their metering reproducibility due to the larger size of the carrier particles.

For M67, a significantly lower mass of 7.71 ± 0.32 mg compared to the other carrier particles (8.81–9.73 mg, Table 4) was observed. The reason for this can be explained by the results of the bulk and tapped density measurements. M67 shows a significantly lower bulk and tapped powder density. As a matter of fact, a lower mass of mannitol is released (volumetric dosing).

3.3. Metering reproducibility of the adhesive mixtures/metered mass

Like the metering reproducibility of the pure carriers, the metering reproducibility of the adhesive mixtures was determined by releasing 50 puffs via the Novolizer® multi-dose inhaler (Fig. 6).

Table 2
Powder characteristics of the carrier particles spray dried at different outlet temperatures (mean ± SD, $n = 3$).

	M67	M80	M84	M92	M102
Bulk density (g/cm^3)	0.41 ± 0.00	0.51 ± 0.01	0.50 ± 0.01	0.49 ± 0.01	0.49 ± 0.01
Tapped density (g/cm^3)	0.48 ± 0.00	0.60 ± 0.00	0.60 ± 0.01	0.60 ± 0.01	0.60 ± 0.01
Powder density (g/cm^3)	1.492 ± 0.001	1.474 ± 0.001	1.421 ± 0.001	1.396 ± 0.001	1.471 ± 0.003
Hausner ratio	1.18 ± 0.01	1.18 ± 0.02	1.20 ± 0.04	1.21 ± 0.01	1.22 ± 0.04

Table 4
Mean mass and coefficient of variation of 50 puffs of the pure carrier particles delivered via a Novolizer® multi-dose inhaler (mean ± SD, n = 3).

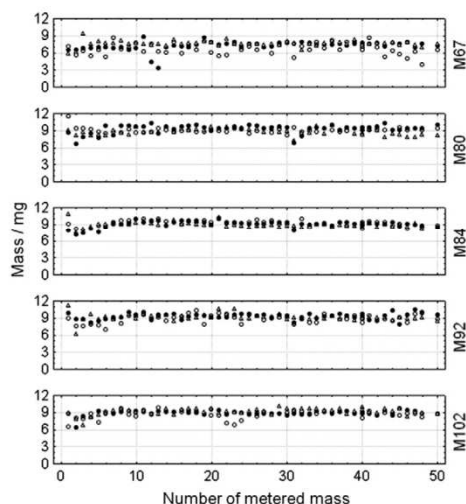|	M67	M80	M84	M92	M102
Mean (mg)	7.71 ± 0.32	9.73 ± 0.09	9.27 ± 0.23	9.05 ± 0.26	8.81 ± 0.18
CV (%)	4.90 ± 0.96	7.04 ± 0.69	4.30 ± 0.50	4.32 ± 0.62	4.63 ± 0.89

Fig. 6. Masses of the adhesive mixtures released from a Novolizer® multi-dose inhaler.

Subsequently, the mean and coefficient of variation of the 50 puffs was calculated (Table 5).

The coefficients of variation of the adhesive mixtures are similar to the ones of the pure carriers. If there is any difference at all, the coefficient of variation of the mixtures is slightly higher (Tables 4 and 5). The reason for the higher coefficient of variation of the mixtures might be a decreased flowability due to adhered API fines present on the carrier surface.

As expected from the measurements of the pure carrier, also the mixture containing M67 showed a significantly lower metered mass (7.14 ± 0.50 mg, Table 5) compared to the other mixtures (8.88–9.06 mg). As already described above, a lower bulk and tapped density of the pure carrier and consequently the mixture is the reason for this behavior. A significant difference of the metered mass between the pure carrier and the mixtures was only observed for M80. A metered mass of 9.73 ± 0.09 mg was measured for the pure carrier, whereas a mass of 9.02 ± 0.20 mg was found for the mixture. The reason for this might be a lower packing density of the mixture compared to the pure carrier due to the increased roughness which is caused by the attached API particles.

Table 5
Mean metered mass and coefficient of variation of 50 puffs of the adhesive mixtures delivered via a Novolizer® multi-dose inhaler (mean ± SD, n = 3).

	M67	M80	M84	M92	M102
Mean (mg)	7.14 ± 0.50	9.02 ± 0.20	9.01 ± 0.09	9.06 ± 0.22	8.88 ± 0.25
CV (%)	11.44 ± 4.20	6.80 ± 1.62	6.32 ± 0.55	7.00 ± 1.16	6.53 ± 1.16
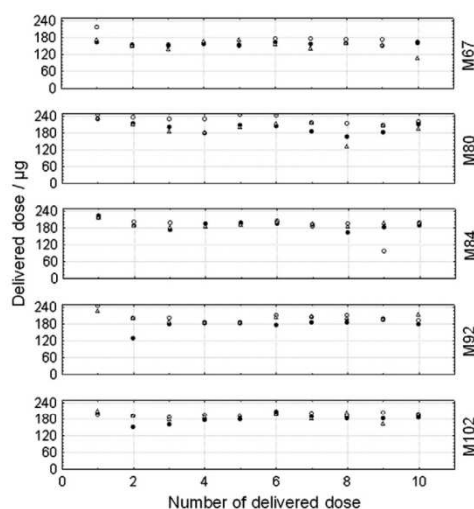
Fig. 7. Delivered dose of the adhesive mixtures delivered via a Novolizer® multi-dose inhaler.

3.4. Delivered dose and uniformity of delivered dose

The delivered dose, which is defined as the mass of the active that leaves the inhaler device during testing, was determined according to the European Pharmacopoeia (preparations for inhalation: inhalanda, Ph. Eur., 7.0). Therefore, for each of the three batches of the adhesive mixtures, 10 puffs from the Novolizer® multi-dose inhaler were delivered (puff 1–5 and 45–50 from a series of 50 puffs) and the amount of active was determined by HPLC (Fig. 7). Subsequently, the mean amount of the active of the 10 discharges (delivered dose) was calculated (Table 6). In order to get an idea how much of the active was lost during testing, the percentage of recovery of the delivered dose (PRDD) was determined also. All values were within a range of 85–95%.

In accordance with the metered mass (Table 5), the delivered dose (Fig. 7, Table 6) of the mixtures containing M67 (159.30 ± 8.85 μg) was significantly lower than those of M80, M84, M92, and M102 (188.70–208.04 μg). As already described, the reason for this behavior is a lower bulk density of the adhesive mixture containing M67 and hence a lower mass of the active that flows into the metering chamber of the inhaler during powder dosing. The bulk densities of M67 and M80 differ by 24%. Multiplying the delivered dose of M67 by 1.24 approximates the delivered dose of M80.

According to the European Pharmacopoeia, the formulation complies with the test of the uniformity of the delivered dose if 9 out of 10 results lie between 75% and 125% of the average value and all lie between 65% and 135%. If 2 or 3 values exceed the limits of 75–125%, the test must be repeated for 2 more inhalers. Altogether not more than 3 of the 30 values must lie outside the limits of 65–135%.

The uniformity was achieved for M67, M80, and M102 (Fig. 7). For the ordered mixtures M84 one (51.62%) and for M92 two (69.00%, 142.54%) out of thirty samples, which were tested during the uniformity of delivered dose experiments, did not fulfill the requirements of the European pharmacopoeia. This is unexpected as all powders and mixtures showed equal flowing behavior and mixing homogeneity. However, an explanation might be that all

Table 6
Aerodynamic characteristics of the adhesive mixtures of micronized salbutamol sulfate and mannitol carrier particles spray dried at different outlet temperatures. (DD = delivered dose; FPD = fine particle dose; ED = emitted dose; FPF = fine particle fraction; PRDD = percentage of recovery of the delivered dose; PRED = percentage of recovery of the emitted dose; mean ± SD, n = 3).

	M67	M80	M84	M92	M102
DD (µg)	159,30 ± 8,85	208,04 ± 17,65	190,84 ± 3,08	196,79 ± 8,82	188,71 ± 6,99
PRDD (%)	91.12 ± 10.61	93.63 ± 6.99	86.91 ± 1.90	88.34 ± 4.21	86.28 ± 3.12
FPF (%)	29.23 ± 4.73	14.62 ± 1.18	10.51 ± 1.03	12.31 ± 1.54	13.05 ± 1.11
FPD (µg)	49.07 ± 5.73	32.34 ± 1.67	22.09 ± 2.19	26.39 ± 3.37	26.95 ± 2.45
ED (µg)	168.79 ± 8.41	221.91 ± 9.01	210.17 ± 7.09	214.33 ± 1.79	206.43 ± 3.02
PRED (%)	96.20 ± 4.40	99.76 ± 3.17	105.45 ± 11.04	96.50 ± 0.29	94.43 ± 1.13

the tests only covered the amount of the powder that left the inhaler and not the amount that might have remained within the device (e.g., at the wall of the cyclone). It is possible that the small active particles accumulate within the device after the delivery because of electrostatic charging and might be discharged as a whole, when a certain agglomerate size is exceeded, resulting in a higher amount that is detected (M92: 142.54%). Another reason for the low emitted doses might be an insufficient actuation of the inhaler dosing due to material wearing of the metering device (M84: 51.62%; M92: 69.00%).

Another explanation for this fail could be an insufficient homogeneity of the powder blend. However, for M67 (4.35%), M80 (5.89%), and M102 (3.75%), which are the carrier particles that complied with the test of the uniformity of the delivered dose, the highest CVs of the mixing homogeneity were found (Table 3), indicating that the variations of the delivered dose for M84 and M92 are not a cause of insufficient powder homogeneity.

3.5. Assessment of fine particles

In order to get an idea how much of the active was lost during testing, the percentage of recovery of the emitted dose (PRED) was determined also. All values were within a range of 94–105%.

Consistently with the metered mass (Table 5) and the delivered dose (Table 6), the emitted dose (Table 6), which is the amount of API found in the whole impactor, of mixtures containing M67 (168.79 ± 8.41 µg) was significantly lower than those of M80,

M84, M92, and M102 (206.43–221.91 µg), because of the lower bulk density of the adhesive mixture containing M67.

The SEM micrographs of the adhesive mixtures (Fig. 8) reveal that the micronized active accumulates within the cavities of the carrier (especially M102). This entrapment of API particles in the carrier surface irregularities and cavities was also reported by de Boer et al. [37]. However, Dickhoff et al. [36] mentioned that drug agglomerate re-dispersion from such cavities might also be observed, especially for higher carrier payloads (4.0% m/m) due to inertial impaction forces during mixing. However, drug agglomerate re-dispersion from the carrier surface irregularities was found to be negligible, if present at all, despite the rather high energy input during Turbula®-mixing (90 min, 62 rpm) and a carrier payload of 2.4% (m/m). One reason for this might be the porous nature of the spray dried carrier particles leading on the one hand to lower inertial impaction forces during mixing compared to particles of higher density. On the other hand, porous particles have a comparably higher outer specific surface, resulting in a comparably lower API surface covering of the carrier particles.

The presence of surface cavities is reported in literature to enhance as well as to decrease the API detachment from the carrier surface. For example, smoother lactose carriers recrystallized from carbopol gels increased the fine particle fraction when using the Rotahaler device [38]. Also, ethanol (70% V/V) smoothed lactose particles delivered by the Spinhaler® device performed better than the untreated ones [39]. Further lactose crystals treated with 95%
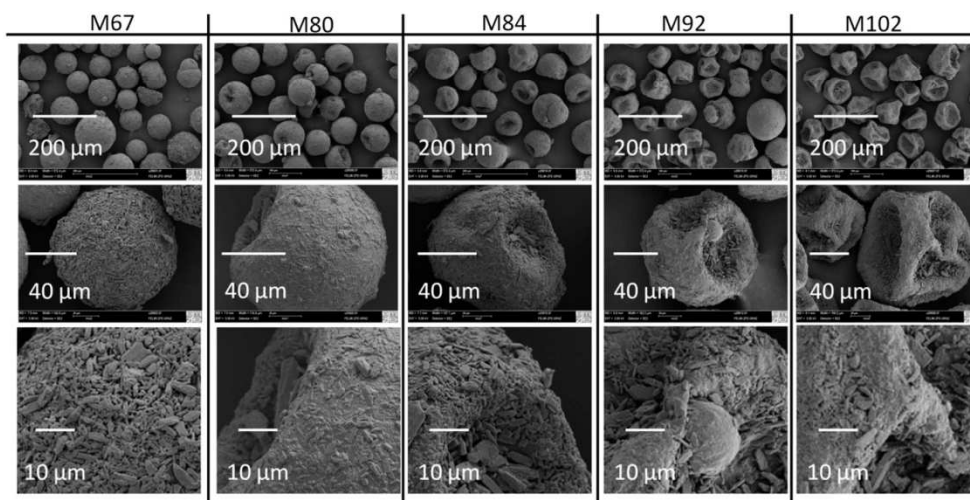

Fig. 8. SEM micrographs (Zeiss) of the adhesive mixtures of micronized salbutamol sulfate and spray dried mannitol carrier particles of different surface roughness and shape.

(V/V) ethanol showed more surface irregularities than the control group and performed worse with the Rotahaler® device [40].

The opposite was shown by Dickhoff et al. [36] when using an air classifier inhaler. He proposed that the presence of surface discontinuities may be beneficial in order to improve the fine particle fraction due to lower press-on forces emerging during mixing. Additionally, the surface asperities provide the detached API particles a free path to fly away from the carrier surface upon collision of the carrier particles (inertial separation forces) [41].

However, the advantages of surface discontinuities might only be beneficial when inhalers are used that rely mainly on inertial separation forces (e.g., Novolizer®). Inhalers where drag, lift, and friction forces are dominant are likely to perform worse in the presence of surface irregularities. The reason for this is that the API particles inside the carrier cavities are sheltered from those removal forces [42].

Interestingly, despite the fact that a Novolizer® device was used, carrier particles with surface cavities performed worse than the perfect spheres. The reason for this might be that the Novolizer® inhaler is optimized for non-porous lactose carrier particles of larger size [43]. When carrier particles with a lower aerodynamic diameter (e.g., smaller size or lower density) are used, the residence time within the inhaler is lower. As a matter of fact, inertial separation forces are lower. Further inertial forces are proportional to the particle density.

The porous, spray dried mannitol carrier particles [34] used in this study are likely to experience comparably low inertial separation forces within the Novolizer®. This might also be the reason why relatively low fine particle fractions (10.51–29.23% vs. 30–46%) were found [42]. However, when inertial forces are low, drag, lift, and friction forces are responsible for API detachment from the carrier surface. But these forces have no access to active particles trapped within surface cavities. This might be the reason why the highest fine particle faction is found for M67 particles (Fig. 9) which are spherically shaped (aspect ratio = 0.925), despite the fact that an air classifier inhaler was used.

Interestingly strong electrostatic charging was observed for all formulations during DPI testing. The influence of electrostatic charging on the performance of the inhalates is still unclear and will be focus of further studies.

Apart from carrier shape, also surface roughness was found to influence the detachment of the active particles from the carrier. Although the difference of the R_a values of M67 (mean R_a = 140.33 ± 27.75 nm) and M80 (mean R_a = 88.73 ± 22.25 nm) (Fig. 3) is not statistically significant (p = 0.06), the SEM micro-

graphs clearly show that they differ in surface roughness (Fig. 1). For those two carrier particles, which are both of almost spherical shape (aspect ratio = 0.925 and 0.918, respectively, Fig. 4), the FPF decreased from 29.23 ± 4.73% (M67) to 14.62 ± 1.18% (M80). This means the rougher the surface the higher the fine particle fraction. Consequently, the surface roughness of M67 is such that it leads to a decrease of the contact area of the active and the carrier and thereby to a decrease of the interparticle forces. The largest difference in FPF was found for M67 (FPF = 29.23 ± 4.73%, aspect ratio = 0.925) and M84 (FPF = 10.51 ± 1.03%, aspect ratio = 0.905). For those two carriers, there is not only a change in surface roughness, but also in shape (Figs. 1 and 4).

In contrast to the experiments that had been carried out by Maas et al. [27] previously, the highest fine particle fraction was observed for mixtures with M67 carrier particles, which were those with the coarse crystalline surface. These results are somehow unexpected as the opposite had occurred at lab-scale [27], where the lowest FPF was found for adhesive mixtures with carrier particles of rough surface. One explanation for this behavior might be that the rough particles at lab-scale showed a different roughness than those at pilot-scale (Fig. 10). As already described by Young et al. [44], the ratio between roughness spacings and API particle size plays a crucial role in interparticle forces (Fig. 11). At pilot-scale, the rough particles might have a roughness as schematically shown on the right hand side of Fig. 11, whereas at lab-scale a long wave roughness as drawn on the left hand side might have been achieved leading to higher interparticle forces. The SEM micrographs clearly show the different roughnesses of the "rough" carrier particles at lab- and pilot-scale (Fig. 10).

Another difference between the experiments performed by Maas et al. [27] and the present experiments was the size of the carrier particles. The median carrier particle size at lab-scale was approximately 14 μm. Considering the porous nature of the spray dried particles, this corresponds to an even lower aerodynamic diameter. Due to the small aerodynamic diameter, the lab-scale carrier particles might not be separated in the preseparator during NGI testing and might have access to the lower stages of the impactor. Hence the amount of the API is detected even though there is no detachment of the active from the carrier surface. This might be the reason, why much higher FPFs (56.3–73.8%) were

Fig. 10. SEM micrographs (Hitachi) of rough particles spray dried at lab-scale (left, [26]) and pilot-scale (M67).

Fig. 11. Influence of surface roughness on interparticle forces between carrier and micronized active. Depending on the size scale of the surface roughness and the particle size of the active, the contact area and hence interparticle forces may be modified.
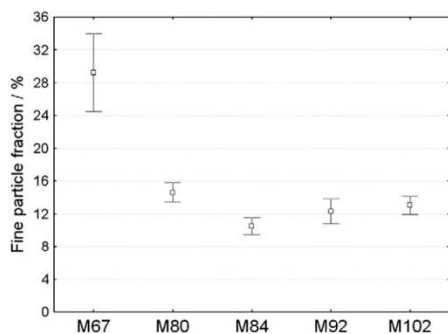

Fig. 9. Fine particle fraction of the adhesive mixtures of micronized salbutamol sulfate and mannitol carrier particles spray dried at different outlet temperatures (mean ± SD, n = 3).
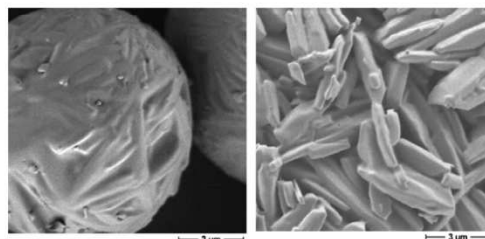
found by Maas et al. [27] compared to the present study (10.51–29.23%). Another difference was the carrier payload (lab-scale: 1/100, pilot-scale: 1/42). This makes the comparison of the fine particle fractions difficult [45].

4. Conclusion and outlook

This study demonstrates that spray drying mannitol is an appropriate technique for the preparation of alternative carrier particles of sufficient size for dry powder inhalers. Surface roughness may be targeted by adjusting the appropriate spray drying outlet temperature. However, particle shape depends on the process parameters also. It was shown that surface roughness as well particle shape influences the detachment of the active particles from the carrier. The highest fine particle fraction was achieved with carrier particles of spherical shape and a rough surface. Smoother surfaces and surface cavities reduced the fine particle fraction released from the carrier.

Acknowledgements

References

[1] D.I. Daniher, J. Zhu, Dry powder platform for pulmonary drug delivery, Particuology 6 (4) (2008) 225–238.

[2] N.R. Labris, M.B. Dolovich, Pulmonary drug delivery. Part I: Physiological factors affecting therapeutic effectiveness of aerosolized medications, British Journal of Clinical Pharmacology 56 (2003) 588–599.

[3] A.J. Hickey, Lung deposition and clearance of pharmaceutical aerosols: what can be learned from inhalation toxicology and industrial hygiene?, Aerosol Science and Technology 18 (3) (1993) 290–304

[4] H.W. Frijlink, A.H. de Boer, Pulmonary Drug Delivery – Basics, Application and Opportunities for Small Molecules and Biopharmaceutics – Chapter III Application Devices. Editio Cantor Verlag für Medizin und Naturwissenschaften GmbH.

[5] A. de Boer, H. Chan, R. Price, A critical view on lactose-based drug formulation and device studies for dry powder inhalation: which are relevant and what interactions to expect? Advanced Drug Delivery Reviews, 2011.

[6] G. Pilcer, K. Amighi, Formulation strategy and use of excipients in pulmonary drug delivery, International Journal of Pharmaceutics 392 (1–2) (2010) 1–19 (review).

[7] D. El-Sabawi, R. Price, S. Edge, Novel temperature controlled surface dissolution of excipient particles for carrier based dry powder inhaler formulation, Drug Development and Industrial Pharmacy 32 (2006) 243–251.

[8] D. El-Sabawi, S. Edge, R. Price, Continued investigation into the influence of loaded dose on the performance of dry powder inhalers: surface smoothing effects, Drug Development and Industrial Pharmacy 32 (2006) 1135–1138.

[9] F. Ferrari, D. Cocconi, R. Bettini, F. Giordano, P. Santi, M. Tobyn, R. Price, P. Young, C. Caramella, P. Colombo, The surface roughness of lactose particles can be modulated by wet-smoothing using a high-shear mixer, AAPS PhramSciTech 5 (2004).

[10] K. Iida, H. Todo, H. Okamoto, K. Danjo, H. Leuenberger, Preparation of dry powder inhalation with lactose carrier particles surface-coated using a wurster fluidized bed, Chemical and Pharmaceutical Bulletin 53 (2005) 431–434.

[11] H.-K. Chan, N.Y.K. Chew, Novel alternative methods for the delivery of drugs for the treatment of asthma, Advanced Drug Delivery Reviews 55 (7) (2003) 793–805.

[12] H. Steckel, P. Markefka, H. teWierik, R. Kammelar, Effect of milling and sieving on functionality of dry powder inhalation products, International Journal of Pharmaceutics 309 (1–2) (2006) 51–59.

[13] K. Iida, Y. Inagaki, H. Todo, H. Okamoto, K. Danjo, H. Luenberger, Effects of surface processing of lactose carrier particles on dry powder inhalation properties of salbutamol sulfate, Chemical and Pharmaceutical Bulletin 52 (2004) 938–942.

[14] H. Adi, I. Larson, H. Chiou, P. Young, D. Traini, P. Stewart, Agglomerate strength and dispersion of salmeterol xinafoate from powder mixtures for inhalation, Pharmaceutical Research 23 (2006) 2556–2565.

[15] R. Guchardi, M. Frei, E. John, J. Kaerger, Influence of fine lactose and magnesium stearate on low dose dry powder inhaler formulations, International Journal of Pharmaceutics 348 (1–2) (2008) 10–17.

[16] M.D. Louey, S. Razia, P.J. Stewart, Influence of physico-chemical carrier properties on the in vitro aerosol deposition from interactive mixtures, International Journal of Pharmaceutics 252 (1–2) (2003) 87–98.

[17] B. Dickhoff, A. de Boer, D. Lambregts, H. Frijlink, The effect of carrier surface treatment on drug particle detachment from crystalline carriers in adhesive mixtures for inhalation, International Journal of Pharmaceutics 327 (1–2) (2006) 17–25.

[18] H. Steckel, N. Bolzen, Alternative sugars as potential carriers for dry powder inhalations, International Journal of Pharmaceutics 270 (2004) 297–306.

[19] P.M. Young, H. Chiou, T. Tee, D. Traini, H.-K. Chan, F. Thielmann, D. Burnett, The use of organic vapor sorption to determine low levels of amorphous content in processed pharmaceutical powders, Drug Development and Industrial Pharmacy 33 (1) (2007) 91–97.

[20] Y. Kawashima, T. Serigano, T. Hino, H. Yamamoto, H. Takeuchi, Effect of surface morphology of carrier lactose on dry powder inhalation property of pranlukast hydrate, International Journal of Pharmaceutics 172 (1–2) (1998) 179–188.

[21] M.I.U. Islam, R. Sherrell, T.A.G. Langrish, An investigation of the relationship between glass transition temperatures and the crystallinity of spray-dried powders, Drying technology 28 (2010) 361–368.

[22] G. Saint-Lorant, P. Leterme, A. Gayot, M. Flament, Influence of carrier on the performance of dry powder inhalers, International Journal of Pharmaceutics 334 (1–2) (2007) 85–91.

[23] W. Kaialy, G.P. Martin, H. Larhrib, M.D. Ticehurst, E. Kolosionek, A. Nokhodchi, The influence of physical properties and morphology of crystallised lactose on delivery of salbutamol sulphate from dry powder inhalers, Colloids and Surfaces B: Biointerfaces 89 (2012), 29–39.

[24] S.K. Tee, C. Marriott, X.M. Zeng, G.P. Martin, The use of different sugars as fine and coarse carriers for aerosolised salbutamol sulphate, International Journal of Pharmaceutics 208 (2000) 111–123.

[25] E.M. Littringer, A. Mescher, S. Eckhard, H. Schröttner, C. Langes, M. Fries, U. Griesser, P. Walzel, N.A. Urbanetz, Spray drying of mannitol as a drug carrier – the impact of process parameters on the product properties, Drying Technology 30 (2012) 114–124.

[26] S.G. Maas, Optimierung trägerbasierter Pulverinhalate durch Modifikation der Trägeroberfläche mittels Sprühtrocknung. PhD Thesis, Heinrich-Heine-Universität Düsseldorf, 2009.

[27] S.G. Maas, G. Schaldach, P.E. Walzel, N.A. Urbanetz, Tailoring dry powder inhaler performance by modifying carrier surface topography by spray drying, Atomization and Sprays 20 (2010) 763–774.

[28] A. Burger, J.-O. Henck, S. Hetz, J.M. Rollinger, A.A. Weissnicht, H. Stöttner, Energy/temperature diagram and compression behaviour of the polymorphs of D-mannitol, Journal of Pharmaceutical Sciences 89 (2000) 457–468.

[29] A. Kaminsky, W. Glazer, Crystal optics of mannitol, c6h14o6: crystal growth, structure, basic physical properties, birefringence, optical activity, Faraday effect, electro-optic related effect and model calculations, Zeitschrift für Kristallographie 212 (1997) 238–296.

[30] G.R.R. Berman, H.M. Jeffrey, The crystal structures of the alpha and beta forms of d-mannitol, Acta Crystallographica Section B – Structural Crystallography and Crystal Chemistry 24 (1968) 442–449.

[31] F.R. Fronczek, H.N. Kamel, M. Slattery, Three polymorphs (alpha, beta and delta) of D-mannitol at 100 k, Acta Crystallographica C59 (2003) o567–o570.

[32] V. Marple, B. Olson, K. Santhanakrishnan, J. Michell, S. Murray, B. Hudson-Curtis, Next generation pharmaceutical impactor (a new impactor for pharmaceutical inhaler testing). Part II: Archival calibration, Journal of Aerosol Medicine 16 (2003) 301–324.

[33] S.G. Maas, G. Schaldach, E.M. Littringer, A. Mescher, U.J. Griesser, D.E. Braun, P. Walzel, N.A. Urbanetz, The impact of spray drying outlet temperature on the particle morphology of mannitol, Powder Technology 213 (2011) 27–35.

[34] E.M. Littringer, A. Mescher, S.G. Maas, P. Walzel, N.A. Urbanetz, Influence of droplet size on the crystallization behaviour of aqueous d-mannitol solutions during spray drying, in: ILASS2011 Conference Proceedings, 2011, pp. 1–8.

[35] X. Kou, L.W. Chan, H. Steckel, P.W. Heng, Physico-chemical aspects of lactose for inhalation, Advanced Drug Delivery Reviews, 2011.

[36] B. Dickhoff, A. de Boer, D. Lambregts, H. Frijlink, The interaction between carrier rugosity and carrier payload, and its effect on drug particle redispersion from adhesive mixtures during inhalation, European Journal of Pharmaceutics and Biopharmaceutics 59 (2005) 197–205.

[37] A.H. de Boer, P. Hagedoorn, D. Gjaltema, D. Lambregts, M. Irngartinger, H.W. Frijlink, The rate of drug particle detachment from carrier crystals in an air classifier-based inhaler, Pharmaceutical Research 21 (2004) 2158–2166.

[38] X.M. Zeng, G.P. Martin, C. Marriott, J. Pritchard, The use of lactose recrystallised from carbopol gels as a carrier for aerosolised salbutamol sulphate, European Journal of Pharmaceutics and Biopharmaceutics 51 (1) (2001) 55–62.

[39] K. Iida, Y. Hayakawa, H. Okamoto, K. Danjo, H. Leuenberger, Preparation of dry powder inhalation by surface treatment of lactose carrier particles, Chemical and Pharmaceutical Bulletin 51 (2003) 1–5.

[40] X.-M. Zeng, G.P. Martin, C. Marriott, J. Pritchard, Lactose as a carrier in dry powder formulations: the influence of surface characteristics on drug delivery, Journal of Pharmaceutical Sciences 90 (2001) 1424–1434.

[41] A.H. de Boer, P. Hagedoorn, D. Gjaltema, J. Goede, H. Frijlink, Air classifier technology (act) in dry powder inhalation Part 1. Introduction of a novel force distribution concept (fdc) explaining the performance of a basic air classifier on adhesive mixtures, International Journal of Pharmaceutics 260 (2003) 187–200.

[42] A. de Boer, P. Hagedoorn, D. Gjaltema, J. Goede, H. Frijlink, Air classifier technology (act) in dry powder inhalation: Part 4. Performance of air classifier technology in the novolizer® multi-dose dry powder inhaler, International Journal of Pharmaceutics 310 (1–2) (2006) 81–89.

[43] A. de Boer, P. Hagedoorn, D. Gjaltema, J. Goede, H. Frijlink, Air classifier technology (act) in dry powder inhalation: Part 3. Design and development of an air classifier family for the novolizer® multi-dose dry powder inhaler, International Journal of Pharmaceutics 310 (1–2) (2006) 72–80.

[44] P.M. Young, D. Roberts, H. Chiou, W. Rae, H.-K. Chan, D. Traini, Composite carriers improve the aerosolisation efficiency of drugs for respiratory delivery, Journal of Aerosol Science 39 (1) (2008) 82–93.

[45] P.M. Young, S. Edge, D. Traini, M.D. Jones, R. Price, D. El-Sabawi, C. Urry, C. Smith, The influence of dose on the performance of dry powder inhalation systems, International Journal of Pharmaceutics 296 (1–2) (2005) 26–33.

Supplement: *"Spray dried mannitol carrier particles with tailored surface properties - The influence of carrier surface roughness and shape"*

Introduction

XRPD is a widely used technique to determine the amorphous content of a material. However one drawback of this method is that the limit of quantification is in the range of 5-10 % [3]. Consequently small amounts of amorphous material which might be present at the particle surface (reactive "hot spots "[2]) will not be detected with this method. However because of the higher sensitivity Buckton and Darcy [1, 2] as well as Pilcer et al. [3] suggest to use moisture sorption analysis in order to measure the amorphous content of powders for inhalation. In order to make sure that the differences of the fine particle fractions are not a result of amorphous spots at the carrier surface, which might have not been detected by XRPD, moisture sorption analysis of the products dried at the lowest (M67), highest (M102) and at intermediate temperature (M84) were performed too.

Materials and Methods - Water sorption analysis

The moisture sorption isotherms were recorded with a SPS-11 moisture sorption analyzer (Projekt Messtechnik, Ulm, Germany) at a temperature of 25°C ± 0.1°C. The measurement cycle was started at 0% relative humidity (RH), RH was increased in two 5% steps to 10% RH, further increased up to 90% RH in 10% steps and from 90% to 95% RH in one step. Subsequently the RH was decreased again to 90% RH, further decreased in 10% steps to 10% RH and in two 5%-steps to 0% RH. The equilibrium condition for each step was set to a mass constancy of ±0.001 % over 60 min. Samples were analyzed in duplicate.

Results

In the presence of amorphous spots a higher amount of water is absorbed than without amorphous spots. The water absorbed acts as a plasticizer and reduces the glass transition temperature (T_g) of the amorphous material. Once the temperature of the experiment is higher than the glass transition temperature the molecules have sufficient mobility to crystallize and vapor is expelled from the crystal lattice [3, 6]. This sudden loss of water can be seen in the moisture sorption isotherms (sudden decrease in mass) and may be used to determine the amorphous content of the sample. In Figure 1 the moisture induced change of mass of one of two runs of the mannitol samples spray dried at different outlet temperatures versus relative humidity is shown.

Figure 1 shows that there is a continuous increase in mass attributed to the sorption of water in the whole RH range studied. No sudden decrease of mass was detected indicating that there are no

amorphous spots. For all samples the sorption isotherm looks similar. The final moisture uptake was determined to be between 5.43 % and 6.97 % (Table 1).
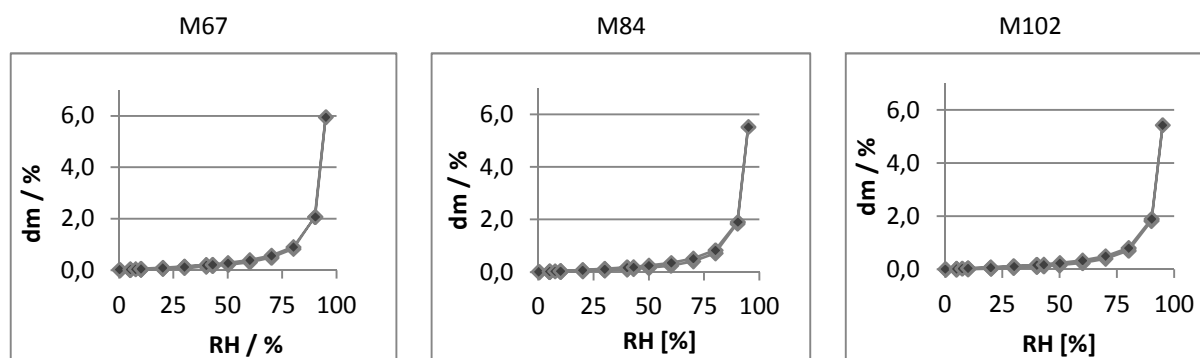
Figure 1. Sorption isotherms of mannitol samples spray dried at different outlet temperatures.

Table 1. Moisture uptake of mannitol samples spray dried at different outlet temperatures.

	M67 / %	M84 / %	M102 / %
Measurement 1	5.95	5.53	5.43
Measurement 2	6.97	5.64	5.54

Conclusion

This study verifies that irrespective of the process parameters adjusted there are no amorphous spots at the particle surface. The differences of the fine particle fractions observed for the different carriers are not a result of amorphous material which might have been present at the surface of the particles.

References

[1] Graham Buckton and Patricia Darcy. The use of gravimetric studies to assess the degree of crystallinity of predominantly crystalline powders. *International Journal of Pharmaceutics*, 123(2):265 – 271, 1995.

[2] Graham Buckton and Patricia Darcy. Assessment of disorder in crystalline powders—a review of analytical techniques and their application. *International Journal of Pharmaceutics*, 179(2):141 – 158, 1999.

[3] Gabrielle Pilcer, Nathalie Wauthoz, and Karim Amighi. Lactose characteristics and the generation of the aerosol. *Advanced Drug Delivery Reviews*, 64(3):233 – 256, 2012.

3.2.5. Homogene Produkteigenschaften in der Sprühtrocknung durch laminare Rotationszerstäubung

Axel Mescher, Eva Maria Littringer, Raphael Paus, Nora Anne Urbanetz, Peter Walzel

Kurzmitteilung

Homogene Produkteigenschaften in der Sprühtrocknung durch laminare Rotationszerstäubung

Axel Mescher[1],*, Eva M. Littringer[2], Raphael Paus[1], Nora A. Urbanetz[2] und Peter Walzel[1]

Der Einfluss der Zerstäubungsmethode auf die Homogenität sprühgetrockneter Produkte wird diskutiert. Eng verteilte Tropfengrößen sind die Voraussetzung für einheitliche Trocknungsverläufe und Morphologien der Einzelpartikel. Am Beispiel der Sprühtrocknung von Polyvinylpyrrolidon und D-Mannitol aus wässriger Lösung wird die laminar betriebene Rotationszerstäubung als geeignete Zerstäubungsmethode für ein eng verteiltes System angewendet. Durch die wenig streuenden Trocknungsbedingungen werden für die verwendeten Stoffsysteme homogene Pulvereigenschaften erzielt. Die besonderen Anforderungen, die die eingesetzte Zerstäubungsmethode an die Heißgasführung im Sprühtrockner stellt, werden erläutert und eine neue Gasverteilungsgeometrie vorgestellt.

Homogeneous Product Quality in Spray Drying with Laminar Operated Rotary Atomizers

The influence of the atomization method on the product homogeneity in spray drying is discussed. For identical drying histories at individual particles, a narrow drop size distribution has to be achieved in order to produce a homogeneous powder. Spray drying experiments with aqueous solutions of polyvinylpyrrolidon and D-Mannitol were carried out. For generation of narrow distributed droplets a laminar operated rotary atomizer is applied. Homogeneous particle properties of the powders were achieved. However, this kind of atomization requires special drying gas distribution. A possible geometry for a proper heating gas distribution is presented.

1 Sprühtrocknung: Anforderungen an Spray und Zerstäuber

Die Sprühtrocknung stellt ein gängiges Verfahren zur Herstellung von Pulvern aus flüssigen Speisen dar. Neben der schonenden Trocknung des Materials ist insbesondere die Formgebung zu runden Partikeln im Trocknungsverfahren vorteilhaft [1]. Zu den Qualitätsmerkmalen eines Feststoffprodukts gehören neben der Partikelform und Partikelmorphologie auch Pulvereigenschaften, wie Fließ- und Rieselfähigkeit sowie die Produkthomogenität [2]. Mit Homogenität ist einerseits die Korngrößenverteilung (KGV)

gemeint, da zumeist staub- und grobkornfreie Pulver verlangt werden. Unter Produkthomogenität ist neben der KGV aber auch die Verteilungsbreite anderer Partikeleigenschaften, wie z. B. Porosität, Partikelform und Morphologie, zu verstehen. Eine enge Verteilung dieser Partikeleigenschaften im Pulver kann ebenfalls ein wesentliches Qualitätsmerkmal eines Produkts sein. Beispielhaft wird dies an einem Modellsystem Polyvinylpyrrolidon (PVP) und an D-Mannitol gezeigt, das zu Trägerpartikeln für Pulverinhalate sprühgetrocknet wird.

Bei den genannten Pulverinhalaten wird der lungengängige Wirkstoff, mit aerodynamischen Durchmessern unter 5 μm, mit Trägerpartikeln, die einen mittleren Durchmesser von 80 μm aufweisen, gemischt und in einem Pulverinhalator vorgelegt. Der Wirkstoff haftet auf der Oberfläche der Trägerpartikel und stellt im Gegensatz zu reinem Wirkstoffpulver ein gut fließfähiges und somit reproduzierbar dosierbares Pulvergemisch dar. Nachdem durch aerodynamische Kräfte bei der Inhalation die Adhäsion zwischen Trä-

[1]Axel Mescher (axel.mescher@bci.tu-dortmund.de), Raphael Paus, Prof. Dr. Peter Walzel, TU Dortmund, Lehrstuhl für Mechanische Verfahrenstechnik, Emil-Figge-Straße 68, 44227 Dortmund, Germany; [2]Eva M. Littringer, Prof. Dr. Nora A. Urbanetz, Research Center Pharmaceutical Engineering GmbH, Inffeldgasse 21/A, 8010 Graz, Austria.

ger und Wirkstoff überwunden wurde, stellt sich an den Verästelungen der Atemwege des Patienten eine Klassierung von Träger- und Wirkstoffpartikel ein. Während der Wirkstoff die tieferen Bereiche der Lunge erreicht, wird das Trägermaterial bereits in Rachen und Luftröhre abgeschieden.

Maas hat gezeigt, dass die Oberflächenmorphologie von sprühgetrockneten *D*-Mannitol-Partikeln stark von den Trocknungsbedingungen abhängt [3, 4]. Es stellen sich verschiedene Oberflächenrauigkeiten ein, die es erlauben die Kontaktfläche und somit die Adhäsionskräfte zwischen Träger und Wirkstoff anzupassen. In vorangegangenen Arbeiten zur Sprühtrocknung von *D*-Mannitol im Technikumsmaßstab wurde der Einfluss der Trocknungsbedingungen auf die Rauigkeit der Partikel systematisch untersucht [5 – 7]. Es konnten geeignete Trocknungsbedingungen zur Herstellung von glatten sowie rauen Partikeln gefunden werden (s. Abb. 1).
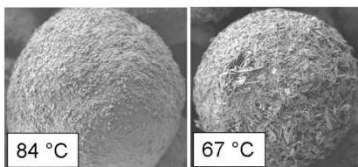

Abbildung 1. Elektronenmikroskopische Aufnahmen von sprühgetrockneten *D*-Mannitol-Partikeln. Bei gleichem Luft- und Flüssigkeitsdurchsatz und gleichen Sprühbedingungen wurde die Trocknungstemperatur variiert. Die Partikel haben beide Durchmesser von ca. 80 μm, weisen jedoch in Abhängigkeit der Luftausgangstemperaturen des Trockners von 84 °C bzw. 67 °C verschiedene Rauigkeiten auf.

Um ein Produkt mit homogenen Eigenschaften durch Sprühtrocknung herzustellen, bedarf es eines eng verteilten Tropfengrößenspektrums [8]. Hinsichtlich der KGV des Pulvers erscheint dies trivial, jedoch wirkt sich die Tropfengrößenverteilung (TGV) auch auf die Homogenität bezüglich der Partikelmorphologie aus. Die charakteristischen Zeiten für Aufheizung, Stofftransport, Keimbildung und Kristallwachstum ergeben für große und kleine Tropfen andere Bedingungen, selbst bei identischen Trocknungsgaszuständen. Zudem bewegen sich vom Zerstäuber ausgehend Tropfen verschiedener Größe aufgrund ihrer unterschiedlichen aerodynamischen Widerstände unterschiedlich schnell und entlang anderer Flugbahnen durch den Trockenturm. Daraus resultieren zunächst verschiedene Umströmungsgeschwindigkeiten der Tropfen. Darüber hinaus ergibt sich durch die unterschiedlichen Flugbahnen auch die Bewegung durch unterschiedliche Temperaturzonen im Trockner. Diese Umstände führen zu voneinander abweichenden Trocknungsverläufen. Sofern die Partikelmorphologie, wie bei *D*-Mannitol, sensitiv auf die Trocknungsbedingungen ist, können stark streuende Trocknungsverläufe zu einem inhomogenen Produkt führen.

In [8] wird die Klassierung verschiedener Tropfengrößen hinsichtlich ihrer Flugbahnen durch einen Sprühtrockner

als Funktion des Sprühwinkels beschrieben. Zerstäuber mit kleinen Sprühwinkeln, wie Einstoff-Druckdüsen aber auch pneumatische Zweistoffdüsen, führen zu geringeren Klassierungseffekten im Spray als Zerstäuber mit großen Sprühwinkeln, wie Hohlkegeldüsen oder Rotationszerstäuber. Einen Überblick über Funktionsweise und Auslegung der genannten Zerstäuber geben [9] und [10]. An klassischen Rotationszerstäubern ergibt sich aufgrund des Sprühwinkels von annähernd 180° eine starke Klassierwirkung auf die Tropfen mit meist breiter Größenverteilung. Bei geeigneter Gestaltung und Betriebsweise von Rotationszerstäubern besteht jedoch die Möglichkeit besonders eng verteilte Tropfengrößen zu produzieren.

Am Beispiel der Sprühtrocknung von Polyvinylpyrrolidon und *D*-Mannitol mit laminar betriebener Rotationszerstäubung zeigt sich, dass aufgrund der dabei erzielten engen TGV homogene Produkteigenschaften erhalten werden können.

2 Laminar betriebene Rotationszerstäubung

Laminar betriebene Rotationszerstäuber (LAMROT-Zerstäuber) [11] weisen vergleichsweise große durchströmte Querschnitte auf. Hierdurch stellen sich im gesamten Zerstäuber ausschließlich Gerinneströmungen ein, die kaum verstopfungsgefährdet sind. Von besonderem Vorteil ist auch die Methode der Flüssigkeitszerteilung durch Zertropfen laminarer Fäden. Die Zerstäuber haben hierfür definierte Abströmstellen, die ebenfalls in Form von Gerinnen durchströmt werden. In Abb. 2 links ist ein Schnitt durch einen solchen Rotationszerstäuber dargestellt. Die vorgegebenen Abströmstellen erlauben die Bildung laminarer Fäden über einen breiten Bereich von Drehzahlen und Flüssigkeitsdurchsätzen. Das Gerinne bildet nach Verlassen der Austrittsbohrung einen Freistrahl aus, der durch die Zentrifugalbeschleunigung zu geringen Durchmessern gedehnt wird. Die Flüssigkeitsfäden sind hydrodynamisch instabil und zerfallen aufgrund ihrer Oberflächenspannung zu Tropfen (s. Abb. 2 rechts).

Da der laminare Strahlzerfall zu eng verteilten Tropfengrößen führt [12] erlaubt dieser Zerstäubertyp die Herstellung von Sprays mit span < 1. Der span-Wert charakterisiert die Breite der TGV:

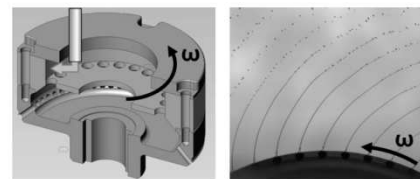$$\text{span} = \frac{d_{90,3} - d_{10,3}}{d_{50,3}} \tag{1}$$

Abbildung 2. Links: Zerstäuber mit 100 mm Durchmesser und 60 Austrittsbohrungen D_B = 3 mm; rechts: Fadenzerfall am Zerstäuber im Betrieb. Die Zerstäuber-Winkelgeschwindigkeit beträgt ω.

Zum Vergleich kann das relativ enge Tropfenspektrum an Hohlkegeldüsen betrachtet werden, das unter günstigen Betriebsbedingungen einen span von 1,5 aufweist [9].

Die jüngste Weiterentwicklung der LAMROT-Zerstäuber [13] zielte auf eine verbesserte und drucklose Flüssigkeitsverteilung im Zerstäuber ab. Abb. 3 zeigt einen fünfreihigen Zerstäuber mit 100 mm Durchmesser und 450 Abströmbohrungen sowie den zugehörigen internen Flüssigkeitsverteiler im ausgebauten Zustand.
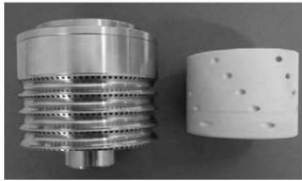

Abbildung 3. Links: Zerstäuber mit 100 mm Durchmesser und 450 Bohrungen in fünf Reihen. Der Bohrungsdurchmesser beträgt $D_B = 2$ mm; rechts: gebohrter Flüssigkeitsverteiler aus einem Polymer im ausgebauten Zustand.

Aus der grundlegenden Arbeit von Schröder [11] lässt sich je nach angestrebter Tropfengröße ein Maximaldurchsatz für den gewünschten Strömungszustand im Zerstäuber ableiten. Die Gleichverteilung dieses Speisevolumenstroms auf viele Abströmstellen stellt jedoch eine Herausforderung dar. Der in Abb. 3 gezeigte Flüssigkeitsverteiler für mehrere Abströmebenen wurde bereits in [14] vorgestellt. Das Konzept sieht einen gebohrten Flüssigkeitsverteiler vor, der als Kern in den eigentlichen Zerstäuber eingesetzt und ebenfalls als Gerinne durchströmt wird. In Abb. 4 ist das Prinzip der Flüssigkeitsverteilung auf mehrere Ebenen im Zerstäuber dargestellt.

Diese Art der internen Flüssigkeitsverteilung erlaubt es auch kleine Volumenströme auf eine Vielzahl von Abström-

stellen aufzuteilen. Die resultierenden bohrungsspezifischen Volumenströme sind dann gering und es können bereits bei moderaten Drehzahlen mit dem Zerstäuber nach Abb. 3 relativ kleine Tropfen mit $d_{50,3}/D_B < 0,1$ hergestellt werden (s. Abb. 5). Bei höheren Drehzahlen nimmt die Sensitivität der Tropfengröße bzgl. des Speisevolumenstroms ab.
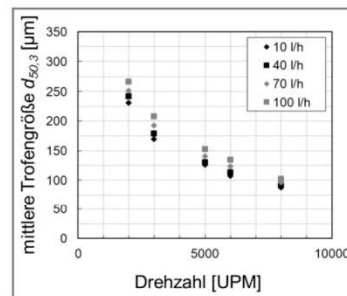
Abbildung 5. Mittlere Tropfengröße am Zerstäuber nach Abb. 2 in Abhängigkeit von der Zerstäuberdrehzahl für verschiedene Speisevolumenströme. Die Tropfengrößenmessung wurde mit einer Newtonschen Glycerin/Wasser-Lösung mit einer Viskosität von 50 mPa s in einem Tropfengrößenmessstand mittels Laserbeugungsspektrometrie (Malvern Spraytec) durchgeführt.

Auch der span der TGV hängt von der Drehzahl des Zerstäubers ab, da größere Drehzahlen eine größere aerodynamische Wechselwirkung der laminaren Fäden mit der umgebenden Gasphase bewirken (s. Abb. 6) [15, 16].

Der vergleichsweise geringe span-Wert der TGV gleicht die besonders ausgeprägte Klassierwirkung aus, die Rotationszerstäuber bei axialer Anströmung im Sprühtrockner durch ihren großen Sprühwinkel aufweisen [8]. Dies erlaubt vergleichbare Flugbahnen der Tropfen im Sprühtrockner und ermöglicht geringe Streuungen der Partikeltrocknungs-

Abbildung 4. Schnittansicht durch einen 3-reihigen Zerstäuber mit integriertem gebohrtem Flüssigkeitsverteiler. Die Bohrungen des Verteilerkerns sind so gegen die wirkende Zentrifugalbeschleunigung angestellt, dass sich gleichförmige und stabile Gerinne ausbilden.

Abbildung 6. span der TGV in Abhängigkeit von der Zerstäuberdrehzahl für verschiedene Speisevolumenströme. Die Tropfengrößenmessung wurde mit einer Newton'schen Glycerin/Wasser Lösung mit einer Viskosität von 50 mPas in einem Tropfengrößenmessstand mittels Laserbeugungsspektrometrie (Malvern Spraytec) durchgeführt.

verläufe. Bei der Sprühtrocknung von *D*-Mannitol war die Verwendung des beschriebenen Zerstäubertyps eine Voraussetzung für die Produktion eines Pulvers mit homogener Morphologie.

3 Sprühtrocknung mit laminarer Rotations-zerstäubung

Am Beispiel der Sprühtrocknung wässriger Lösungen von Polyvinylpyrrolidon sowie *D*-Mannitol sollen die Vorteile der Verwendung von Rotationszerstäubern mit enger TGV aber auch die zusätzlichen Anforderungen, die dieser Zerstäubertyp an die Trocknungsanlage stellt, deutlich gemacht werden.

Die verwendete Technikums-Sprühtrocknungsanlage ist in Abb. 7 dargestellt. Der Sprühturm besitzt einen Durchmesser von 2,7 m und eine Gesamthöhe von 3,7 m. Die Anlage ist mit Temperatur-, Druck- und Feuchtemessfühlern ausgerüstet. Von Bedeutung ist auch die Überwachung der Luftdurchsätze und des Zerstäubungsbetriebspunkts, also Drehzahl und Speisedurchsatz, da eine abgestimmte Heißgasführung eine wichtige Voraussetzung für den Betrieb des Zerstäubers ist.
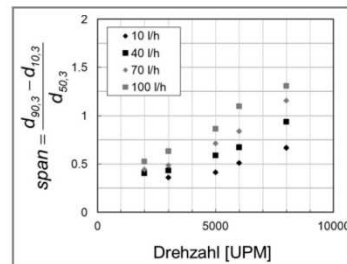
Bei typischen Betriebszuständen eines laminar betriebenen Rotationszerstäubers liegt die Startgeschwindigkeit eines Tropfens in der Größenordnung von 30 m s^{-1}. Wegen der hohen Tropfenanfangsgeschwindigkeit und des Sprühwinkels des Zerstäubers von annähernd 180° müssen die Tropfen durch das Trocknungsgas axial abgelenkt werden, um ein Auftreffen auf die Wand des Trockners zu verhindern.

Typischerweise wird das Trocknungsgas dazu in axialer Richtung durch einen koaxialen Ringschlitz oberhalb des Zerstäubers in den Trockenturm eingeleitet. Obwohl die

axiale Ablenkung der Tropfen für den Betrieb von Rotationszerstäubern erforderlich ist, bewirkt die Heißgaseinleitung im Nahbereich des Zerstäubers eine starke Störung des Tropfenbildungsvorgangs. In [14] wurde der Einfluss einer axialen Anströmung des Rotationszerstäubers untersucht und ein Anstieg des span-Wertes der TGV mit steigender Anströmungsintensität festgestellt. Es wurden Ähnlichkeitsexperimente zum Zerfall angeströmter Strahlen durchgeführt [15–17], die eine Störung des Strahlzerfalls und erhöhte span-Werte bereits bei sehr geringen Anströmungsintensitäten zeigten. In Sprühtrocknern mit Zerstäubern auf Basis des laminaren Strahlzerfalls müssen die Tropfen zwar axial abgelenkt werden, das Heizgas sollte dabei aber den Strahlzerfall möglichst wenig stören. Um die enge TGV des ungestörten Strahlzerfalls bestmöglich zu erhalten, muss daher ein geeigneter Heißgasverteiler installiert werden. In Abb. 8 ist eine mögliche Konstruktion für einen solchen Heißgasverteiler dargestellt [18].

Die Heißgasverteilungsgeometrie wurde zusammen mit dem in Abb. 2 gezeigten Rotationszerstäuber für Sprühtrocknungsversuche mit PVP und *D*-Mannitol benutzt. Der

Abbildung 7. Schematische Darstellung der verwendeten Technikums-Sprühtrocknungsanlage. Die Heizleistung beträgt 60 kW, der Luftdurchsatz ca. 1000 m³h^{-1} i.N. Der Durchmesser des Sprühturms beträgt 2,7 m, die Gesamthöhe ist 3,7 m. In geringer Menge anfallendes Feingut kann an einem nachgeschalteten Zyklon und in einem Taschenfilter abgetrennt werden. Relevante Prozessgrößen werden durch einen elektronischen Datenschreiber erfasst.

Abbildung 8. Skizze des Gasverteilers der Technikums-Sprühtrocknungsanlage. Mitte: Durch Variation der Heißgasvolumenströme A und B kann der Drallanteil der Heizgaseinströmung in den Sprühtrockner eingestellt werden. Deckengängige drallbehaftete sowie strahlartige axiale Einströmungen können realisiert werden.

Gasverteiler hat tangentiale sowie axiale Einlässe und erlaubt über geeignete Mischverhältnisse das Heizgas mit variablem Drall in den Trockenturm einzuleiten. Als Grenzfälle stellen sich eine an der Decke anliegende Drallströmung oder ein axialer Schlitzstrahl ein. Zunächst wurden Sprühtrocknungsversuche mit PVP zur Charakterisierung des Gasverteilers durchgeführt. Zur Anpassung der Luftführung auf den gewählten Zerstäubungsbetriebspunkt wurde der Drallanteil der Strömung, von der rein deckengängigen Strömung ausgehend, solange verringert bis die Ablenkung der Tropfen ausreichte, um Wandablagerungen zu verhindern. Die ständige Aufzeichnung der Prozessdaten, wie Gesamt- und Tangentialvolumenstrom, aber auch Zerstäuberdrehzahl und Speisevolumenstrom bildet eine breite Datengrundlage von Luftführungs- und Zerstäuberbetriebspunkten.

Auf Basis der Erfahrungswerte, die mit dem vergleichsweise einfachen Modellsystem PVP (Luvitec K30) für verschiedene Trocknungs- und Zerstäubungsbedingungen erhalten wurden, lässt 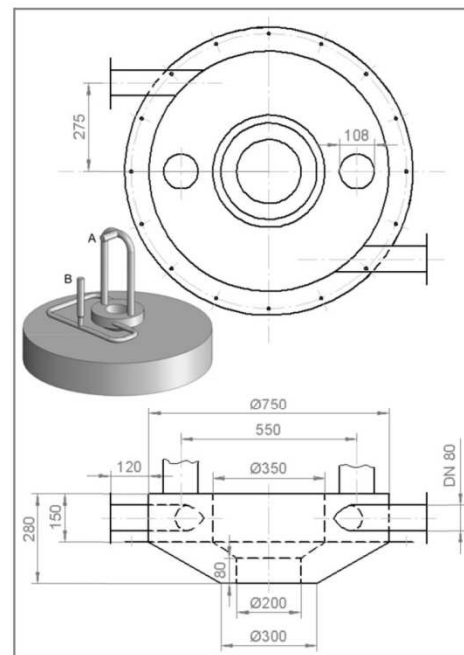sich auch bei anderen zu trocknenden Stoffen und bei beliebigen Zerstäubungsbetriebspunkten eine Luftführung mit geeignetem Drallanteil einstellen. Auf diese Weise kann eine gerade ausreichende axiale Ablenkung der Tropfen eingestellt werden, die den Strahlzerfall geringstmöglich stört. Wesentlich ist dabei jedoch, dass die Drehzahl des Zerstäubers und schließlich die Tropfengröße mit den PVP-Basisversuchen vergleichbar sind.

Zunächst soll anhand der Sprühtrocknung einer wässrigen PVP-Lösung der Einfluss der Luftführung auf die Produktqualität, insbesondere auf die Korngrößenverteilung des Pulvers vorgestellt werden. In Tab. 1 sind die Betriebsbedingungen der Sprühtrocknung einer wässrigen Lösung mit einem PVP-Anteil von 40 Gew.-% sowie die erzielte mittlere Korngröße und der span-Wert der Korngrößenverteilung dargestellt.

Tabelle 1. Parameter und Ergebnisse der Sprühtrocknungsversuche mit wässriger PVP-Lösung. Die Korngrößen wurden mittels Laserbeugungsspektrometrie (Malvern Spraytec) gemessen.

Parameter	Einheit	Werte	
Flüssigkeitsdurchsatz	$[L\,h^{-1}]$	10	
Zerstäuberdrehzahl	[rpm]	5000	
Trocknereinlasstemperatur	[°C]	150	
Trocknerauslasstemperatur	[°C]	110	
Heißluftdurchsatz	$[m^3h^{-1}]$	1500	
Drallanteil	[%]	10	40
$d_{50,3}$	[µm]	207	207
$d_{P,10,3}$	[µm]	91,7	76,7
$d_{P,50,3}$	[µm]	146,2	121,9
$d_{P,90,3}$	[µm]	232,1	186
$span_{KGV}$	[–]	0,96	0,89

In Abb. 9 sind die erhaltenen Korngrößenverteilungen dargestellt. Neben dem geringeren span bei höherem Drallanteil der Strömung fällt ebenfalls der geringere mittlere Partikeldurchmesser auf. Wie in [16] gezeigt, kann die geringere Korngröße $d_{P,50,3}$ ebenso wie der kleinere span auf eine günstigere Gas/Flüssigkeits-Wechselwirkungen mit geringerer Gas-Relativgeschwindigkeit der Flüssigkeitsfäden zurückgeführt werden.
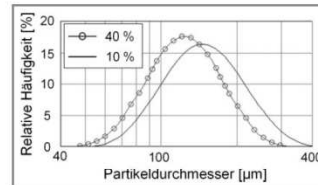
Abbildung 9. Vergleich der Korngrößenverteilungen aus Sprühtrocknungsversuchen mit wässriger PVP-Lösung. Außer dem Drallanteil der Heißgaseinströmung sind alle Versuchsparameter identisch. Bei einem Drallanteil von 40 % sind eine geringere mittlere Korngröße und eine geringere Verteilungsbreite der KGV zu erkennen.

Die in Tab. 1 und Abb. 9 gezeigten Trocknungsversuche stellen zwei der beschriebenen PVP-Basisversuche dar, anhand derer der Gasverteiler für beliebige Stoffsysteme und Zerstäubungsbedingungen eingestellt werden kann. Das verwendete PVP (Luvitec K30) kann als verhältnismäßig leicht zu trocknendes Material bezeichnet werden.

Die Sprühtrocknung von *D*-Mannitol hingegen ist deutlich anspruchsvoller, da restfeuchte Mannitol-Partikel leicht an der Trocknerwand anhaften und rasch zu Ablagerungen führen. Nachfolgend werden die Ergebnisse von Sprühtrocknungsversuchen mit wässriger *D*-Mannitol-Lösung vorgestellt. Erste Versuche zur Sprühtrocknung von *D*-Mannitol wurden ohne die beschriebene Messtechnik und ohne die systematische Einstellung der Luftführung um den Zerstäuber gemäß der PVP-Basisversuche durchgeführt. Zum einen verursachten ungeeignete Luftführungseinstellungen ausgeprägte Decken- und Wandablagerung des Zuckers. Während der relativ kurzen Sprühversuchsdauer von 1–2 Stunden lag die Ausbeute an fließfähigem Material teilweise unter 5 %. Darüber hinaus wiesen die Pulver teilweise breit verteilte Eigenschaften hinsichtlich Korngröße, vor allem aber hinsichtlich ihrer Morphologie auf.

Durch gezielte Einstellung der Luftführung auf Basis der Erfahrungswerte aus den Modellversuchen mit PVP konnten jedoch Deckenablagerungen des Materials gänzlich verhindert werden. Wandablagerungen beschränkten sich im Wesentlichen auf den konischen unteren Teil des Trocknerturms. Die Ausbeute stieg während der ebenfalls 1–2 stündigen Sprühversuche auf etwa 50 %, wobei das abgelagerte Material auf dem Trocknerkonus lose auflag und nicht etwa anhaftete. Bei längeren Sprühzeiten sind daher höhere Aus-

beuten wahrscheinlich. Durch die gezielt eingestellte Luft-führung wurde auch die Homogenität der getrockneten Pulver hinsichtlich Morphologie deutlich verbessert. Man kann daher davon ausgehen, dass der ringfömige, ange-nähert kegelige Trocknungsgasstrahl die Tropfen erst außer-halb der sensiblen Fadenzerfallszone ablenkt.

4   Zusammenfassung und Ausblick

In Sprühtrocknungsverfahren mit LAMROT-Zerstäubung können eng verteilte Tropfen in ein qualitativ hochwertiges Pulver mit eng verteilten Eigenschaften überführt werden. Neue Flüssigkeitsverteiler und mehrreihige Zerstäuber er-lauben die zuverlässige Verteilung des Speisevolumen-stroms auf eine Vielzahl von Abströmstellen. Insbesondere bei einphasigen Speisen, wie der hier vorgestellten D-Man-nitol-Lösung, lassen sich auch sehr geringe Volumenströme gleichmäßig verteilen.

Der Betrieb des genannten Zerstäubers erfordert jedoch eine geeignete Gasführung im Sprühturm. Einerseits müssen die Tropfen, wie bei allen Rotationszerstäubern, axial abgelenkt werden, um Wandablagerungen zu verhin-dern. Andererseits wird der gleichmäßige Strahlzerfall durch zu große Relativgeschwindigkeiten zum Gas im Nah-bereich des Zerstäubers gestört. Es wurde eine mögliche Gasverteilungsgeometrie vorgestellt, die durch variablen Drall der Gasströmung eine vergleichsweise geringe Stö-rung der Zerstäubung bei ausreichender Tropfenablenkung ermöglicht. Die Weiterentwicklung des Gasverteilungskon-zepts für laminare Rotationszerstäuber ist aktueller For-schungsgegenstand. Das Entwicklungsziel ist hierbei eine hinreichende axiale Tropfenablenkung außerhalb der Tropfenbildungszone bei gleichzeitig möglichst geringer Strömungsintensität in unmittelbarer Nähe des Zer-stäubers.

Die vorgestellten Sprühversuche mit PVP dienten dazu, eine Erfahrungsbasis für die Einstellung der Luftverteilung in Abhängigkeit von den Zerstäubungsbedingungen zu schaffen. Auf dieser Basis konnten D-Mannitol-Trägermate-rialien mit verschiedenen Oberflächenrauigkeiten sprüh-getrocknet werden. Die beschriebenen Träger/Wirkstoff-Mischungen wurden durch die Autoren hinsichtlich ihrer medizinischen aber auch ihrer mechanischen Eigenschaf-ten bewertet [19]. Die Ergebnisse der Studie sollen die For-mulierung einer Prozessfunktion zwischen den Sprühtrock-nungsbedingungen und der medizinischen Funktionalität des D-Mannitol-Pulvers erlauben.

Formelzeichen

$d_{10,3}$	[m]	Tropfengröße, entsprechend dem 10 %-Perzentil der Tropfenvolumen-verteilung
$d_{50,3}$	[m]	Volumetrische mittlere Tropfengröße
$d_{90,3}$	[m]	Tropfengröße, entsprechend dem 90 %-Perzentil der Tropfenvolumenver-teilung
$d_{P,10,3}$	[m]	Korngröße, entsprechend dem 10 %-Perzentil der Tropfenvolumen-verteilung
$d_{P50,3}$	[m]	Volumetrische mittlere Korngröße
$d_{P,90,3}$	[m]	Korngröße, entsprechend dem 90 %-Perzentil der Tropfenvolumen-verteilung
D_B	[m]	Durchmesser einer Austrittsbohrung
ω	[s^{-1}]	Winkelgeschwindigkeit

Literatur

[1] K. Masters, *Spray Drying Handbook*, 4th ed., George Godwin Ltd., London **1985**.
[2] P. Walzel, T. Furuta, in *Modern Drying Technology: Product Quality and Formulation* (Eds: E. Tsotsas, A. S. Mujumdar), Wiley-VCH, Weinheim **2011**.
[3] S. G. Maas, *Dissertation*, Heinrich-Heine-Universität Düssel-dorf **2009**.
[4] S. G. Maas, G. Schaldach, P. Walzel, N. A. Urbanetz, *Atomiza-tion Sprays* **2010**, *20 (9)*, 163 – 774.
[5] E. M. Littringer et al., *17th International Drying Symposium*, Magdeburg, October **2010**.
[6] E. M. Littringer et al., in *Proc. of the ILASS – Europe 2010, 23rd Annual Conference on Liquid Atomization and Spray Systems*, Brno, Czech Republic **2010**.
[7] S. G. Maas et al., *Powder Technol.* **2011**, *213*, 27 – 35.
[8] P. Walzel, *Chem. Eng. Technol.* **2011**, *34 (7)*, 1039 – 1048.
[9] P. Walzel, in *Ullmann's Encyclopedia of Industrial Chemistry*, Wiley-VCH, Weinheim **2009**.
[10] P. Walzel, *Chem. Ing. Tech.* **1990**, *62 (12)*, 983 – 994.
[11] T. Schröder, P. Walzel, *Chem. Ing. Tech.* **1996**, *68 (5)*, 562 – 566.
[12] A. H. Lefebvre, *Atomization and Sprays*, Taylor Francis, Boca Raton, FL **1989**.
[13] P. Walzel, *DE 102007047411A1*, **2009**.
[14] P. Walzel, G. Schaldach, H. Wiggers, *Int. Conf. on Liquid Ato-mization and Spray Systems*, Como Lake, Italy **2008**.
[15] A. Mescher, P. Walzel, *17th Int. Drying Symposium*, Magde-burg, October **2010**.
[16] A. Mescher, A. Möller, M. Dirks, P. Walzel, *Chem. Eng. Sci.* **2011**, in press. DOI: 10.1016/j.ces.2011.10.021
[17] S. Gramlich, A. Mescher, M. Piesche, P. Walzel, *Chem. Ing. Tech.* **2011**, *83 (3)*, 273 – 279.
[18] M. Koch, *Dissertation*, Universität Dortmund **2003**.
[19] E. M. Littringer et al., *Drying Technol.* **2012**, *30 (1)*, 114. DOI: 10.1080/07373937.2011.620726

3.3. Differences at lab and pilot scale

3.3.1. The morphology of spray dried mannitol particles - The vital importance of droplet size

Eva Maria Littringer, Raphael Paus, Axel Mescher, Hartmuth Schroettner, Peter Walzel, Nora Anne Urbanetz

The morphology of spray dried mannitol particles - The vital importance of droplet size

E M Littringer[1*], R Paus[2], A Mescher[2], H Schroettner[3], P Walzel[2], N A Urbanetz[1]

[1]Research Center Pharmaceutical Engineering GmbH, Inffeldgasse 21a/II, Graz, Austria

*Corresponding author: Tel: +43 316 873 9743; Fax: +43 316 873 109743; Email: eva.littringer@tugraz.at

[2]Department of Biochemical and Chemical Engineering, TU Dortmund, Emil-Figge-Str. 68, Dortmund, Germany

[3]Austrian Centre for Electron Microscopy and Nanoanalysis, TU Graz, Steyrergasse 17/III, Graz, Austria

Abstract

As the morphology of spray dried aqueous mannitol solutions is strongly influenced by the scale of the used spray dryer or more correctly by the droplet size generated in the spray dryer the purpose of this work is to carefully study and compare the morphologies and underlying particle formation mechanisms on lab and pilot scale. Therefore drying experiments of 15 % [w/w] aqueous mannitol solutions were performed on a lab and pilot scale spray dryer at different outlet temperatures. The obtained spray dried products are intended to be used as carrier particles for pulmonary drug delivery. In order to show that the morphology is highly dependent on the initial droplet size, irrespective of the size of the used spray dryer, droplets of different size were dried in the pilot scale spray dryer at different air outlet temperatures. Additionally the influence of feed temperature on particle morphology was studied.

For small droplets crystallization from a highly viscous liquid or even water-free melt is observed, leading to rough particles at high outlet temperatures and smooth particles at low temperatures. When drying larger droplets, however crystallization obviously starts from a more diluted solution leading to rougher surfaces, containing larger single crystals at lower outlet temperatures than at higher ones. For large droplets an increase in the mannitol solution feed temperature leads to particles of comparably rougher surface. No influence of feed temperature was observed for smaller droplets.

Introduction

Powder bulk characteristics such as flowability, reproducibility of dosing, compactability or aerodynamic behavior are strongly influenced by the particle size, shape and surface of individual powder particles. Therefore the control of particle size and morphology is very important. Often spray drying is used to improve or even adjust the desired powder properties. Usually before drying

at an industrial scale preliminary experiments at lab scale are performed. These experiments are needed to study the influence of process parameters on product properties.

However, there are always constraints in the transfer of the lab to the pilot scale as the droplet and the maximum achievable particle size largely depends on the size of the spray dryer. Droplets must be small enough to allow complete drying within the residence time of the droplet in the spray dryer. The larger the spray dryer, the larger is the residence time and therefore the larger is the size of the droplets which still can be dried. When moving from lab to pilot or even industrial scale there is often not only a change in the amount of product produced per time but also in particle size. However this change in droplet size may have a strong impact on the particle morphology as will be shown below.

Maas et al. [18] studied the suitability of spray dried mannitol as a carrier in dry powder inhaler (DPI) formulations. In such formulations the reproducible delivery of the active pharmaceutical ingredient (API) to the lower part of the lung is mandatory. However the target site within the lung is only reached when API particles with an aerodynamic diameter of 1 µm to 5 µm are used [3, 15, 7]. Powders consisting of particles of this size are highly cohesive and exhibit poor flowing properties. The solution to cope with cohesivity is the addition of excipients of larger size. In a mixing procedure the fine API particles are mixed with so called "carrier particles". During mixing the API particles are attached to the surface of the larger excipient particles. Interparticulate forces are highly important in such mixtures. In order to guarantee mixing homogeneity and stability of the mixture during transport and dosing adhesion forces should be preferably high. However, in order to increase API detachment from the carrier surface that is crucial upon inhalation, these forces have to be overcome. In case the API particles do not detach from the surface of the carrier, due to the inertia of the larger carrier they will impact in the throat and will not have access to the lung. Interparticle forces in such mixtures are influenced by various factors such as particle size, particle shape, surface roughness, powder moisture, mixing rate and many more. There are several studies showing the importance of surface roughness on the performance of e.g. DPI lactose carrier particles [6, 5, 8, 14, 2, 24, 13, 4].

Maas et al. [18] showed that spray drying of aqueous mannitol solutions at different spray dryer air outlet temperatures on lab scale resulted in the formation of carrier particles of different surface topography. They also demonstrated that the amount of API reaching the lung could be successfully targeted by adjusting the surface topography of the carrier particles [11]. However one problem encountered by Maas was the lack of reproducibility of dosing due to the small particle size of the carriers, which was not large enough to guarantee adequate flowability. The particle size of the carrier was restricted to approximately 12 µm because of the small size of their spray tower. Larger droplets, leading to larger particles, require larger drying times and hence larger spray towers.

Therefore the aim of Littringer et al. [10] was the preparation of larger mannitol carrier particles of adjustable surface roughness and sufficient flowability on a larger, i.e. pilot scale spray dryer.

Besides surface roughness, Littringer et al. [10] studied the influence of spray drying process parameters on particle size, polymorphism and breaking strength of the mannitol particles [10]. One of the main results concerning surface roughness, mentioned in [10], was that low outlet temperatures lead to rough, coarse crystalline particles and higher temperatures to smoother ones. These results are in contrast to those of Maas et al. [18] who showed smooth surfaces at low outlet temperatures and rough surfaces at higher ones. Maas et al. [18] as well as Littringer et al. [10] mentioned that the different roughness is a result of the underlying crystallization processes. Further at lab scale not only surface roughness changed, depending on the outlet temperature, but also particle shape. This change in particle shape, which had been firstly described in [11] but never explained, largely affects the DPI performance when used as a carrier. As surface roughness as well as the shape of spray dried mannitol carrier particles strongly influence the DPI performance [11, 19], the focus of this work is to study and thoroughly compare the mechanisms leading to diverging morphologies at lab and pilot scale. Additionally the influence of droplet size, irrespective of the size of the used dryer, as well as the influence of feed temperature is investigated. This finally leads to a comprehensive understanding of the underlying particle formation mechanisms and will open up the possibility to tailor particle shape and surface roughness independent of the particle size.

Materials and methods

Materials

Mannitol (Pearlitol® 200SD and Pearlitol® 160C) which was kindly provided by Roquette Frères (Lestrem, France) was used for the spray drying experiments.

Spray drying at lab scale

Spray dried particles were prepared on a Niro MOBILE MINOR™ (Niro Atomizer, Copenhagen, Denmark) equipped with a 50 mm rotary atomizer Type 010084-0001 (Niro Atomizer, Copenhagen, Denmark) having 24 openings of 6 mm in height and 3 mm in width. A pneumatic wheel drive pressure of 4 bar, which according to the manufacturer corresponds to an atomizer revolution rate of 23000 min^{-1} was adjusted. The spray drying tower had an inner diameter of 0.800 m and a total height of 1.315 m. The spray was produced from a solution of mannitol dissolved in water (15 % [w/w]) at room temperature dosed at a feed rate of 0.84 l/h. Four products were prepared at 65 °C, 114 °, 140 °C and 150 °C outlet temperature (T2, Figure 1) which are termed L65, L114, L140 and L150.

Spray drying at pilot scale

Spray drying at pilot scale was performed using self-built tower. A laminar operated rotary atomizer (LAMROT-atomizer [22]) with a diameter of 100 mm and containing 60 bores of 3 mm was used. The atomizer was running at a speed of 7200 min^{-1}. The dimensions of the pilot scale spray dryer were: diameter 2.7 m, total height 3.7 m. The spray was again produced from a solution of mannitol dissolved in water (15 % [w/w]) at room temperature with a feed rate of 10 l/h. Three products at 67 °C, 80 °C and 92 °C outlet temperature (T4, Figure 1), termed M67, M80 and M92, were prepared according to [11].

Droplet size experiments at pilot scale

Three different atomizers, producing droplets of different size, were operated in the pilot scale spray dryer (see above). Atomizers and atomizer operation settings were chosen in order to obtain droplets with approximately 130 µm, 50 µm and 20 µm mass mean diameter. 15 % [w/w] aqueous mannitol solutions at 20 °C and 70 °C with a feed rate of 10 l/h were atomized by a LAMROT [22] atomizer (7400 rpm see spray drying at pilot scale), a Niro rotary atomizer (4.1 bar, 24000 rpm; see spray drying at lab scale) and a Caldyn pneumatic nozzle (1.9 bar, Caldyn CSL A, 2.5 mm, Caldyn Apparatebau GmbH, Ettlingen, Germany). To prevent evaporation of the feed and hence an increase in feed concentration at 70 °C feed temperature a closed feed stock vessel was used. The experiments were carried out at two different drying gas inlet temperatures (T1, Figure 1, 100 °C and 140 °C), corresponding to outlet temperatures of approximately 70 °C and 100 °C (T4, Figure 1).

Due to tower optimization, the temperature measuring points for the droplet size studies were changed (Figure 10) and differ from those in the first experiments at pilot scale (M67, M80 and M92, Figure 1). This is the cause of the slightly different temperature profiles.

Droplet size analysis of the atomizing spray (LAMROT, Niro, Caldyn)

The droplet size distribution of the sprays generated by the three different atomizers (see above; LAMROT atomizer at 7400 rpm, Niro rotary atomizer at 4.1 bar and Caldyn pneumatic nozzle at 1.9 bar) was measured with a laser diffraction system in an offline arrangement (Malvern Spraytec, Malvern Instruments, Worcestershire, UK). A 15 % [w/w] aqueous mannitol solution at 20 °C with a feed rate of 10 l/h was analyzed.

Particle size distribution

The particle size distribution of pilot scale spray dried products (M67, M80 and M92) was determined by analytical sieving for 15 min (amplitude 20 %) on a sieving machine (Analysette Type 3010, Fritsch GmbH, Idar-Oberstein, Germany). The mesh sizes of the sieves were 45 µm, 53 µm, 63 µm, 90 µm, 125 µm and 160 µm.

Laser light diffraction (Helos/KF-Magic, Sympatec, Clausthal-Zellerfeld, Germany) including a dry dispersing system (Rodos, Sympatec, Clausthal-Zellerfeld, Germany) was used to determine particle size distributions of powders dried at lab scale (L65, L114 and L140). The powder was fed to the disperser via a vibrating chute (Vibri, Sympatec, Clausthal-Zellerfeld, Germany). The measurements were carried out at a dispersing pressure of 4.0 bar. Evaluation of the data was performed using the software Windox 5 (Sympatec, Clausthal-Zellerfeld, Germany).

The particle size of products of the droplet size experiments at pilot scale was measured with a laser diffraction system (Malvern Spraytec, Malvern Instruments, Worcestershire, UK) with a wet dispersion unit. Prior to measurements the powder samples were finely dispersed in silicon oil (Tegiloxan 20, Evonik Industries, Krefeld, Germany) by ultrasonification for one minute.

Particle surface investigations

The powder samples were examined using a scanning electron microscope (SEM) (Zeiss Ultra 55, Zeiss, Oberkochen, Germany; Particles were sputtered with gold-palladium prior to analysis; Figure 2 and Figure 5) operating at 5kV and a SEM (Hitachi H-S4500 FEG, Hitachi High-Technologies Europe, Krefeld, Germany; Particles were unsputtered; Figure 6, Figure 11 and Figure 16) operating at 1kV.

Particle cross section investigations

Pilot scale spray dried particles were embedded into epoxy resin (Spezifix 40, Struers, Willich, Germany) and after polymerization cross sections were prepared by using a microtom (Ultracut UCT, Leica Microsystems, Wetzlar Germany). Cross sections were investigated by SEM (Zeiss Ultra 55, Zeiss, Oberkochen, Germany; Particles were sputtered with pure carbon prior to analysis) at 5 kV.

Hot stage microscopy

The drying process was studied by using an Olympus BH2 polarization microscope (Olympus Optical, Vienna, Austria) equipped with a Kofler hot stage (Reichert Thermovar, Vienna, Austria) at 120 °C. Aqueous mannitol solutions of 15 % (w/w) were studied. Photomicrographs were acquired using the Olympus BH2 and a stereomicroscope (Olympus SZX-12, Olympus Optical, Vienna, Austria) equipped with a ColorViewIII CCD camera using the software Cell-D (Olympus Optical, Vienna, Austria).

Results and discussion

Spray drying at lab and pilot scale

Scale-up experiments were carried out using a lab and pilot scale spray dryer. Both spray dryers were operated with rotary atomizers, producing droplets with a mass mean diameter of $\approx 30\mu m$ and $\approx 140\mu m$ respectively (towers and atomizers are shown in Figure 1).

Spray drying at lab scale

Lab scale spray drying experiments were carried out on a Niro MOBILE MINOR™ spray dryer equipped with a rotary atomizer. As already described by Maas et al. [18] it was not possible to measure the droplet size of the atomizer spray due to the low feed rate of 0.84 l/h. At this feed rate a pulsating spray is generated disturbing the measurement of the droplet size by laser diffraction. Pulsation ceases when higher feed rates are employed as continuous feeding via the flexible-tube pump becomes possible. Therefore when using a feed rate of 10 l/h (see below, droplet size experiments at pilot scale) the droplet size can be determined by laser diffraction and will be discussed below. However, in order to get an idea about droplet sizes at the feed rate of 0.84 l/h the mean droplet size was calculated [18] as proposed in [29] and determined to 27 μm [18].

Table 1 shows that the products spray dried at lab scale have a mass mean particle size between 10.4 μm and 15.2 μm. The lowest value of 10.4 μm was observed for the product that had been dried at the lowest temperature (L65), whereas the highest value of 15.2 μm was measured for the product dried at the highest temperature. The increase in particle size with drying temperature had been described before by Vehring et al. [15] and can be explained by the drying history of a droplet in the spray-drying tower. As soon as the droplet enters the hot tower, evaporation of water at the droplet surface will take place. The increase in solute concentration at the droplet surface due to the evaporation of the solvent causes diffusion of the solute towards the droplet center [23, 15, 25]. If the diffusion is fast enough compared to the evaporation the concentration gradient of the solute along the droplet radius will be small. However if the diffusion is significantly slower than the evaporation, there will be a higher solute concentration at the droplet surface compared to the droplet center. The ratio of evaporation rate to diffusion is described by the dimensionless Peclet number (Equation 4). High Peclet numbers indicate a fast increase of the solute concentration at the surface. Peclet numbers below 1 indicate that the concentration remains more evenly distributed along the droplet radius during drying. As soon as the concentration at the surface exceeds the solubility or even a certain supersaturation of the solute, crystallization will take place and a shell will form. With higher temperatures, hence higher Peclet numbers, the increase in surface concentration will be much faster and shell formation will take place at an earlier instant when the particle volume is still large and thus, larger and hollow particles will be obtained at higher temperatures.

As a dimensionless number the peclet number is the same for all droplet sizes. Consequently also at pilot scale the particle size should increase with increasing Peclet numbers. However this was not observed for the products dried at pilot scale (Table 1). The reason for this might be that during drying the surface area decreases linearly with time (Equation 1). Consequently smaller droplets show a comparably larger relative change in size for a given drying temperature and for a given time

interval than larger droplets. Therefore the influence of drying temperature can easier be observed at the smaller the droplets. Additionally at pilot scale at higher temperatures the spray dried products lose their spherical shape (see below) which leads to changes in the mean particle size determined.

Maas et al. [18] did not observe any influence of outlet temperature on the mean particle size when they performed experiments at lab scale. Drying at 60 °C resulted in particles of 13.5 µm. At 90 °C the particles exhibited a mean diameter of 13.6 µm and at 120 °C a mean diameter of 13.2 µm was observed. One possible reason of the different findings by Maas et al. is that the temperature range they studied (90 °C to 120 °C) was smaller with respect to the one covered in the present study (65 °C to 140 °C). Especially towards higher temperatures (L140) the increase in particle size is comparably large.

The morphology of spray dried products will now be discussed with respect to the shape and the surface roughness of the particles.

Figure 2 shows that the particle morphology is highly dependent on the drying air temperature. The influence of drying air temperature on the morphology of products prepared from aqueous solutions had been described before [20, 18]. At the drying air outlet temperature of 65 °C (L65, corresponding inlet temperature: 117 °C (Table 2)) nearly perfect spheres with a smooth surface are obtained (Figure 2, left). Despite the rather smooth looking surface the products are crystalline [20, 18], indicating that the surface consists of rather small single crystals which are too small to be seen at as individual crystals at the given resolution. With higher temperatures (L114, corresponding to inlet temperature: 177 °C and L140, corresponding to inlet temperature: 207 °C (Table 2)) the particles are still spherical, however a hole in the shell of some particles can be seen (Figure 2, middle and right). Such "blow holes" have already been described by Walton [27] and Vehring [25]. Like the particle size this phenomenon may be explained by the drying history of the droplet in the spray drying tower. At first water will evaporate from the droplet surface. Due the evaporation of the water, the droplet has a much lower temperature than the drying air (Equation 10, i. e. a temperature close to the so-called wet bulb temperature. However after the formation of the shell a lower amount of water is evaporated and the temperature of the droplet increases. The higher the drying temperature the higher is the temperature of the solidifying droplet. As soon as it is high enough the liquid trapped inside particle reaches the boiling temperature of the solution and bubble nucleation will occur. Due to the rapid volume expansion caused by the phase transition from liquid to vapor the sudden increase in pressure finally breaks the particle shell at its weakest point leaving a so-called "blow hole".

At lower drying temperatures the liquid trapped inside the particle after the formation of the shell does not reach boiling temperature. The vaporizing water will then leave the particle by diffusion or capillary transport through the shell. Although at lower temperatures a certain pressure might built-up inside the particle as well. Due to the restriction of the shell the increase in pressure will not be high enough to cause a visible rupture of the particle shell.

With higher temperatures not only "blow holes" occur, but also surface roughness increases due to the emergence of large single crystals that form the particle shell (Figure 2, right). This behavior is somehow unexpected as usually slow crystallization, expected when drying at comparably lower temperature should result in the formation of larger crystals (see below, spray drying at pilot scale). For low temperatures the supersaturation is expected to be comparably low and usually the lower the supersaturation, the larger is the critical size of the thermodynamically stable nuclei. Consequently fewer crystals, which then grow larger, are expected to form. However larger crystals, which form the particle shell, are observed at higher temperatures and not as expected at low temperatures. Maas et al. [18] explain this behavior to be caused due to the progressive evaporation of the solvent and the formation of a highly concentrated viscous solution or even a melt at the droplet surface during drying. The high viscosity might hinder crystal nucleation. For this reason fewer crystals, which however are larger in size, can be found at higher temperatures.

Figure 3 shows the crystallization of a droplet placed on a hot stage at 120 °C roughly simulating the conditions at high drying temperatures. At the beginning the size of the droplet decreases due to the evaporation of water (image not shown). After the evaporation of the water is complete, the droplet remains liquid and forms a highly viscous liquid that then crystallizes instantaneously upon mechanical stressing or lowering the temperature of the hot stage. Large single, laminary growing crystals can be seen.

Figure 4 shows SEM micrographs of cross sections of products spray dried at lab scale. The figure gives insight into the inner structure of the spray dried products. As already stated the images reveal that the particles consist of a shell and a hollow or porous core. Due to the emergence of "blow holes" at higher temperatures most of the particles of L114 and L140 are filled with epoxid resin that had been used for particle embedding. Via the hole the epoxid resin entered the particles and solidified there. Interestingly, the largest magnification of L65 (Figure 4, left) shows that the outermost layer of the shell consists of very small crystals. However the inner shell is formed of larger crystals. The reason for this shape may be the preceding shell formation, consisting of very small single crystals causing the evaporation rate to decrease because of the constraint the shell presents to evaporation. Due to the decrease of evaporation rate the increase in concentration is

slower and the crystals are given more time to grow. The same structural composition is also found at pilot scale (Figure 9).

At even higher temperatures (L150, Figure 5) most of the particles have lost their spherical shape and compact particles without a hollow or porous core are found [20]. At higher temperatures evaporation is so fast that there is no time for crystal nucleation and all the water vaporizes, before a shell could have formed. As long as there is evaporation of water, the temperature of the droplet is far below the surrounding air temperature. This temperature is close to the wet bulb temperature and can be estimated using Equation 10. Once the water is evaporated the temperature of the particle will rise, eventually above the melting point of mannitol (166 °C, [1]), leaving a droplet consisting of molten mannitol. This melt will then crystallize instantaneously when arriving at cooler regions of the spray dryer or when colliding with other particles or the tower wall giving rise to mechanical stress forming a single mannitol crystal.

Spray drying at pilot scale

At pilot scale the feed rate was increased (10 l/h vs. 0.84 l/h) as well as the droplet size by using the LAMROT rotary atomizer instead of the NIRO rotary atomizer. The droplet sizing of the spray [10] showed that at an atomizer rotation speed of 7200 rpm leads to mean droplet sizes of approximately 140 μm. Products spray dried at pilot scale have a mean particle size of 80 μm (Table 1), a proper size to be used as a carrier in dry powder inhaler formulations. Table 3 shows the temperature profile at the pilot drying tower.

As already described by Littringer et al [10] the surface roughness of the spray dried products at pilot scale decreases with increasing temperature (Figure 6). This was somehow unexpected at first sight as the opposite was observed at lab scale where higher temperatures led to rougher surfaces (Figure 2) [18] obviously due to the formation of a highly viscous liquid at higher temperatures. Figure 6 (left) shows that at 67 °C (P67) outlet temperature, the particle shell is made-up of single, rod shaped crystals which are approximately 3 μm in length. With increasing temperatures the size of the crystals decreases and the surface appears smoother (P92, Figure 6, right). However, this behavior is also expected from a theoretical point of view as slow drying favors crystal growth, whereas fast drying results in the formation of smaller crystals.

Calculations of the drying time of droplets of 140 μm and a 40 μm at a drying temperature of 120 °C were performed, in order to understand the different crystallization processes at different spray dryer and particle size scales i.e. anticipated crystallization from a highly viscous liquid at higher temperatures in the lab scale and crystallization from a solution at the pilot scale, as a reason for different particle morphologies. For droplets of 140 μm a droplet drying time τ of 1.567 s was approximated. A much shorter drying time of 0.128 s is required to theoretically dry droplets of

40 µm. Figure 7 shows the calculated mannitol concentration at the droplet surface. Due to the different surface-to-volume ratio, the surface concentration increases faster for smaller droplets. This fast increase in concentration (high supersaturation rate) might be the reason why a highly viscous liquid is able to form on the droplet surface at high temperatures at lab scale. The supersaturation rate is so high that there is simply not enough time for the formation of crystal nuclei. Another difference is that the atomizer at lab scale rotates with a much higher speed of 23000 rpm, whereas at pilot scale a rotation speed of 7200 rpm is used. For this reason there are much higher relative velocities between the droplets leaving the lab scale atomizer and the surrounding drying air resulting in a smaller drying boundary layer and consequently faster drying and a higher supersaturation rate. There might also be differences due to the used spray towers, having different drying capacities, air flow pattern and temperature profiles. In order to exclude the influence of the spray tower, atomizers shaping droplets of different size were operated with the same feed rate in the same pilot spray dryer (see droplet size experiments below) leaving the airflow conditions also unchanged.

Besides the changes in surface morphology, Figure 6 shows that the particle shape also changes with increasing outlet temperature. At 67 °C inlet temperature (P67, corresponding inlet temperature: 120 °C, Table 3) perfect spheres are obtained (Figure 6, left). At intermediate temperatures (P80, corresponding to inlet temperature of 130 °C, Table 3) most of the particles show a single indentation at the particle surface. This morphology was described by Walton as mushroom cap-shaped [27]. At even higher temperatures, (P92, corresponding inlet temperature of 153 °C, Table 3) the particle surface contains several indentations giving the particle a raisin like appearance, see p92. In contrast to the experiments at lab scale no "blow-holes" were found when increasing the temperature at pilot scale.

Also at pilot scale, collisions with other particles, particle wall collisions, the presence of submicron dust or even air friction might initiate shell formation. As already discussed above (see results and discussion, spray drying at lab scale) at higher temperatures bubble nucleation will then lead to a pressure increase followed by expansion and rupture of the shell which will after pressure release collapse, giving the particles a mushroom cap-shaped or raisin like appearance. The higher the temperature, the more violent is the surface distortion, leading to larger morphological changes. At lab scale the particle shell is more stable, due to the smaller size of the particles. Additionally a comparably lower amount of water in relation to the particle surface is trapped. Upon bubble nucleation the shell breaks at its weakest point leaving a "blow hole". However, unlike at pilot scale, the shell has enough strength to keep the initial spherical shape and does not collapse. Products dried at 67 °C keep their spherical shape as the shell allows sufficient diffusion of vapor.

In order to mimic bubble nucleation and the impact on particle morphology crystallization experiments of a droplet on a hot stage at 120 °C were performed. In order to prevent water evaporation and the formation of a highly viscous liquid (as described above, Figure 3) crystal seeds were added to the solution. Figure 8 shows the crystallization process. In the presence of crystal seeds a shell is immediately formed. It can be seen that inside the droplet vapor bubbles are generated. The bubbles then expand and disrupt the particle shell (Figure 8, right). This violent particle structure distortion by internal bubble nucleation was also observed by Walton and Mumford [28] for crystalline particles during levitation experiments. At pilot and lab scale a similar process is likely to take place at higher temperatures resulting in either irregularly shaped particles at pilot scale or surfaces with "blow holes" at lab scale.

As already described above the SEM micrographs of cross sections of pilot scale spray dried products reveal that also these particles consist of a shell and a porous inside (Figure 9). Similarly the shell outside consists of smaller crystals than at the core of the particle. Interestingly also the inner particle crystal size decreases with increasing temperature due to the higher drying rate. In contrast to the lab scale particles (Figure 4) the core of the pilot scale particles is not filled with epoxid resin, verifying that "blow holes" are not present at pilot scale.

Droplet size experiments at pilot scale

In order to study the influence of droplet size on the morphology of spray dried mannitol particles irrespective of the size and drying capacity of the used dryer three different atomizers, the LAMROT, the Niro rotary atomizer as well as a Caldyn pneumatic nozzle, were operated at the same feed rate (10 l/h) in the pilot scale spray dryer at two drying outlet temperatures, i. e. at 70 °C and at 100 °C. Additionally the influence of feed temperature (20 °C and 70 °C) on particle morphology was studied. Figure 10 shows the experimental set-up.

The droplet size of the three atomizers was analyzed by laser diffraction. The largest mean droplet diameter of 130.2 µm was measured with the LAMROT atomizer (Table 4). Due to the slightly higher rotation speed of 7400 rpm the mean droplet size is smaller compared to the first pilot scale experiments which are described above (7200 rpm, 140 µm). Higher rotation speeds result in stronger thinning of the threads leaving the atomizer. Thinner threads will subsequently disintegrate into smaller droplets (Rayleigh break-up) [10].

As mentioned above, the feed rate used for the droplet size experiments was higher (10 l/h) than the feed rate at lab scale (0.84 l/h). This increase in feed rate made it possible to determine the droplet size of the Niro atomizer by laser diffraction. In contrast to the calculated value of the mean droplet diameter of 27 µm for the spray generated at lab scale [18] the mean diameter determined in the present experiments was 48.9 µm. Although the calculation model is based on simplified

assumptions, the increase in droplet diameter when operating the Niro atomizer at 10 l/h is a result of the higher feed rate. When higher feed rates are used the ligaments that leave the atomizer have a larger diameter and will subsequently disintegrate into droplets of larger size [10]. The smallest droplets were generated by the pneumatic nozzle (mean drop size: 19.1 µm, Table 4).

The largest droplet sizes and consequently the largest mean particle sizes (73.8 µm – 78.6 µm) were measured for products generated with the LAMROT atomizer (Table 4). Spray generation with the Niro atomizer resulted in particles with a smaller mass mean diameter of 11.6 µm – 13.4 µm. The smallest mass mean diameters of the solidified droplets were observed with the Caldyn nozzle (8.9 µm - 9.8 µm). In Table 5 the dryer outlet temperatures, the feed temperatures and the resulting particle sizes are given. The surface morphologies of the corresponding dry products are shown in Figure 11 and Figure 12.

Figure 11 verifies the findings of the lab and pilot scale experiments that irrespective of the size of the used dryer the particle roughness depends on the initial droplet size. For large droplets (≈ 130 µm) an increase in the air outlet temperature leads to a decrease in surface roughness of the mannitol particles and vice versa for smaller initial droplets (≈ 50 µm and ≈ 20 µm).

The 50 µm Niro droplets dried in the pilot scale spray dryer show the same dependence of the shell surface roughness on the outlet temperature as the ones dried at lab scale. However, there is a big difference concerning the particle shape. The SEM images reveal that most of the particles are broken-up (Figure 11). Particle rupture might have taken place due to a higher pressure caused by the higher amount of water compared to the smaller lab scale droplets and subsequent vapor expansion. However in relation to the larger pilot scale particles, the shell is more stable and does not collapse. The shape of the LAMROT based particles is the same as described above for the former pilot scale products. At 70 °C outlet temperature perfect spheres are obtained whereas at higher temperature raisin-like structures are found. Also the Caldyn nozzle based particles have the expected spherical shape.

Because of the fact that crystallization, and consequently particle morphology, is highly dependent on temperature, the influence of feed temperature was also studied. Therefore the feed was heated-up to 70 °C prior to spray drying. All the other experiments described above had been carried out at a feed temperature of 20 °C.

For the LAMROT particles an increase in feed temperature leads to larger single crystals building up the shell of the particles. The surface appears rougher. No influence of feed temperature on surface roughness was found for the smaller Niro and Caldyn particles.

The mechanism for larger droplets might be that with higher feed temperatures the solubility of mannitol is increased. Therefore the supersaturation at the droplet surface during drying is smaller

than for lower feed temperatures for the initial drying stage. However the smaller the supersaturation the larger is the critical size of thermodynamically stable nuclei. Therefore fewer crystals, which then can grow larger, will form.

Conclusion and outlook

This study shows that particle morphology of spray dried mannitol, especially surface roughness, largely depends on the initial drop size. Due to the fact that large droplets can only be dried in large spray drying towers, the scale of the used spray dryer implicitly influences the drying result. Depending on the droplet size, two different crystallization regimes of aqueous mannitol solutions can be observed; either crystallization from a solution or delayed crystallization from a highly supersaturated viscous liquid or even water-free melt. For small droplets in lab scale trials and low outlet temperatures crystallization from a solution is observed, leading to smooth surfaces composed of numerous small crystals at the surface. At higher outlet temperatures crystallization obviously takes place within a highly supersaturated viscous liquid and crystals at the surface become larger giving the surface a rougher appearance. When drying larger droplets at pilot scale no viscous liquid is formed due to slower increase in concentration (lower supersaturation rate). For that reason for all temperatures studied at pilot scale, crystallization of mannitol takes place from solution, where usually drying at low temperatures results in the formation of larger crystals due to low nucleation rates. In contrast, drying at higher temperatures leads to higher nucleation rates and then to smoother surfaces. For large droplets it could be also demonstrated that higher feed temperatures result in comparably rougher surfaces.

Acknowledgements

Appendix A: Calculation of the droplet surface concentration

In order to calculate the mannitol concentration profiles of droplets of 140 µm and 40 µm in diameter of an aqueous mannitol solution (15 % w/w) during spray drying at 120 °C (393.15 K) a simplified analytical treatment was chosen [25, 15]. Equation 1 [11, 25, 15], also called d^2-law, can be used to calculate the droplet size d at a certain time t depending on the initial droplet size d_0, the drying time t and the evaporation rate of a single droplet κ.

$$d^2(t) = d_0^2 - \kappa * t$$

Equation 1

This equation shows that the droplet surface area decreases linearly with the drying time. With this equation the time τ_D that is required to completely evaporate a droplet of a certain size d_0 can be estimated [25]:

$$\tau_D = \frac{d_o^2}{\kappa}$$

Equation 2

The mean solute concentration of a drying droplet at a certain time can be calculated by dividing the mass of the solute by the volume of the droplet at the time t. The volume of the droplet is calculated using Equation 1. Several rearrangements lead to the following equation where c_m is the mean solute concentration, c_0 the initial solute concentration (15 % w/w), t the drying time and τ_D the time that is required to completely evaporate a droplet of an initial droplet size d_0.

$$c_m = c_0 * (1 - \frac{t}{\tau_D})^{-3/2}$$

Equation 3

In order to describe, if there is an enrichment of the solute at the droplet surface the Peclet number (Pe), which is the ratio of the evaporation rate (κ) and the diffusion coefficient of the solute (D_s) can be used [15, 25]:

$$Pe = \frac{\kappa}{8 * D_s}$$

Equation 4

For drying of a droplet at 120 °C, which exhibits the evaporation rate κ of 0,012509 mm^2/s (see calculation evaporation rate below) and the diffusion coefficient of the solvent (see below, Equation 5) of 4,59-06 cm^2/s a Peclet number of 3.4 is obtained.

$$D_s = \frac{k_B * T}{6 * \pi * \eta * r_0}$$

Equation 5

The diffusion coefficient of the solute is calculated by using the Stokes-Einstein equation where k_B is the Boltzmann constant, T the temperature (here the calculated wet bulb temperature, see below), η the dynamic viscosity of the solution (0.00121 Pa*s) and r_0 the hydrodynamic solute radius (4.1 Å).

The surface enrichment (E), which is defined as the ratio of the concentration of the solute at the surface (c_s) and the mean solute concentration (c_m), can be approximated by using the following formula (Pe<20) [15, 25]:

$$E = \frac{c_s}{c_m} = 1 + \frac{Pe}{5} + \frac{Pe^2}{100} + \frac{Pe^3}{4000}$$

Equation 6

With a Peclet number of 3.4 the surface enrichment E of 1.8 is obtained.

In reality the calculation or measurement of the evaporation rates of droplets in a spray dryer is complex due to a variety of unknown and changing process parameters and physical properties of the liquid mixture. However it can be estimated with Equation 7 [9]:

$$\kappa = 8 * D_g * \frac{\rho_g}{\rho_l} * (Y_S(T_e) - Y_\infty)$$

Equation 7

Here we see that the evaporation rate (κ) depends on the diffusion coefficient in the gas phase (D_g, see below), the density of the gas (ρ_g) and the liquid ($\rho_l = 1050$ g/dm^3) phase, the mass fraction of solvent in the gas phase at the droplet surface (Y_S, see below) and the mass fraction of the solvent far from the surface ($Y_\infty = 0$). The density of the gas at 120 °C was calculated with the ideal gas law (0.8976 g/dm^3).

The required diffusion coefficient of vapor within the gas phase can be estimated at low pressures according to Fulder [10], where T is the temperature of the drying gas (in Kelvin), M_i the molar mass of solvent (here H_2O), M_j the molar mass of the drying air, ($\sum\Delta v_i$) the diffusion volume of the solvent and ($\sum\Delta v_j$) the diffusion volume of the drying air, p the atmospheric pressure.

$$D_g = \frac{0.00143 * T^{1.75} * [(M_i^{-1}) + (M_j^{-1})]}{p * \sqrt{2} * [(\sum\Delta v_i)^{1/3} + (\sum\Delta v_j)^{1/3}]^2}$$

Equation 8

At 393.15 K (120 °C) a D_g of 0.43188648 cm^2/s was calculated.

In order to calculate the mass fraction of the water vapor at the surface Equation 9, with p_s being the vapor pressure of the solvent at the corresponding equilibrium temperature (T_e in Kelvin) was used:

$$Y_s(T_e) = 0.622 * \frac{p_s}{p - p_s}$$

Equation 9

The vapor pressure of the solvent (0,06459252 bar) at the corresponding equilibrium temperature of 310,73 K (37.58 °C, T_e, see below) can be calculated by using the Clausius- Clapeyron relationship.

In order to approximate the equilibrium temperature, an empirical correlation [21] of the wet bulb temperature (T_{wb} in Kelvin) , which is the temperature that establishes at the droplet surface during evaporation, as a function of the boiling temperature of the solution (T_b in Kelvin) and the gas temperature (T_g in Kelvin) was used:

$$T_{wb} = 137 * (\frac{T_b}{373.15})^{0.68} * \log(T_G) - 45$$

Equation 10

Assuming a boiling temperature of the solution (T_b) of 373.57 K and a gas temperature (T_G) of 393,15 K the wet bulb temperature (T_{wb}) of 31.,73 K (37.58 °C) is obtained.

References

[1]   Artur Burger, Jan-Olav Henck, Silvia Hetz, Judith M. Rollinger, Andrea A. Weissnicht, and Hemma Stöttner. Energy/temperature diagram and compression behaviour of the polymorphs of d-mannitol. *Journal of pharmaceutical sciences*, 89:457–468, 2000.

[2]   Hak-Kim Chan and Nora Y. K. Chew. Novel alternative methods for the delivery of drugs for the treatment of asthma. *Advanced Drug Delivery Reviews*, 55(7):793 – 805, 2003.

[3]   Derek Ivan Daniher and Jesse Zhu. Dry powder platform for pulmonary drug delivery. *Particuology*, 6(4):225 – 238, 2008.

[4]   B.H.J. Dickhoff, A.H. de Boer, D. Lambregts, and H.W. Frijlink. The interaction between carrier rugosity and carrier payload, and its effect on drug particle redispersion from adhesive mixtures during inhalation. *European Journal of Pharmaceutics and Biopharmaceutics*, 59:197 – 205, 2005.

[5]   Dina El-Sabawi, Stephen Edge, and Robert Price. Continued investigation into the influence of loaded dose on the performance of dry powder inhalers: surface smoothing effects. *Drug development and industrial pharmacy*, 32:1135–1138, 2006.

[6]   Dina El-Sabawi, Robert Price, and Stephen Edge. Novel temperature controlled surface dissolution of excipient particles for carrier based dry powder inhaler formulation. *Drug development and industrial pharmacy*, 32:243–251, 2006.

[7]   Jessica Elversson and Anna Millqvist-Fureby. Particle size and density in spray drying- effects of carbohydrate properties. *Journal of pharmaceutical sciences*, 94(9):2049–2060, 2005.

[8]   F. Ferrari, D. Cocconi, R. Bettini, F. Giordano, P. Santi, M. Tobyn, R. Price, P. Young, C. Caramella, and P. Colombo. The surface roughness of lactose particles can be modulated by wet-smoothing using a high-shear mixer. *AAPS PhramSciTech*, 5, 2004.

[9]   W.H Finlay. *The mechanics of inhaled pharmaceutical aerosols*. Academic press, 2001.

[10]   Fulder. *Verfahrenstechnik, VDI Wärmeatlas*, volume 10. Springer-Verlag Berlin Heidelberg, 2006.

[11]   G.A.E. Godsave. Studies of the combustion of drops in a fuel spray—the burning of single drops of fuel. *Symposium (International) on Combustion*, 4(1):818 – 830, 1953.

[12]   Anthony J. Hickey. Lung deposition and clearance of pharmaceutical aerosols: What can be learned from inhalation toxicology and industrial hygiene? *Aerosol Science and Technology*, 18(3):290–304, 1993.

[13]   Kotaro Iida, Yukari Inagaki, Hiroaki Todo, Hirokazu Okamoto, Kazumi Danjo, and Hans Luenberger. Effects of surface processing of lactose carrier particles on dry powder inhalation properties of salbutamol sulfate. *Chem. pharm. bull.*, 52:938–942, 2004.

[14]   Kotaro Iida, Hiroaki Todo, Hirokazu Okamoto, Kazumi Danjo, and Hans Leuenberger. Preparation of dry powder inhalation with lactose carrier particles surface-coated using a wurster fluidized bed. *Chem. pharm. bull.*, 53:431–434, 2005.

[15]   N. R. Labris and M. B. Dolovich. Pulmonary drug delivery.part i: Physiological factors affecting therapeutic effectiveness of aerosolized medications. *British journal of clinical pharamcology*, 56:588–599, 2003.

[16]   Eva Maria Littringer, Axel Mescher, Susanna Eckhard, Hartmuth Schröttner, Christoph Langes, Manfred Fries, Ulrich Griesser, Peter Walzel, and Nora Anne Urbanetz. Spray drying of mannitol as a drug carrier – the impact of process parameters on the product properties. *Drying Technology*, 30:114–124, 2012.

[17]   Eva Maria Littringer, Axel Mescher, Hartmuth Schroettner, Peter Walzel, and Nora Anne Urbanetz. Spray-dried mannitol carrier particles with optimized surface properties – the influence of carrier surface roughness and shape. *European Journal of Pharmaceutical Sciences*, page in press, 2012.

[18]   S. G. Maas, G. Schaldach, E. M. Littringer, A. Mescher, U. J. Griesser, D. E. Braun, P. Walzel, and N. A. Urbanetz. The impact of spray drying outlet temperature on the particle morphology of mannitol. *Powder Technology*, 213:27–35, 2011.

[19]   Stephan G. Maas, Gerhard Schaldach, Peter E. Walzel, and Nora A. Urbanetz. Tailoring dry powder inhaler performance by modifying carrier surface topography by spray drying. *Atomization and Sprays*, 20:763–774, 2010.

[20]   Stephan Gerhard Maas. *Optimierung trägerbasierter Pulverinhalate durch Modifikation der Trägeroberfläche mittels Sprühtrocknung*. PhD thesis, Heinrich-Heine-Universität Düsseldorf, 2009.

[21]   R.S. Miller, K. Harstad, and J. Bellan. Evaluation of equilibrium and non-equilibrium evaporation models for many-droplet gas-liquid flow simulations. *International Journal of Multiphase Flow*, 24(6):1025 – 1055, 1998.

[22]   Thomas Schröder and Peter Walzel. Gestaltung laminar betriebener rotationszerstäuber unter berücksichtigung der abströmgeometrie. *Chemie Ingenieur Technik*, 70:400–405, 1998.

[23]   Chi Sung Song and Charn Jung Kim. Freeze-drying of skim milk in a cylindrical container. *Drying Technology*, 21(9):1811–1838, 2003.

[24]   H. Steckel, P. Markefka, H. teWierik, and R. Kammelar. Effect of milling and sieving on functionality of dry powder inhalation products. *International Journal of Pharmaceutics*, 309(1-2):51 – 59, 2006.

[25]   Reinhard Vehring. Pharmaceutical particle engineering via spray drying. *Pharmaceutical research*, 25:1000–1022, 2008.

[26]   Reinhard Vehring, Willard R. Foss, and David Lechuga-Ballesteros. Particle formation in spray drying. *Aerosol Science*, 38:728–746, 2007.

[27]   D. E. Walton. The morphology of spray-dried particles a qualitative view. *Drying technology*, 18:1943–1986, 2000.

[28]   D.E. Walton and C.J. Mumford. The morphology of spray-dried particles: The effect of process variables upon the morphology of spray-dried particles. *Chemical Engineering Research and Design*, 77(5):442 – 460, 1999.

[29]   Peter Walzel. *Ullmann's Encyclopedia of Industrial Chemistry*. Wiley online, 2010.

Table 1. Particle size distribution of the products spray dried at lab scale at 65°C (L65), 114 °C (L114) and 140 °C (L140) outlet temperature (T2) determined by laser diffraction and of the products spray dried at pilot scale at 67°C (P67), 80 °C (P80) and 92 °C (P92) outlet temperature (T4) determined by sieving.

		$X_{10.3}$ / µm	$X_{50.3}$ / µm	$X_{90.3}$ / µm
Lab	L65	3.5	10.4	20.4
	L114	4.9	11.9	23.8
	L140	7.6	15.2	26.9
Pilot	P67	54.8	84.0	123.7
	P80	60.2	84.4	118.8
	P92	56.4	77.4	110.9

Table 2. Temperature profile of the products spray dried at lab scale at 65°C (L65), 114 °C (L114) and 140 °C (L140) outlet temperature (T2, location of temperature points T see Figure 1).

	T1 / °C	T2 / °C
L65	117	65
L114	177	114
L140	207	140

Table 3. Temperature profile of products spray dried at pilot scale at 67°C (P67), 80 °C (P80) and 92 °C (P92) outlet temperature T1 to T4, (location of temperature points T see Figure 1).

	T1 / °C	T2 / °C	T3 / °C	T4 / °C
P67	120	78	78	67
P80	130	92	92	80
P92	153	110	110	92

Table 4. Droplet size distribution of the spray generated by the three different atomizers obtained from offline drop size measurements by laser diffraction.

	$X_{10.3}$ / µm	$X_{50.3}$ / µm	$X_{90.3}$ / µm
LAMROT / 7400 rpm	104.1	130.2	164.8
Niro / 4.1 bar 24000 rpm	33.4	48.9	71.1
Caldyn / 1.9 bar	9.1	19.1	39.3

Table 5. Particle size distribution of the spray dried products generated by the three different atomizers studied in the droplet size experiments and determined by laser diffraction.

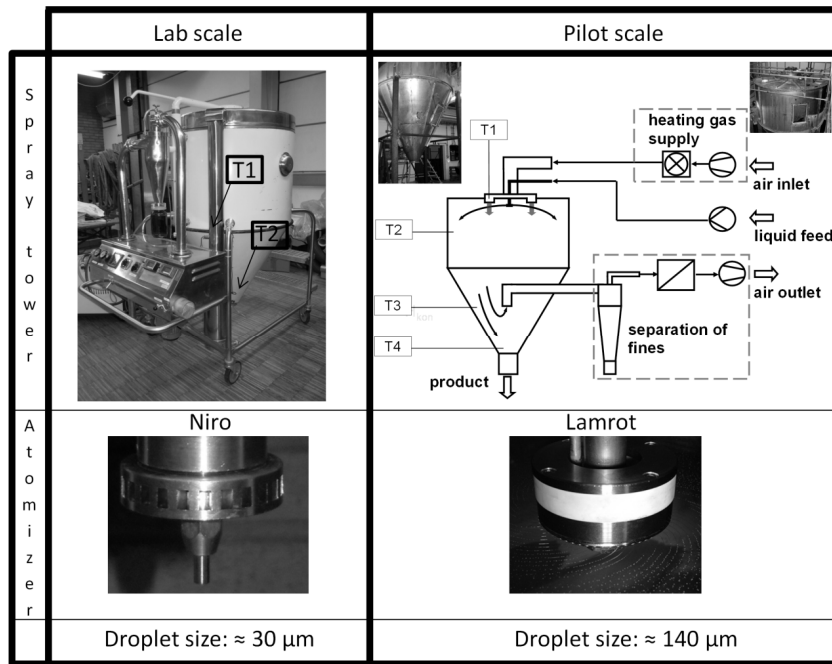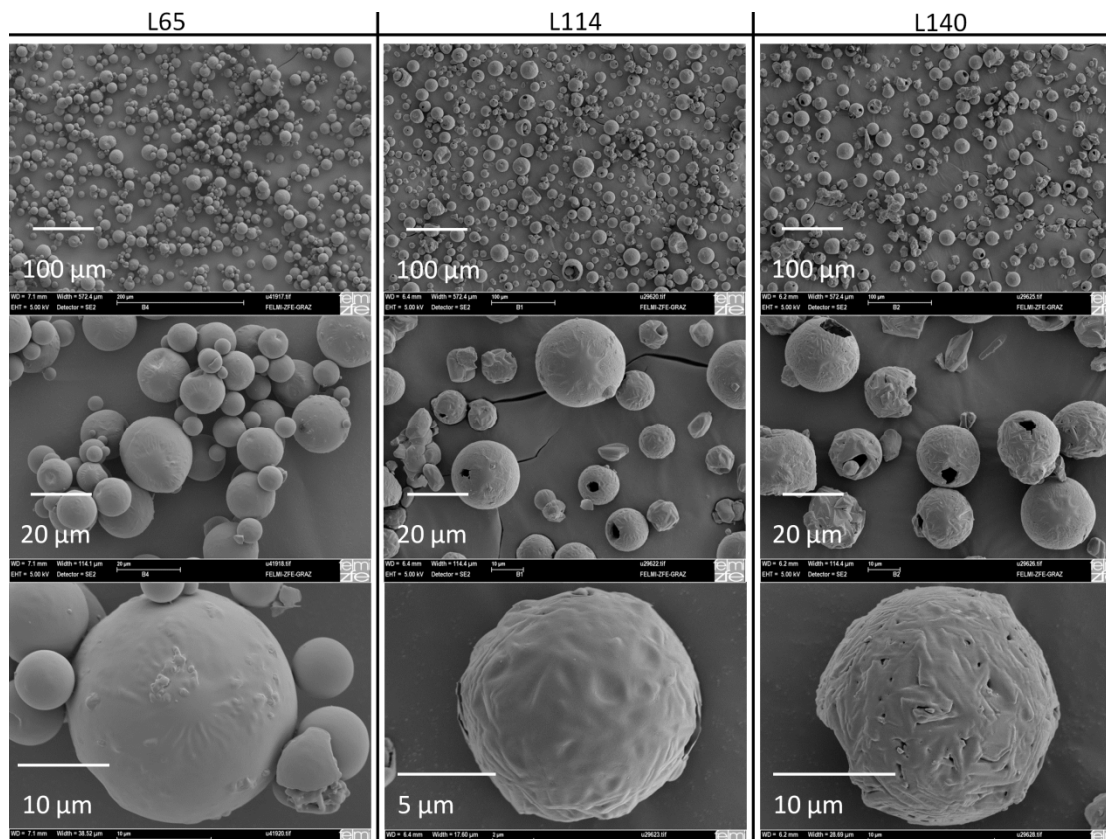|	T4 / °C	Feed temp. / °C	$X_{10.3}$ / µm	$X_{50.3}$ / µm	$X_{90.3}$ / µm
LAMROT	70	20	33.5	78.6	161.9
	100	20	47.0	78.1	121.7
Niro	70	20	4.1	11.6	24.0
	100	20	2.7	11.6	22.8
Caldyn	70	20	3.0	8.9	18.4
	100	20	2.3	9.3	19.6
LAMROT	70	70	31.3	74.1	134.8
	100	70	40.0	73.8	126.4
Niro	70	70	4.2	12.3	25.8
	100	70	3.4	13.4	27.5
Caldyn	70	70	3.0	9.3	21.0
	100	70	2.2	9.8	21.4

Figure 1. Schematic of lab and pilot scale spray drying.

Figure 2. SEM micrographs of the products spray dried at lab scale at 65°C (L65), 114 °C (L114) and 140 °C (L140) outlet temperature (T2).
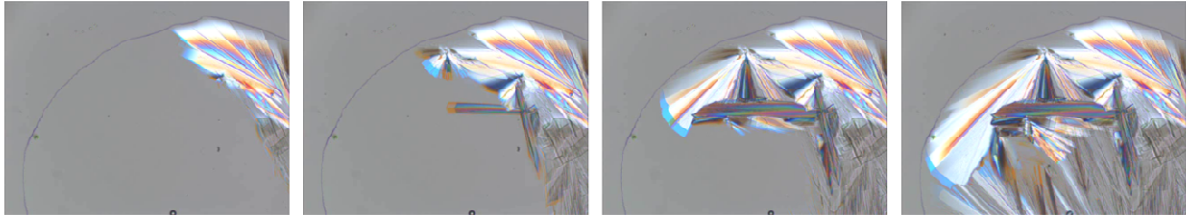
Figure 3. Polarized light micrographs of the progress of crystallization from a highly viscous liquid at the hot stage at 120 °C (droplet size approximately 2 mm).
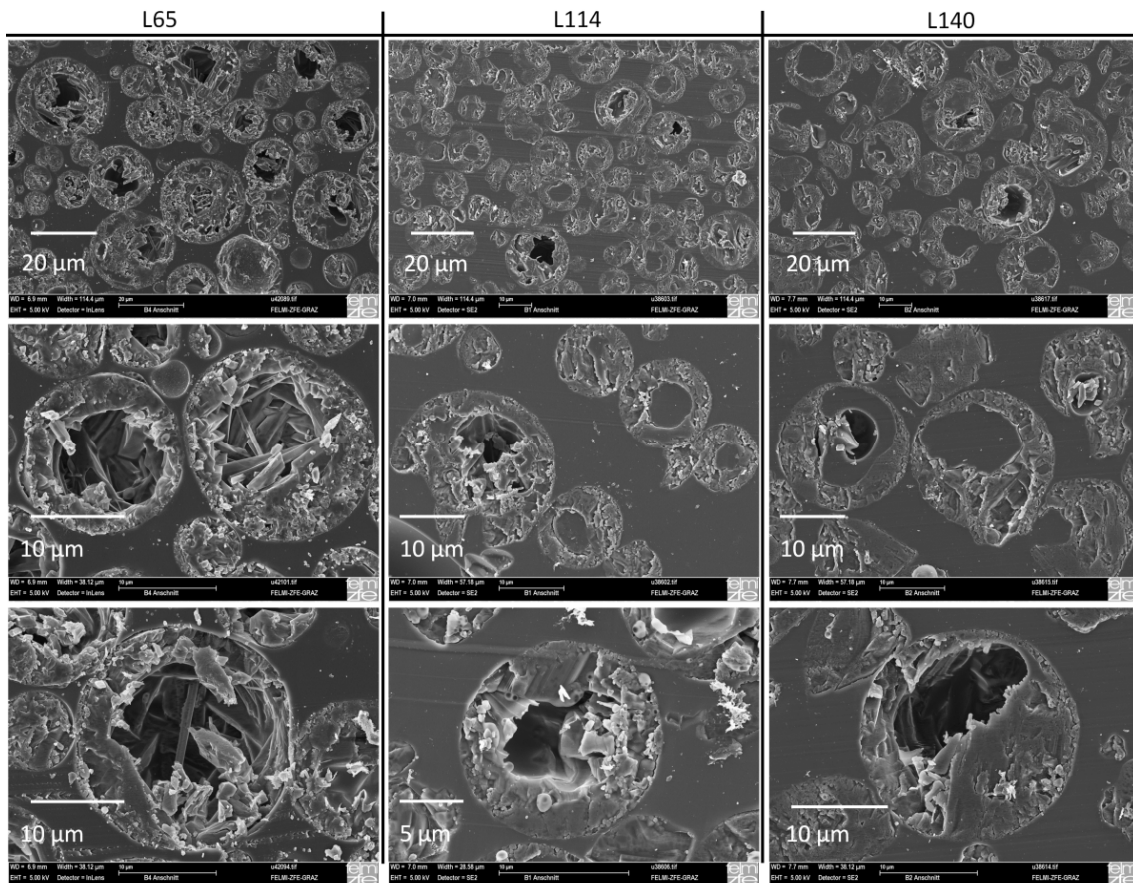

Figure 4. SEM micrographs of cross sections of products spray dried at lab scale at 65°C (L65), 114 °C (L114) and 140 °C (L140) outlet temperature (T2).
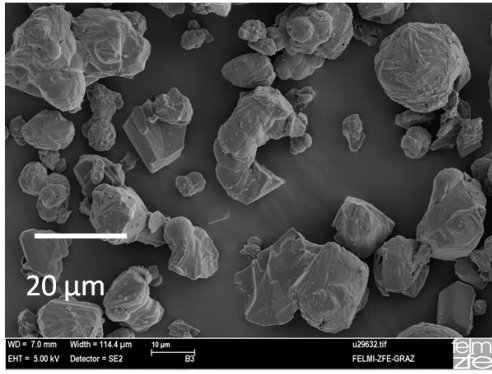
Figure 5. SEM micrograph of a product spray dried at lab scale at 150 °C (L150) outlet temperature (T2).
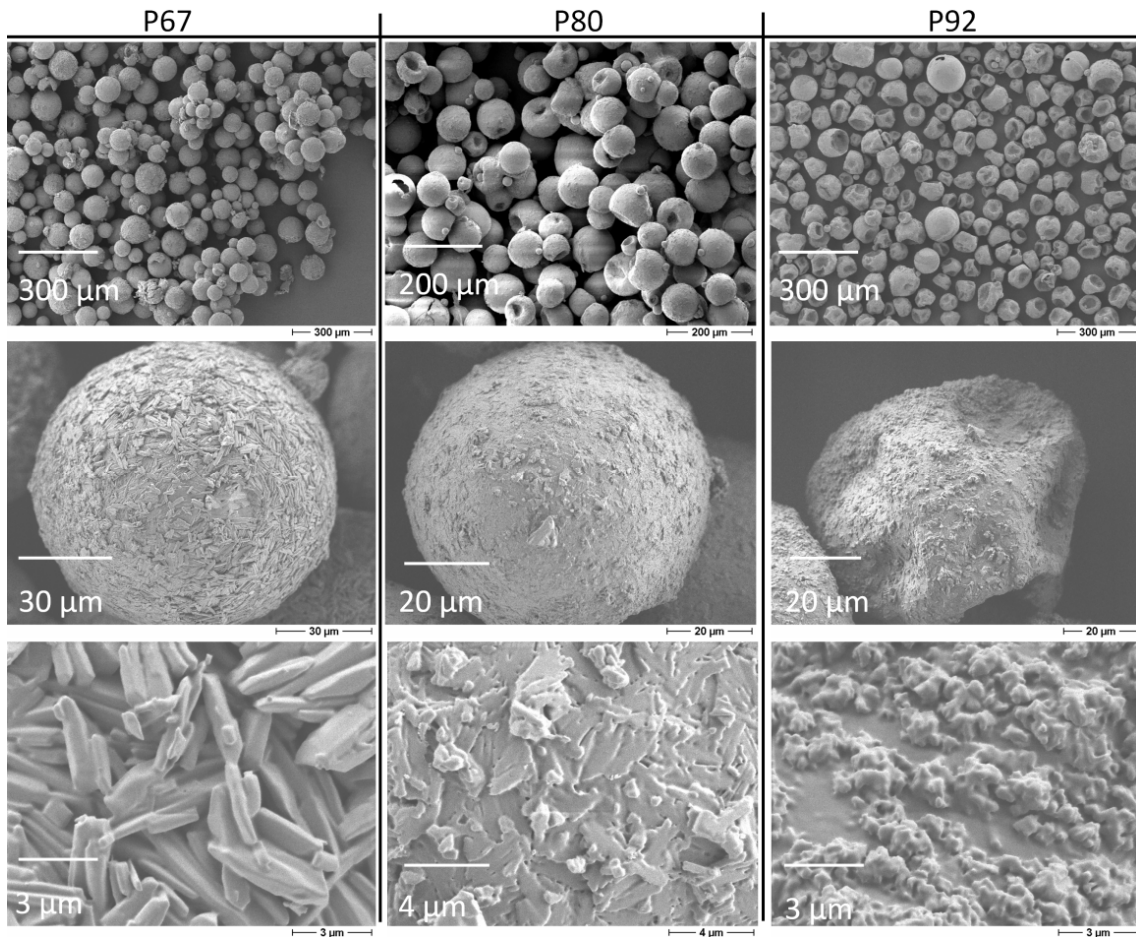

Figure 6. SEM micrographs of the mannitol particles spray dried at pilot scale at 67°C (P67), 80 °C (P80) and 92 °C (P92) outlet temperature (T4).
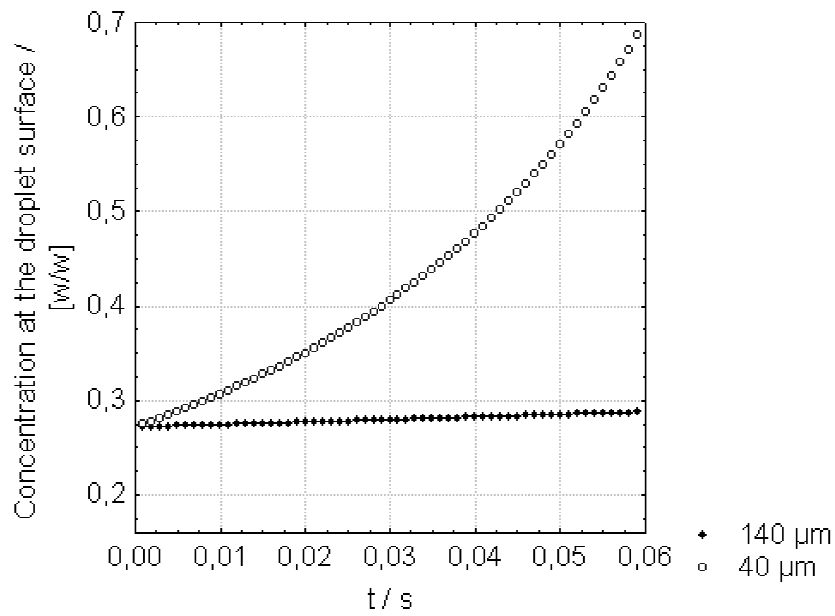
Figure 7. Calculated mannitol concentration profiles at the droplet surface when drying a droplet of 140 µm and 40 µm at a drying temperature of 120 °C.
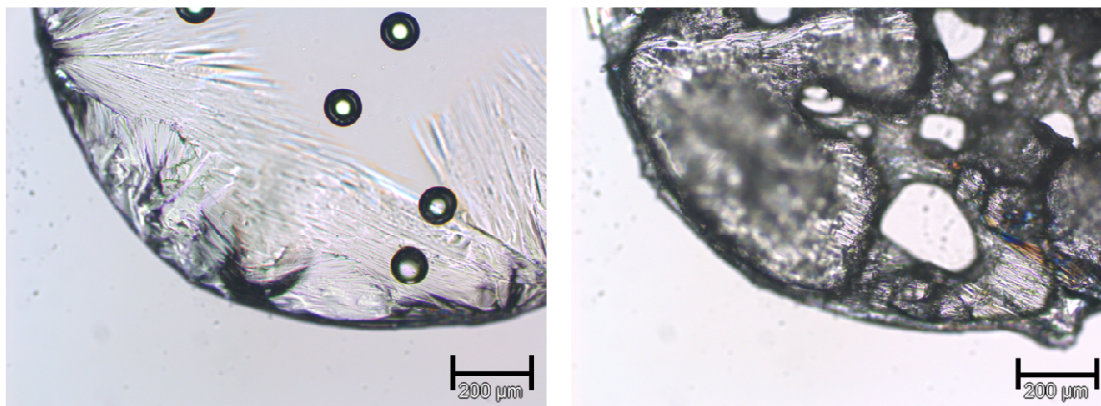
Figure 8. Polarized light micrographs of bubble nucleation (left) and subsequent shell distortion (right) at the hot stage at 120 °C.
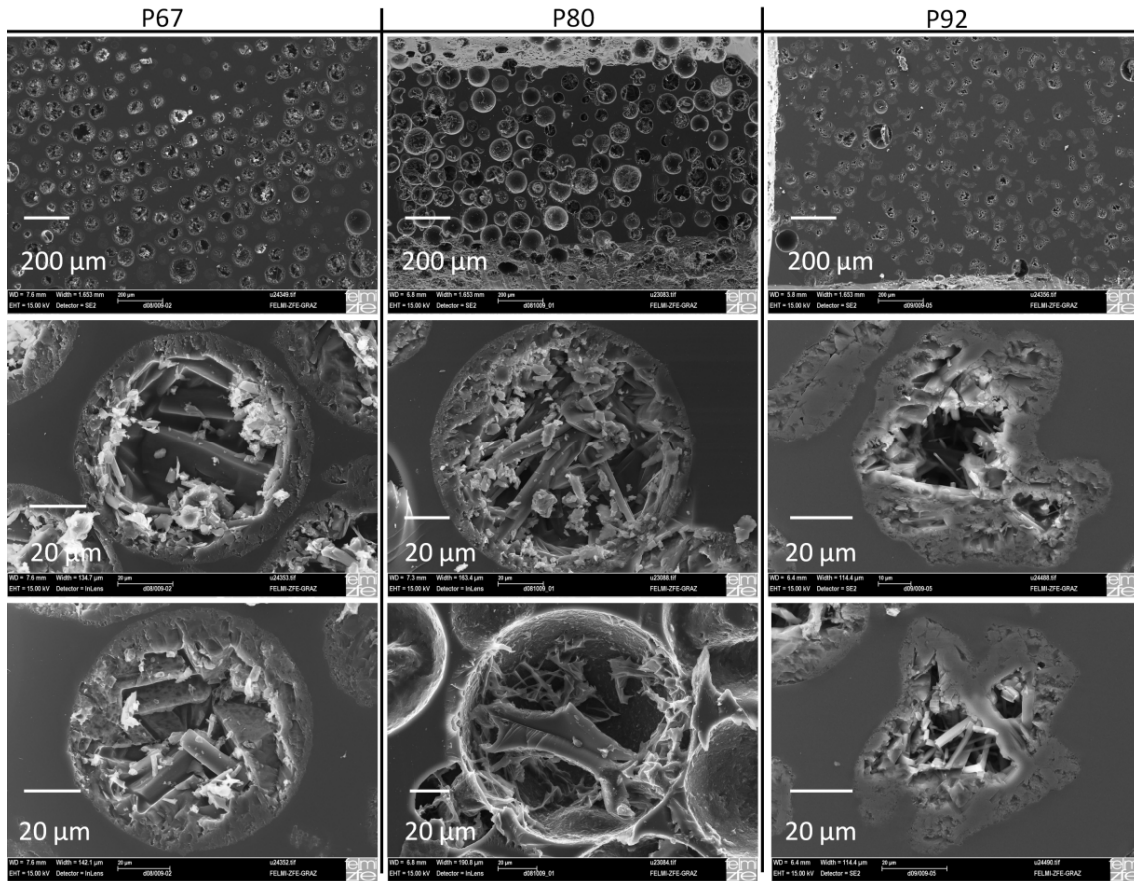
Figure 9. SEM micrographs of the cross sections of products spray dried at pilot scale at 67°C (P67), 80 °C (P80) and 92 °C (P92) outlet temperature (T4).
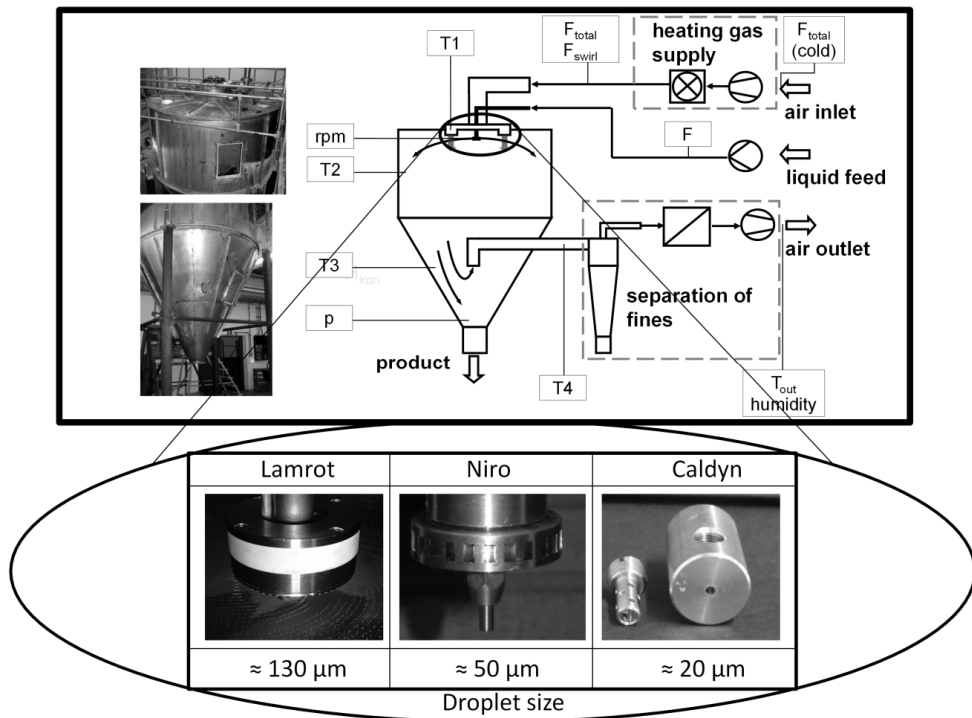
Figure 10. Schematic of the droplet size experiments.
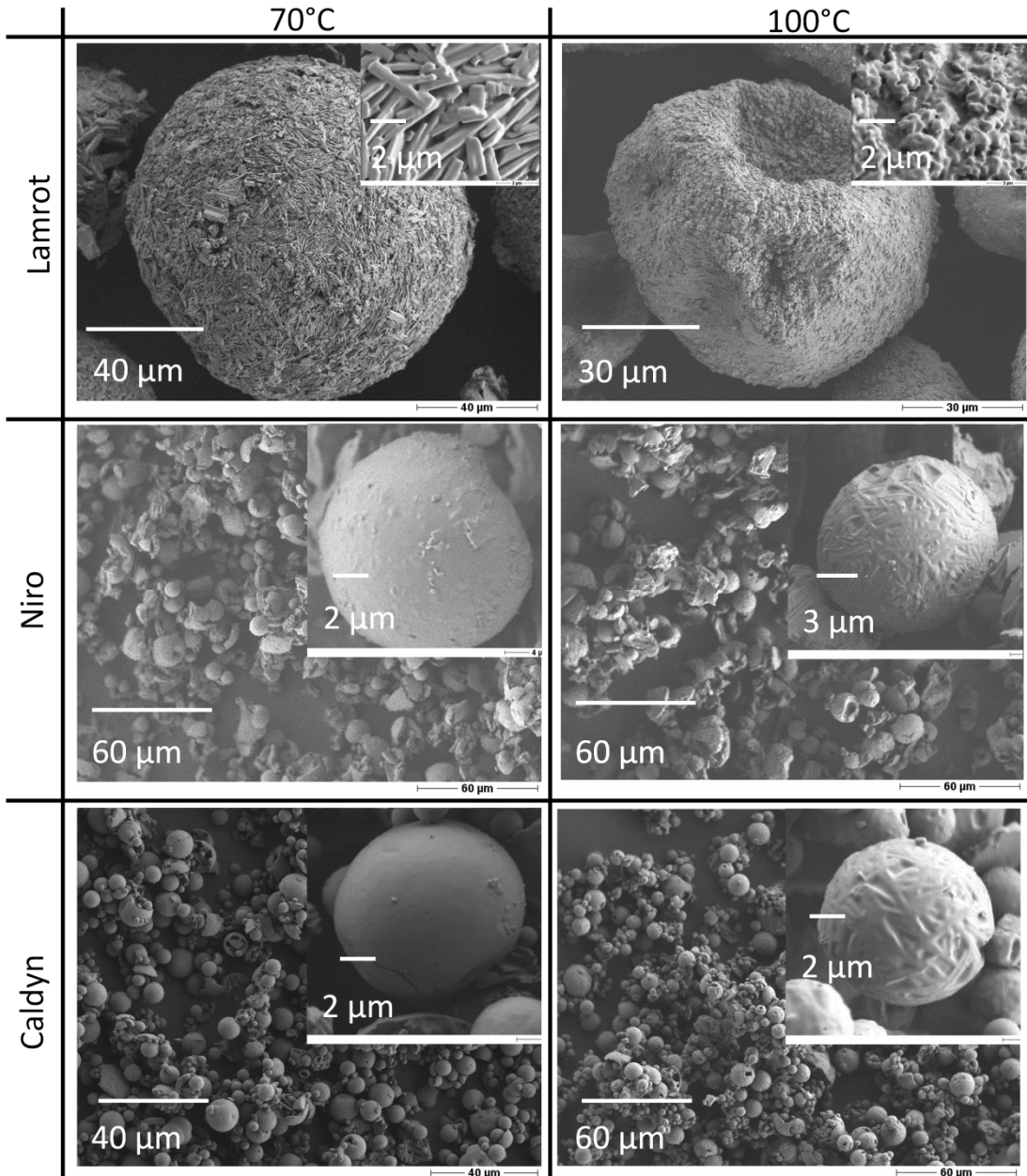
Figure 11. SEM micrographs of spray dried droplets of different size dried at 70°C and 100 °C outlet temperature (feed temp. 20°C).
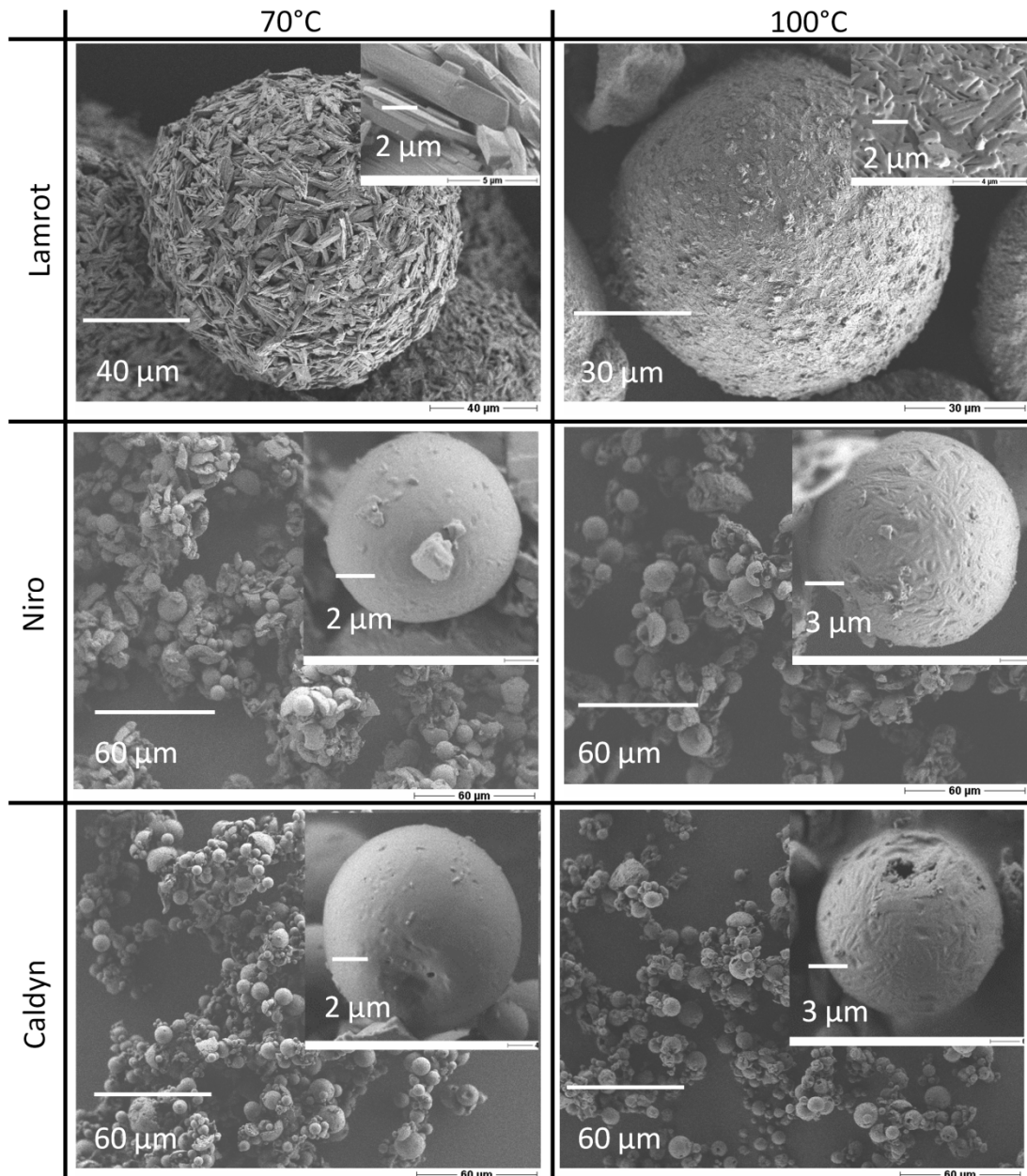
Figure 12. SEM micrographs of spray dried droplets of different size dried at 70°C and 100 °C (feed temp. 70°C).

3.4. Outlook- API morphology and size optimization

3.4.1. Spray drying of aqueous salbutamol sulfate solutions using the Nano Spray Dryer B-90 - The impact of process parameters on particle size

Eva Maria Littringer, Sarah Zellnitz, Kerstin Hammernik, Verena Adamer, Herwig Friedl, Nora Anne Urbanetz

Spray drying of aqueous salbutamol sulfate solutions using the Nano Spray Dryer B-90 - The impact of process parameters on particle size

E M Littringer[1*], S Zellnitz[2], K Hammernik[1], V Adamer[3], H Friedl[4], N A Urbanetz[1]

[1]Research Center Pharmaceutical Engineering GmbH, Inffeldgasse 21a/II, Graz, Austria

*Corresponding author: Tel: +43 316 873 9743; Fax: +43 316 873 109743; Email: eva.littringer@tugraz.at

[2]Institute for Process and Particle Engineering, Graz University of Technology, Inffeldgasse 21a, Graz, Austria

[3]Department of Pharmaceutical Technology, University of Innsbruck, Innrain 80/82, Innsbruck, Austria

[4]Institute of Statistics, Graz University of Technology, Kopernikusgasse 24/III, Graz, Austria

Abstract

In order to prepare spherical salbutamol sulfate particles of adjustable size the Nano Spray Dryer B-90 was employed. A 3^3 full factorial design was used to investigate the influence of process parameters (mesh size, feed concentration and drying air temperature) on the particle size (median size and width of the particle size distribution), the amount of product produced per time and the product yield. The median particle size was significantly influenced by all three factors of the statistical design. Within the design space studied particle sizes of 1.01 μm to 6.39 μm were obtained. The width of the particle size distribution (span) increased with increasing mesh sizes. All particles with a particle size above 2.39 μm showed a bimodal particle size distribution. Generally larger mesh sizes as well as larger concentrations led to an increase in the amount of product prepared per time. The corresponding values observed were from 0.44 mg/min to 75.83 mg/min. The product yield was independent of the process parameters studied. All products were amorphous after spray drying and were stable up to a relative humidity of 60 %.

Introduction

Dry powder inhalers (DPI) are widely used in the treatment of respiratory diseases like asthma bronchiale and chronic obstructive pulmonary disease (COPD). In such formulations, which usually comprise an excipient that ensures sufficient flowability and the active pharmaceutical ingredient (API), the dry powder is directly administered to the lung. However in order to reach the targeted regions of the lung, the bronchioles, the API must have an aerodynamic particle size in the range of 1 μm to 5 μm [14, 7, 17]. Particles that are too large cannot follow the air stream. They will impact in the throat and will have no access to the bronchiolar region. However if the particle size is below

1 μm the particles will travel deeper into the lung during inhalation and will be deposited mainly in the alveolar region.

Usually the preparation of particles in the low micrometer range involves micronization. The disadvantages of this procedure are the need of high energy input and the high variability of the morphology of the obtained single particles leading to unpredictable dry powder inhaler (DPI) performance. For this reason narrowly size distributed, isometric, preferably spherical particles would be desirable. A rather easy and widely used technique to prepare spherical particles with narrow size distribution is spray drying where a liquid feed is dispersed into small droplets which subsequently are dried in a heated tower. There are several studies which show the suitability of spray drying for the preparation of API particles for pulmonary drug delivery [16, 4, 18]. Therefore the aim of this work is the preparation of spherical salbutamol sulfate particles as a model API with adjustable particle size.

Instead of a conventional spray dryer the recently launched Nano Spray Dryer B-90 was used in the present study. The droplet generation as well as the particle collection of this spray dryer differs from a conventional one. A vibrating mesh, that is piezoelectrically driven, enables droplet generation. Further, instead of using the cyclone technology, particles are collected with an electrostatic particle collector [8, 1]. Several studies have been performed using this novel spray dryer already. For example protein solutions were dried by Bürki et al. [2] and Lee et al. [8]. Cyclosporin A and dexamethasone were encapsulated by Schafroth et al. [13]. Also potential wall materials for encapsulation (arabic gum, whey protein, polyvinyl alcohol, modified starch and maltodextrin) were investigated [9]. However to the knowledge of the authors there are no studies on the thorough investigation of the impact of process parameters of the Nano Spray Dryer B-90 on the particle size (median, width of the particle size distribution), the mass of product generated per time and yield of a low molecular weight compound, here salbutamol sulfate, spray dried from aqueous solutions available.

The obtained salbutamol sulfate particles may be used finally to study the complex interplay of API size and carrier surface roughness in dry powder inhaler formulations as optimizing carrier surface roughness (spacing distance, see [11, 10]) and API size might be a useful approach to optimize the performance of carrier-based inhalates.

Materials and methods

Materials

Salbutamol sulfate (USP25 quality) was provided by Selectchemie (Zuerich, Switzerland). Aqueous salbutamol sulfate solutions used for spray drying were prepared with purified water (TKA Micro

Pure UV ultra pure water system, TKA Wasseraufbereitunssysteme GmbH, Niederelbert, Germany) equipped with a capsule filter (0.2 µm).

Spray drying

The spray dried products were prepared on a Nano Spray Dryer B-90 (Buechi Labortechnik AG, Flawil, Switzerland) equipped with the long version of the drying chamber. Drying air flow rate (110 l/h) and spray rate (30 %) were constant and the same for all experiments. Atomizer mesh size, feed concentration and drying air temperature were varied according to the experimental design (see below and Table 1). Products were stored desiccated after spray drying until further required.

Statistical design

The influence of atomizer mesh size (4.0 µm, 5.5 µm, 7.0 µm), feed concentration (1.0 %, 7.5 %, 15.0 %; (m/m)) and drying air temperature (80 °C, 100 °C, 120 °C) on median particle size, the amount of product spray dried per time and product yield was studied using a full-factorial 3^3 design (Table 1, Table 2). The statistical analysis was carried out using Modde 9.0 software (Umetrics AB, Umeå, Sweden). In order to get normally distributed data the responses median particle size and amount of product spray dried per time were logarithmically transformed prior to statistical analysis. Only significant terms were considered in the model. A significance level of 0.05 was used.

Particle size distribution

The particle size distribution of the spray dried products was determined by laser light diffraction (Helos/KR, Sympatec, Clausthal-Zellerfeld, Germany). A dry dispersing system (Rodos/L, Sympatec, Clausthal-Zellerfeld, Germany) and a vibrating chute (Vibri, Sympatec, Clausthal-Zellerfeld, Germany) were used for powder dispersion. A dispersing pressure of 2.0 bar was applied. Evaluation of the data was performed using the software Windox 5 (Sympatec, Clausthal-Zellerfeld, Germany). The volumetric median particle size and particle span (span=$(X_{90.3}-X_{10.3})/X_{50.3}$) were obtained from the analysis.

Amount of product produced per time

The amount of product spray dried per time was calculated by dividing the mass of product collected after spray drying by the time that was required to produce the product.

Product yield

Product yield was determined as the ratio of spray dried mass by the initial mass of salbutamol sulfate used for the preparation of the feed solution.

Particle surface investigations

The powder samples were examined using a scanning electron microscope (SEM) (Zeiss Ultra 55, Zeiss, Oberkochen, Germany) operating at 5kV. The particles were sputtered with gold-palladium prior to analysis.

Water sorption analysis

The moisture sorption isotherms were recorded with a SPS-11 moisture sorption analyzer (Projekt Messtechnik, Ulm, Germany) at a temperature of 25°C ± 0.1°C. The measurement cycle was started at 0% relative humidity (RH), increased in two 5% steps to 10% RH, further increased up to 90% RH in 10% steps and from 90% to 95% RH in one step. Subsequently the RH was decreased again to 90% RH, further decreased in 10% steps to 10% RH and in two 5%-steps to 0% RH. The equilibrium condition for each step was set to a mass constancy of ±0.001 % over 60 min.

X-Ray powder diffraction analysis

The powder X-Ray diffraction patterns (PXRD) were obtained with a X'Pert PRO diffractometer (PANalytical, Almelo, The Netherlands) equipped with a theta/theta coupled goniometer in transmission geometry, programmable XYZ stage with well plate holder, Cu-Kα1,2 radiation source (wavelength 0.15419 nm) with a focussing mirror, a 0.5° divergence slit, a 0.02° soller slit collimator and a 0.5° anti-scattering slit on the incident beam side, a 2 mm anti-scattering slit, a 0.02° soller slit collimator, a Ni-filter and a solid state PIXcel detector on the diffracted beam side. The patterns were recorded at a tube voltage of 40 kV, tube current of 40 mA, applying a stepsize of 0.013° 2Θ with 40s per step in the angular range of 2° to 40° 2Θ.

Results and discussion

In order to study the influence of mesh size, feed concentration and drying air temperature on the median particle size, the width of the particle size distribution (span), the product produced per time as well as the product yield when spray drying aqeous mannitol solutions using the Nano Spray Dryer B-90 a full-factorial 3^3 design was used. Table 1 shows the three factor levels of the statistical design. The mesh sizes used (4.0 µm, 5.5 µm and 7.0 µm) were the three sizes which are available for the Nano Spray Dryer. The high level of the drying air temperature (120 °C) is the highest temperature the Nano Spray Dryer can be operated at. In order to allow complete drying of the aqueous solutions the lower level was set to 80 °C. The high level of the feed concentration was 15.00 % (m/m), which is close to the solubility of salbutamol sulfate at room temperature (≈ 18.00 % (m/m)).

In order to keep the number of experiments at a reasonable level and as the main target was to study the influence of process parameters on particle size, drying air flow rate (110 l/h) and spray rate (30 %), which are both expected not to impact particle size, were kept constant.

For a conventional spray dryer a change of the drying air flow rate might alter the deposition efficiency of the cyclone. Via this mechanism particle size could change. However this is not expected for the Nano Spray Dryer as particle collection relies on electrostatic deposition.

When using conventional atomizers (rotary as well as nozzle) a change of the atomizing conditions (e.g. spray rate) influences the droplet size and consequently the particle size. However for the novel vibrating mesh spray technology an increase in the spray rate increases the oscillation frequency of the mesh. The higher oscillation frequency results in the formation of more droplets per time. However the size of the droplets should not change.

Drying air flow rate as well as spray rate impact the drying temperature. Via a change of drying temperature the two factors might impact particle size. However preliminary experiments showed that the change of drying air temperature was small compared to the temperature range studied within the experimental design (80 °C-120 °C).

Particle size

Within the design space studied particles with a median size of 1.01 μm to 6.39 μm (Table 2, see also Figure 9) were observed. All of the three factors studied significantly influenced the size of the spray dried products. Besides the three main factors the quadratic terms concentration*concentration and mesh size*mesh size as well as the interaction term mesh size* concentration significantly impacted particle size (Figure 1). The complex interplay of these terms and their effect on particle size at intermediate temperature (100 °C) is graphically displayed in Figure 2. In this contour plot factor settings where particles of the same size are obtained are displayed by regions of equal color. Because of the fact that the influence of drying air temperature was only small the impact of this factor is not graphically displayed.

For all mesh sizes studied an increase in feed concentration from 1 % to 12 % led to an increase in particle size. The correlation between feed concentration and particle size had already been described by Masters [12] and was explained by Elversson and Millqvist-Fureby [5] for a spray drying process with a conventional spray dryer. Lee et al. [8] observed the same impact, albeit less pronounced, when spray drying protein solutions using the Nano Spray Dryer B-90. Although the Nano Spray Dryer relies on atomization and particle collection principles different from the conventional ones and is therefore a novel spray dryer, the mechanism of drying of the droplets once generated is the same. A liquid feed is dispersed into small droplets. Those droplets then are dried in the tower and are collected after drying at the bottom of the dryer. In order to understand the influence of feed concentration the progress of drying of the droplet should be understood. As soon as the droplet enters the tower evaporation of water at the droplet surface takes place. Due to the evaporation of water the concentration of salbutamol sulfate at the droplet surface increases. When

the concentration exceeds the solubility solidification starts. With higher concentration the concentration where solidification starts is reached at an earlier point of time when the droplet is comparably larger. Therefore larger feed concentrations lead to larger particle sizes.

Figure 2 shows that the increase in particle size is more pronounced the larger the mesh size, hence the larger the droplets generated. Although the ratio of the solid salbutamol sulfate content of droplets with a concentration of 1 % and 12 % is independent of the droplet size (e.g. for a droplet of 10 µm: $(10*4/3*\pi)$ /$(120*4/3*\pi)$, for a droplet of 1 µm: $(0.01*4/3*\pi)$ /$(0.12*4/3*\pi)$; ratio=1/12) the subsequent change of size of the solidified particle (assuming a solid particle) is larger, the larger the size of the initial droplet (e.g. for a droplet of 10 µm: $(10)^{1/3}$ /$(120)^{1/3}$; droplet of 1 µm: $(0.01)^{1/3}$ /$(0.12)^{1/3}$).

A further increase in feed concentration from 12 % to 15 % did not increase or even slightly decreased particle size. One explanation for this might be that the impact of feed concentration on particle size is more pronounced at comparably lower concentration. For example a change of feed concentration from 1 % to 2 % leads to a larger change of particle size than an increase from 14 % to 15 %. This correlation was also described by Elversson and Millqvist-Fureby [5] when spray drying carbohydrate solutions. Therefore the higher the concentration, the sooner the solidification will start and the change of volume and hence in size is comparably smaller. Additionally the particles of larger size exhibit a corrugated surface (Figure 9), that may result in a slightly lower particle size detected with laser diffraction.

For all concentrations studied an increase in mesh size resulted in the formation of larger particles. This is not much of a surprise as with larger mesh sizes the size of the droplets generated increases [1]. Consequently the larger the droplets, the larger the size of the solidified particles.

Also drying air temperature was found to significantly influence the median particle size, although the impact was only small compared to the one of the mesh size and the feed concentration. Vehring et al. [15] describe this phenomenon with the help of the Peclet number, which is the ratio of the evaporation rate to the diffusion coefficient of the solute. During drying the increase in solute concentration at the particle surface causes a diffusion of the solute towards the droplet center. If the diffusion is equal to the evaporation rate there will not be any concentration gradient along the radius of the droplet. However if the evaporation is faster than the diffusion the concentration at the particle surface will be higher than in the center of the droplet. With higher drying air temperatures the evaporation rate rises and larger Peclet numbers are observed leading to comparably higher concentrations at the particle surface. Therefore shell formation takes place at an earlier point of time, when the droplet volume is still larger resulting in larger particles.

Chawla et al. [4] who studied the influence of process parameters when spray drying aqueous mannitol solutions using a conventional Mini Spray Dryer B-190 on particle size observed that none of the single process parameters studied (pump speed, aspirator level, inlet temperature, feed concentration) impact particle size. However they reported that the interaction term of feed concentration and aspirator level was significant. When both factors were at their highest level, the largest particles were obtained. The authors further reported that the spray dried particles had a median diameter of 4.4 µm. In contrast to the study performed by Chawla et al. [4] on the Mini Spray Dryer B-190 this work shows that by using the Nano Spray Dryer B-90 particle size can be successfully adjusted by controlling the process parameters. A larger change of particle size with the Mini Spray Dryer might have been achieved by varying the atomizer settings.

In order to get an idea about the influence of process parameters on the width of the particle size distribution the span values were evaluated too. A change of mesh size significantly altered particle span (Figure 3). Figure 4 shows that the particle span significantly increases with increasing mesh sizes. The change was even larger the larger the mesh size (mesh size*mesh size). Exemplarily the particle size distribution of the sample with the highest (Sample 2) and the lowest (Sample 26) median particle size is displayed in Figure 5. Interestingly all samples with a median particle size larger than 2.39 µm showed a bimodal particle size distribution.

The increase in particle span with increasing mesh size, and the change from a mono- to a bimodal distribution, could be a result of secondary droplet break-up or the generation of satellite droplets during atomization, especially when larger mesh sizes are used.

Amount of product spray dried per time

In order to get an idea about the time that is required to produce a certain amount of product the influence of process parameters on the amount of product spray dried per time was investigated. Values from 0.44 mg/min to 75.83 mg/min were observed (Table 2).

Figure 6 shows that two factors, mesh size and feed concentration as well as their quadratic terms, significantly impact the amount of product that is produced per time. The drying air temperature had no influence on the response studied. Generally larger mesh sizes as well as larger concentrations led to an increase in the amount of product prepared per time. With larger mesh sizes there is an increase in the size of the droplets generated [1]. Due to the higher volume those droplets contain a higher amount of dissolved salbutamol sulfate finally leading to a higher amount of product produced per time. Also higher concentrations mean a higher amount of dissolved salbutamol sulfate and consequently a higher value of the effect studied.

Interestingly there was a minimum of the product produced per time at a mesh size of approximately 4.7 µm and a concentration of 9.5 %. Further at large mesh sizes and high concentrations the mass

prepared per time slightly decreased. These findings are unexpected and should be further investigated.

Product yield

Product yields from 41.21 % to 90.38 % (Table 2) were observed. The statistical analysis of the experimental design revealed (data not shown) that there was no correlation between the process parameters studied and the product yield. Although the result that product yield is independent on process parameters is primarily positive the high scatter of values observed needs further understanding and will be the focus of further work.

Initially the idea was to use the same initial mass of salbutamol sulfate for all the experiments studied. However the experiments showed that especially with a low feed concentration and small mesh size the time to spray the whole feed prepared was too long. When comparably lower initial masses are used the yield is expected to be lower due to comparably higher losses e.g. during particle collection after spray drying. In the case of losses which are attributed to the different initial masses of spray dried salbutamol sulfate the statistical analysis of process parameters on product yield would be invalid. In order to exclude this, the influence of initial mass on the product yield was studied. Figure 8 shows that there is no correlation between the initial mass and the product yield indicating that the analysis of the influence of process parameters on product yield is valid.

Particle shape

The SEM micrographs of the products reveal (Figure 9) that all products are of spherical shape. Although the overall particle shape is spherical, the particles of larger size exhibit a corrugated surface whereas the smaller particles show no corrugation.

The drying history of the droplets will explain the different morphologies of the small and large particles. As already described above (see particle shape) water will evaporate at the droplet surface as soon as the droplet enters the tower. Due to the evaporation of water there is a continuous increase in the surface concentration at the droplets surface and once the concentration is high enough a shell will form. After the formation of the shell there is still water trapped inside the drying particle. Due to the high temperature the water trapped inside the solidifying particles continues to vaporize and a pressure will form inside the particle. The increase in pressure leads to particle inflation. Due to the fact that the stability of the shell is higher the smaller the particles the shell of the smaller particles has sufficient mechanical stability to remain spherical whereas the shell of the larger particles will collapse after inflation, giving the particles a corrugated surface.

Powder crystallinity

As already shown by Chawla et al. [4] spray drying of aqueous salbutamol sulfate solutions results in the formation of amorphous products. Exemplarily the XRPD pattern of sample 10, which is a sample with an intermediate particle size (see Table 2), is shown (Figure 11).

Water vapor sorption

In order to get an idea about the stability of the amorphous spray dried products upon storage at elevated relative humidities water vapor sorption experiments were carried out.

In Figure 10 the moisture induced change of mass of the spray dried salbutamol sulfate versus relative humidity of sample 10 (see also powder crystallinity) is shown. In the experiment the relative humidity was increased from 0 % to 95 %. It can be seen that there is a continuous increase in mass attributed to the sorption of water in the RH range of 0 % to 60 %. Suddenly at 60 % RH the mass decreases, which is ascribed to crystallization. The water absorbed acts as a plasticizer and reduces the glass transition temperature (T_g) of the amorphous salbutamol sulfate. Once the temperature of the experiment is higher than the glass transition temperature the molecules have sufficient mobility to crystallize and vapor is expelled from the crystal lattice that forms [3, 6]. After the transformation of the amorphous material the RH was further increased and the final water uptake at 95% RH was measured to be 4 % for the crystalline material. Subsequently the humidity was reduced back to 0 % again resulting in the decrease of the water content.

In order to prove that there is a change from the amorphous to the crystalline state XRPD experiments before and after the moisture sorption were performed. Figure 11 shows that after moisture sorption diffraction peaks appear verifying the transition from amorphous to crystalline.

Moisture sorption experiments indicate that as long as the RH is below 60 % spray dried salbutamol sulfate products are stable and can be used in order to study interparticle interactions in dry powder inhaler formulations.

<u>Conclusion</u>

This study shows that particle size can be successfully modified by changing the process parameters of the Nano Spray Dryer B-90 when spray drying aqueous salbutamol sulfate solutions. The particle size can be tailored by adjusting the mesh size, feed concentration as well as drying air temperature. Although termed "Nano" Spray Dryer all products were in the micrometer range (1.01 µm to 6.39 µm) and had an appropriate size to be used in pulmonary drug delivery. Small particles had a monomodal size distribution whereas for particles with a mean size above 2.39 µm there was a shift to bimodal distributed sizes. The width of the particle size distribution (span) increased with increasing mesh sizes. The changes in particle size distribution might be a result of the formation of

satellite droplets or secondary droplet break-up during atomization. A thorough characterization of the spray generated with the novel vibrating mesh technology seems therefore necessary and will be the focus of further research. The amount of product prepared per time was observed to be from 0.44 mg/min to 75.83 mg/min. Mesh size as well as concentration significantly impacted the amount of product prepared per time. No correlation between product yield (41.21 % to 90.38 %) and spray drying process parameters was observed. Further studies are suggested to identify the reasons for the high variability in product yield. Consistent with the findings of Chawla et al. [4] who spray dried aqueous salbutmol sulfate solutions on a conventional Mini Spray Dryer B-190 all products were amorphous after spray drying. There was a change from the amorphous to the crystalline state at a relative humidity of 60 %.

Acknowledgements

References

[1]   BÜCHI Labortechnik AG. Brochure nano spray dryer b-90. *Flawil, Switzerland*, 2009.

[2]   K. Bürki, I. Jeon, C. Arpagaus, and G. Betz. New insights into respirable protein powder preparation using a nano spray dryer. *International Journal of Pharmaceutics*, 408(1–2):248 – 256, 2011.

[3]   Graham Buckton. Characterisation of small changes in the physical properties of powders of significance for dry powder inhaler formulations. *Advanced Drug Delivery Reviews*, 26(1):17 – 27, 1997.

[4]   A. Chawla, K.M.G. Taylor, J.M. Newton, and M.C.R. Johnson. Production of spray dried salbutamol sulfate for use in dry powder aerosol formulation. *International Journal of Pharmaceutics*, 108:233–240,

[5]   Jessica Elversson and Anna Millqvist-Fureby. Particle size and density in spray drying- effects of carbohydrate properties. *Journal of pharmaceutical sciences*, 94(9):2049–2060, 2005.

[6]   Bruno C. Hancock and Sheri L. Shamblin. Water vapour sorption by pharmaceutical sugars. *Pharmaceutical Science & Technology Today*, 1(8):345 – 351, 1998.

[7]   Anthony J. Hickey. Lung deposition and clearance of pharmaceutical aerosols: What can be learned from inhalation toxicology and industrial hygiene? *Aerosol Science and Technology*, 18(3):290–304, 1993.

[8]   Sie Huey Lee, Desmond Heng, Wai Kiong Ng, Hak-Kim Chan, and Reginald B.H. Tan. Nano spray drying: A novel method for preparing protein nanoparticles for protein therapy. *International Journal of Pharmaceutics*, 403(1–2):192 – 200, 2011.

[9]   Xiang Li, Nicolas Anton, Cordin Arpagaus, Fabrice Belleteix, and Thierry F. Vandamme. Nanoparticles by spray drying using innovative new technology: The büchi nano spray dryer b-90. *Journal of Controlled Release*, 147(2):304 – 310, 2010.

[10]   Eva Maria Littringer, Axel Mescher, Susanna Eckhard, Hartmuth Schröttner, Christoph Langes, Manfred Fries, Ulrich Griesser, Peter Walzel, and Nora Anne Urbanetz. Spray drying of mannitol as a drug carrier – the impact of process parameters on the product properties. *Drying Technology*, 30:114–124, 2012.

[11]   Eva Maria Littringer, Axel Mescher, Hartmuth Schroettner, Peter Walzel, and Nora Anne Urbanetz. Spray-dried mannitol carrier particles with optimized surface properties – the influence of carrier surface roughness and shape. *European Journal of Pharmaceutical Sciences*, page in press, 2011.

[12]   K. Masters. *Spray drying*. Leonhard Hill Books, 1972.

[13]   Nina Schafroth, Cordin Arpagaus, Umesh Y. Jadhav, Sushil Makne, and Dennis Douroumis. Nano and microparticle engineering of water insoluble drugs using a novel spray-drying process. *Colloids and Surfaces B: Biointerfaces*, 90(0):8 – 15, 2012.

[14]   Gerhard Scheuch, William C. Zimerlich, and Ruediger Siekmeier. *Pulmonary drug delivery - Basics, Application and Opportunities for Small Molecules and Biopharmaceutics- Chapter I Biophysical Parameters Determing Pulmonary Drug Delivery*. Editio Cantor Verlag für Medizin und Naturwissenschaften GmbH, 2007.

[15]   Reinhard Vehring, Willard R. Foss, and David Lechuga-Ballesteros. Particle formation in spray drying. *Aerosol Science*, 38:728–746, 2007.

[16]   M.T. Vidgrén, P.A. Vidgrén, and T.P. Paronen. Comparison of physical and inhalation properties of spray-dried and mechanically micronized disodium cromoglycate. *International Journal of Pharmaceutics*, 35(1–2):139 – 144, 1987.

[17]   Claudius Weiler, Marc Egen, Michael Trunk, and Peter Langguth. Force control and powder dispersibility of spray dried particles for inhalation. *Journal of pharamceutical sciences*, 2009.

[18]   Min Zhao, Yu You, Yachao Ren, Yu Zhang, and Xing Tang. Formulation, characteristics and aerosolization performance of azithromycin dpi prepared by spray-drying. *Powder Technology*, 187(3):214 – 221, 2008.

Table 1. Process parameters used in the 3^3 full-factorial design.

Parameter	Factor level			Unit
	1	**2**	**3**	
Mesh size	4.0	5.5.	7.0	µm
Feed concentration	1.0	7.5	15.0	% (m/m)
Drying air temperature	80	100	120	°C

Table 2. Design matrix of the 3^3 full-factorial design and the data collected from the analyses.

| Sample ID	Factor			Response			
	Mesh size / µm	Conc. / % (w/w)	Temp. /°C	Size / µm	Span	Mass per time / mg/min	Product yield / %
1	7	15	120	6,36	1,79	75,84	90,38
2	7	15	100	6,39	1,99	36,67	70,34
3	7	15	80	5,41	2,08	20,31	72,98
4	7	7,5	120	5,43	2,13	42,00	83,79
5	7	7,5	100	4,86	1,98	15,12	72,15
6	7	7,5	80	3,97	1,94	3,71	75,44
7	7	1	120	2,04	1,96	2,27	46,37
8	7	1	100	2,33	2,01	0,00	0,00
9	7	1	80	2,25	2,06	1,76	57,07
10	5,5	15	120	3,37	1,68	3,17	86,07
11	5,5	15	100	3,53	1,69	4,86	51,42
12	5,5	15	80	3,07	1,71	7,47	70,80
13	5,5	7,5	120	2,94	1,78	4,37	82,69
14	5,5	7,5	100	2,84	1,68	4,03	48,34
15	5,5	7,5	80	2,74	1,64	6,77	65,17
16	5,5	1	120	1,44	1,59	3,94	49,59
17	5,5	1	100	1,55	1,67	0,61	59,05
18	5,5	1	80	1,17	1,76	0,73	78,14
19	4	15	120	2,39	1,66	0,79	71,73
20	4	15	100	2,31	1,59	4,12	41,21
21	4	15	80	2,37	1,59	4,56	73,82
22	4	7,5	120	2,3	1,54	6,14	61,91
23	4	7,5	100	2,3	1,58	4,39	61,21
24	4	7,5	80	1,93	1,48	9,05	63,12
25	4	1	120	1,17	1,65	3,01	72,16
26	4	1	100	1,01	1,86	0,55	56,03
27	4	1	80	1,09	1,72	0,44	57,16
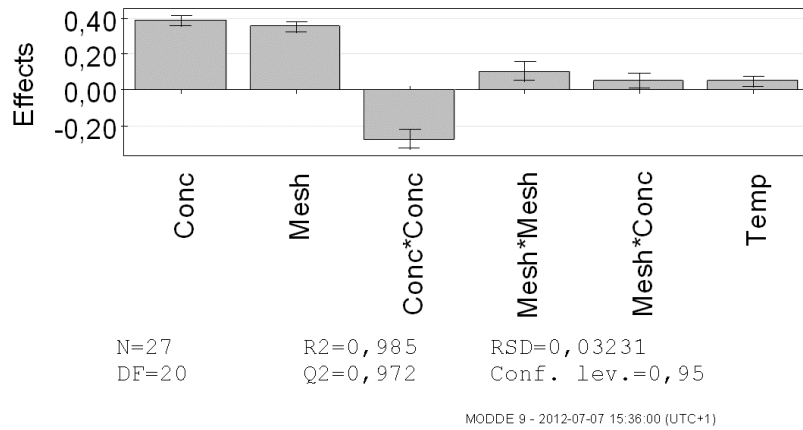
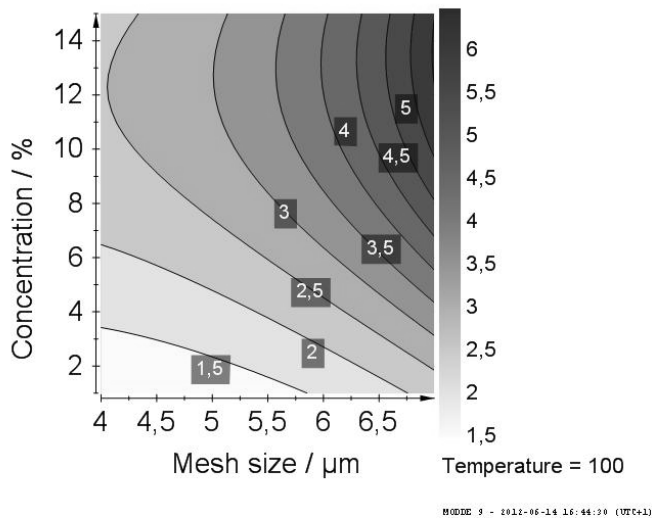*Figure 1. Effect plot displaying the influence of process parameters on the median particle size.*

Figure 2. Contour plot of the influence of feed concentration and mesh size on the median particle size (μm) of the spray dried products.
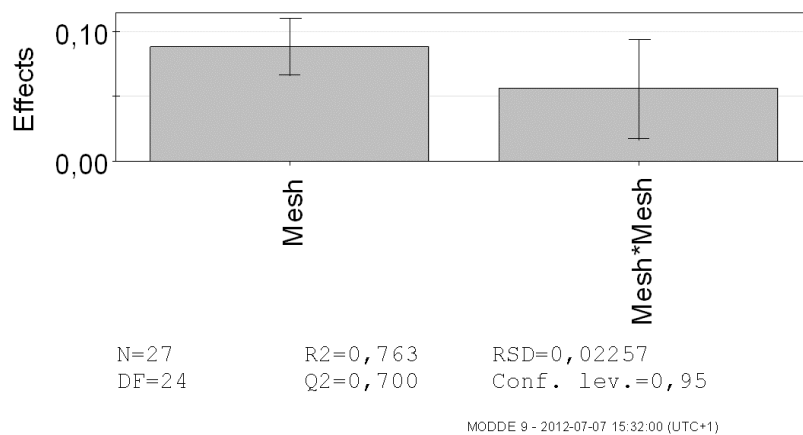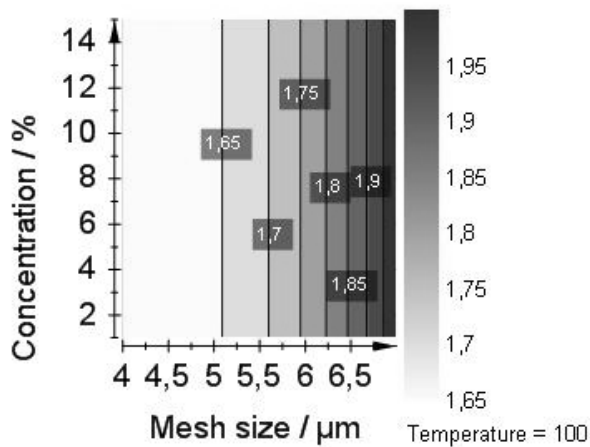

Figure 3. Effect plot displaying the influence of process parameters on particle span.

Figure 4. Contour plot of the influence of feed concentration and mesh size on particle span of the spray dried products.

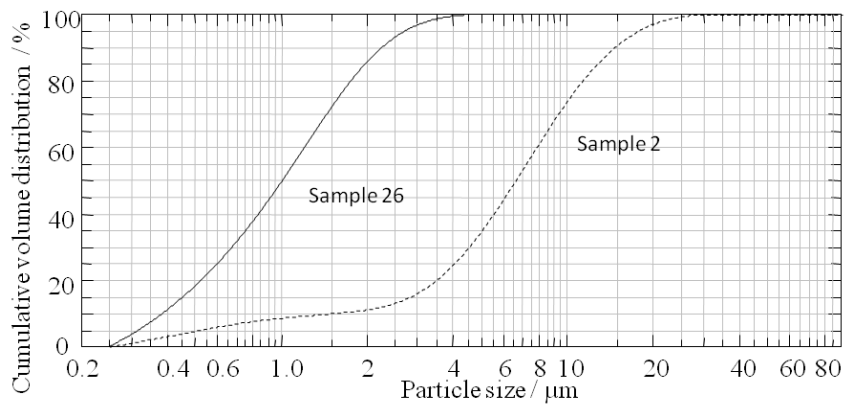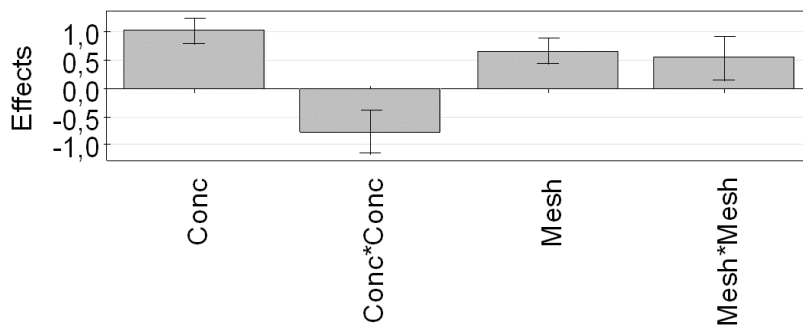*Figure 5. Particle size distribution of sample 26 and sample 2.*

Figure 6. Coefficient plot displaying the influence of process parameters on the product produced per time.
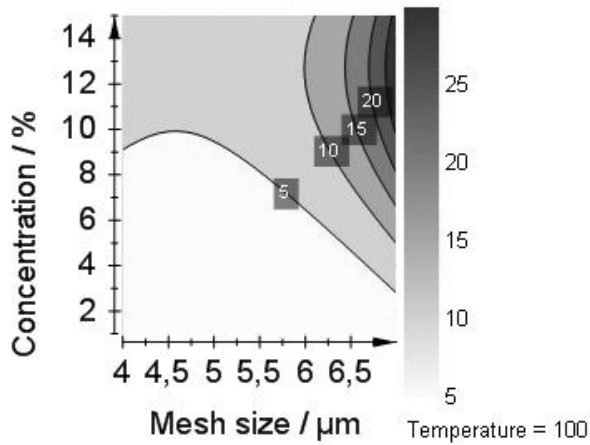
Figure 7. Contour plot of the influence of feed concentration and mesh size on the spray dried product produced per time (g/min).
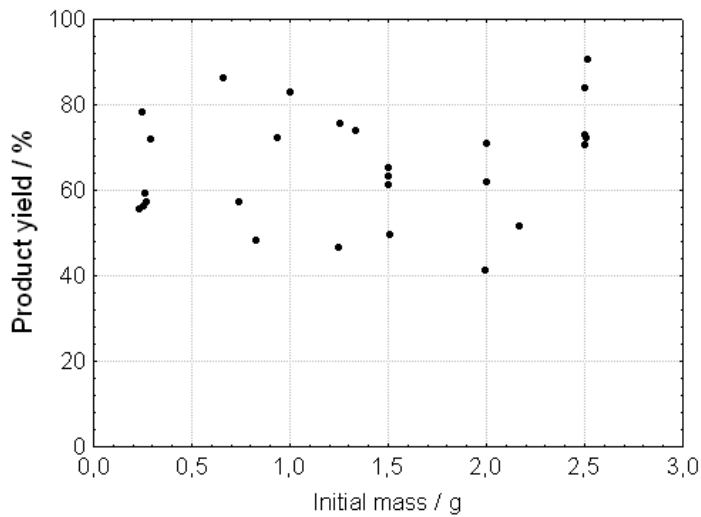
Figure 8. Correlation between the initial mass of salbutamol sulfate spray dried and the corresponding product yield.

Figure 9. SEM micrographs of the products with the largest (Sample 1, left) and smallest (Sample 27, right) particle size.

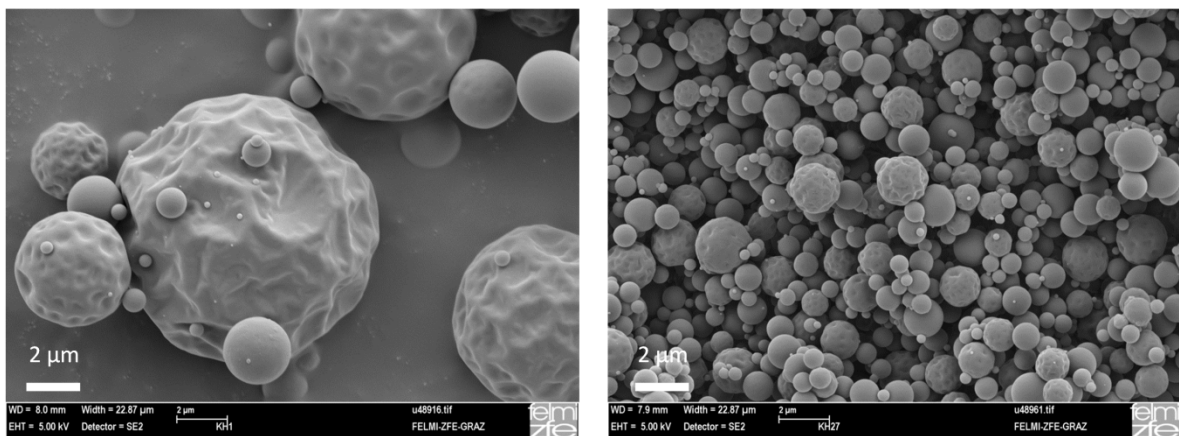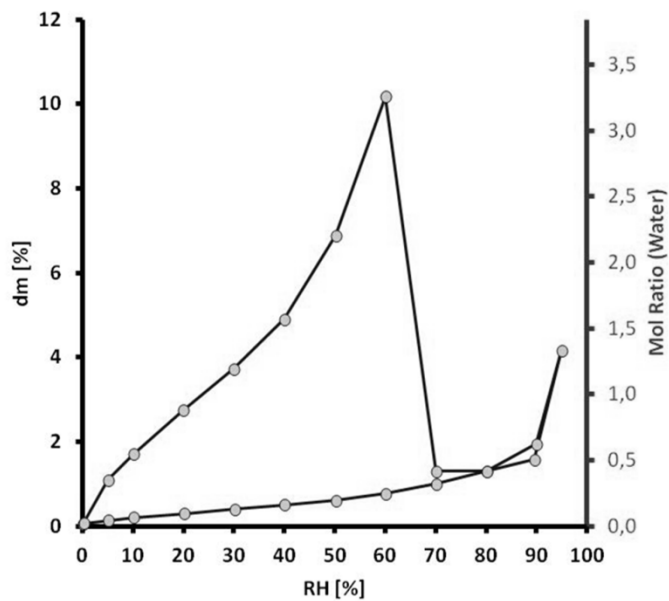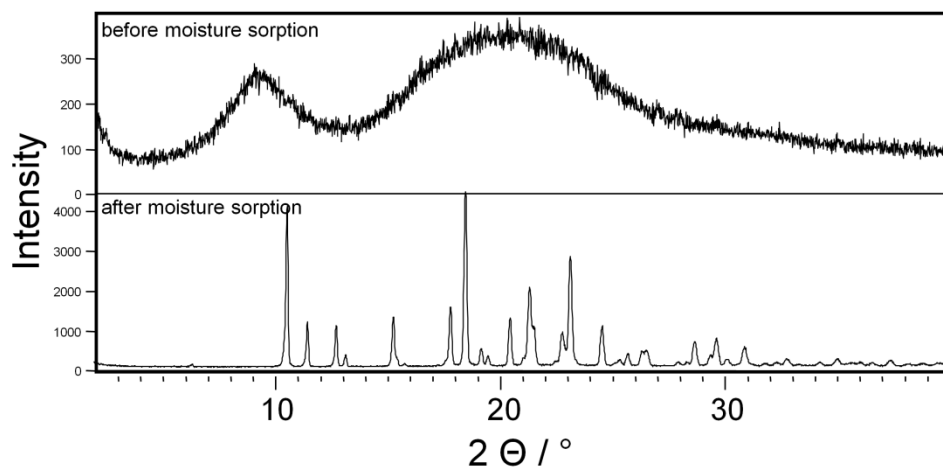*Figure 10. Sorption isotherm of spray dried salbutamol sulfate (Sample 10, see Table 2).*

Figure 11. XRPD pattern of Sample 10 (see Table 2) before and after the moisture sorption experiments.

4. Appendix

4.1. Curriculum vitae

Eva Maria Littringer

Born on February 12th, 1985 in Kirchdorf/Krems (Austria)

Austrian citizen

Education

04/2009 -	**Doctoral Program in Natural Sciences**
	Graz University of Technology, Austria
	Project manager of the B6 project of the DFG (German research foundation) priority program SPP 1423 "Process-spray" at the Research Center Pharmaceutical Engineering GmbH, Graz, Austria
	Thesis „Optimizing the quality attributes of carrier based dry powder inhaler formulations by carrier surface modification via spray drying"
	Supervisor: Prof. Urbanetz
10/2008 - 01/2011	**Master Pharmaceutical Engineering**
	University of Graz, Austria
	With distinction
10/2003 - 04/2008	**Diploma study Pharmacy**
	University of Graz, Austria
	With distinction
	Thesis: „Investigating protein ligand interactions by biophysical and cellular biological means" at the Institute of Pharmaceutical Sciences and ProtAffin AG
	Supervisor: Prof. Kungl
09/1995 - 06/2003	**Bundesrealgymnasium Kirchdorf/Krems**
	School leaving examination, with distinction

Professional experience

01/2012 – 05/2012	**Austrian Agency for Health and Food Safety (AGES)**
	Inspections GDP/GMP
10/2009 - 11/2009	**Visiting researcher at the Department of Mechanical Process Engineering, Dortmund University of Technology, Germany**
	Spray drying experiments (pilot-plant)
10/2008 - 12/2008	**University of Graz, Institute of Pharmaceutical Sciences, Austria**
	Scientific project staff, Glycosaminoglycan analysis

08/2008	**Internship at the Institute of BioAgricultural Sciences, Academia Sinica, Taipei, Taiwan**
	Laboratory work
06/2008 - 07/2008	**Parmacy Kirchdorf/Krems, Austria**
	Preparation of magistral formulations, start of the practical year
12/2007 - 12/2008	**University of Graz, Institute of Pharmaceutical Sciences, Austria**
	Tutor in the practical course „ Pharmaceutical clinical diagnostics and biochemical methods"
09/2007	**Hospital Pharmacy, Wels, Austria**
	Aseptical preparation of magistral formulations (eye drops, infusions)
08/2006	**Pharmacy Kirchdorf/Krems, Austria**
	Internship

Grants and Distinctions

12/2011	Pat Burnell New Investigator Award at the conference "Drug delivery to the lungs" (DDL22, Edinburgh, UK)
12/2011	Excellence scholarship of the Faculty of Technical Chemistry, Chemical & Process Engineering and Biotechnology, Graz University of Technology, Austria
11/2011	Travel grant of the Austrian Research Association (Österreichische Forschungsgemeinschaft) for participation at the conference „Drug delivery systems" (SDSS-2011, Shenzhen, China)
09/2011	Paul Eisenklam Travel Award for participation at the "European Conference on liquid atomization and spray systems "(ILASS2011, Estoril, Portugal)
10/2010	Nomination for the Pat Burnell New Investigator Award within the conference Drug delivery to the lungs (DDL21, Edinburgh, UK)
05/2010	Scholarship for short time academic research and expert courses abroad (International Relations and Mobility Programs, Graz University of Technology) for participation at the "International school of crystallization" (Laboratorio de Estudios Cristalograficos, Granada, Spain)
10/2009	Scholarship of the Faculty of Technical Chemistry, Chemical & Process Engineering and Biotechnology (Graz University of Technology); Visiting researcher at the Department of Mechanical Process Engineering, Dortmund University of Technology, Germany
2006, 2007	Excellence scholarship of the Natural Science Faculty, University of Graz, Austria

4.2. Publications

Research Papers

Littringer, E. M.; Noisternig, M. F.; Mescher, A.; Schroettner, H.; Walzel, P.; Griesser, U. J. & Urbanetz, N. A., The morphology and various densities of spray dried mannitol, Journal of pharmaceutical sciences, 2012, submitted for publication

Littringer, E. M.; Zellnitz, S.; Hammernik, K.; Adamer, V.; Schroettner, H.; Griesser, U. & Urbanetz, N., Spray drying of aqueous salbutamol sulphate solutions using the Nano Spray Dryer B-90 – The impact of process parameters on particle size, *European Journal of Pharmaceutics and Biopharmaceutics,* **2012**, submitted for publication

Littringer, E. M.; Paus, R.; Mescher, A.; Schroettner, H.; Walzel, P. & Urbanetz, N. A., The morphology of spray dried mannitol particles – The vital importance of droplet size, *European Journal of Pharmaceutics and Biopharmaceutics,* **2012**, submitted for publication

Littringer, E. M.; Mescher, A.; Schroettner, H.; Walzel, P. & Urbanetz, N. A., Spray-dried mannitol carrier particles with optimized surface properties – The influence of carrier surface roughness and shape, *European Journal of Pharmaceutical Sciences,* 2011, in press

A. Mescher, **E. M. Littringer**, R. Paus, N. A. Urbanetz und P. Walzel; Homogene Produkteigenschaften in der Sprühtrocknung durch laminare Rotationszerstäubung; Chem.-Ing.-Techn., DOI: 10.1002/cite.201100155

Littringer E M, Mescher A, Eckhard S, Schröttner H, Langes C, Fries M, Griesser U, Walzel P, Urbanetz, N A, Spray drying of mannitol as a drug carrier – The impact of process parameters on the product properties, Drying Technology, 2012, 30, 114-124

Maas S G, Schaldach G, **Littringer E M,** Mescher A, Griesser U, Braun D E, Walzel P, Urbanetz N A, The impact of spray drying outlet temperature on the particle morphology of mannitol, Powder Technology, 2011, 213, 27-35

Conference proceedings

Noisternig, M. F.; **Littringer, E. M.**; Urbanetz, N. A. & Griesser, U. J., Mercury Intrusion Porosimetry – A powerful method for the characterisation of spray dried products, *Spray2012 – in Spray 2012. Berlin,* 2012, 1-8

Littringer, E. M.; Mescher, A.; Schröttner, H.; Achelis, L.; Walzel, P.; Urbanetz, N. A.:The influence of carrier shape and surface roughness of carrier-based dry powder inhalates on the fine particle fraction. - in: Drug delivery to the lungs 2011. Edinburgh, 2011, 1 - 4

Littringer, E. M.; Mescher, A.; Paus, R.; Schröttner, H.; Maas, S.; Walzel, P.:Influence of droplet size on the crystallization behaviour of aqueous D-mannitol solutions during spray drying. - in: ILASS2011- Proceedings. Estoril, 2011

Littringer E M., Mescher A, Schröttner H, Walzel P, Urbanetz N A, Tailoring particle morphology of spray dried mannitol carrier particles by variation of the outlet temperature, Conference Proceedings, 23rd Annual Conference on Liquid Atomization and Spray Systems. Brno, 2010

Littringer E. M., Mescher A, Schröttner H, Walzel P, Urbanetz N A, The use of design of experiments to study the effect of process parameters on surface topography and size of spray dried D-Mannitol, Conference Proceedings, 17th International Drying Symposium. Magdeburg, 2010

Littringer, E. M.; Mescher, A.; Schröttner, H.; Walzel, P.; Urbanetz, N. A.; Surface modification of dry powder inhaler carrier particles by spray drying. - in: Workshop über Sprays, Techniken der Fluidzerstäubung und Untersuchungen von Sprühvorgängen. Heidelberg, 2010, 1 - 8

Littringer, E. M.; Mescher, A.; Schröttner, H.; Walzel, P.; Urbanetz, N. A.; Surface modification of mannitol inhaler carrier particles via spray drying. - in: Drug delivery to the lungs 21. Edinburgh, 2010, 264 – 267

Poster presentations

Littringer, E. M.; Mescher, A.; Paus, R.; Luger, T.; Schröttner, H.; Walzel, P.; Urbanetz, N. A.: The influence of droplet size on the crystallization behavior of aqueous mannitol solutions during spray drying. - in: 8th World Meeting on Pharmaceutics, Biopharmaceutics and Pharmaceutical Technology. Istanbul, 03.2012

Littringer, E. M.; Mescher, A.; Schröttner, H.; Achelis, L.; Walzel, P.; Urbanetz, N. A.: The influence of carrier shape and surface roughness of carrier-based dry powder inhalates on the fine particle fraction. - in: Drug delivery to the lungs 22. Edinburgh, 12.2011

Littringer, E. M.; Mescher, A.; Schröttner, H.; Walzel, P.; Urbanetz, N. A.: The influence of carrier morphology on the fine particle fraction of dry powder inhaler formulations. - in: JOINT MEETING OF THE AUSTRIAN AND GERMAN PHARMACEUTICAL SOCIETIES. Universität Innsbruck, 09.2011

Littringer, E. M.; Maas, S.; Schröttner, H.; Urbanetz, N. A.: Studien zur Ausbildung der Partikelmorphologie im Sprühtrocknungsprozess zur Steuerung der Leistungsmerkmale von Pulverinhalaten. - in: Berichterstattung und Begutachtung zur zweiten Periode des SPP 1423 „Prozess-Spray" . Frankfurt/Main, 01.2011

Littringer, E. M.; Schröttner, H.; Mescher, A.; Maier, M.; Walzel, P.; Urbanetz, N. A.: Influence of carrier particle morphology on the performance of dry powder inhalers. - in: Central European symposium on pharmaceutical technology. Graz, 09.2010

Littringer, E. M.; Mescher, A.; Schröttner, H.; Walzel, P.; Urbanetz, N. A.:Surface modification of mannitol inhaler carrier particles via spray drying. - in: Drug delivery to the lungs 21. Edinburgh, 12.2010

Littringer, E. M.; Maas, S.; Mescher, A.; Walzel, P.; Urbanetz, N. A.: Influence of process scale on the crystallization behaviour of spray dried D-Mannitol. - in: International school of crystallization. Granada, 05.2010

Littringer, E. M.; Maas, S.; Mescher, A.; Schröttner, H.; Walzel, P.; Urbanetz, N. A.: SPRAY DRIED MANNITOL CARRIER PARTICLES WITH OPTIMIZED SURFACE PROPERTIES. - in: Lactose as a Carrier for Inhalation Products. Parma, 09.2010

Littringer, E. M.; Schröttner, H.; Mescher, A.; Walzel, P.; Urbanetz, N. A.: The benefit of design of experiments (DOE) for studying the influence of spray drying conditions on particle morphology . - in: 11th International Conference on Pharmacy and Applied Physical Chemistry . University of Innsbruck, 02.2010

Littringer, E. M.; Maas, S.; Mescher, A.; Walzel, P.; Urbanetz, N. A.: Sprühtrocknung wässriger Mannitollösungen im Labor- und Pilotmaßstab. - in: 6. Minisymposium Verfahrenstechnik. Tulln, 06.2010

Littringer, E. M.; Mescher, A.; Walzel, P.; Urbanetz, N. A.: Influence of spray drying conditions on the morphology of mannitol carrier particles intended for the use in DPI. - in: 7th world meeting on pharmaceutics, biopharmaceutics and pharmaceutical technology. Malta, 03.2010

Littringer, E. M.; Mescher, A.; Walzel, P.; Urbanetz, N. A.: Tailor-made carrier particles for dry powder inhalers . - in: 3. International Congress for Pharmaceutical Engineering. Graz, 09.2009

Oral Presentations

Noisternig, M. F.; Littringer, E. M.; Urbanetz, N. A. & Griesser, U. J., Mercury Intrusion Porosimetry – A powerful method for the characterisation of spray dried products, *Spray2012 – in Spray 2012. Berlin, 22.05.2012*

Littringer, E. M.; Mescher, A.; Schröttner, H.; Walzel, P.; Urbanetz, N. A.:
Influence of process parameters on the D-mannitol particle formation during spray drying. - in: 12th International Conference on Pharmacy and Applied Physical Chemistry. Graz, 06.05.2012

Littringer, E. M.; Mescher, A.; Schröttner, H.; Achelis, L.; Walzel, P.; Urbanetz, N. A.: The influence of carrier shape and surface roughness of carrier-based dry powder inhalates on the fine particle fraction. - in: Drug delivery to the lungs 22. Edinburgh, 05.12.2011

Littringer, E. M.; Mescher, A.; Paus, R.; Walzel, P.; Urbanetz, N. A.: Particle formation of mannitol during spray drying - a scale-up problem. - in: SPP 1423 "Prozess-Spray" Jahrestreffen. TU Darmstadt, 07.11.2011

Littringer, E. M.; Mescher, A.; Walzel, P.; Urbanetz, N. A.: Carrier particle engineering for pulmonary drug delivery via spray drying. - in: 1st annual symposium of drug delivery systems. Shenzhen, 03.11.2011

Littringer, E. M.; Mescher, A.; Schröttner, H.; Schutting, S.; Walzel, P.; Urbanetz, N. A.: Optimized carrier particles for dry powder inhalers by the use of spray drying. - in: 5th International Congress on Pharmaceutical Engineering, Graz. 29.09.2011

Littringer, E. M.; Mescher, A.; Schröttner, H.; Walzel, P.; Urbanetz, N. A.: Influence of process parameters on the D-mannitol particle formation during spray drying. - in: 8th European Congress of Chemical Engineering. Berlin, 25.09.2011

Littringer, E. M.; Mescher, A.; Schröttner, H.; Maas, S.; Walzel, P.; Urbanetz, N. A.: Influence of droplet size on the crystallization behaviour of aqueous D-mannitol solutions during spray drying. - in: 24th European Conference on Liquid Atomization and Spray Systems - ILASS-Europe 2011. Estoril, 05.09.2011

Littringer, E. M.; Mescher, A.; Paus, R.; Schröttner, H.; Maas, S.; Walzel, P.; Urbanetz, N. A.: Influence of droplet size on the crystallization behaviour of aqueous D-mannitol solutions during spray drying. - in: 7. Minisymposium der Verfahrenstechnik. Graz, 30.06.2011

Littringer, E. M.; Urbanetz, N. A.: Influence of surface roughness on the quality attributes of dry powder inhalers. - in: Summerschool/workshop "Rheologie und Phasengrenzen bei der Zerstäubung", Universität Bremen, 08.06.2011

Littringer, E. M.; Schröttner, H.; Urbanetz, N. A.: Sprühtrocknungsverfahren zur Erzeugung inhalierbarer Pulver. - in: Sprühtrocknung zur Herstellung fester Arzneiformen. Arbeitsgemeinschaft für Pharmazeutische Verfahrenstechnik, Fulda, 28.02.2011

Littringer, E. M.; Urbanetz, N. A.: Carrier particle engineering for pulmonary drug delivery via spray drying. - in: Pharmazeutisches Kolloquium - Uni Innsbruck., 24.01.2011

Littringer, E. M.; Urbanetz, N. A.:Tailoring the performance ofcarrier based dry powder inhalates by surface modification of the carrier using spray drying. - in: Berichterstattung und Begutachtung zur zweiten Periode des SPP 1423 „Prozess-Spray" . Frankfurt/Main, 10.01.2011

Littringer, E. M.; Mescher, A.; Schröttner, H.; Walzel, P.; Urbanetz, N. A.: „Surface modification of mannitol inhaler carrier particles via spray drying". - in: Drug delivery to the lungs 21. Edinburgh, 08.12.2010

Urbanetz, N. A.; Littringer, E. M.: „The use of design of experiments to study the effect of process parameters on surface topography and size of spray dries D- mannitol, Conference Proceedings. - in: International Drying Symposium. Magdeburg, 03.10.2010

Littringer, E. M.; Mescher, A.; Schröttner, H.; Maier, M.; Walzel, P.; Urbanetz, N. A.: „Surface modification of dry powder inhaler carrier particles by spray drying. - in: 2. Workshop des SPP Prozess-Spray. Erlangen, 13.09.2010

Littringer, E. M.; Mescher, A.; Schröttner, H.; Walzel, P.; Urbanetz, N. A.: „Tailoring particle morphology of spray dried mannitol carrier particles by variation of the outlet temperature". - in: 23rd European Conference on Liquid Atomization and Spray Systems. Brno, 06.09.2010

Schnepfleitner, S. K.; Littringer, E. M.; Urbanetz, N. A.: „Nanosprühtrocknung - ein Erfahrungsbericht". - in: Büchi Seminar Sprühtrocknung und Chromatographie, Graz, 10.06.2010

Littringer, E. M.; Mescher, A.; Schröttner, H.; Walzel, P.; Urbanetz, N. A.: „Surface modification of dry powder inhaler carrier particles by spray drying. - in: Spray 2010. Heidelberg, 03.05.2010

Littringer, E. M.; Mescher, A.; Schröttner, H.; Walzel, P.; Urbanetz, N. A.: „Morphologie sprühgetrockneter Trägerpartikel für Pulverinhalatoren - Einfluss der Prozessparameter. - in: ProcessNet-Fachausschuss Trocknungstechnik. Göttingen, 28.02.2010

Littringer, E. M.; Urbanetz, N. A.: „Tailor-made carrier particles for dry powder inhalers". - in: Mitarbeiter Workshop DFG SPP 1423, Hamburg, 04.11.2009

Littringer, E. M.; Urbanetz, N. A.: „Steuerung der Leistungsmerkmale trägerbasierter Pulverinhalate durch gezielte Oberflächenmodifikation des Trägers mittels Sprühtrocknung". - in: Kick-Off Meeting des DFG SPP 1423. Bremen, 24.06.2009